HYDROSALINITY MODELLING OF THE BERG RIVER USING ACRU*SALINITY*

by

Wageed Kamish

Thesis presented in partial fulfilment of the requirements for the Degree of Master of Science in Engineering (Civil)

at

Stellenbosch University

Department of Civil Engineering

Study Leader : Professor GR Basson (internal)
Co-Study Leader : Dr AHM Görgens (external)

December 2008

Declaration

By submitting this thesis electronically, I declare that the entirety of the work contained therein is my own, original work, that I am the owner of the copyright thereof (unless to the extent explicitly otherwise stated) and that I have not previously in its entirety or in part submitted it for obtaining any qualification.

Date: 25 November 2008

Copyright © 2008 Stellenbosch University

All rights reserved

ABSTRACT

In recent years, concern about the water quality in the Berg River received a fair degree of attention, particularly with the imminent construction of the Berg Water Project (BWP). Particular concerns have been expressed about the water quality with respect to total dissolved salts (TDS) at Misverstand Dam. In previous studies (Fourie and Görgens, 1977) it was identified that the saline water was mostly generated in the lower portion of the Berg River Catchment (Matjies, Moorreesburg and Sandspruit Rivers) and that the abstraction of acceptable quality water higher up in the Berg River could possibly result in salinity problems at Misverstand Dam. Contrary to expectation, these studies also showed that for the most saline catchments, a winter peak in TDS concentrations also existed.

To help address these concerns, a Water Research Commission (WRC) project was initiated in 2003 in which the newly-developed salinity module of the daily Agricultural Catchment Research Unit (ACRU) agrohydrological model, known as ACRU*Salinity*, would be configured for the Berg River Catchment. This model had previously been configured and calibrated for the Mkhomazi Catchment (Teweldebrhan, 2003) which exhibited relatively low streamflow TDS concentrations (100 mg/l) and it was deemed necessary to ascertain whether comparable TDS values could be simulated in the Berg River Catchment, where TDS concentration could rise to well above 1 000 mg/l in certain tributaries.

In this project, ACRU*Salinity* was configured for the Berg River Catchment on a distributed basis, aiming to capture the spatial distribution of rainfall and geophysical characteristics which inherently exist in a catchment as expansive as the Berg. Initial application of the "Beta version" of ACRU*Salinity* to the Berg River Catchment revealed that it failed to produce simulated TDS values which were representative of the observed data. It became evident that the model required both additional salinity-related functions and modifications of existing functions. After the implementation of these algorithm changes the correspondence of simulated and observed TDS concentrations improved markedly.

Verification of the ACRU*Salinity* simulated flows and calibration of the salinity-related parameters was based on the values of predefined objective functions. Reasonably representative flows could be obtained provided that the catchment discretisation and driver rainfall selection process were adequate. Salinity related parameters were determined purely on an iterative basis, although *a priori* estimation of these parameters was possible. Preliminary interdependency tests of these parameters revealed that the final *calibrated* set of salinity-related parameters was probably not unique and that some *a priori* decision making would be required when selecting the most realistic set of parameters.

Quantification of the potential effect of the Berg River Dam on the TDS concentrations at Misverstand Dam was achieved as follows: the ACRU*Salinity* model was verified for flow and calibrated for TDS at available and reliable flow gauging stations. This was then followed by a long-term simulation run which yielded daily TDS time series for comparison, on an exceedance basis, with the observed record. Since the concern about the possible deterioration of water quality at Misverstand Dam was only a winter concern (May to September), comparisons were only drawn over this period. The flow-routing option in ACRU*Salinity* was not activated and a 1:1 daily comparison of flows and TDS concentrations, based on values of the objective function, was thus not possible. Results from this study showed that even with a daily model, the exceedance percentages of the TDS concentrations after the construction of the Berg River Dam were comparable with the exceedance percentages obtained from the original monthly modelling study (DWAF, 1993). In this study, however, it was possible to capture the increasing TDS concentration which was evident over winter months in the observed data record for the Matjies River and Sandspruit River catchments.

The testing of the model's effectiveness in the evaluation of engineering options was accomplished as follows: several options for ameliorating the possible deterioration of water quality at Misverstand Dam were defined, based on its practicality and cost of implementation. For example, the Withoogte water treatment works abstracts water from Misverstand Dam for supply to the West Coast region when water quality is acceptable (i.e. a TDS lower than 450 mg/l). It was proposed that to minimise the effect of periods when no abstraction from Misverstand could occur due to unacceptable water quality, a second reservoir at the treatment works should be lined and used to provide bridging storage for water from Misverstand Dam when the water quality was acceptable. The calibrated ACRU*Salinity* model was then modified to reflect the physical attributes of this engineering scenario of interest to produce sets of flow and TDS time series which could be further analysed to determine assurance of supply, in terms of predetermined TDS concentration thresholds in Misverstand Dam. Using this particular engineering option, the analysis revealed that a 300 mg/l TDS upper-limit at Misverstand was too stringent and that 450 mg/l was probably more realistic.

OPSOMMING

In die laaste jare het kommer oor die watergehalte van die Bergrivier redelik baie aandag ontvang, veral met die oprigting van die Bergwaterprojek (BWP). Kommer is spesifiek uitgespreek oor die watergehalte van die Misverstanddam ten opsigte van die totale opgeloste soute (TOS). Met vorige navorsing (Fourie & Görgens, 1977) is daar vasgestel dat die soutwater meestal afkomstig is van die laerliggende gedeelte van die Bergrivier-opvanggebied (die Matjies-, Moorreesburg- en Sandspruitrivier), en dat die onttrekking van water met ’n aanvaarbare gehalte hoër op in die Bergrivier moontlik kan lei tot probleme met die soutgehalte van die Misverstanddam. Anders as wat verwag is, het hierdie studies ook getoon dat die TOS-konsentrasie in die meeste soutopvanggebiede in die winter die hoogste was.

Om hierdie probleme te help oplos het die Waternavorsingskommissie (WNK) in 2003 begin met ’n projek waarin die pas ontwikkelde soutmodule van die Navorsingseenheid vir Landbou-opvanggebiede (NLO) se daaglikse agrowaterkundige model – bekend as ACRU*Salinity* –vir die Bergrivier-opvanggebied aangepas sou word. Hierdie model is voorheen aangepas en gekalibreer vir die Mkhomazi-opvanggebied (Teweldebrhan, 2003) waar die stroomvloei relatiewe lae TOS-konsentrasies (100 mg/ℓ) getoon het. Daar moes dus bepaal word of vergelykbare TOS-waardes nageboots kon word in die Bergrivier-opvanggebied, waar die TOS-konsentrasie tot ver bokant 1 000 mg/ℓ in sekere sytakke kan styg.

In hierdie projek is ACRU*Salinity* aangepas om wyd verspreid in die Bergrivier-opvanggebied gebruik te word, met die doel om die ruimtelike verspreiding van reënval en geofisiese eienskappe wat eie is aan ’n opvanggebied so omvangryk soos dié van die Bergrivier, te bepaal. Die aanvanklike toepassing van die “Beta-weergawe” van ACRU*Salinity* op die Bergrivier-opvanggebied het aan die lig gebring dat dit nie nagebootste TOS-waardes wat verteenwoordigend van die waargenome waardes was, kon voortbring nie. Dit het duidelik geword dat die model sowel bykomende soutverwante funksies en aanpassings van bestaande funksies sou vereis. Ná die instelling van hierdie algoritmiese veranderings het die ooreenstemming tussen die nagebootste en waargenome TOS-konsentrasies merkbaar verhoog.

Stawing van ACRU*Salinity* se nagebootste stroomvloei en kalibrering van die soutverwante parameters is gegrond op die waardes van vooraf bepaalde objektiewe funksies. Redelike verteenwoordigende stroomvloei kon verkry word mits die diskretisasie en hoofreënval-seleksieproses in die opvanggebied voldoende was. Soutverwante parameters is slegs op ’n herhalingsgrondslag bepaal, al was ’n a-priori skatting van hierdie parameters moontlik. Voorlopige interafhanklikheidstoetse op hierdie parameters het getoon dat die finale gekalibreerde stel soutverwante parameters waarskynlik nie uniek was nie en dat ’n

mate van a-priori besluitneming vereis sou word wanneer die mees realistiese stel parameters gekies sou word.

Kwantifisering van die moontlike invloed van die Bergrivierdam op die TOS-konsentrasies van die Misverstanddam is soos volg bereik: Die ACRU*Salinity*-model is by beskikbare en betroubare vloeimeetstasies vir stroomvloei getoets en vir TOS gekalibreer. Dit is toe gevolg deur ’n langtermyn-nabootsingstoets wat daaglikse TOS-tydreekse voorsien het, wat op ’n oorskrydingsgrondslag met die waargenome data vergelyk kon word. Aangesien die besorgdheid oor die moontlike verswakking van die watergehalte by die Misverstanddam net in die winter (Mei tot September) ’n bekommernis was, is vergelykings net in hierdie tydperk gedoen. Die stroomvloei-opsie van ACRU*Salinity* is nie gebruik nie, en ’n 1:1- daaglikse vergelyking van stroomvloei en TOS-konsentrasies, gegrond op waardes van die objektiewe funksie, was dus nie moontlik nie. Resultate van hierdie studie het getoon dat, selfs met ’n daaglikse model, die oorskrydingspersentasies van die TOS-konsentrasies ná die oprigting van die Bergrivierdam vergelykbaar was met die oorskrydingspersentasies wat uit die oorspronklike maandelikse modelstudie verkry is (DWAF, 1993). In hierdie studie was dit egter moontlik om die toenemende TOS-konsentrasie wat in die wintermaande sigbaar was, vas te lê in die waargenome data vir die Matjiesrivier- en die Sandspruitrivier-opvanggebied.

Die toetsing van die model se doeltreffendheid in die evaluering van ingenieursopsies is soos volg bereik: Verskeie opsies om die moontlike verswakking van die watergehalte van die Misverstanddam te beperk, is gedefinieer op grond van die praktiese uitvoerbaarheid daarvan en die koste daaraan verbonde. Die Withoogte-waterbehandelingsaanleg onttrek byvoorbeeld water uit die Misverstanddam vir watervoorsiening aan die Weskusstreek wanneer die watergehalte aanvaarbaar is (m.a.w., met ’n TOS laer as 450 mg/ℓ). Om die invloed van tydperke wanneer geen water weens ’n onaanvaarbare watergehalte uit die Misverstanddam onttrek kan word nie tot die minimum te beperk, is daar voorgestel dat ’n tweede reservoir by die behandelingsaanleg gevul en gebruik moet word vir oorbruggingsberging van water uit die Misverstanddam wanneer die watergehalte aanvaarbaar is. Die gekalibreerde ACRU*Salinity*-model is toe aangepas om die fisiese kenmerke van hierdie belangwekkende ingenieurscenario te weerspieël om stelle stroomvloei en TOS-tydreekse voort te bring wat verder geanaliseer kan word om watervoorraad te verseker in terme van vooraf bepaalde TOS-konsentrasiedrumpels in die Misverstanddam. Deur die gebruik van hierdie spesifieke ingenieursopsie het die ontleding getoon dat ’n boonste perk van 300 mg/ℓ TOS by die Misverstanddam te streng was en dat 450 mg/ℓ waarskynlik meer realisties sou wees.

ACKNOWLEDGMENTS

The research presented in this report would not have been possible without the support and contributions of numerous organisations and individuals. Foremost, I thank the Almighty for allowing me to keep an open mind and bestowing me with the patience to deal with the many challenging periods which were encountered during the study.

I would like to express my sincere gratitude to the following organisations and individuals:

- Professor A H M Görgens for his insightful guidance, knowledge and motivation throughout the study. It was greatly appreciated.
- Mr Andrew Pike for providing the initial training on the use of the standard ACRU model.
- The Water Research Commission for the funding of this study.
- The Department of Water Affairs and Forestry for additional funding which allowed for evaluation of the engineering options as part of the West Coast Study.
- The School of Bioresources Engineering and Environmental Hydrology (SBEEH) of the University of KwaZulu-Natal for performing the many code modifications to the salinity module of ACRU*Salinity*.
- Ms Simone Maharaj and Ms Louise Hayes for performing the many ACRU*Salinity* runs during calibration of the ACRU*Salinity* model.
- All my colleagues at Ninham Shand (Pty) Ltd who assisted in various ways in the completion of the research reported in this study.
- My wife, Shahieda and sons Moegamad Aarif and Mustafa for allowing me the time and providing the support when it was most required.

TABLE OF CONTENTS

Page No

CHAPTER 1: INTRODUCTION 1

1.1 BACKGROUND 1
1.2 ACRU – A BRIEF REVIEW 1
1.3 FOCUS OF THIS STUDY 2
1.4 OBJECTIVES OF STUDY 2
1.5 LAYOUT OF REPORT 2

CHAPTER 2: SALINITY SITUATION OF THE BERG RIVER 4

2.1 SALINITY PATTERNS IN THE BERG RIVER AND PREVIOUS SIMULATIONS 4
2.2 REVIEW OF AVAILABLE DATA SETS AND SIMULATED OUTPUTS OF TDS PATTERNS AT MISVERSTAND DAM 10

2.2.1 Data and model simulation used in the investigation 10
2.2.2 Comparison of flow-weighted monthly TDS series 12
2.2.3 Previously simulated future scenarios 16

2.3 DRYLAND SALINITY RESEARCH FINDINGS 18

2.3.1 Mineralization of Western Cape Rivers (Fourie, 1976) 18
2.3.2 Water and soil quality information for integrated water resource management: The Riviersonderend-Berg River System (De Clercq *et al*., 2005) 18
2.3.3 Research on Berg River water management - Land use impacts on salinity in Western Cape waters (Fey *et al.*, 2008) 19

2.4 DRYLAND SALINITY STATEMENTS FOR THE BERG RIVER 20

CHAPTER 3: MODEL CONCEPTUALISATION 21

3.1 INTRODUCTION 21
3.2 RANGE OF MODEL DEVELOPMENT APPROACHES 22

3.2.1 Stochastic models 23
3.2.2 Deterministic models 23

3.3 DESCRIPTION OF THE ACRU MODELLING SYSTEM 25

3.3.1 ACRU*Salinity* Concepts 28

CHAPTER 4: APPLICATION OF ACRU TO THE BERG RIVER FOR FLOW SIMULATION 44

4.1 INTRODUCTION 44
4.2 DELINEATION OF THE BERG RIVER CATCHMENT 44

4.2.1 Origin to Berg River at Dal Josafat (G1H020) 45

4.2.2 Berg River at Dal Josafat (G1H020) to Berg River at Vleesbank (G1H036) 45
4.2.3 Berg River at Vleesbank (G1H036) to Berg River at Drieheuwels (G1H013) 49
4.2.4 Berg River at Drieheuwels (G1H013) to Berg River at Misverstand Dam (G1R003) 50

4.3 DATA PREPARATION FOR THE ACRU MODEL 52

4.3.1 Preparation of the rainfall data 52
4.3.2 Land-use 60

4.4 FARM DAMS 66

4.4.1 G1H020 to G1H036 69

4.5 FLOW VERIFICATION OF THE ACRU MODEL 71

4.5.1 Objective functions 72
4.5.2 Verification at G1H037 (Krom River at Wellington) 74
4.5.3 Verification at G1H041 (Kompanjies River at De Eikeboomen) 78
4.5.4 Verification at G1H036 (Berg River at Vleesbank) 82
4.5.5 Verification at G1H002/G1H028 (24 Rivers at Drie-Das Bosch) 85
4.5.6 Verification at G1H008 (Klein Berg River at Nieuwkloof) 91
4.5.7 Verification at G1H043 (Sandspruit River at Vrisgewaagd) 93
4.5.8 Verification at G1H013 (Berg River at Drieheuwels) 96
4.5.9 Verification at G1H035 (Matjies River at Matjiesfontein) 97
4.5.10 Simulated naturalised flow sequences 100

CHAPTER 5: APPLICATION OF ACRU*SALINITY* TO THE BERG RIVER FOR SALINITY SIMULATION 102

5.1 INTRODUCTION 102
5.2 APPROACH TO DAILY AND MONTHLY SALINITY CALIBRATIONS 102

5.2.1 Approach to daily TDS calibrations 102
5.2.2 Approach to monthly salinity calibrations 103

5.3 SENSITIVITY ANALYSIS 103

5.3.1 Effect of varying the salt uptake rate (SALTUPT) 104
5.3.2 Effect of varying soil surface layer depth (DEPSS) 106
5.3.3 Effect of varying runoff event contact time (SALTCTIME) 109
5.3.4 Effect of varying the monthly salt saturation (SALTSAT) 111
5.3.5 Summary of sensitivity analysis outcomes 114

5.4 INTER-DEPENDENCE OF SALINITY-RELATED PARAMETERS 114
5.5 SALINITY CALIBRATION OF THE ACRU*SALINITY* MODEL 117

5.5.1 Salinity calibration at G1H037 (Krom River at Wellington) 118
5.5.2 Salinity calibration at G1H041 (Kompanjies River at De Eikeboomen) 121
5.5.3 Salinity calibration at G1H036 (Berg River at Vleesbank) 124
5.5.4 Salinity calibration at G1H043 (Sand Spruit at Vrisgewaagd) 127

5.5.5 Salinity calibration at G1H013 (Berg River at Drieheuwels) 130
5.5.6 Salinity calibration at G1H035 (Matjies River at Matjiesfontein) 133
5.5.7 Salinity calibration at G1R003 (Berg River at Misverstand Dam) 136
5.5.8 Summary of objective function values for salinity calibrations 139

5.6 DISCUSSION 140

CHAPTER 6: EVALUATION OF ENGINEERING OPTIONS FOR SALINITY MANAGEMENT OF THE BERG RIVER 142

6.1 INTRODUCTION 142
6.2 OUTLINE OF THE BERG RIVER DAM AND VOËLVLEI AUGMENTATION SCHEMES 142

6.2.1 The Berg River Dam scheme 142
6.2.2 The Voëlvlei Augmentation scheme 142

6.3 FLOW SCENARIOS AND MANAGEMENT OPTIONS 143

6.3.1 Current Day flow at G1H020 143
6.3.2 Post Berg River Dam flow for G1H020 144
6.3.3 Post Voëlvlei abstraction scheme 146

6.4 SIMULATED FLOWS AT MISVERSTAND DAM 147
6.5 EVALUATION OF MANAGEMENT OPTIONS 147

6.5.1 Spreadsheet model developed for the evaluation of management options 147
6.5.2 Analysis of the salinity impact of a conditional abstraction at Misverstand Dam 148
6.5.3 Analysis of the salinity impact of the VAS on conditional abstraction at Misverstand Dam 150

6.6 DISCUSSION 152

CHAPTER 7: CONCLUSIONS AND RECOMMENDATIONS 153

7.1 CONCLUSIONS 153

7.1.1 Salinity situation of the Berg River 153
7.1.2 ACRU*Salinity* modelling 153
7.1.3 Evaluation of engineering options using ACRU*Salinity* 154

7.2 RECOMMENDATIONS 155

LIST OF TABLES

Table 1 Comparison of Average TDS values at Misverstand Dam 12
Table 2 Classification of hydrosalinity models according to Jewitt's (1998) classification system 23
Table 3 Salinity related parameters for soil surface layer 32
Table 4 Summary of information for calibration sub-catchments 45
Table 5 Irrigated and non-irrigated areas between gauging stations G1H020 and G1H036 65
Table 6 Irrigated and non-irrigated areas between gauging stations G1H036 and G1H013 65
Table 7 Irrigated and non-irrigated areas between gauging stations G1H013 and G1R003 66
Table 8 Coefficients used to relate farm dam capacity to surface area for the catchment between G1H020 and G1H036 70
Table 9 Objective function values for simulated and observed flows at G1H037 77
Table 10 Statistics for simulated and observed flows at G1H041 81
Table 11 Water imported and exported to the catchment gauged by G1H036 (DWAF, 1999) 82
Table 12 Objective function values for simulated and observed flows at G1H036 84
Table 13 Objective functions for simulated and observed flows at G1H002 87
Table 14 Statistics for simulated and observed flows at G1H028 90
Table 15 Objective function values for the Simulated and Observed flows at G1H008 91
Table 16 Objective values for simulated and observed flows at G1H043 95
Table 17 Objective function values for simulated and observed flows at G1H013 97
Table 18 Objective function values for simulated and observed flows at G1H035 99
Table 19 Simulated naturalised MARs 101
Table 20 Sensitivity of daily simulated TDS statistics to variations in the value of SALTUPT (for quickflow) 105
Table 21 Sensitivity of daily simulated TDS statistics to variations in the value of SALTUPT (for baseflow) 106
Table 22 Sensitivity of daily simulated TDS statistics to variations in the value of DEPSS (for quickflow) 107
Table 23 Sensitivity of daily simulated TDS statistics to variations in the value of DEPSS (for baseflow) 108
Table 24 Sensitivity of daily simulated TDS statistics to variations in the value of SALTCTIME (for quickflow) 110
Table 25 Sensitivity of daily simulated TDS statistics to variations in the value of SALTCTIME (for baseflow) 111
Table 26 Sensitivity of daily simulated TDS statistics to variations in the value of SALTSAT (for quickflow) 112
Table 27 Sensitivity of daily simulated TDS statistics to variations in the value of SALTSAT (for baseflow) 113
Table 28 Summary of sensitivity of daily simulated TDS statistics 114
Table 29 Gauges used for the calibration of the Salt Module in ACRUSalinity 117
Table 30 Values of salinity -related parameters used in the Berg River 117
Table 31 Objective functions values for comparison of daily TDS concentrations (May to September) 139
Table 32 Objective function values based on the comparison of monthly TDS loads (May to September) 140
Table 33 Baseflow requirements for the Supplement Scheme 145
Table 34 Environmental baseflow releases (m^3/s) from Berg River Dam based on historical average daily natural inflow (m^3/s) 146
Table 35 Operating rule for the Voëlvlei Augmentation Scheme 147
Table 36 Impact of conditional abstraction: current demands (20 x 106 m^3/a) 149
Table 37 Impact of salinity on the abstraction at Misverstand Dam post BRP and post VAS 150

LIST OF FIGURES

Figure 1 Schematic of gauging stations in the Berg River Catchment up to Misverstand Dam 5
Figure 2 Variation in TDS along the Berg River mainstem 6
Figure 3 Monthly distribution of TDS concentrations at Misverstand Dam 6
Figure 4 TDS load and run-off for tributaries of the Berg (after DWAF, 1993) 8
Figure 5 Seasonal distribution of TDS concentrations (grab samples) on the Matjies River 9
Figure 6 Simulated and observed TDS at Misverstand Dam (DWAF, 2005) 12
Figure 7 Frequency plot of TDS at Misverstand Dam – FLOSAL calibration period (1983 – 1988) (DWAF, 2005) 13
Figure 8 TDS data at Misverstand Dam - including DWAF grab samples (DWAF, 2005) 14
Figure 9 High TDS values at Misverstand Dam - including DWAF grab samples (DWAF, 2005) 14
Figure 10 Exceedence probability plot of TDS at Misverstand Dam - DWAF grab samples only (DWAF, 2005) 15
Figure 11 Exceedence probability plot of TDS at Misverstand Dam - full record periods 16
Figure 12 Frequency plot of simulated TDS at Misverstand Dam - future scenarios (DWAF, 2005) 17
Figure 13 Water quality modelling process, after Chapra (2003) 21
Figure 14 Classification of model approaches (after Jewitt, 1998) 22
Figure 15 The ACRU agrohydrological modelling system : general structure (after Schulze 1995) 26
Figure 16 The ACRU agrohydrological modelling system : concepts (after Schulze 1995) 27
Figure 17 Soil movement within the root zone of the soil profile (after Görgens et al., 2001) 29
Figure 18 Flow diagram for salt addition (extracted and adapted from Teweldebrhan, 2003) 30
Figure 19 Sub-surface salt movement in non-irrigated lands (extracted and adapted from Teweldebrhan, 2003) 38
Figure 20 Flow diagram for salt calculations in reservoirs (after Teweldebrhan, 2003) 39
Figure 21 Salt generation curves (after Ferguson et al., 1994 and extracted from Teweldebrhan, 2003) 41
Figure 22 Sequence of enrichment and mixing processes (after Ferguson et al., 1994 and extracted from Teweldebrhan, 2003) a) instantaneous mixing and b) real world mixing 42
Figure 23 Primary sub-catchments defined for the Berg River Catchment between gauging stations G1H020 and G1H036 47
Figure 24 ACRU system layout for the Berg River Catchment between gauging stations G1H020 and G1H036 48
Figure 25 Primary sub-catchments defined for the Berg River Catchment between gauging stations G1H036 and G1H013 49
Figure 26 ACRU system layout for the Berg River Catchment between gauging stations G1H036 and G1H013 50
Figure 27 Primary sub-catchments defined for the Berg River Catchment between gauging stations G1H013 and G1R003 51
Figure 28 ACRU system layout for the Berg River Catchment between gauging stations G1H013 and G1R003 52
Figure 29 Possible rainfall gauges to be used as the driver rainfall stations in the various primary (distributed) catchments between G1H020 and G1H036 58
Figure 30 Possible rainfall gauges to be used as the driver rainfall stations for the primary (distributed) sub-catchments between G1H036 and G1H013 59
Figure 31 Possible rainfall gauges to be used as the driver rainfall stations for the primary (distributed) sub-catchments between G1H013 and G1R003 60
Figure 32 Land-use used in the VAFS study 61

Figure 33 Extent of coverage of the the WfW aerial photography 62
Figure 34 Land-use coverage for the lower Berg River Catchment 64
Figure 35 Relationship between farm dam surface area and capacity in catchment gauged by G1H008 69
Figure 36 Farm dam catchment boundaries for the Berg River Catchment between gauging stations G1H020 and G1H036 70
Figure 37 Monthly simulated and observed flows at gauging station G1H037 75
Figure 38 Daily simulated and observed flows at gauging station G1H037 76
Figure 39 Daily flow duration curves for simulated and observed flows at G1H037 76
Figure 40 Daily flow duration curves for simulated and observed flows at G1H037 (flow of winter 1990 removed) 77
Figure 41 Rainfall distribution in the Berg River Catchment between gauging stations G1H020 and G1H036 78
Figure 42 Monthly simulated and observed flows at G1H041 79
Figure 43 Daily simulated and observed flows at gauging station G1H041 80
Figure 44 Daily flow duration curves at gauging station G1H041 81
Figure 45 Monthly simulated and observed flows at G1H036 83
Figure 46 Daily Simulated and Observed Flows at Gauging Station G1H036 84
Figure 47 Simulated and Observed Flow duration curves at Gauging Station G1H036 85
Figure 48 Comparison of observed and simulated flows at G1H002 87
Figure 49 Daily flow duration curve for simulated and observed flows at gauging station G1H002 88
Figure 50 Monthly simulated and observed flows at gauging station G1H028 89
Figure 51 Daily flow duration curves for simulated and observed flows at G1H028 90
Figure 52 Simulated and observed monthly flows at gauging station G1H008 92
Figure 53 Daily simulated and observed flows at gauging station G1H008 92
Figure 54 Daily flow duration curves for simulated and observed flows at G1H008 (1977 to 1994) 93
Figure 55 Monthly simulated and observed flows at gauging station G1H043 94
Figure 56 Daily Simulated and Observed Flows at G1H043 95
Figure 57 Flow Duration Curves Simulated and Observed Flows at G1H043 96
Figure 58 Monthly simulated and observed flows at gauging station G1H013 96
Figure 59 Monthly simulated and observed flows at G1H035 98
Figure 60 Daily simulated and observed flows at G1H035 99
Figure 61 Flow duration curves simulated and observed flows at G1H035 100
Figure 62 Variation in quickflow salinity in response to variation in SALTUPT value in the A and B Horizons 105
Figure 63 Variation in baseflow salinity in response to variation in SALTUPT value 106
Figure 64 Variation in quickflow salinity in response to variation in DEPSS 107
Figure 65 Sensitivity of baseflow salinity to variations in DEPSS 108
Figure 66 Sensitivity of quickflow salinity to variations in SALTCTIME 109
Figure 67 Sensitivity of baseflow salinity to variations in SALTCTIME 110
Figure 68 Sensitivity of quickflow salinity to variations in SALTSAT 112
Figure 69 Sensitivity of baseflow salinity to variations in SALTSAT 113
Figure 70 Two-dimensional response surface (objective function = r^2) 115
Figure 71 Two-dimensional response surface (objective function = r^2/coefficient of efficiency) 115
Figure 72 Seasonal distribution of observed (grab sample) TDS concentrations at gauging station G1H037 118
Figure 73 Exceedance of observed and simulated daily TDS at gauge G1H037 119
Figure 74 Daily Simulated and Observed TDS Concentrations at G1H037 120
Figure 75 Comparison of seasonality of simulated and infilled observed TDS values at G1H037 120

Figure 76 Seasonal distribution of observed (grab sample) TDS concentrations at Gauge G1H041 121
Figure 77 Exceedance of observed and simulated daily TDS at gauge G1H041 122
Figure 78 Daily Simulated and Observed TDS Concentrations at G1H041 123
Figure 79 Comparison of seasonality of simulated and infilled observed TDS values at G1H041 123
Figure 80 Seasonal distribution of observed (grab sample) TDS concentrations at gauge G1H036 124
Figure 81 Exceedance of observed and simulated daily TDS at Gauge G1H036 125
Figure 82 Daily Simulated and Observed TDS Concentrations at G1H036 126
Figure 83 Comparison of seasonality of simulated and infilled observed TDS values at G1H036 126
Figure 84 Seasonal variation of observed (grab sample) TDS concentration at gauging station G1H043 127
Figure 85 Exceedance of simulated and observed daily TDS concentrations at G1H043 128
Figure 86 Daily Simulated and Observed TDS Concentrations at G1H043 129
Figure 87 Comparison of seasonality of simulated and infilled observed TDS values at G1H043 129
Figure 88 Seasonal distribution of observed (grab sample) TDS concentration at Gauge G1H013 130
Figure 89 Exceedance of simulated and observed daily TDS concentrations at G1H013 131
Figure 90 Daily Simulated and Observed TDS Concentrations at G1H013 132
Figure 91 Comparison of seasonality of simulated and infilled observed TDS values at G1H013 132
Figure 92 Seasonal distribution of observed (grab sample) TDS concentration at G1H035 133
Figure 93 Exceedance of observed and simulated daily TDS at G1H035 134
Figure 94 Daily Simulated and Observed TDS Concentrations at G1H035 135
Figure 95 Comparison of seasonality of simulated and infilled observed TDS values at G1H035 136
Figure 96 Seasonal distribution of TDS concentration at Gauge G1R003 136
Figure 97 Exceedance of observed and simulated TDS at G1R003 137
Figure 98 Daily Simulated and Observed TDS Concentrations at G1R003 138
Figure 99 Comparison of seasonality of simulated and infilled observed TDS values at G1R003 138
Figure 100 Estimated level of assurance based on a conditional abstraction based on TDS = 300 mg/l (extracted from Cullis and Kamish, 2006) 151
Figure 101 Estimated level of assurance based on a conditional abstraction based on TDS = 450 mg/l (extracted from Cullis and Kamish, 2006) 151

APPENDICES

Appendix A : Example of Rainfall Station Ranking for Primary Sub-catchments

ABBREVIATIONS

ACRU	Agricultural Catchment Research Unit
ARC	Agricultural Research Council
BEEH	Bioresources Engineering and Environmental Hydrology
BRD	Berg River Dam
BRP	Berg River Project
BWP	Berg Water Project
CCT	City of Cape Town
CSIR	Council for Scientific and Industrial Research
DEPSS	Soil Surface Layer Depth
DISA	Daily Irrigation and Salinity Analysis
DSS	Decision Support System
DUL	Drained Upper Limit
DWAF	Department of Water Affairs and Forestry
EC	Electrical Conductivity
FLOSAL	Monthly Hydrosalinity model
GIS	Geographical Information System
HIS	Hydrological Information System
HSPF	Hydrological Simulation Progam - Fortran
IWRM	Integrated Water Resources Management
km^2	Square kilometres
LEACHM	Leaching Estimation and Chemistry Model
MAP	Mean Annual Precipitation
MAR	Mean Annual Runoff
mg	Milligram
mg/l	Milligram per litre
mS/m	Milli Siemens per meter
$x\ 10^6\ m^3$	Million Cubic metres
Mm^3	Million Cubic metres
MMR	Mean Monthly Runoff
NetRFL	Net Rainfall
NLCDP	National Landcover Database Project
r^2	Coefficient of Determination
RESCON	Reservoir Constant
RESEXP	Reservoir Exponent
SALTCTIME	Runoff Event Conatct Time
SALTSAT	Salt Saturation Parameter
SALTUPT	Salt Uptake Rate Constant
SAWS	South African Weather Services
SWAT	Soil and Water Assessment Tool

TCTA	Trans Caledon Tunnel Authority
TDS	Total Dissolved Salts
VAFS	Voëlvlei Augmentation Feasibility Study
VAS	Voëlvlei Augmentation Scheme
WCDM	West Coast District Municipality
WCSA	Western Cape Systems Analysis
WEMCO	West Coast Monitoring Committee
WfW	Working for Water
WRC	Water Research Commission
WQIS	Water Quality Information System
WQT	Water Quality TDS model
WTW	Water Treatment Works

CHAPTER 1: INTRODUCTION

1.1 BACKGROUND

The lower Berg River has a long history of salinity concerns (Fourie and Görgens, 1977) and with the construction of the Berg River Dam (BRD) in the upper reaches of the river the deterioration in water quality with respect to Total Dissolved Salts (TDS) may be exacerbated.

The possible deterioration in water quality at Misverstand Dam was addressed in the *Western Cape System Analysis* (WCSA) study initiated by the Depertment of Water Affairs and Forestry (DWAF) where the monthly flow-weighted TDS concentrations at Misverstand Dam (G1R003) were simulated based on the assumption that the Berg River Dam had been constructed (DWAF, 1993). The major short-coming of this study, however, was that the TDS concentrations were simulated on a monthly basis and therefore lacked the required daily variation to fully describe the TDS behaviour for a fast responding river such as the Berg River.

To address this concern, a Water Research Commission (WRC) project was initiated in 2003 in which the newly-developed salinity module of the ACRU*Salinity* model would be configured for the Berg River Catchment. This model had previously been configured and calibrated for the Mkhomazi Catchment (Teweldebrhan, 2003) which has low TDS concentrations and it was necessary to ascertain whether comparable TDS values could be simulated in the Berg River where TDS concentration could rise to well above 1 000 mg/l in certain tributaries.

1.2 ACRU – A BRIEF REVIEW

This study employed the Agricultural Catchment Research Unit (ACRU) model (Schulze, 1995), enhanced with salinity modelling functionality, for the simulation of daily flow and TDS concentrations from the sub-catchements comprising the Berg River basin. The ACRU model is a daily rainfall-runoff model which compartmentalizes rainfall into the various components of runoff, taking into consideration factors such as evaporation, interception losses and landuse, etc. The salinity module of ACRU, incorporated in the ACRU*Salinity* version of the model, was developed by Teweldebrhan (2003) and assumes that salt generation in the catchment follows a first order rate of production.

1.3 FOCUS OF THIS STUDY

This study will focus on the application of the salinity module of ACRU*Salinity* (Teweldebrhan, 2003 and Teweldebrhan *et al*., 2003) to the Berg River Catchment in the Western Cape Province of South Africa, to quantify the potential effect on the salinity in the lower Berg River as a result of the Berg River Dam. It forms part of the follow-up study to the WRC project commissioned in 1997, in which hydrodynamic and water quality river (DUFLOW, STOWA/EDS, 1998) and reservoir (CE-QUAL-W2, Cole and Wells, 2001) models were integrated into a Water Quality Information System (WQIS) to support Integrated Water Resources Management (IWRM).

The version of ACRU*Salinity* used in this study is "v1.2.5".

1.4 OBJECTIVES OF STUDY

The objectives of this study were:

- To improve the functionality of the ACRU*Salinity* model
- To configure the ACRU*Salinity* model for the Berg River Catchment, where salinity problems are known to exist
- To verify the model's water quantity component and to calibrate the salinity related parameters of the salinity module
- To perform sensitivity analyses of the salinity-related parameters
- To test various engineering options using the configured model, and
- To assimilate the necessary database to complete the aforementioned tasks

1.5 LAYOUT OF REPORT

The remainder of the report consists of the following chapters:

Chapter 2 describes the salinity situation in the Berg River and highlights the reasons why it was necessary to configure a daily water quality model, such as ACRU*Salinity* for this catchment.

Chapter 3 describes the range of approaches that can be employed in the development of water quality models; including a table classifying commonly used models in South Africa. Finally, the scientific principles of the salinity module used in ACRU*Salinity* are presented.

Chapter 4 presents the application of the ACRU model to the Berg River for flow verification. In particular, this chapter will describe data preparation and flow verifications.

Chapter 5 presents the sensitivity analyses that were performed for the salinity-related parameters of the salinity module of the ACRU*Salinity* simulation model. The results of the interdependency tests performed on the salinity-related parameters are also presented. The chapter is then concluded with the outputs from the salinity calibration of the ACRU*Salinity* model.

Chapter 6 describes the application of the ACRU*Salinity* model to test various engineering options relating to the operation of the Berg River system to ameliorate the potential deterioration in water quality with respect to TDS in the lower Berg River (Misverstand Dam).

Chapter 7 presents the conclusions and recommendations drawn from the study.

CHAPTER 2: SALINITY SITUATION OF THE BERG RIVER

2.1 SALINITY PATTERNS IN THE BERG RIVER AND PREVIOUS SIMULATIONS

The possible deterioration in water quality at Misverstand Dam was evaluated in the Western Cape System Analysis (WCSA) (DWAF, 1993) where the monthly flow-weighted total dissolved salts (TDS) concentrations at Misverstand Dam (G1R003) were simulated based on the assumption that the Berg River Dam had been constructed (see **Figure 1** for the layout of the Berg River Catchment).

A possible short-coming of the approach used in the WCSA, however, was that the model had been calibrated using only the monthly salt loads from the various catchments and as a result, lacked the required intra-monthly variation of TDS concentrations necessary to address water quality in the Berg River. It was previously shown (Fourie and Görgens, 1977 and DWAF, 2005) that two peaks in TDS concentrations occurred in the Lower Berg River, *viz.* the summer peak which is mostly associated with the irrigation return flows and the winter peak which is associated with the mobilisation of salts from the catchment, the latter being partially natural and partially caused by dryland agriculture. The variation in TDS concentrations along the Berg River mainstem is depicted in **Figure 2** which shows a gradual increase in TDS from the Berg River Dam site (G1H004) to immediately below Misverstand Dam (G1H031). The graph is based on DWAF TDS grab sample data. This increase in TDS concentration could be attributed to the contribution of the salt loads from the very saline tributaries, *viz* Sandspruit River, Matjies River and the Moorreesburg Spruit.

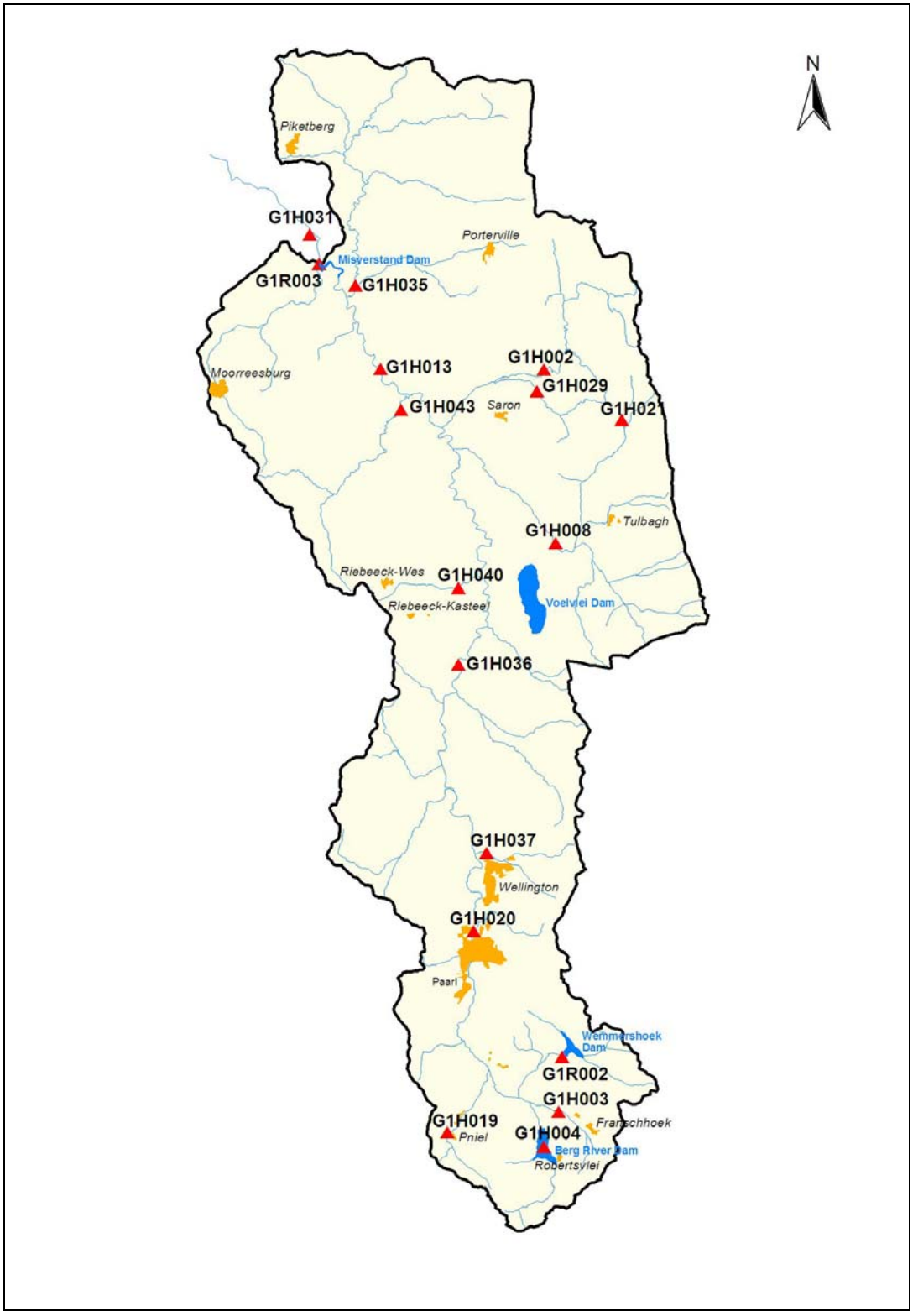

Figure 1 Schematic of gauging stations in the Berg River Catchment up to Misverstand Dam

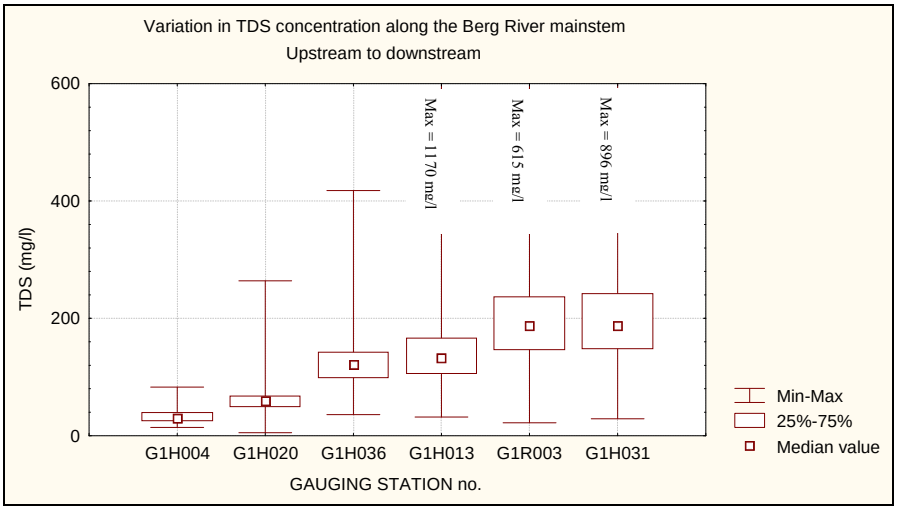

Figure 2 Variation in TDS along the Berg River mainstem

It is usually expected in semi-arid winter-rainfall catchments that the highest concentration of salts will occur in summer when the flow is made up almost entirely of irrigation return flows. At Misverstand Dam, however, this is not true and high concentrations of TDS are also experienced during the winter months. This phenomenon is depicted in **Figure 3**, in which month 1 is January and month 12 is December.

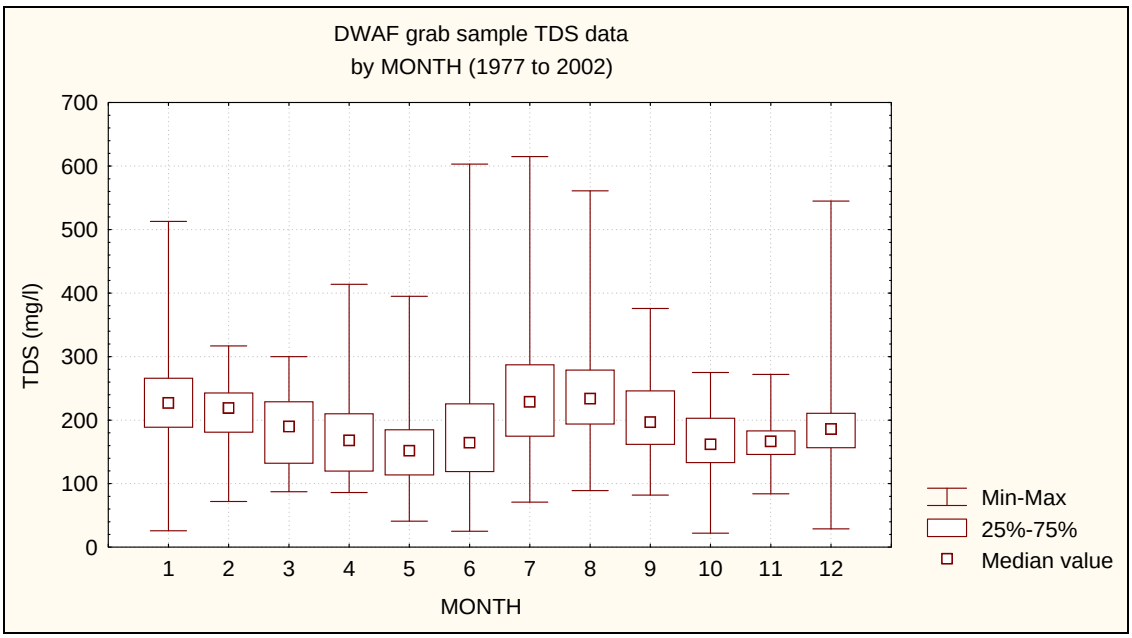

Figure 3 Monthly distribution of TDS concentrations at Misverstand Dam

Misverstand Dam (G1R003) on the Berg River provides a storage facility for the abtraction of drinking water to the Withoogte treatment works. Treated water is then supplied from here to the

greater West Coast region. TDS concentrations of up to 450 mg/l are acceptable for domestic use (DWAF, 1996). Saldanha Steel and other industries in the Saldanha Bay area also rely on water from Misverstand Dam for their evaporative cooling system. It was noted at a meeting (12 December 2001) at the DWAF's offices in Bellville that abstracted water with a TDS concentration of 250 mg/l could be used for four cycles while water with a TDS concentration of 500 mg/l could be used for only two cycles.

Much of the dryland agriculture in the Berg River is practiced on soils which spread over the Malmesbury Shale geological formation and these soils are almost always associated with high salt concentrations. Flügel (1995) explains that the dryland salinity is initiated by clearing the deep rooting natural vegetation which causes the natural groundwater table to rise. He concluded, after intensive sampling in the Sandspruit river catchment, that the bulk of the mobilised salt was delivered by groundwater and interflow from the weathered shale and soils in the catchment. A more in depth discussion on historical and current research findings as it relates to dryland salinity is presented in **Section 2.3** of this report.

The grab sample data show an increase in TDS over the winter months (months 5- 8) which is contrary to expectations, as it is assumed that enough fresh water is supplied by winter rainfall to cause a substantial dilution of salts washed out from the more saline catchments. The pulse of TDS in mid-to late-winter is most likely caused by the infiltrating excess rainfall in the Malmesbury Shale dominated profiles of the middle to Lower Berg catchment which mobilises weathering-related salt loads. This TDS pulse is further augmented by tillage practices in the dryland grain farming areas during the preceding summer. Between gauging stations G1H036 and G1R003 and based on a 1998 level of development, 1 725 km^2 of the sub-catchment was under dryland cultivation while only 159 km^2 was irrigated (DWAF, 1999).

DWAF (1993) showed that between gauging stations G1H036 and Misverstand (see **Figure 4**), the biggest TDS loads are contributed by the Matjies River (G1H035) and the Sandspruit River (G1H043). As an example, the TDS load input to the Berg mainstem for the 1988 hydrological year is depicted in **Figure 4**.

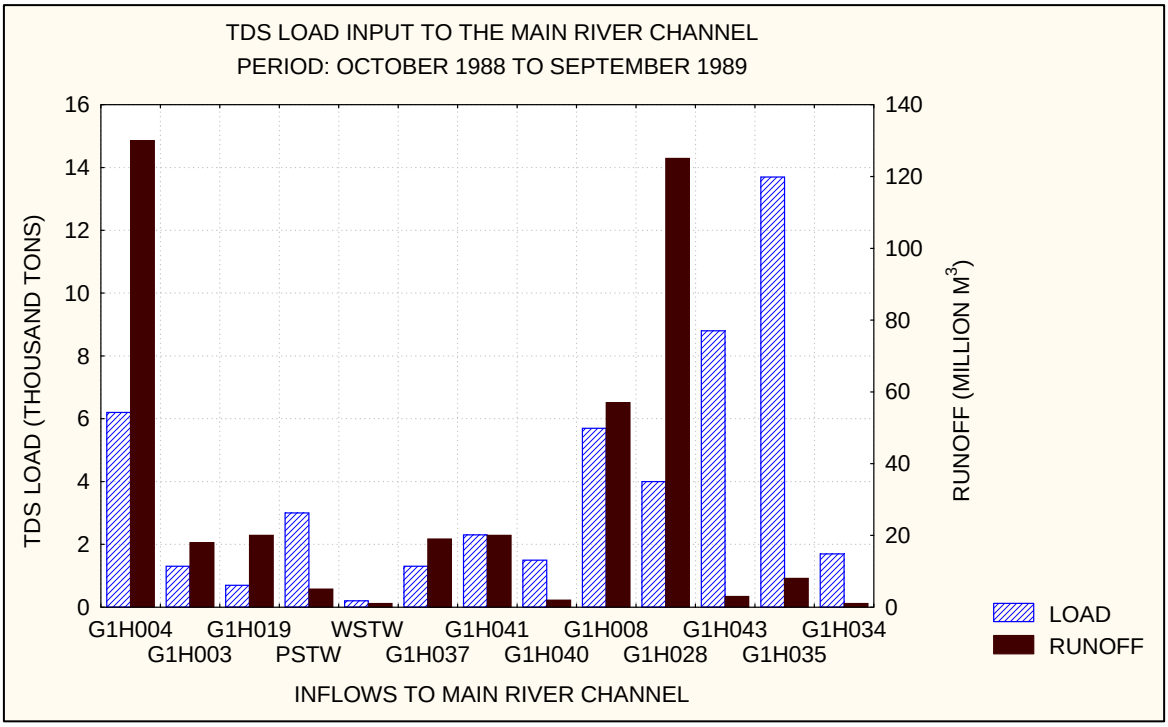

Figure 4 TDS load and run-off for tributaries of the Berg (after DWAF, 1993)

From **Figure 4** it can be seen that the flows contributed by the Matjies (G1H035) and Sandspruit (G1H043) rivers are small in comparison to their loads, indicating that high concentrations could be expected in these rivers. The monthly distribution of the TDS grab samples collected from the Matjies River and depicted in **Figure 5** shows a marked increase in TDS concentration over the winter months. These high concentrations are also accompanied by higher flows that lead to high TDS loads. Although fairly high concentrations also occur during the dry summer months, the resultant contribution to the mainstem, in terms of the TDS load, is insignificant as the Matjies River is non-perennial.

Based on the above argument, it is reasonable to assume that the TDS load contributed by the Matjies (and probably the Sandspruit) would have a marked effect on TDS distribution at Misverstand Dam – especially during winter when these loads are mobilised.

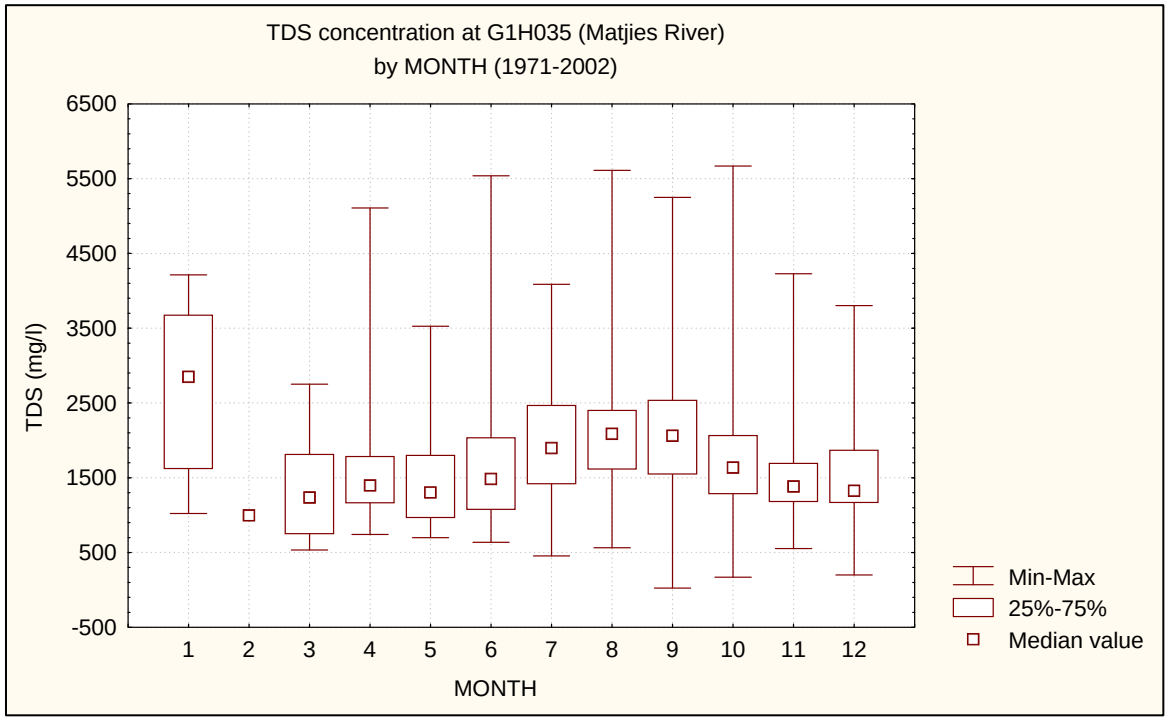

Figure 5 Seasonal distribution of TDS concentrations (grab samples) on the Matjies River

Previous concerns with the modelling undertaken in the WCSA, related to the phenomena that higher TDS in the Lower Berg River was actually associated with the wet winter months, when sufficient flow should be available for dilution and that the storage of fresh water in the Berg River Dam would of necessity result in a further deterioration with regard to TDS at Misverstand Dam. It was also added that the approach of focusing on the winter months in the pre- and post-construction scenario analysis was not adopted in the WCSA.

During the detailed design stage for the Berg River Dam DWAF commissioned several additional reports focusing specifically on the TDS at Misverstand Dam. These reports were prepared by the author and comprised the following:

I. *Review of Observed and Simulated TDS Patterns at Misverstand Dam, Berg River* – Unpublished DWAF report (DWAF, 2005). Prepared by Ninham Shand, September 2005. NS Report no. 3285/6950.

II. *Updating of FLOSAL Salinity Parameters for the Berg River* - Unpublished DWAF report (DWAF, 2005(1)). Prepared by Ninham Shand, September 2005. NS Report no. 4032/6950.

III. *Review of Dr Fourie's Calculations of Projected TDS concentrations at Misverstand Dam as a Result of the Berg River Dam* - Unpublished DWAF report (DWAF, 2005(2)). Prepared by Ninham Shand, September 2005. NS Report no. 3828/6950.

A specific recommendation of **Report no. II** above was that daily salinity modelling be undertaken with the ACRU*Salinity* model (Teweldebrhan, 2003 and Teweldebrhan *et al.*., 2003) based on the fact that the monthly models were considered to be unable to capture single rainfall-runoff events which could lead to high TDS concentrations in the run-off generated.

Based on the preceeding discussion, the focus was placed on the highly saline catchments and the ability of the model to capture the high TDS concentrations during the wet winter months. It should be noted that salinity calibrations were only undertaken at gauges where a sufficient number of grab samples were available.

In **Chaper 4** the flow verification and salinity calibrations of the ACRU*Salinity* model, undertaken for the Berg River at the various gauges are described. However, in the rest of this Chapter, an overview of the salinity patterns and earlier attempts to simulate these patterns at Misverstand Dam are presented.

2.2 REVIEW OF AVAILABLE DATA SETS AND SIMULATED OUTPUTS OF TDS PATTERNS AT MISVERSTAND DAM

At a meeting held on the 12th December 2001, to discuss the potential water quality impacts of the Berg River Dam, it was noted by certain stakeholders that, according to the information available to them, the salinity at Misverstand Dam had generally been higher in recent years than had been shown in the FLOSAL hydrosalinity modelling exercise, which had been undertaken as part of the Western Cape System Analysis Study, prior to the decision to construct the dam (DWAF, 1993(2)). To examine these claims, it was decided that a comparison of available TDS information at Misverstand Dam should be undertaken.

2.2.1 Data and model simulation used in the investigation

Two sets of flow-weighted monthly TDS series at Misverstand Dam were considered, namely:

- TDS series prepared before December 2001 by the late Dr Martin Fourie, formerly of the Council for Scientific and Industrial Research (CSIR) and member of the West Coast Monitoring Committee (WEMCO), covering the period 1974 to 2001.

- TDS series prepared in 2005 by the author from data collected by DWAF as grab samples at Misverstand Dam (G1R003).

The abovementioned TDS series were also compared with outputs from the FLOSAL model used in the Western Cape System Analysis (DWAF, 1993). FLOSAL monthly flow-weighted TDS output was available from 1927 to 1988 for irrigation, with water use conditions and return flows set at a 1988 level of development (i.e. conditions that existed during 1988).

The TDS series prepared by Dr Fourie was made up of monthly flow-weighted average TDS values. The values up to 1979 were calculated from daily TDS measurements and daily flows while the values from 1980 onwards were aggregated from DWAF electrical conductivity (EC) measurements (in mS/m), converted to TDS values (in mg/l) using a scaling factor of 6 (personal communication with Dr Fourie), collected as grab samples on a weekly basis and combined with daily observed flows.

For the TDS series generated by the author, DWAF grab sample data collected on a weekly basis, was used. Where TDS values had not been chemically analysed, a scaling factor of 5.3 (obtained from the best straight line fit between EC and TDS) was used to convert EC (in mS/m) to TDS (in mg/l). This data was supplied by the DWAF from their Hydrological Information System (HIS) national database. The grab sample TDS concentrations were subsequently infilled, through a daily infilling procedure based on a rolling forwards regression of daily flow against TDS, to provide monthly flow-weighted TDS values. Infilling of DWAF grab sample data was done using an infilling routine developed for the Vaal Dam Salinity Study and described by Herold and Görgens (1991). This routine creates a synthetic daily TDS series in which the observed values are imbedded. Daily concentration is converted to daily load by multiplying it by the observed total daily flow volume. The daily loads are then aggregated to a monthly load and divided by the total monthly flow volume to create a flow-weighted monthly TDS. Unfortunately, the infilling method creates daily TDS values that remain almost constant where ***large gaps*** in the grab sample data exist. This results in false monthly flow-weighted TDS values during those large gaps.

The average values of the two "raw" TDS data sets from which the above series was generated are compared in **Table 1**.

Table 1 Comparison of Average TDS values at Misverstand Dam

Data Set	Start Date	End Date	Average TDS (mg/l)
Dr J M Fourie's average TDS, based on grab samples of EC (mS/m) converted to TDS (mg/l)	May 1974	Aug 2001	248
DWAF TDS grab samples (992 samples)	Feb 1977	Aug 2001	189

While both raw TDS sets go back as far as the 1970s, it was found that from December 1978 to April 1983 large gaps exist in the DWAF grab sample data. The flow-weighted values were therefore falsely stable over this period as described above, and were not suitable for this investigation. Hence the comparison of a flow-weighted monthly TDS series could only be done from April 1983 to August 2001.

2.2.2 Comparison of flow-weighted monthly TDS series

A comparison of the flow-weighted monthly TDS presented by Dr. Fourie, the flow weighted DWAF series and the results of the original FLOSAL modelling performed as part of the WCSA study are given in **Figure 6**. From **Figure 7** it is evident that the series presented by Dr. Fourie tended to be higher than the DWAF series.

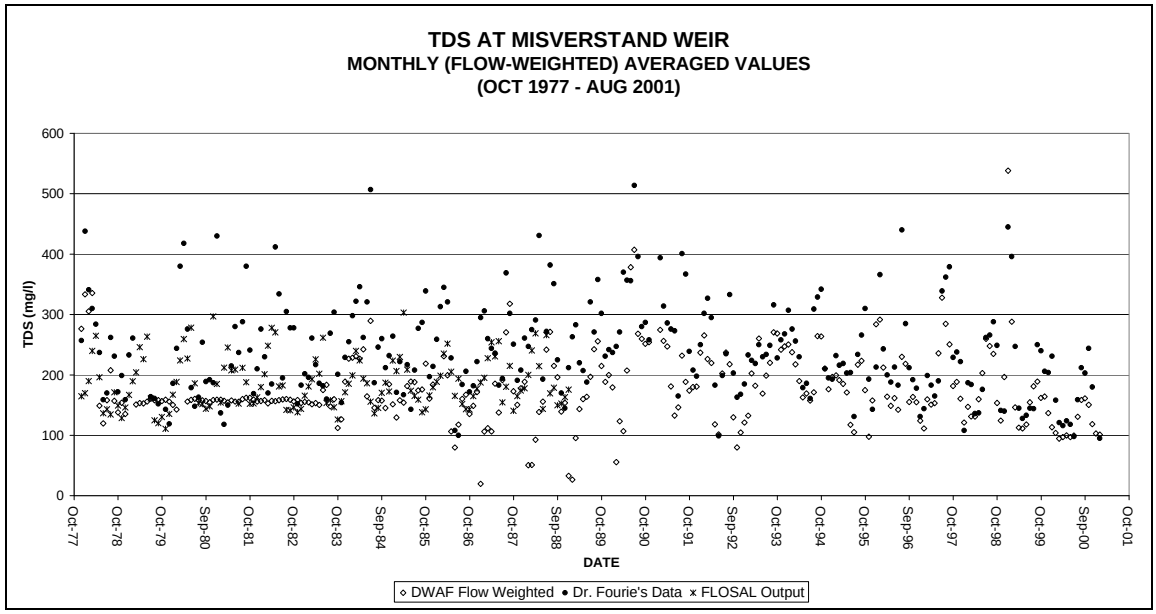

Figure 6 Simulated and observed TDS at Misverstand Dam (DWAF, 2005)

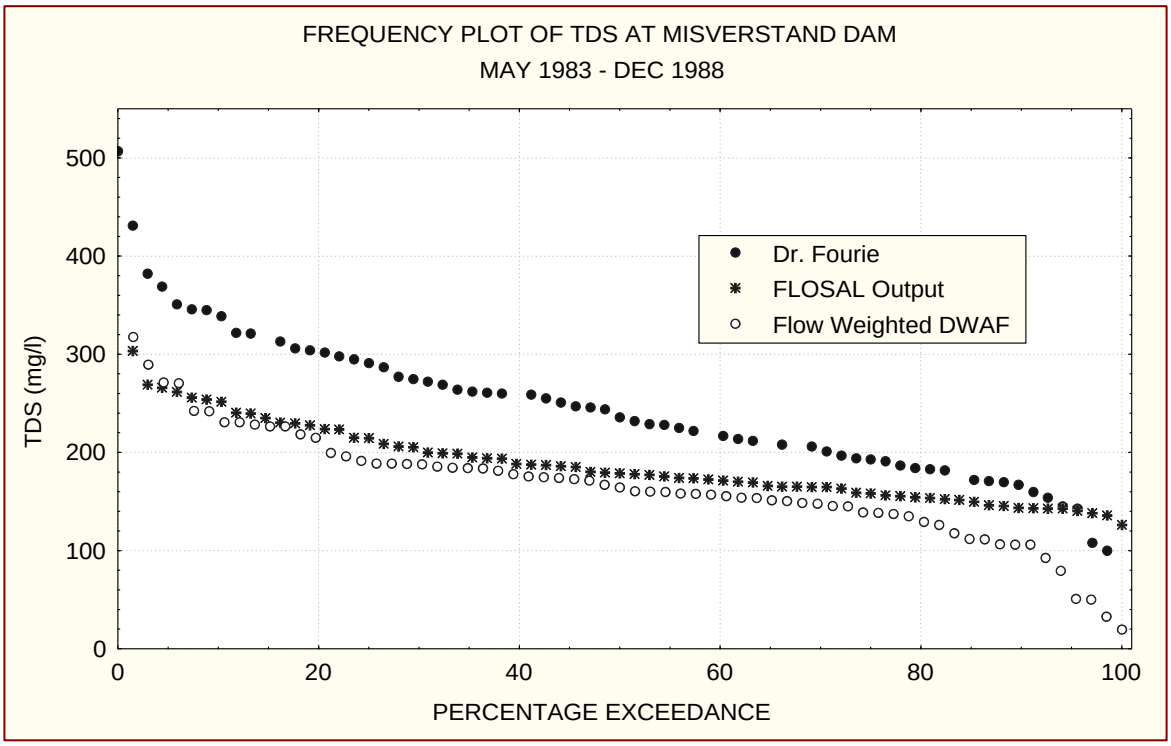

Figure 7 Frequency plot of TDS at Misverstand Dam – FLOSAL calibration period (1983 – 1988) (DWAF, 2005)

The FLOSAL output compared favourably with the DWAF flow-weighted series. Nevertheless, it could be postulated that the reason for the lower probabilities of higher values in the DWAF flow-weighted data could be due to the infilling process. To test this postulation, the raw DWAF grab sample data was compared with the flow-weighted DWAF TDS values and Dr Fourie's flow-weighted series in **Figure 8**. As expected, the DWAF grab samples plotted higher than the flow weighted data, but were still not as high as indicated by Dr Fourie's flow-weighted values. As stated earlier, this can be partly attributed to the fact that Dr Fourie only worked with ECs and used a scaling factor of 6 to convert from EC to TDS, whereas the DWAF flow-weighted monthly TDS series comprised TDS values based on full chemical analysis, while a factor of 5.3 was applied to the DWAF data on occasions where separate TDS readings where not available.

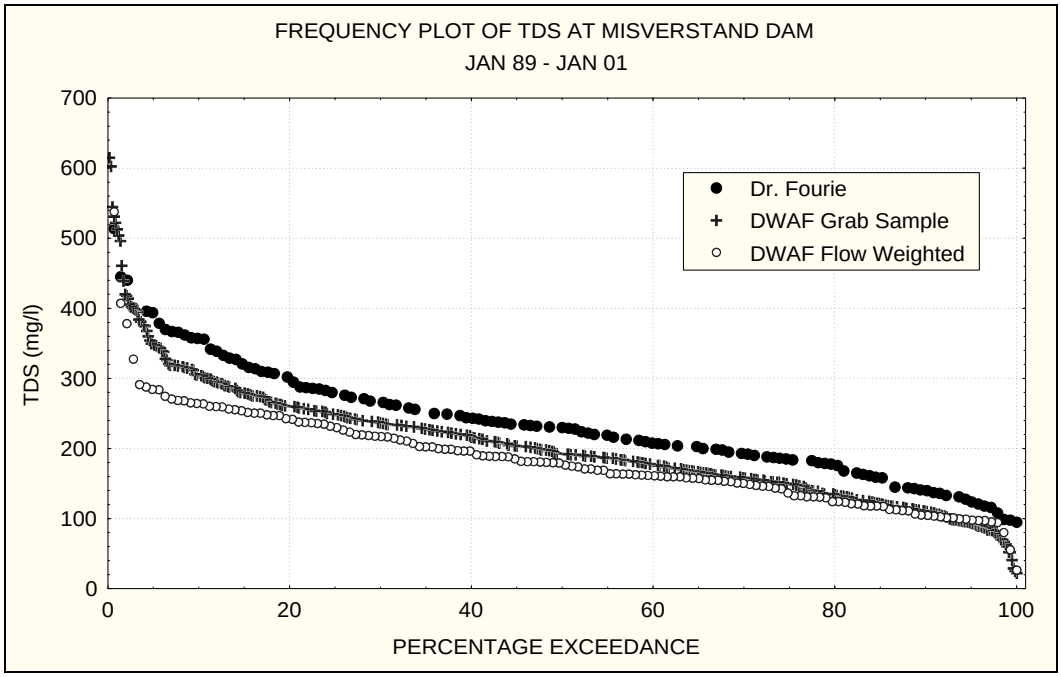

Figure 8 TDS data at Misverstand Dam - including DWAF grab samples (DWAF, 2005)

The periods of concern to the industrial water users are those values with high TDS concentration and a low probability of occurrence. This high-end portion of the exceedance probability plot is enlarged in **Figure 9**. This figure shows that the DWAF grab samples exceeded the monthly average TDS values of Dr Fourie for approximately 3% of the time, but were markedly lower than Dr Fourie's values for the rest of the time.

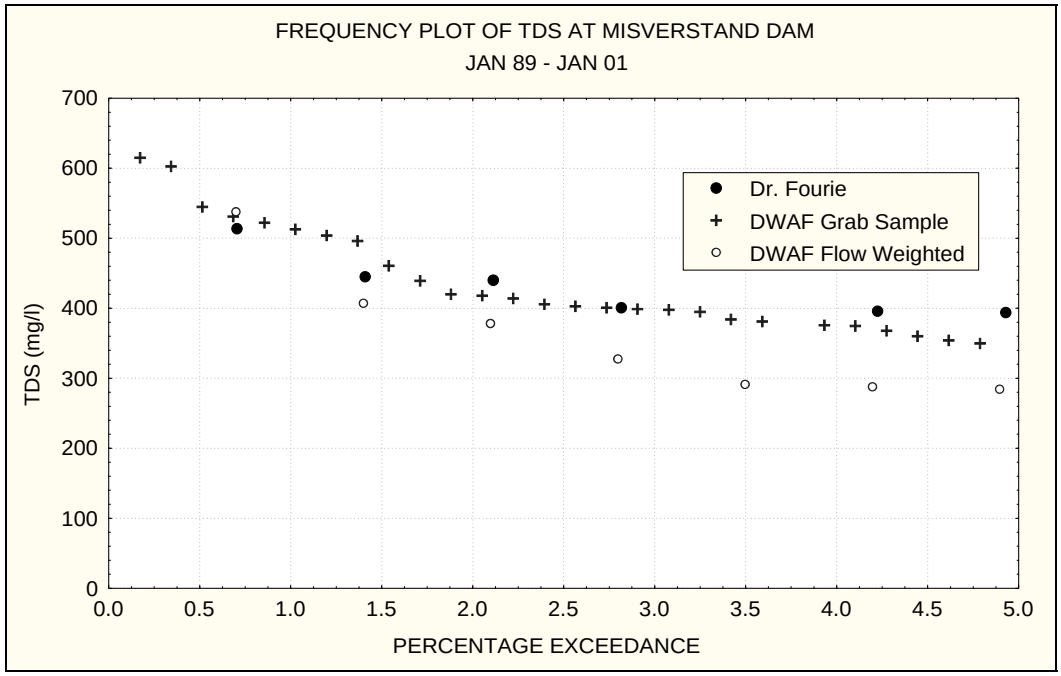

Figure 9 High TDS values at Misverstand Dam - including DWAF grab samples (DWAF, 2005)

DWAF grab sample data is available from 1977 and a frequency plot of the entire period of sampling may be more representative of reality, given the longer period of climatic variations that is included in the frequency counts. **Figure 10** shows the frequency plot for the entire period of available DWAF data.

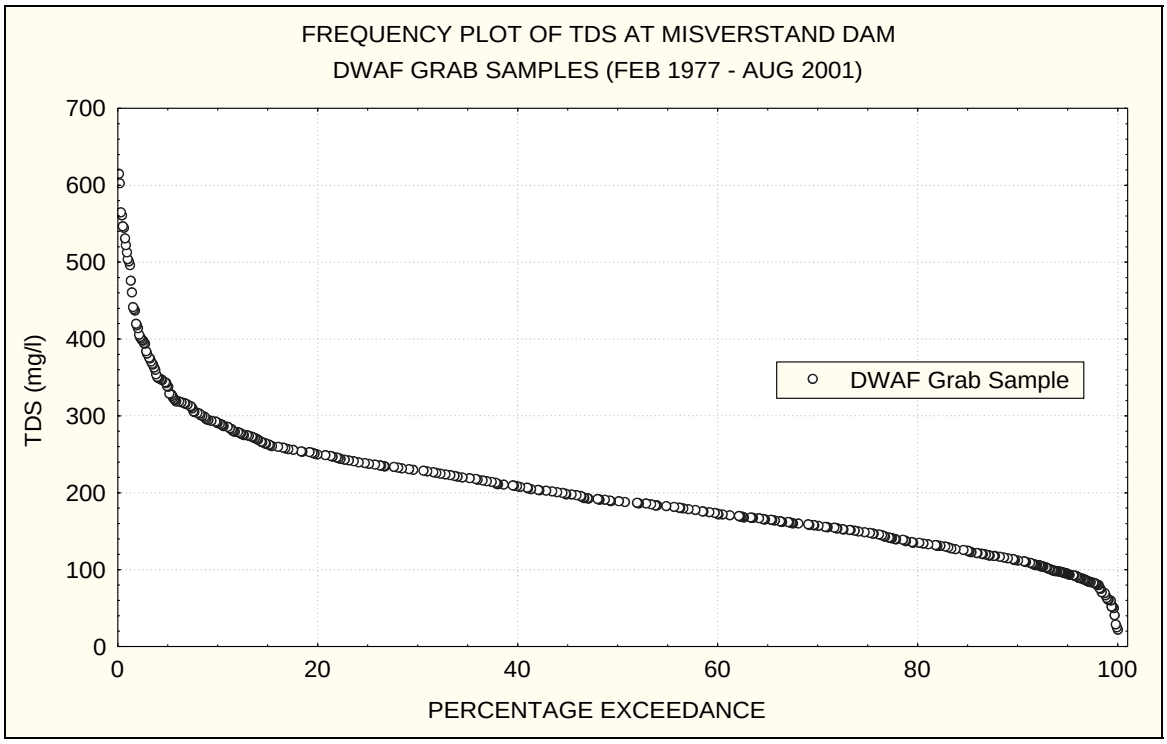

Figure 10 Exceedence probability plot of TDS at Misverstand Dam - DWAF grab samples only (DWAF, 2005)

Figure 10 shows that 20% of the grab samples had concentrations above 250 mg/l and that 500 mg/l was exceeded by less than 1% of the samples. In the absence of daily data it is difficult to say whether TDS concentrations actually escalated or declined during two successive grab samples, which are typically a week apart. The possibility of sustained high TDS concentrations occurring cannot be ruled out. This is particularly evident between 23 December 1998 (545 mg/l) and 6 January 1999 (513 mg/l) when three grab samples in the aforementioned period had TDS values of over 500 mg/l.

Figure 11 depicts the frequency plot of the FLOSAL output as well as the respective monthly flow-weighted TDS values over their respective full periods. Since the DWAF flow-weighted data is constructed from the DWAF grab sample data, it is necessary to exclude the periods in the flow-weighted sequence that correspond with the large gaps in the grab sample data.

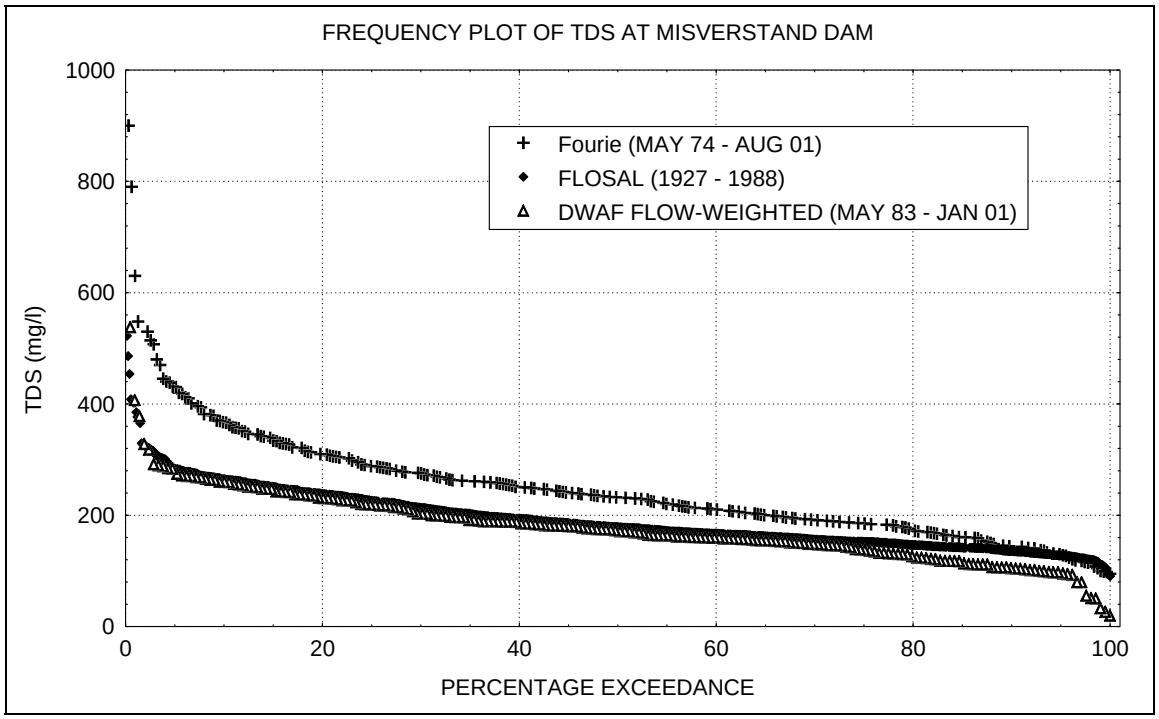

Figure 11 Exceedence probability plot of TDS at Misverstand Dam - full record periods

It can be seen that Dr Fourie's flow-weighted monthly TDS values again exceeded the DWAF flow-weighted values while the FLOSAL output compared favourably with the DWAF values, being slightly conservative throughout the full range of TDS values.

2.2.3 Previously simulated future scenarios

Further FLOSAL simulations, assuming projected irrigation development for 2010, were performed as part of the Skuifraam Feasibility Study (DWAF, 1997). The scenarios covered in that work were as follows:

- **Optimistic scenario** - assumed that newly developed areas would not generate new salt loads, and that increased irrigation return flow salinities would mainly be a function of consumptive use by crops.

- **Worst scenario** - assumed that new areas would generate 150 tons of new or residual salt per million cubic metres of water applied.

The 'worst' scenario is based on the interpretation of field data collected by Dr Martin Fourie in the 1970s (CSIR, 1976). In both the above scenarios, it was assumed that Skuifraam Dam had

been constructed and that Misverstand Dam had been raised (pumping from Skuifraam Supplement Scheme was not included).

Frequency plots of TDS, for both future scenarios (2010) as well as the then "present-day scenario" (i.e. dating from 1988) are depicted in **Figure 12**.

According to the above analysis, if the 'worst' scenario should be realised, salinities of 450 mg/l may be exceeded for 30% of the time at Misverstand Dam. In the 'optimistic' scenario, 450 mg/l might be exceeded for only 2% of the time, whereas, for the 1988-level of development this exceedence is less than 1% of the time. It is clear from **Figure 12**, that growth in irrigation could have a severe effect on the TDS concentrations at Misverstand Dam and that measures to reduce this effect should be instituted at an early stage in the planning of any development in the catchment.

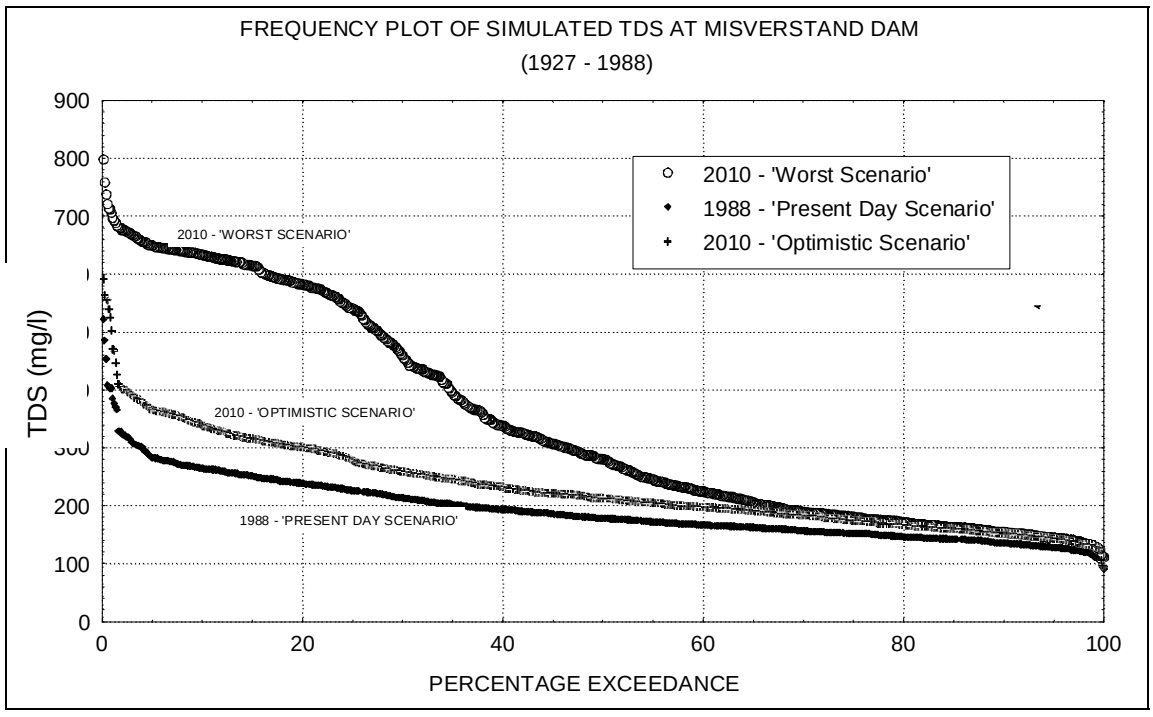

Figure 12 Frequency plot of simulated TDS at Misverstand Dam - future scenarios (DWAF, 2005)

2.3 DRYLAND SALINITY RESEARCH FINDINGS

Several South African studies focusing on catchment scale salinity generation have been undertaken in the past and a summary of the pertinent findings from selected studies are presented below:

2.3.1 Mineralization of Western Cape Rivers (Fourie, 1976)

Fourie analysed weathered and unweathered samples of the Malmesbury shale and found that the unweatherd shale had insignificant quantities of sodium (on average 13 mg/kg to 22 mg/kg) and chloride (on average 5 mg/kg to 8 mg/kg), whereas the weathered material contained large quantities of both sodium (on average 465 mg/kg to 1 008 mg/kg) and chloride (on average 605 mg/kg to 962 mg/kg). He concluded that a secondary mechanism was responsible for the enrichment of the weathered shale and hypothesised that this could be attributed to the inundation of the area by sea water during the *Late Tertiary* (i.e. 38 to 1.6 million years ago) and the subsequent adsorption of the salt molecules onto the weathered shale or accumulation thereof in the interstitial spaces of the weathered material. He further proposed that this salt had remained *in-situ* until conditions favouring their leaching were induced. Several other hypotheses relating to the secondary enrichment of the weathered shale were also discussed in that thesis.

2.3.2 Water and soil quality information for integrated water resource management: The Riviersonderend-Berg River System (De Clercq *et al*., 2005)

In work by (De Clercq *et al*., 2005), another possible origin of the salt content in the catchments giving rise to the highly saline tributaries was mentioned. It stated that dust transported by prevailing wind and rain could possibly have deposited salts over millions of years. Salt fallout from this source had previously been estimated (Jurinak, 1990) at 100 to 200 $kg.ha^{-1}.a^{-1}$ in those parts of the catchment that are close to the ocean, with the effect dissipating with increased distance from the sea.

Additionally, the study found that the saline runoff from the dryland areas had a significant impact on the runoff quality from irrigated lands. It could, however, not quantify the effect on the salt budget of changing from the natural Renosterveld to dryland wheat cultivation. A specific recommendation from this study was further investigation into the mechanism of dryland salinity mobilization.

2.3.3 Research on Berg River water management - Land use impacts on salinity in Western Cape waters (Fey *et al.*, 2008)

In a pilot study (Fey and De Clercq, 2004), preceeding this one, it was estimated that dryland salinity had a larger influence on the river salinity than any other source in the catchment. Their study initially hypothesised that the mechanism of soil salinisation was similar to the Australian scenario, where salinisation was caused by deep-rooted natural vegetation being cleared to make way for shallow-rooted dryland crops. This subsequently results in the rise of saline groundwater.

As part of the project the total evaporation (i.e. evaporation plus transpiration) from the natural Renosterveld and a wheat field was determined. The study found that the average daily total evaporation was 1 $mm.day^{-1}$ higher for the Resnosterveld and therefore supported (although not overwhelmingly) the Austalian approach in defining dryland salinity.

The study also found that tillage practices, in part, also contributed to the mechanism of salt mobilisation. For example, it was found that shallow tillage before wheat planting caused a reduction in runoff and runoff salinity. No "first flush" effect was observed and this was attributed to the salt quantities being below the surface.

Througout the soil profiles, salinity concentrations were found to be higher in the top-soil during the drier summer months while the reverse was observed during the wetter winter months. This effect was attributed to the increased dissolution and mobilization of salts with the increased availability of water. This was particularly evident at the sites where the soil overlies the Malmesbury Shales.

Final conclusions from the study were that the salts in the catchment are probably derived meteorically (and not by previous inundation by the sea) and that the current rate of salt discharge could persist for decades or possibly a century or two. The study proposes that methods of decreasing discharge from these catchments should be considered due to the large volumes of water that would need treatment in the case of an end-of-pipe treatment option being used.

2.4 DRYLAND SALINITY STATEMENTS FOR THE BERG RIVER

Based on the preceeding discussions in this Chapter the following statements concerning the salinity mobilization mechanisms in the Berg River can be made:

i) Although many hypotheses on the origin of the salinity-enriched Malmesbury Shales exist, a definitive statement in this regard is not possible at this stage. The effect of these salt-enriched Shales on runoff salinity, however, cannot be disputed.

ii) Runoff salinity in the sub-catchments overlying the Malmesbury Shale increases during the winter months when sufficient rainfall has occurred to dissolve and mobilize the salts in the deeper soil layers. This indicates that specific mechanisms for salt generation in these sub-catchments should be considered in addition to the evapo-concentration effect.

iii) The effect of tillage practices and change in crop types on the salinity generation and mobilization potential of soils overlying the Malmesbury Shale has not been formulated mathematically. This effect should, however, be acknowledged during the modelling process.

CHAPTER 3: MODEL CONCEPTUALISATION

3.1 INTRODUCTION

Chapra (2003) points out that a wide range of models have been developed over the last 75 years for modelling the fate of pollutants in receiving waterbodies. More recently, these models have been integrated with catchment models to provide comprehensive tools for predicting the effects of human activities on water quality. He warns, however, that the proliferation of these models would necessitate the model user to become extra cautious when applying them. Therefore, he proposes a roadmap (**Figure 13)** which should be followed in the lead-up to the implementation of an installed water quality model within the framework of a decision support system (DSS).

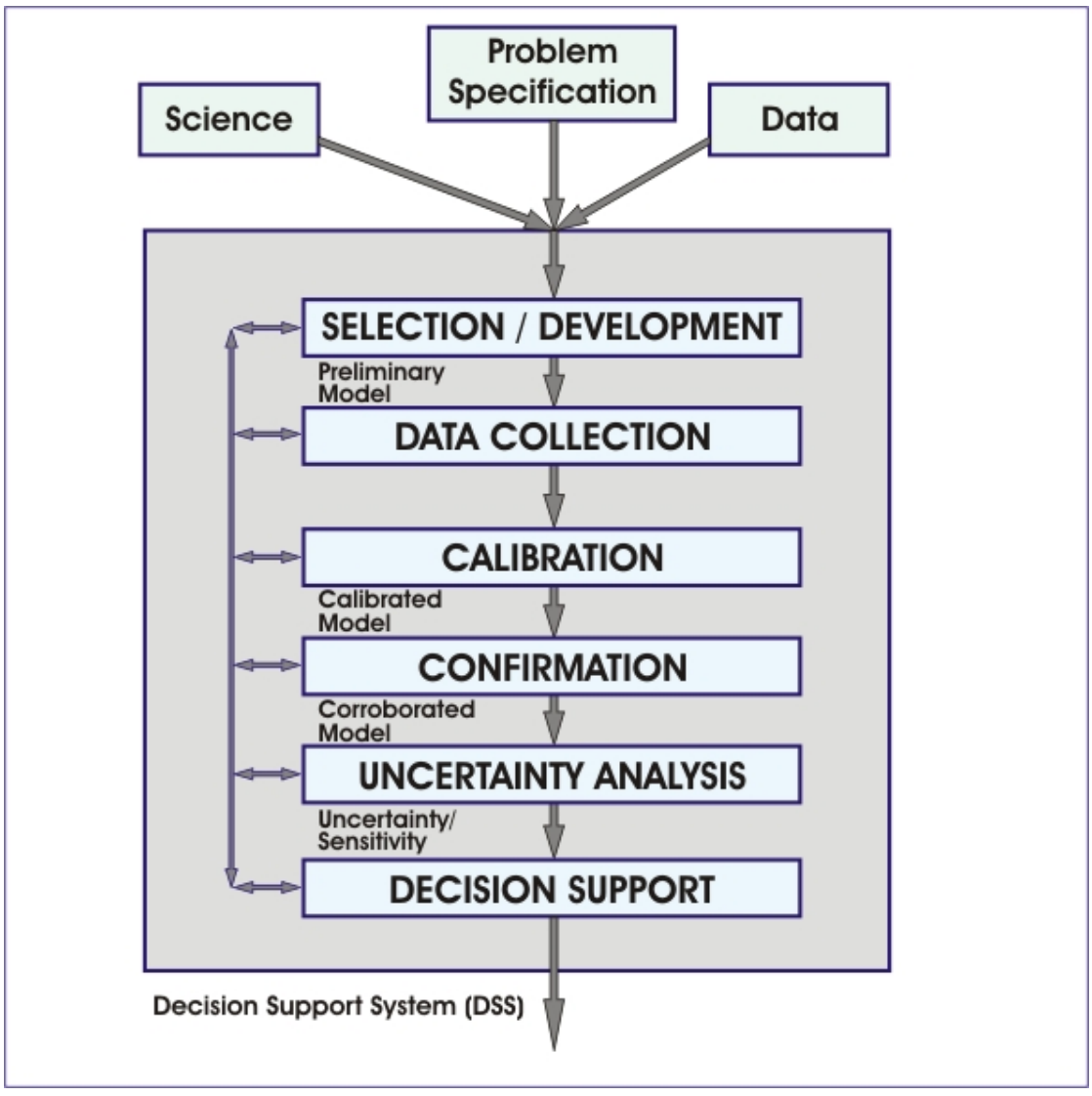

Figure 13 Water quality modelling process, after Chapra (2003)

Model selection and application is usually dependent on the outcome of a process in which the level of data requirement is aligned with model complexity to satisfy a predefined problem specification. This initial task already demands an understanding of the model's underlying science and an evaluation of the adequacy of the available data to ensure that reliable results are obtained. Taking the aforementioned into consideration, the model development and application will be discussed in the ensuing sections.

3.2 RANGE OF MODEL DEVELOPMENT APPROACHES

In the hydrological and water quality literature there have, in the past, been many attempts to classify models, e.g. Kienzle *et al.*(1997) as well as Addiscot and Wagenet (1985) and Schultz, (1987). The classification in this thesis, however, will be based on that presented by Jewitt (1998) and depicted in **Figure 14**. **Table 2** shows a limited range of hydrosalinity models used nationally and internationally.

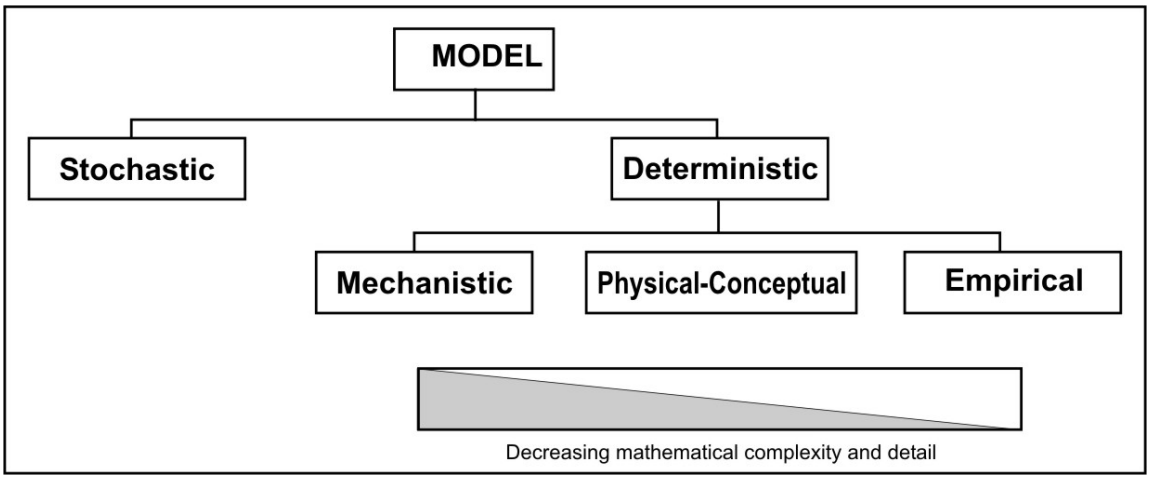

Figure 14 Classification of model approaches (after Jewitt, 1998)

Table 2 Classification of hydrosalinity models according to Jewitt's (1998) classification system

Model Name	Model Classification	Temporal Resolution	Variables Simulated	Runoff Simulation
FLOSAL (Hall and Du Plessis,1981)	*Physical-Conceptual*	Monthly	TDS	Moisture budget Pitman routine
WQT (Herold, 1980 and 1990)	*Physical Conceptual*	Monthly	TDS	Needs monthly naturalised flows as input
LEACHM (Wagenet and Hutson, 1989)	*Mechanistic*	Sub-daily	TDS, Nitrogen Phosphorous	Richards Equation
DISA (NSI, 1990)	*Physical-Conceptual*	Daily	TDS	Moisture Budget Multi-layer soil budgeting
ACRU*Salinity* (Schulze, 1995 and Teweldebrhan, 2003)	*Physical-Conceptual*	Daily	TDS	Moisture Budget Multi-layer soil budgeting
SWAT (Neitsch *et al*., 2002)	*Physical-Conceptual*	Sub-daily	Nitrogen, Phosphorous and Pesticide degradation	SCS Curve Number or Green and Ampt Infiltration method
HSPF *(Bicknell et al., 1997)*	*Physical-Conceptual*	1 minute to daily	TDS, organics and inorganics	Moisture budgeting-empirical functions

3.2.1 Stochastic models

Stochastic models aim to conserve the statistical parameters of a particular series (e.g. flow or TDS) and typically produce outcomes with different levels of probability. These types of models were not used in this study and will not be discussed further in this thesis, because a 1:1 comparsion of simulated and observed TDS sequences is what is desired as an output from this modelling study. The Water Resources Yield Model used for determination of reservoir yields is an example of a stochastic model.

3.2.2 Deterministic models

Bowie *et al*. (1985) explains that these types of models typically consist of fundamental underlying science (mathematical formulations and equations), default parameters and modelled parameters (e.g. evaporation and re-aeration formulae). Data is classified as being directly-measurable numerical values that can be used as input to the model and can consist of site specific values (e.g. land-use, soil types and topography), driving functions (meteorology) and rate data (e.g. settling rates or kinetic rate constants).

This class of models can be further sub-divided into mechanistic models, physical-conceptual models and empirical models.

Mechanistic models

This class of model seeks to solve the fundamental equations of momentum, mass and heat transfer using coupled partial differential equations which describe the underlying science. These equations have analytical solutions for a limited number of cases and often, only time-consuming computational methods can be employed to obtain a solution for a real-world problem. The LEACHM (Wagenet and Hutson, 1989) and HYDRUS (Simunek *et al*., 1996) models fall within this category of models. Although these models are theoretically sound they require large amounts of input data which could be expensive and time-consuming to obtain. As a result, the application of these models has been limited to the academic environment or to controlled situations, such as leaching reactors.

Physical-Conceptual models

These models provide a simplified representation of the fundamental equations which describe flow and solute transport and thus require less input data (Addiscott and Wagenet, 1985). The ACRU model (Schulze, 1995), WQT model (Herold, 1980 and 1990) and the FLOSAL model (Hall and Du Plessis, 1981) fall into this category.

Empirical models

These models can be thought of as the input-response class of models, where a particular input would always result in the same output. The constants in these equations or relationships are often determined from experiment, having no physical meaning and as such, cannot be transferred to other catchments. An example would be the "rational formula" (Mulvaney, 1850).

The following quote (Nestorov, 1999), however, suggests that strict definitions for empirical and mechanistic models can seldom be applied.

> "*In fact, there are no purely empirical or mechanistic models. Philosophically, all mechanistic models involve an element of empiricism (even if it were in the modelling assumptions). Otherwise, one should be able to describe "fully and completely" the studied phenomenon, which is definitely impossible in the continuous and infinite world. The reverse (all empirical models contain a mechanistic element in them) is also true, even if this element is the list of factors (inputs), influencing the modelled*

output. Therefore, no strict formal definition of an empirical or mechanistic model can be given. The distinction can only be relative, reflecting the predominance of the empirical or mechanistic elements in a particular model. Consequently, one should not underestimate the extrapolation capabilities of empirical models or, alternatively, overestimate the ability of the mechanistic models to extrapolate. In reality, both empirical and mechanistic models have found various and successful implementations and developments in different scientific areas."

3.3 DESCRIPTION OF THE ACRU MODELLING SYSTEM

The ACRU agrohydrological model was developed by the Department of Agricultural Engineering at the University of KwaZulu-Natal in Pietermaritzburg, South Africa (Schulze, 1995). The main modelling philosophies as reported by Kienzle (1997) are as follows:

- It is a *physical conceptual* model - conceptual in that it conceives a catchment system in which hydrological processes are idealised and physical in that physical processes are presented explicitly.
- It is not a parameter optimising model since parameter values are intended to be estimated from the physical characteristics of the catchment..
- It is a *multi-purpose* model that compartmentalises (see **Figure 15**) rainfall into various components of runoff. It can be applied in design hydrology, reservoir yield simulation, determination of irrigation demand and supply and regional water resource assessments.
- It is a daily time-step model which can be used to highlight the daily responses of fast responding rivers. Data to which the model is relatively insensitive (e.g. temperature and reference potential evaporation) can be entered on a monthly basis to be transformed to daily values by Fourier Analysis.
- It is a multi-layered model which allows for a variety of approaches for estimating the values of certain parameters, depending on the available information. The parameters include reference potential evaporation, interception losses, values of soil water retention constants, leaf area index, etc.
- It can operate in lumped (1 sub-catchment) or in distributed mode (many sub-catchments), depending on the size of the catchment and the complexity of land-use within the catchment.

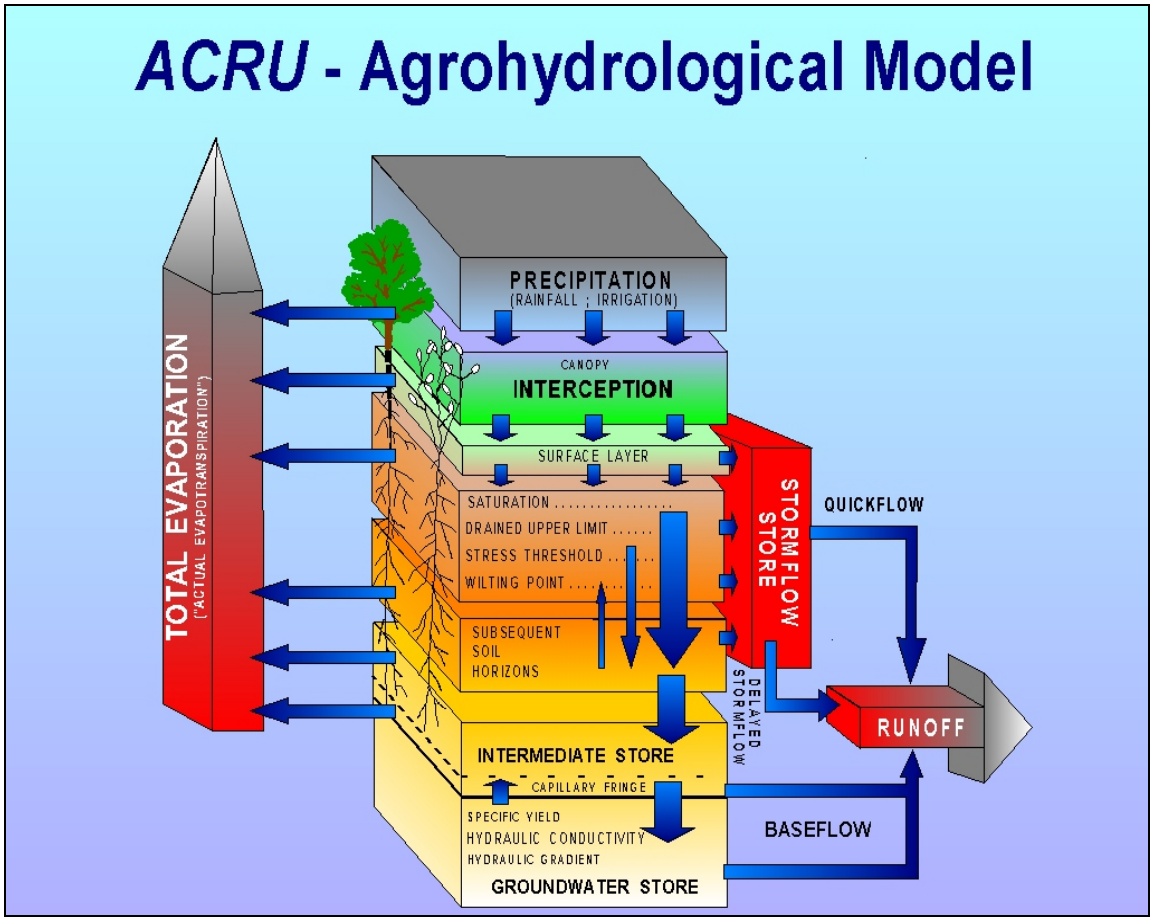

Figure 15 **The *ACRU* agrohydrological modelling system : general structure (after Schulze 1995)**

The processes modelled on a daily basis using the ACRU model (as described by Kienzle *et al*., 1997) are as shown in **Figure 15**:

- Canopy interception of rainfall by vegetation.
- Net rainfall reaching the ground surface.
- Infiltration of net rainfall into the soil.
- Total evaporation (transpiration as well as soil water evaporation) from the various horizons of the soil profile.
- The redistribution of soil water in the soil profile (saturated and unsaturated), and
- Percolation of soil water into the immediate groundwater zone.

The concepts and uses of the ACRU model are depicted in **Figure 16**.

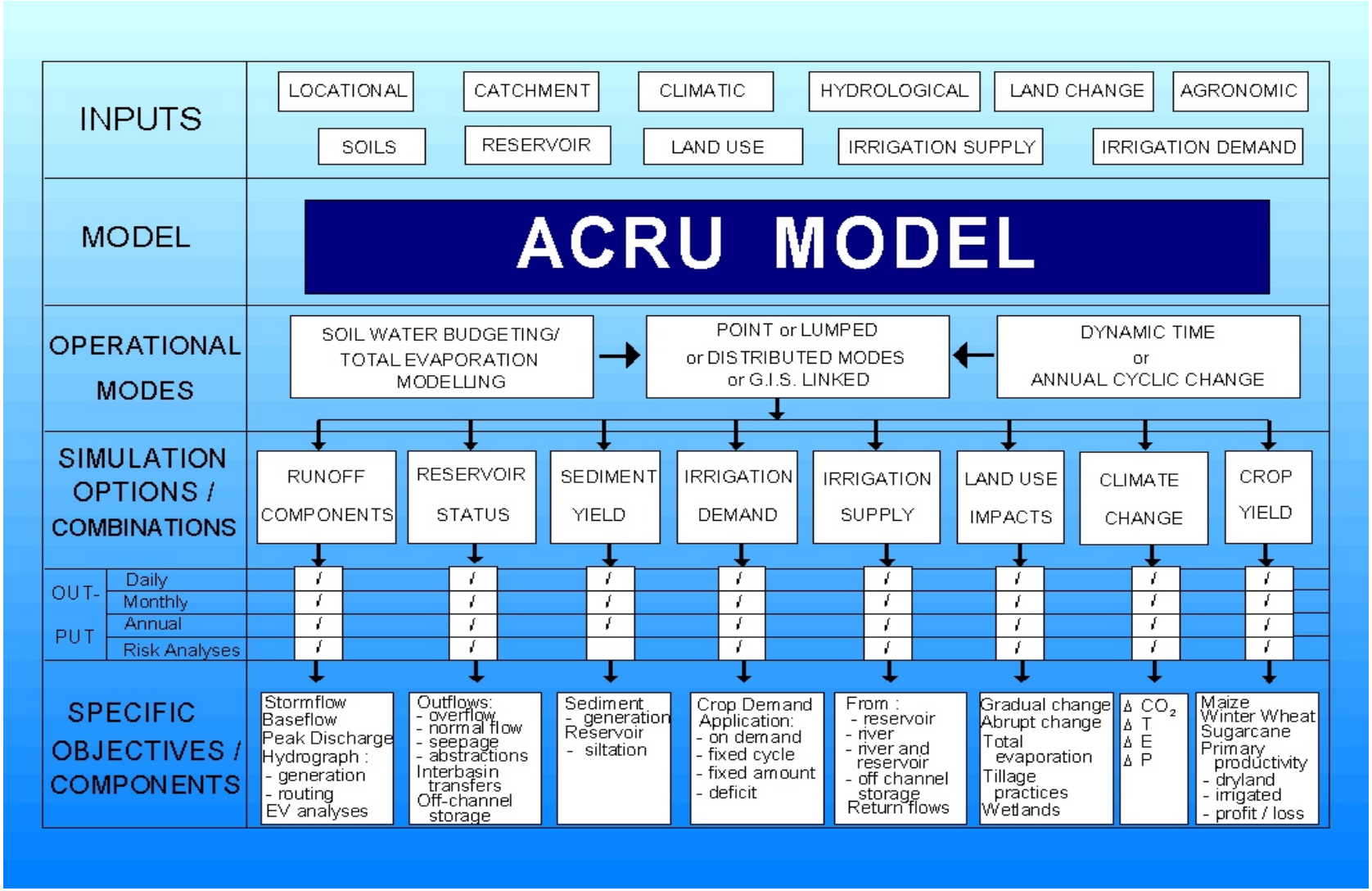

Figure 16 The *ACRU* agrohydrological modelling system : concepts (after Schulze 1995)

3.3.1 ACRU*Salinity* Concepts

Teweldebrhan (2003) described the processes that influence salt balance and movement through the soil profile by examining:

- Mechanistic modelling approaches to salt balance and movement in soils, and
- Conceptual modelling approaches to soil salt balance and movement..

Mechanistic modelling of these processes would consist of advective and diffusive mass transport, topics beyond the scope of this report. The focus of the ensuing sections will instead be on the conceptual model which was developed for the salinity module of ACRU*Salinity*.

The salt movement processes considered in ACRU*Salinity* are ***Initialising Salt Load***, ***Salt Input***, ***Surface Salt Movement***, ***Sub-surface Salt Movement***, ***Reservoir Salt Budget*** and ***Channel Salt Movement***.

During the development of ACRU*Salinity* the following Daily Irrigation and Salinity Analysis (DISA) model (Görgens *et al*., 2001) concepts relating to the movement of salt and water through the irrigated profile were considered for incorporation into ACRU*Salinity*:

- The irrigated soil profile consists of a layered soil structure, allowing for a root zone, unsaturated zone and a saturated zone.
- The model takes into account the capillaric rise of water and salts into the unsaturated zone.
- Movement of water between layers occurs only when the field capacity is exceeded and is controlled by a percolation factor as a function of the soil moisture status.
- Groundwater movement is controlled in the saturated zone and is modelled by the 1-dimensional Dupuit (Dupuit, 1863) approximation. This approximation assumes that groundwater would move horizontally and that groundwater discharge is proportional to the saturated aquifer thickness.
- Salt transport through the saturated zone is controlled by a Lagrangian layering approach, ensuring different time lags for water and salt responses (eventually not incorporated into ACRU*Salinity*).

Görgens *et al.* (2001) explained that the total volume of water entering a unit is divided into sub-units depending on the unit from which the water originated. **Figure 17** depicts the movement of salts within the root zone which shows that if the volume entering a unit (Q_{in}) is more than the initial soil moisture content of the layer immediately above it ($SMC_{S(i-1)}$) the excess water would have a salt concentration equal to $S_{S(i-2)}$. If the volume for Q_{in} still exceeds the initial soil moisture content of the two overlying layers, the additional volume and salt concentration would be obtained from the next layer. This process would continue until the total volume for Q_{in} had been accounted for.

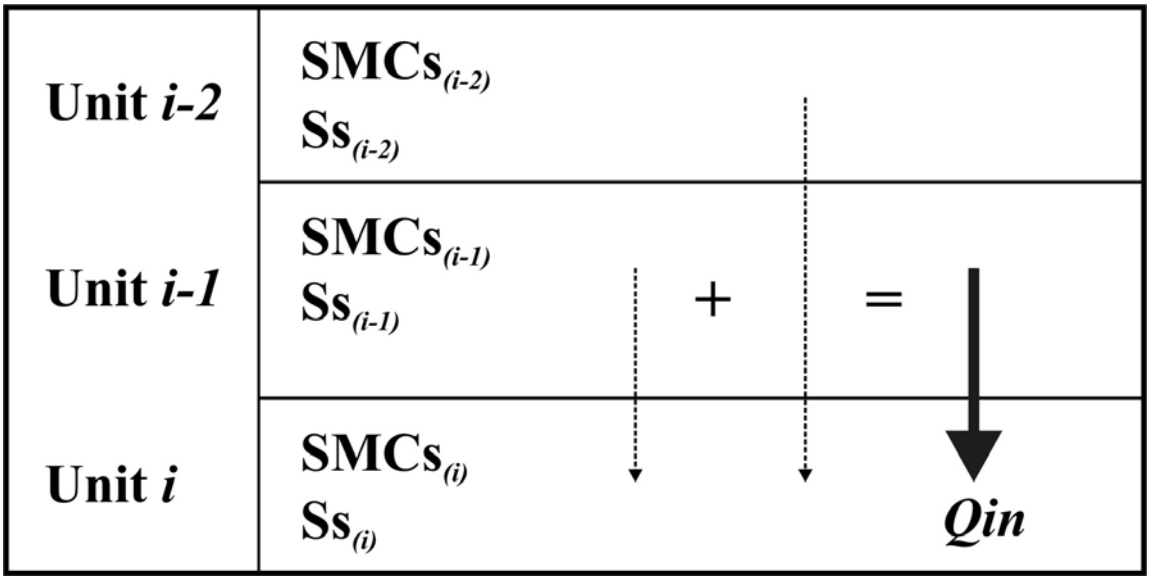

Figure 17 Soil movement within the root zone of the soil profile (after Görgens *et al.*, 2001)

The ACRU*Salinity* sub-surface TDS salt balance and movement algorithms were based on the concepts used in the DISA model except that the Lagrangian salt lagging that accounts for the various sources of percolated water and its influence on TDS in the various layers was not employed. This omission was based on the assumption (in the work by Görgens *et al*. (2001)) that each soil layer in ACRU*Salinity* would be deep enough to store more water in comparison with the water percolating out of that layer on a particular day.

Initial Salt Load

This object allows for the conversion of the user-specified inputs for initial salt concentration in the soil (in mg/l) to salt load, taking into consideration the volume of water in that soil layer.

Salt Input

This object contains algorithms that are responsible for salt load input from rainfall and irrigation water to the top-soil horizon of irrigated and non-irrigated lands as well as to reservoirs. Rainfall is the external salt input to irrigated, non-irrigated lands and reservoirs, while irrigation water provides an additional source of salt input to irrigated lands only. TDS concentration timeseries data for rainfall is not always available and can, in the model, only be specified as a constant value estimated from adhoc rainfall salinity analyses. Irrigation water TDS concentrations are more readily available and need to be specified on a monthly basis. The quantity of salt load added is the product of the added volume of water (rainfall and/or irrigation) and the salinity of the added water. **Figure 18** depicts the flow diagram for salt addition to the top-soil horizon in irrigated and non-irrigated lands.

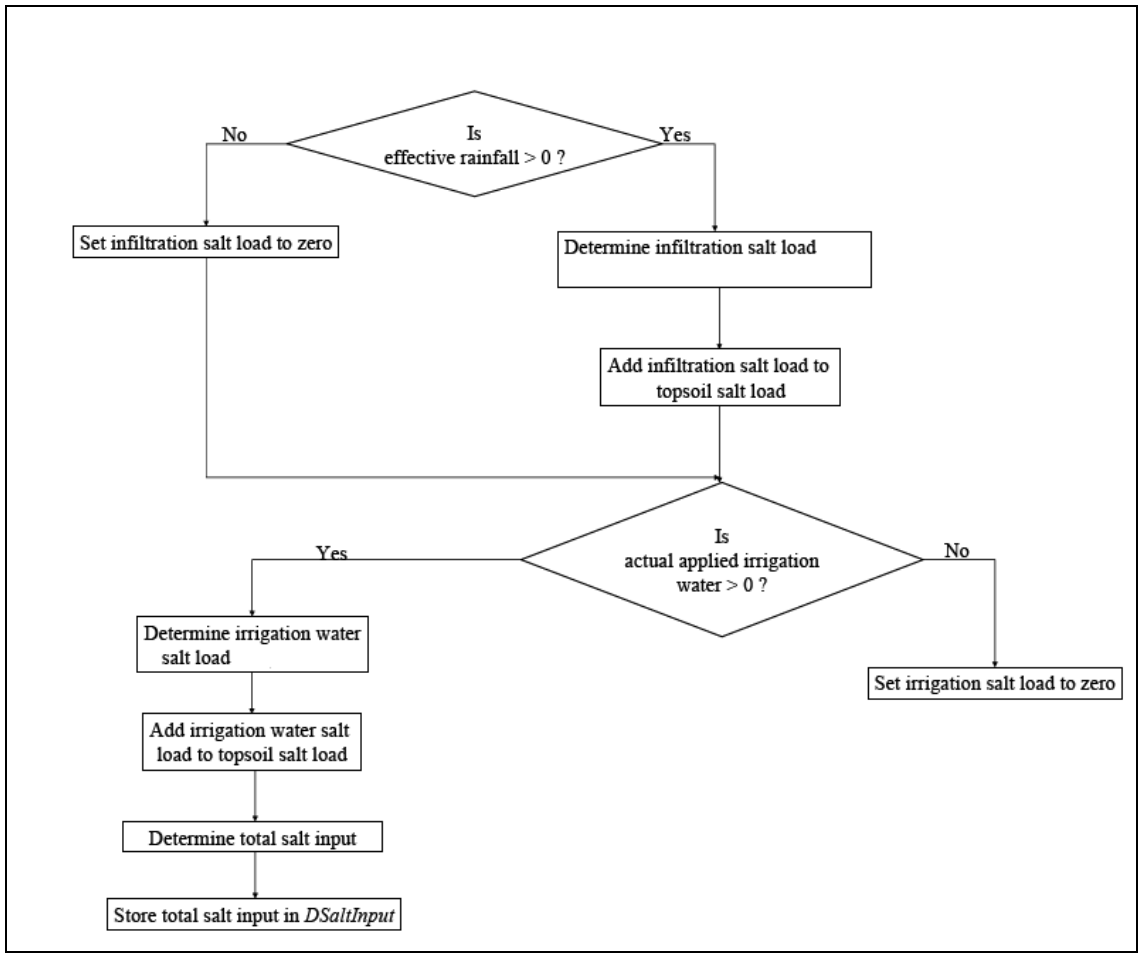

Figure 18 Flow diagram for salt addition (extracted and adapted from Teweldebrhan, 2003)

Surface Salt Movement

In the "Beta version" of ACRU*Salinity* v0.1 (released in February 2004), the salinity of the stormflow was assumed to be equal to rainfall or irrigation water salinity. It is reasonable to assume that the winter run-off would consist of a substantial percentage of "Quickflow" (immediate near-surface runoff) and it can be hypothesised that it would be accompanied by high TDS concentrations.

In response to understanding the salt mobilisation process in the Berg Catchment gained from the work of Fourie and Görgens (1977), as well as the current research by Fey *et al*. (2008), for this study, the following routines were added to the routines in land segments with no irrigation

- Additional surface layer of 10mm depth
- Dissolving a portion of the precipitated salts in the soil surface layer back into the solute state during an event, based on event contact time and soil characteristics,
- Mixing of salts in the soil surface layer with rainfall when calculating stormflow salinity, and
- Precipitation of dissolved salts in the soil layers if the salt concentration exceeds a maximum value.

These changes are detailed by Thorton-Dibb *et al*. (2005) in v1.2.5 of ACRU*Salinity.*

During the calibration process several other modifications to the source code of ACRU*Salinity* were required. Since this is one of the first applications of the ACRU*Salinity* model, it was necessary to make a series of improvements to the model in order to correctly simulate the salinities of the Berg River and its tributaries.

Modifications to the source code were followed by a reviewing process which consisted of recalibration of a highly saline catchment followed by a sensitivity analysis of each of the input parameters. This was an essential step since the acceptable range for a particular input parameter was not necessarily the same after coding changes had been made. After this step, the salinity-related input parameters were calibrated to obtain a simulated time series for TDS that was representative of the observed data record. If a comparative fit between the simulated and observed data could not be obtained, it was then necessary to identify where the formulations for salinity generation were not representative of reality and to suggest possible code modifications to be introduced.

In summary, the processes that were not accounted for in the "Beta version" of ACRU*Salinity* and which are now included in the latest version (v1.2.5) are:

- Unsaturated upward movement of water and salts from the A-horizon to the soil surface layer driven by the hydraulic gradient induced by evaporation in the soil surface layer.
- Evaporation of water and retention of salts in the soil surface layer.
- Precipitation of salts out of solution in the soil surface layer once the maximum dissolved salt concentration has been reached.
- Dissolving of precipitated salts into stormflow during a rainfall event controlled by rain water/soil water contact time and soil properties.
- Mixing of dissolved salts with rainfall in the soil surface layer during an event.
- Removal of salts in stormflow, proportioned on a daily runoff basis, and
- Redistribution of salts from surface layer into A-horizon after a rainfall event.

Initial versions of the ACRU*Salinity* model were unable to reproduce the observed effect of high TDS concentrations associated with the "Quickflow" because it allowed for no interaction between this component of the flow and the soil profile. In subsequent versions, however, the thin surface layer was introduced allowing for higher TDS values to be associated with the "Quickflow" component of the flow.

With the addition of the surface soil layer several new parameters were introduced and are listed in **Table 3**.

Table 3 Salinity related parameters for soil surface layer

Variable	Description
SMSINI	Soil surface layer initial value of soil water content as a depth (m) i.e. soil water content converted to a depth.
DEPSS	Soil surface layer depth (m)
FCSS	Soil water content ($m.m^{-1}$) at drained upper limit for the soil surface layer
SARESP	Fraction of soil water in the soil surface layer above drained upper limit to be redistributed daily from the soil surface layer into the top-soil i.e. "saturated" soil water movement
POSS	Soil water content ($m.m^{-1}$) at saturation (i.e porosity) for the soil surface layer
WPSS	Soil water content ($m.m^{-1}$) at permanent wilting point for soil surface layer
SSINIPRSALT	Initial amount of precipitated salt in the soil surface layer (mg/g)
SALTCTIME	Runoff event contact time (minutes)

Variable	Description
SALTSATSS	Monthly salt saturation of the soil surface layer
SALTDISCNST	Dissolution constant based on soil characteristics
SALTDISALFA	Dissolution constant for a given soil (α)
SALTDISBETA	Dissolution constant for a given soil (β)
INISSLSA	Initial soil surface salinity (mg/l)

The stormflow salinity algorithm was changed to include the dissolving of precipitated salts from the precipitated salt store in the soil surface layer, into stormflow during a rainfall event, as well as the calculation of mixed stormflow salinity.

If the net rainfall (NetRFL) is greater than 0 then the salt load dissolved from the soil surface layer's precipitated salt store is calculated as follows (Thorton–Dibb *et al.*, 2005):

$$DISS1 = K_{diss} \cdot T_{s,i} \cdot t^{\alpha} \cdot WR^{\beta} \qquad \textbf{Equation 1}$$

Where

DISS1	=	Dissolved Precipitated Salts (If DISS1 > $T_{s,i}$ then DISS1 = $T_{s,i}$)	(mg)
Kdiss	=	Salt Dissolution Constant	
$T_{s,i}$	=	Precipitated Salt Flux Record	(mg)
t	=	Runoff Event Salt Contact Time	(minutes)
α	=	Salt Dissolution Constant Alpha	
β	=	Salt Dissolution Constant Beta	
$\theta_{s,i}$	=	Water content of soil surface layer as a depth	(m)
ds lay	=	Soil surface layer depth	(m)
NetRFL	=	Total rainfall – interception	(m)
WR	=	(NetRFL + $\theta_{s,i}$) / ds lay	(m/m)

Also,

$T_{s,i+1}$	=	$T_{s,i}$ - DISS1

Where

$T_{s,i+1}$	=	PrecipitatedSaltFluxRecord (current)
$T_{s,i}$	=	PrecipitatedSaltFluxRecord (previous day's value)

If the net rainfall (NetRFL) is greater than 0 then the mixed stormflow salinity is calculated as follows (Thorton–Dibb *et al.*, 2005):

$$DISS = \left(SL_{RFL} + S_{SLay} + SL_{\inf lows}\right) / \left(\theta_{s,iVol} + NetRFL_{Vol} + WV_{\inf lows}\right) \qquad \textbf{Equation 2}$$

Where,

DISS	=	Mixed stormflow salinity	(mg/l)
SL_{RFL}	=	Salt load from the RFL (RFL converted to litres x RainfallSalinity)	(mg)
SL_{Slay}	=	Dissolved salt load in soil surface layer	(mg)
$SL_{inflows}$	=	Salt load from any other surface inflows (Currently these surface inflows are from disjunct impervious areas)	(mg)
$\theta_{s,iVol}$	=	Water content of soil surface layer as a volume	(litres)
$NetRFL_{vol}$	=	Volume of NetRFL	(litres)
$WV_{inflows}$	=	Water volume from any other surface inflows (Currently these surface inflows are from disjunct impervious areas)	(litres)

Important assumptions made during the development of the salinity model for the thin soil surface layer were as follows:

- It is assumed that there is a thin soil surface layer approximately 10mm thick.
- When using ACRU*Salinity*, the option for estimation of total evaporation (EVTR) must be set to 2, i.e. soil water evaporation (Es) and transpiration (Et) are calculated separately.
- The soil surface layer does not contain any roots and therefore no transpiration takes place from the soil surface layer.
- There is no salt uptake (i.e. mineralisation-based salt generation) in this soil surface layer.
- Even though a portion of the rainfall may be intercepted, the salt load associated with the intercepted rainfall is assumed to still contribute to the system and is therefore still added to the land segment or the impervious area.

Sub-surface Salt Movement

As with the DISA model, ACRU*Salinity* was also divided into vertical layers, *viz*. the top-soil and sub-soil together with a groundwater store and is based on the assumption that each layer is deep enough to store more volume of water than that percolated out of the particular layer for each day.

Teweldebrhan (2003) explained that in conceptualising the salinity module in ACRU*Salinity* careful consideration was given to the hydrological processes which led to a change in concentration of soil salinity, i.e. evaporation and transpiration. In the standard version of ACRU the water balance is active within the defined top-soil and sub-soil horizons. These horizons constitute the region of root development, soil water extraction/uptake and drainage. The soil water budgeting process (which is the main driving force for salt movement) as summarised by Teweldbrhan (2003) occurs as follows:

- Stipulation of soil water content at total porosity, drained upper limit (DUL), and permanent wilting point for each active soil horizon.
- Re-assessment of soil water content after addition of net rainfall.
- If soil water content exceeds the DUL for the top-soil horizon, a proportion of the excess water is drained to the sub-soil horizon.

Similarly, if the soil water content of the sub-soil horizon exceeds the DUL for this horizon, a portion of the excess water drains to the groundwater store. Baseflow is then calculated as the product of the previous day's groundwater store and the user specified baseflow recession coefficient. If drainage rates from the lower horizons are very low (low permeability rock), water can accumulate through the sub-soil and top-soil to eventually contribute to stormflow runoff, if the top-soil porosity is exceeded.

Unsaturated soil water redistribution can also be modelled. This slow movement of water will occur from the top-soil horizon, when the soil water content is below its DUL, to the sub-soil horizon if the top-soil horizon is relatively wetter than the sub-soil horizon. Unsaturated redistribution depends on the soil water gradient, the head of water and soil texture. Upward soil water redistribution in ACRU mimics capillary movement, and takes place when the sub-soil horizon contains a higher relative soil water fraction compared to that of the top-soil (Schulze, 1995c).

Since the salt movement in ACRU*Salinity* is based on the routines in the DISA model, it is controlled by the movement of water. More specifically, the movement of salt is dependent on the net movement of water between the layered soil profiles.

Sub-surface salt movement in ACRU*Salinity* can either be upwards or downwards. Downwards movement is dependent on the percolation of water from the top-soil horizon to the lower horizons while upward salt movement is dependent on saturated upward flow of water, i.e. when the water inflow rate to the bottom horizons is faster than the rate at which water is drained from this horizon, with subsequent accumulation of water in the horizon.

Although the original ACRU allows for the option of unsaturated water movement, the original salinity module in ACRU*Salinity* was not linked to this option and downward salt movement was only allowed to proceed once the DUL of the top-soil was exceeded. The later version (v1.2.5) of ACRU*Salinity* developed during this research project (Thorton–Dibb *et al.*, 2005), however, does allow for unsaturated salt movement making surface salt accumulation possible. Algorithms for sub-surface salt movement were written assuming a multi-layered soil even though ACRU only has two soil layers and a groundwater store, making it possible for additional layers to be added should the need arise. Even though sub-surface movement occurs in both irrigated and non-irrigated lands only the equations for the non-irrigated lands will be discussed in the ensuing sections as the two sets of equations are really identical.

Sub-surface salt movement in irrigated lands proceeds along the same lines except that a single horizon and the groundwater store are considered (this is ACRU's approach for irrigated lands). Additionally, since the irrigation months in ACRU are user-specified, the sub-surface salt movement algorithms in irrigated lands are only activated during those months.

Downward sub-surface salt movement

All salt balance calculations are only performed after all the hydrological processes have been calculated for a particular day and salt loads in a particular horizon are only calculated after water percolation from a higher- to lower-lying soil horizon. The salinity in each horizon is then calculated using the equation (Teweldebrhan, 2003):

$$C_i = \frac{SL_i}{SW_i + PW_i}$$ **Equation 3**

Where

C_i = salt concentration of the i-th horizon before salt generation (mg/l)
SL_i = current salt load of the i-th horizon before salt generation (mg)
SW_i = volumetric soil water content of the i-th horizon after percolation has taken place out of the horizon (l), and
PW_i = volume of percolated water out of the i-th horizon (l)

The updated salt concentration and load added as a result of salt generation can be calculated using **Equations 4** and **5 (**Teweldebrhan, 2003).

$$SL_{upd\_i} = C_{upd\_i}.(SW_i + PW_i) \quad \textbf{Equation 4}$$

$$SL_{gen\_i} = SL_{upd\_i} - SL_i \quad \textbf{Equation 5}$$

Where

SL_{upd_i} = salt load in the i-th horizon after salt generation (mg)
C_{upd_i} = updated horizon salinity (mg/l) and
SL_{gen_i} = salt load generated for the day in the i-th horizon (mg).

It should be noted that C_{upd_i} is obtained from **Equation 8**, after the salt generation process.

The salt load associated with the water percolating out of the *i-th* horizon (SL_{p_i}) is then given by **Equation 6**. In ACRU*Salinity*, the water entering each layer originates only from the overlying layer. If more layers with smaller volumes were to be introduced, this assumption would have to be revisited to possibly include the Lagrangian lagging technique used in the DISA model **(**Teweldebrhan, 2003).

$$SL_{p\_i} = C_{upd\_i}.PW_i \quad \textbf{Equation 6}$$

Percolation of water to the groundwater store is treated in a similar manner. A flow diagram depicting salt movement in non-irrigated lands is shown in **Figure 19**.

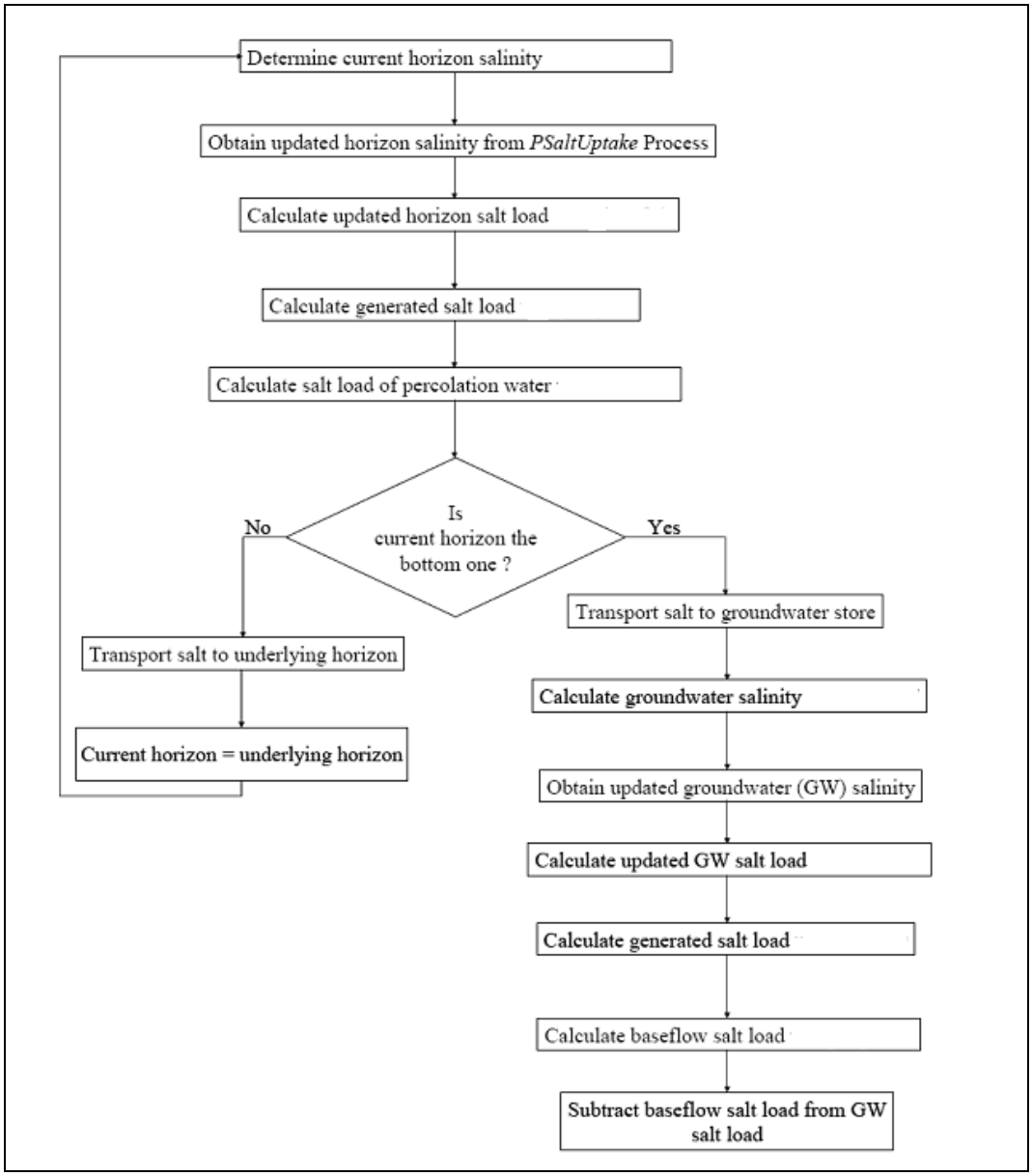

Figure 19 Sub-surface salt movement in non-irrigated lands (extracted and adapted from Teweldebrhan, 2003)

Upward sub-surface salt movement

In the model, upward salt movement through the soil profile and its influence on surface and sub-surface salt balance is determined by the upward salt transport algorithm. In this process, salt load moves from the bottom horizon through the overlying horizons to quickflow under a saturated condition. Hence, upward salt movement under this process occurs only if the rate of water recharge to a layer exceeds the rate of water loss from that particular layer.

In the version of ACRU*Salinity* (v1.2.5) used in this study the sub-surface salt movement is also linked to the unsaturated water movement to provide a more accurate account of salt movement.

Reservoir Salt Budget

Reservoir salt balances are performed on a daily basis considering all the inflow volumes and concentrations to the dam and assuming instantaneous mixing of dam contents. A flow diagram depicting the process of salinity calculation for reservoirs is depicted in **Figure 20**.

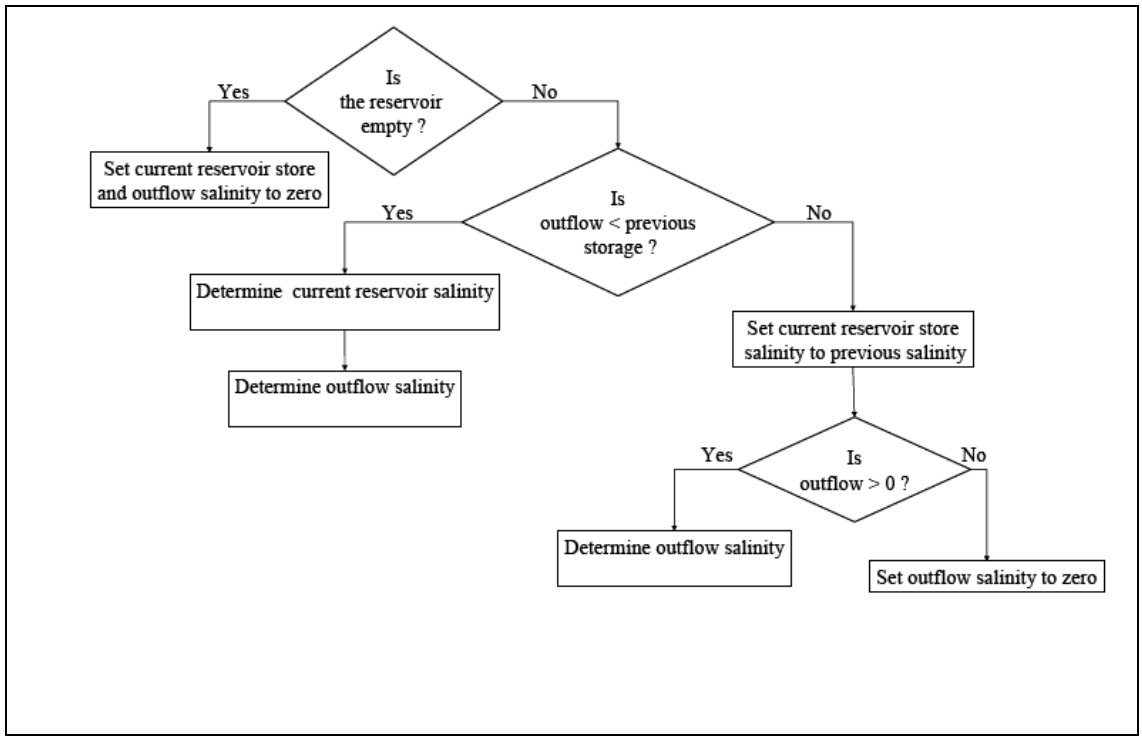

Figure 20 Flow diagram for salt calculations in reservoirs (after Teweldebrhan, 2003)

Channel Salt Movement

Channel reach concentrations are calculated as the daily salt load in the channel reach divided by the volume in the channel reach for that day.

Salt Generation

Many chemical processes are involved in the weathering process and according to Ross (1989) these would include adsorption onto the surface, reaction on the surface and desorption of reaction products. Each of these steps could be controlled by chemical kinetics but, unless all the chemical characteristics of the soil in question are known, it would be difficult to determine what the "rate determining step" would be in the overall process. Aris (1975) explained that adsorption

models can have various levels of sophistication. The solid surface is normally assumed to have a number of sites at which molecules of the adsorbate (reactants) may attach. Furthermore these reactants may be bound by physical forces (e.g. Van der Waal's) or chemical forces when attached to the surface. This treatment, however, is normally reserved for highly controlled cases where steady state conditions are induced. What is evident from this approach though, is that a rigorous mechanistic approach on a catchment scale is almost impossible due to the variability inherent in natural systems.

The development of the salinity generation module (Teweldebrhan, 2003) in ACRU*Salinity* was essentially based on the "combined salt generation and mixing model" and adopts the first order approach proposed by Ferguson *et al.* (1994). In principle, this approach assumes that all the discrete steps involved in the weathering process can be captured in one equation, presented as **Equation 7.** The rate of change of the solute concentration is proportional to how far the current concentration (*C*) is from the equilibrium concentration (*Ce*). The rate constant (*k*) is introduced as the proportionality constant in **Equation 7** (Nernst (1889), Ferguson *et al.* (1994)):

$$\frac{\partial C}{\partial t} = k(Ce - C) \qquad \textbf{Equation 7}$$

For the initial concentration C_0 at time $t = 0$, integration of **Equation 7** for the time period ($0 \rightarrow t$) and concentration ($C_0 \rightarrow C$) results in **Equation 8**:

$$C = C_0 + \left(C_e - C_0\right)\left[1 - \exp\left(-kt\right)\right] \qquad \textbf{Equation 8}$$

If C_0, C_e and k are known, then the contact (residence) time, u, can then be estimated from **Equation 9:**

$$u = -\frac{1}{k}\ln\left(\frac{C_e - C}{C_e - C_0}\right) \qquad \textbf{Equation 9}$$

For pre-selected high and low values of k the equation depicts higher and lower rates of "production" of solutes with a decrease in the rate as the equilibrium concentration is approached. The phenomenon is depicted in **Figure 21**.

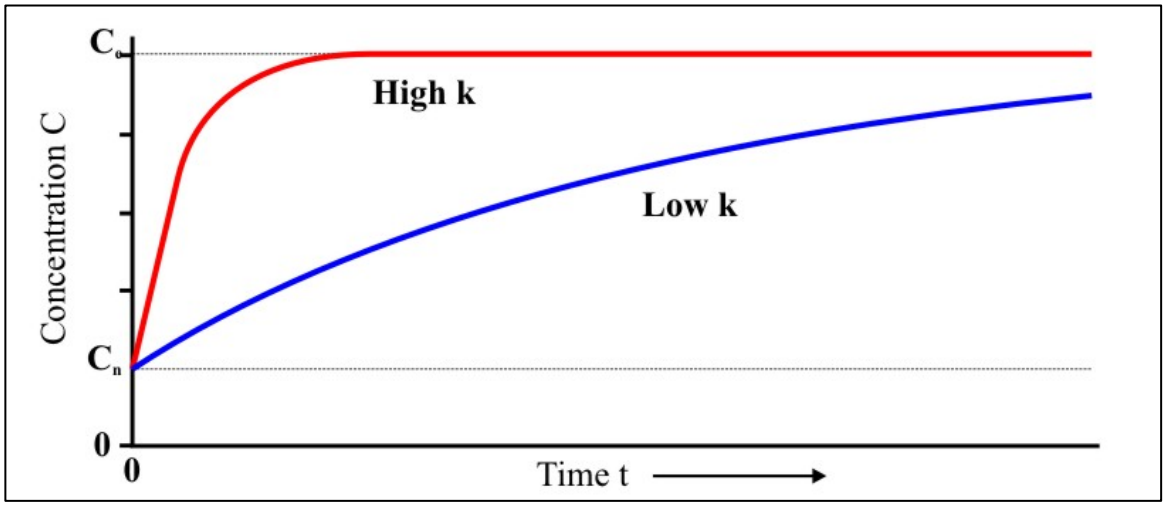

Figure 21 Salt generation curves (after Ferguson *et al.*, 1994 and extracted from Teweldebrhan, 2003)

The mixing of chemically-enriched (old water) and chemically-diluted water in ACRU*Salinity* is based on the approach put forward by Walling and Webb (1986). This approach is in fact a simple mass balance which states that the updated volume (Q) is equal to the sum of the old volume (Q_0) and the new volume (Q_n). This can be mathematically stated as:

$$Q = Q_0 + Q_n \qquad \textbf{Equation 10}$$

The mixture concentration is then given by:

$$C = C_n R + C_0 (1\text{-}R) \qquad \textbf{Equation 11}$$

Where C_0 is the initial concentration, C_n is the new concentration and R is the volumetric ratio of old to new water, i.e. (Q_n/Q_0). Between rainfall events the water in the ground is enriched using **Equation 7.** Combining **Equations 8** and **11** results in **Equation 12.**

$$C = C_e - (C_e - C_n) \exp(-kt) [R + \exp(-ku) (1 - R)] \qquad \textbf{Equation 12}$$

where u and t refers to the age of the "old" and the "new" water before the occurrence of the new rainfall event.

Equation 12 shows that the old water is chemically enriched before a rainfall event and thereafter the mixture becomes diluted with the new water. The mixture then once again becomes enriched before the next rainfall event. Additionally, the equation suggests instantaneous mixing which is

not realistic as rainfall and mixing are not instantaneous in the real world. A graphical depiction of **Equation 12** for the instantaneous and real-world scenarios is depicted in **Figure 22**.

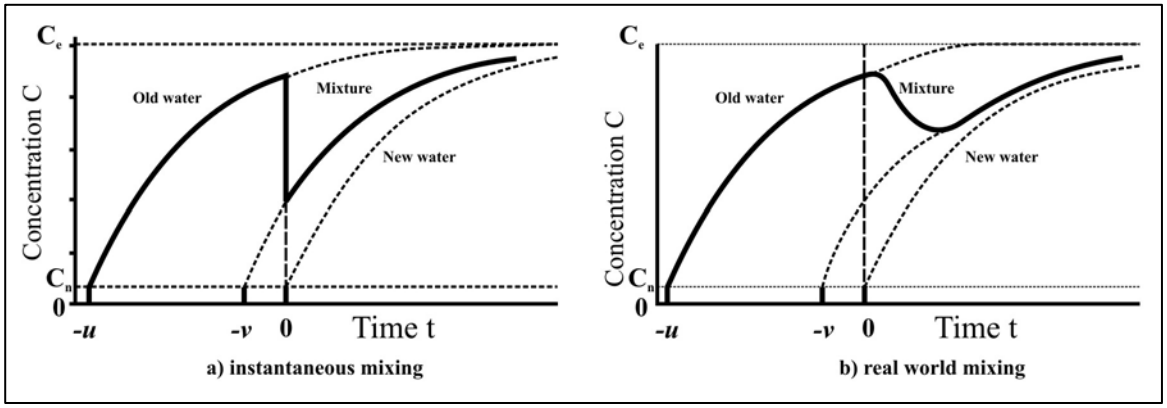

Figure 22 Sequence of enrichment and mixing processes (after Ferguson *et al.*, 1994 and extracted from Teweldebrhan, 2003) a) instantaneous mixing and b) real world mixing

An alternative approach for tracking the change in soil concentration involves the construction of a differential equation describing the processes of water mixing, solute mixing and solute enrichment. This equation is depicted below, where *P* is the rainfall rate, *S* is the volume of water stored in the soil and *Q* is the rate of water discharged.

$$\frac{dS}{dt} = P - Q \qquad \textbf{Equation 13}$$

The rate of change in salt mass would then be represented by:

$$\frac{dL}{dt} = PC_n - QC + Sk(C_e - C) \qquad \textbf{Equation 14}$$

Where *L* is the salt mass and all other variables are as defined before. The solute concentration can then be updated as

$$C = \frac{L}{S} \qquad \textbf{Equation 15}$$

By differentiating **Equation 15** it is possible to obtain **Equation 16** which can be further simplified if it is assumed that volume discharged (Q) is a linear function of the volume of water stored (S):

$$\frac{dC}{dt} = k(C_e - C) - \frac{(C - C_n)P}{S} \qquad \textbf{Equation 16}$$

If one assumes that Q = mS (m = slope of straight line for graph of Q vs S) then **Equation 16** becomes

$$\frac{dC}{dt} = k(C_e - C) - \frac{(C - C_n)mP}{Q} \qquad \textbf{Equation 17}$$

The first term in **Equation 17** is the Nernst (Nernst, 1889) equation and the second term is the dilution effect of the new water. **Equation 17** can then be solved using finite difference methods and without having to keep track of the volume of water storage (S).

According to Ferguson *et al*. (1994) the concentration of the new water (C_n) can be estimated from TDS measurements of rainwater while the equilibrium concentration can be estimated from the river TDS measurements under low flow conditions and after a long spell of dry weather. It is further suggested that the rate constant (k) should be estimated from the rate of change in solute concentration (C) during an inter-event period after mixing has occurred. The proposed method would require a least squares, straight line regression fit of the differential form of the Nernst equation (**Equation 7**).

CHAPTER 4: APPLICATION OF ACRU TO THE BERG RIVER FOR FLOW SIMULATION

4.1 INTRODUCTION

The application of the ACRU hydrological model to a developed catchment such as the Berg is a challenging task. Several factors contribute to a high level of complexity. These include:

- The presence of many farm dams.
- The varying abstraction rates of irrigation water from these farm dams.
- Variation in Mean Annual Precipitation (MAP) throughout the catchment, and
- The spatial distribution of crops (irrigated and dryland) within the catchments.

The approach employed to accommodate these complexities in the study will be discussed below.

4.2 DELINEATION OF THE BERG RIVER CATCHMENT

The delineation of the sub-catchments of interest is probably one of the most important steps in the configuration of the model.

To facilitate the process of catchment delineation two terms were defined:

- ***Primary sub-catchment*** – a sub-catchment that occurs within the confines of natural watersheds or within the confines of natural watersheds and the Berg River mainstem.
- ***Pseudo sub-catchment*** – a sub-catchment that consists of a particular land-use and that is not necessarily confined within natural watersheds, e.g. irrigated grapevines, dryland crops or natural vegetation.

A summary of the irrigated and dryland areas in the middle Berg is shown in **Table 4**.

Table 4 Summary of information for calibration sub-catchments

Calibration gauge	Total Area (km^2)	Dryland Area (km^2)	Irrigated Area (km^2)	Natural vegetation (km^2)
G1H037	72.4	0.0	34.8	37.6
G1H041	121.1	69.0	21.9	30.2
G1H036 incremental	494.4	277.0	165.7	51.7
G1H002/G1H028	185.4	0.0	0.0	185.4
G1H008	375.3	180.8	54.2	140.3
G1H043	154.9	147.9	1.3	5.7
G1H013	917.9	641.0	67.5	209.4
G1H035	674.3	613.0	9.5	51.7

Only one rainfall file can be used for a primary catchment and it was therefore important to recognise areas that had a distinctly different MAP from the rest of the catchment at an early stage in the configuration.

Criteria used for the delineation of the sub-catchment are, as follows:

- Points of interest, e.g. gauging stations with acceptable observed flow records.
- Discharge points of tributaries into the Berg River mainstem, and
- Areas with a distinctly different MAP compared with other zones in the rest of the catchment.

4.2.1 Origin to Berg River at Dal Josafat (G1H020)

This sub-catchment was the only one not configured as part of this project and an existing configuration was used instead. The reader is refererred to Dzvukamanja *et al*. (2005) for a full description of the ACRU configuration for this portion of the Berg River Catchment.

4.2.2 Berg River at Dal Josafat (G1H020) to Berg River at Vleesbank (G1H036)

Delineation into primary sub-catchments

The sub-catchment between gauging stations G1H20 and G1H036 is depicted in **Figure 23**. In the initial delineation of this sub-catchment in this study, the primary sub-catchments were

defined based on watersheds. With this approach, however, it was necessary to define conglomerates of farm dams, called "dummy" dams, within the primary sub-catchment and to specify the percentage of the primary sub-catchment that contributed run-off directly to these dummy dams. Although this approach was possible, it had several practical drawbacks. These are explained below:

The method of creating pseudo sub-catchments from a primary menu was done by using the CreateMenuFromGIS (Pike, 2004) pre-processor which automatically created a pseudo sub-catchment for each land-use within a particular primary sub-catchment, based on the land-use intersection data obtained via a Geographical Information System (GIS). If the percentage of the total sub-catchment contributing run-off directly to the dummy dam was specified in the primary menu, the CreateMenuFromGIS pre-processor would then create a dummy dam in each pseudo sub-catchment comprising the primary sub-catchment. This method preserved the run-off into the dam but gave rise to numerous dummy dams that had to be modelled.

An alternative method of dealing with the dummy dams was to convert the primary menu (for the primary sub-catchments) into an exploded menu (for the pseudo sub-catchments) before adding the dummy farm dam. In this method, it was necessary to locate a dam at a node where all the areas upstream of the node added up to the area upstream of the dummy dam (i.e. contributing run-off directly do the dam) as it would be defined in the configuration of the primary sub-catchment. This proved to be a difficult task because the pseudo sub-catchments created would not necessarily group together such that their area represented exactly that which contributed run-off directly into the dummy farm dam. In fact, this was never the case and the approach was subsequently abandoned.

Because of the impracticalities of the above methods it was decided that a different approach to primary sub-catchment definition was needed and that this should correspond to the dummy farm dam boundaries as defined in the *Western Cape Systems Analysis Study* (WCSA) (DWAF, 1993 (1)). The resultant effect was that the number of primary sub-catchments now increased from 14 to 46 and was no longer based on watersheds only. In the WCSA (DWAF, 1993 (1)) these boundaries were demarcated at the 1990 level of development and represented the boundary of the sub-catchment area contributing run-off directly into the "dummy" farm dam, which represented the combined capacity of all the farm dams upstream of this boundary. In this way it was possible to create an exploded menu (i.e. containing pseudo sub-catchments) where artificial nodes were placed at the outlet of each primary catchment boundary, accumulating the run-off

from all the upstream pseudo sub-catchments and thus marking the exact position within the configuration for the placement of "dummy" farm dams.

The primary catchments defined for the Berg River between gauging stations G1H020 and G1H036 are depicted in **Figure 23**.

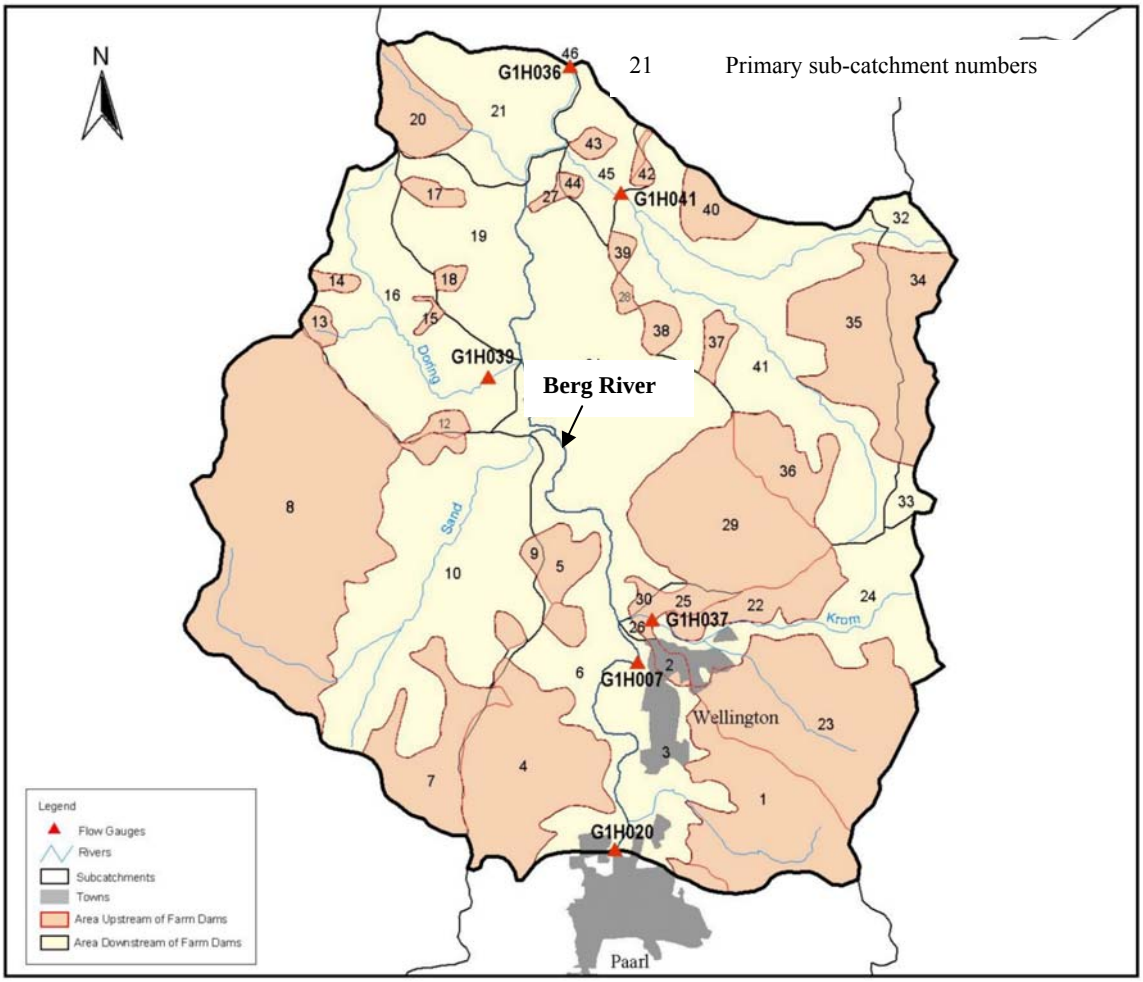

Figure 23 Primary sub-catchments defined for the Berg River Catchment between gauging stations G1H020 and G1H036

Tributaries discharging into the Berg River mainstem from the west include the Doring River (G1H039) and Sand River while tributaries discharging from the east include the Kompanjies River and Krom River. Numerous other small tributaries discharge into the Berg River but these are mostly non-perennial and have no formal names.

In previous hydrological studies on the Berg River (DWAF, 1993 (1) and DWAF, 1999) flow calibrations were undertaken at flow gauging stations G1H020, G1H037, G1H041 and G1H036.

In one of the WCSA series of reports (DWAF,1994 (1)), it was shown that the aforementioned gauges had an accuracy rating of 4 or higher (1 = low, 5 = high) and were suitable for calibration.

It should be noted that the aim of this modelling exercise was to obtain a daily time-series of flow and concentrations of the tributaries discharging into the Berg River mainstem and that the delineation of sub-catchments had to be structured to provide this information as an output. The ACRU system configuration for the primary sub-catchment is depicted in **Figure 24** where the circled numbers represent the primary sub-catchments.

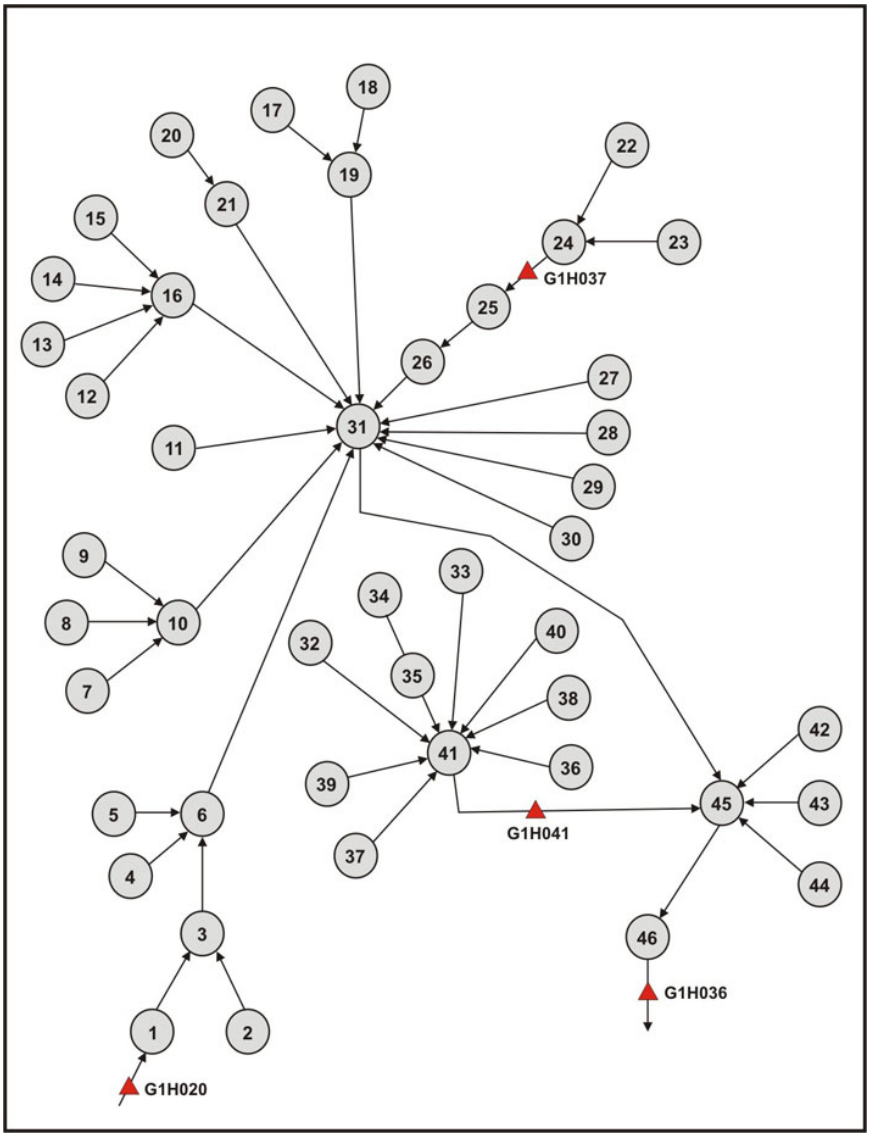

Figure 24 **ACRU system layout for the Berg River Catchment between gauging stations G1H020 and G1H036**

4.2.3 Berg River at Vleesbank (G1H036) to Berg River at Drieheuwels (G1H013)

Delineation into primary sub-catchments

The sub-catchment between gauging stations G1H036 and G1H013 is depicted in **Figure 25**. This sub-catchment contains the off-channel Voëlvlei Dam which is filled by flows diverted at gauging stations G1H028, G1H029 and G1H008. Voëlvlei Dam was not modelled as a dam in the ACRU configuration, instead the diversions were modelled as abstractions and the release from the Dam was introduced into the receiving sub-catchment as a specified inflow, constructed from the observed release record. Pertinent tributaries discharging into the Berg River mainstem include the saline Sandspruit (G1H043) (which is important because of the high salt load that it contributes to the mainstem), the Twenty-Four-Rivers (G1H028), the Leeu River (G1H029) and the Klein Berg River.

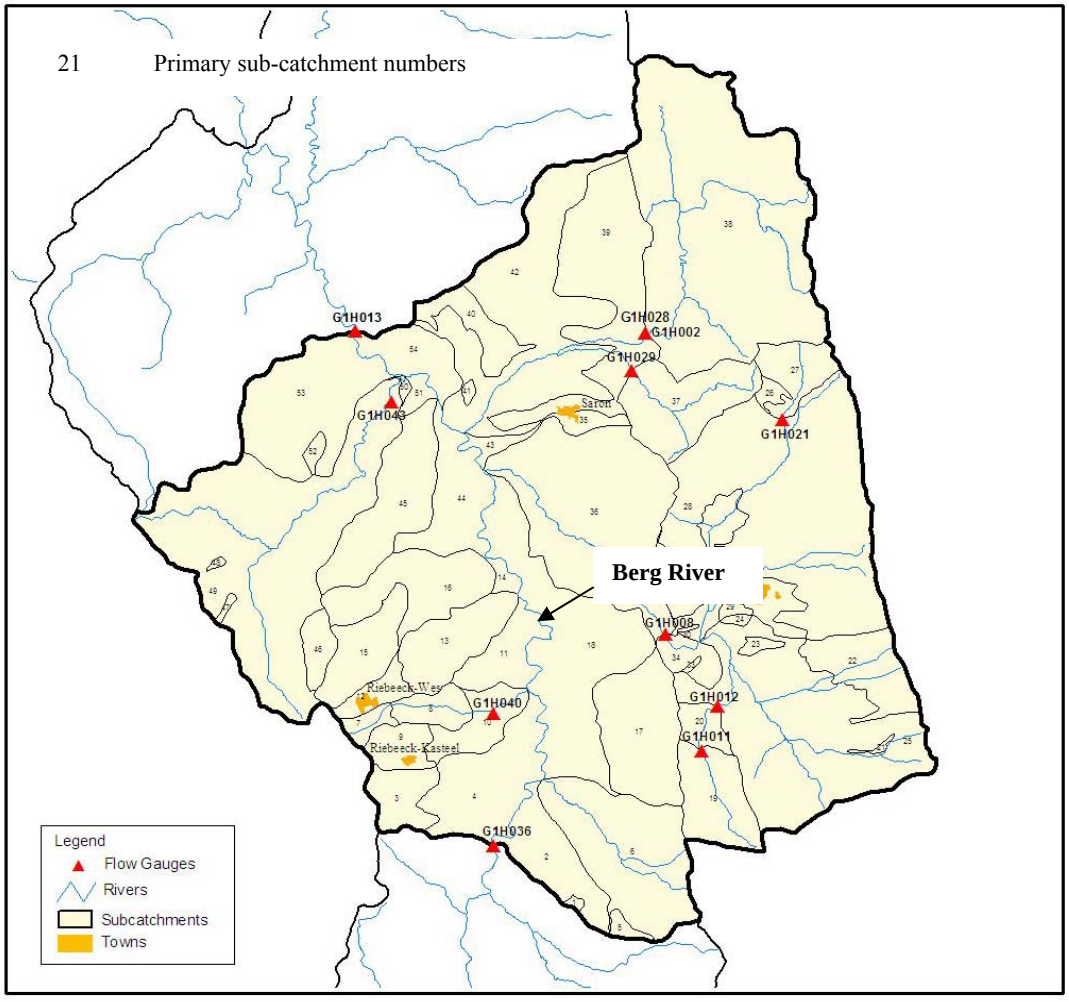

Figure 25 Primary sub-catchments defined for the Berg River Catchment between gauging stations G1H036 and G1H013

It should be noted that **Figure 25** represents the initial delineation into primary catchments and that some refinement was expected, based on quality of the comparison between simulated and observed flows during the verification procedure.

The ACRU system configuration for the sub-catchment is depicted in **Figure 26**.

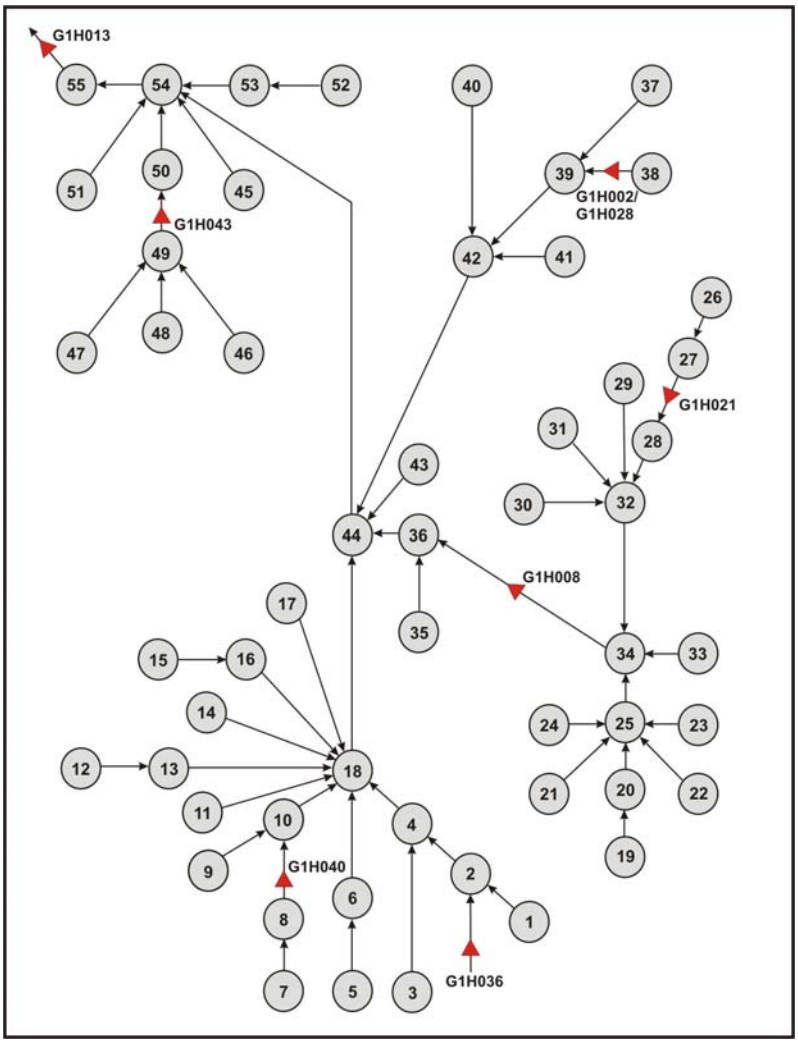

Figure 26 ACRU system layout for the Berg River Catchment between gauging stations G1H036 and G1H013

4.2.4 Berg River at Drieheuwels (G1H013) to Berg River at Misverstand Dam (G1R003)

Delineation into primary sub-catchments

The initial sub-catchment delineation between gauging stations G1H013 and Misverstand Dam G1R003 is depicted in **Figure 27**. Although the run-off contribution from the sub-catchment between G1H013 and G1R003 was substantially less than that of the more upstream portions of

the Berg River Catchment, this sub-catchment still required a fairly detailed delineation because of the contributions to the salt load in the mainstem of the Berg River. This is particularly relevant for the sub-catchments upstream of gauging stations G1H035 and G1H034.

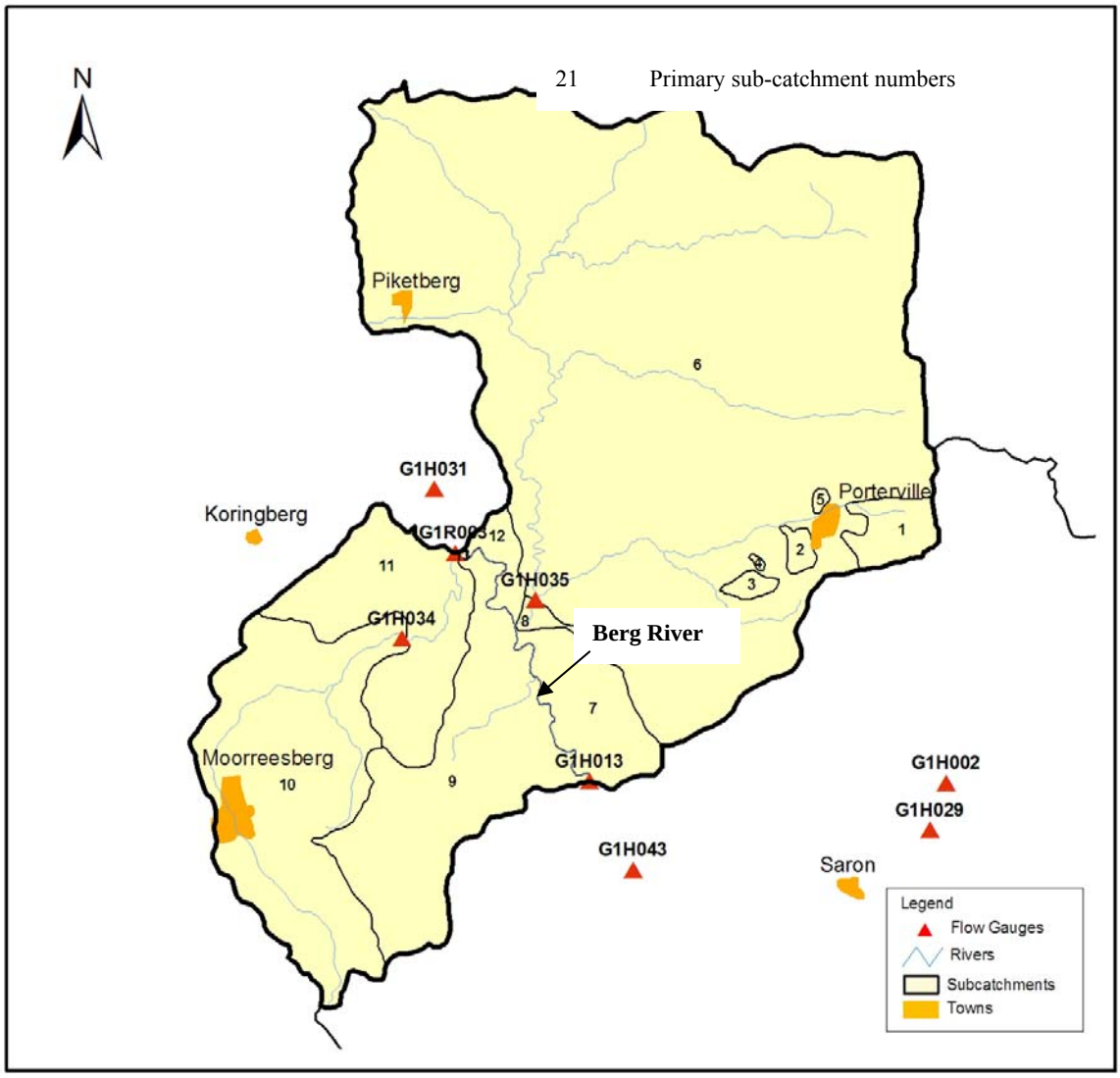

Figure 27 Primary sub-catchments defined for the Berg River Catchment between gauging stations G1H013 and G1R003

The ACRU System layout for this catchment is depicted in **Figure 28**.

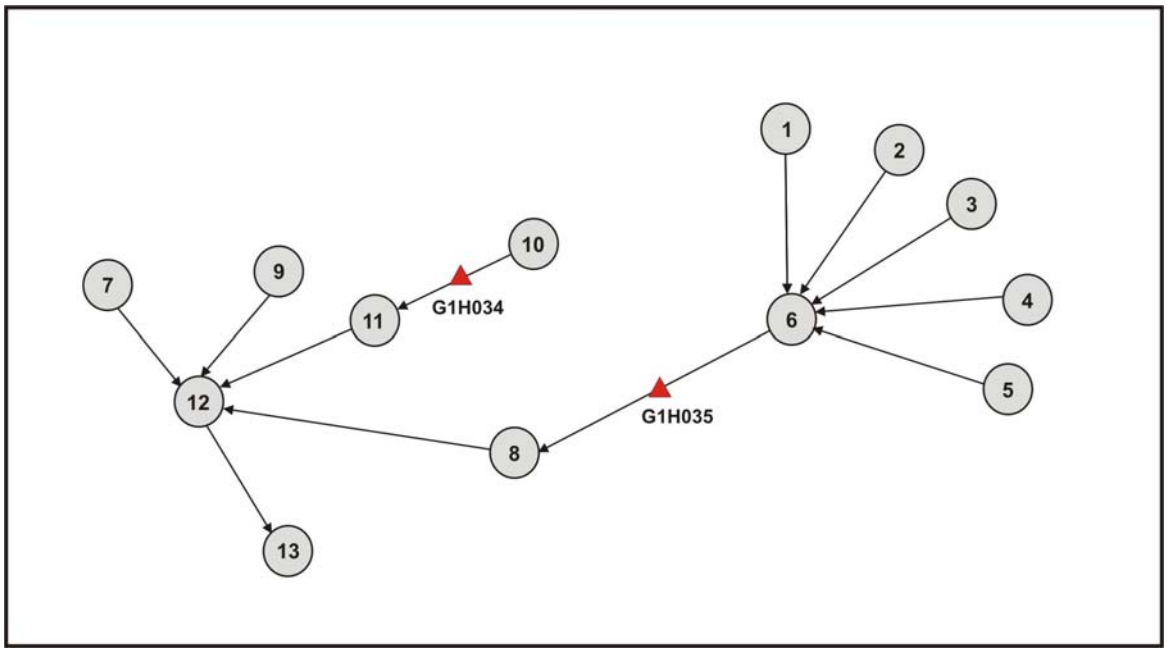

Figure 28 ACRU system layout for the Berg River Catchment between gauging stations G1H013 and G1R003

4.3 DATA PREPARATION FOR THE ACRU MODEL

In general, it can be expected that a daily model, such as ACRU, would require many inputs and in many cases the preparation of this information is the most time-consuming task in the modelling process. ACRU is furthermore supported by a suite of pre-and post-processors that are useful in the preparation of the input information.

The major input parameters to ACRU per primary catchment includes daily rainfall, farm dam sizes and location and land-use data (e.g. vegetation type, area).

The ensuing sections present not only the input information that was prepared for the modelling but also the pre-processor programs that were used in the preparation as well as their availability to the model user.

4.3.1 Preparation of the rainfall data

This is probably the most important data set required to run the model and sufficient time and effort should be invested in the preparation of this data.

The preparation and manipulation of rainfall data can be tedious when done by hand and also allows for the possibility of many "finger errors" being made. With the aid of a GIS and other pre-processor programs, however, it can be done faster and with a reduced probability of mistakes.

Selection of most appropriate daily rainfall sequence

Schulze *et al.* (1995) describe two approaches for selecting the most appropriate rainfall sequence for driving the run-off generating processes within a sub-catchment, *viz*. the driver station approach and the ACRU-300 trend surface approach.

- *Driver Station Approach*

In this approach, the driver station is selected based on:

- Its proximity to the catchment.
- Its altitude relative to the catchment's mean altitude.
- The length of the record, and
- The extent of missing data.

Missing data in the best driver station is replaced with data from the "next best" driver station. Correction factors are then applied to the rainfall of each month in the driver station so that it is more representative of the daily areal catchment rainfall. The correction factor for each month is calculated as the ratio of the median monthly precipitation of the driver to median monthly precipitation of the catchment (Schulze, *et al*., 1995)

According to Schulze *et al*. (1995), the advantage of this method is the preservation of the statistical properties of the point rainfall and the fact that it is fairly straightforward to apply. The major disadvantage of the approach, however, is the over-simplification of the daily areal rainfall distribution, e.g. the method would presume that the temporal rainfall pattern experienced at that particular rainfall gauge was experienced throughout the catchment.

This method is recommended when:

- The aim of the study is for planning rather than operational hydrology.

- The catchment is smaller than 28 km^2 (Seed, 1992). Seed (1992) showed that the rainfall at a rain gauge may be considered representative of the area within a 3 km radius around the rain gauge.
- Topography exerts little influence within the catchment.

➢ *The ACRU-300 Trend Surface Approach*

This method was described in detail by Schulze, Schäfer and Lynch (1989) and Schäfer (1991). A summary of the pertinent steps of the method as applied to the Lions River catchments is given below (Tarboton *et al.,* 1992):

- Rainfall records with a minimum record length of five complete years within a period from January 1960 to December 1990 were extracted for stations in and around the catchment of concern.
- A file containing the median monthly rainfalls over the entire rainfall record length (i.e. 1960 to 1990) for each of the stations selected should be set up.
- For each day, the daily rainfall of each rainfall file should be scanned and for days where rainfall is recorded it should be expressed as a ratio of the median monthly rainfall for that particular file.
- These ratios should then be interpolated onto a rectangular 1 minute by 1 minute of a degree latitude and longitude grid and combined with the 1 minute by 1 minute of a degree latitude and longitude median monthly rainfall image produced by Dent, Lynch and Schulze (1987) for the month in which the rain fell in order to produce a 1 minute by 1 minute daily rainfall surface of point values.
- The 1 minute by 1 minute daily rainfall values within each sub-catchment should then be averaged to produce an estimate of areal daily rainfall for each distributed catchment.

For this study, data gathered by Lynch (2001) was used. The data contained in that database was obtained from the South African Weather Services (SAWS), the South African Sugar Association, the Agricultural Research Council (ARC) and private individuals. The database has not been updated since its completion in 2001.

Spatially, rainfall information was also available in a shape file (personal communication, Pike, 2004(1)) and this was used for identifying all the rainfall gauges in the immediate area that could be used as input files to ACRU by intersecting the shape file with the applicable sub-catchment boundaries.

The pre-processor CALC_PPTCOR (personal communication, Pike, 2004(2)) was used for prioritizing the rainfall gauges that could be used for a specific sub-catchment. The prioritisation was based on the following criteria (as described in the output file of CALC_PPTCOR):

- Record length of the station in years.
- MAP of the rainfall station compared to that of the sub-catchment.
- Altitude of the station compared to the altitude of the centroid of the catchment.
- Distance of the rainfall gauge from the centroid of the catchment.
- The number of out – of – range months, i.e. months where the correction factors are less than 0.70 or more than 1.30.

The abovementioned criteria are consistent with those mentioned by Tarboton *et al.* (1992) and Kunz (2004).

The program is used in conjunction with the 1 minute by 1 minute grid of median monthly rainfall and altitude developed by Dent *et al*. (1989). After the top four rainfall files had been selected from the prioritization process these were extracted from the rainfall database using the program "BR_SAWB.exe" (Lynch, 2001). During the latter stages of this study, the aforementioned procedure for patching daily rainfall data was replaced with the process based on the "Daily Rainfall Data Extraction Utility" program (Kunz, 2004), which allowed for the extraction of previously patched rainfall data from its database. This utility also had the built-in functionality which allowed the user to match the most appropriate rainfall station (driver rainfall station) to the co-ordinates of interest, i.e. the centroid of the catchment.

Tarboton *et al.* (1992) compared these two rainfall estimation techniques and concluded that the ACRU-300 trend surface approach was less suitable for estimating daily rainfall for distributed catchment modelling with a sparse gauging network. They attributed this to the attenuation caused in the peak rainfall events as well as the exaggerated number of raindays which was in turn caused by the interpolation between adjacent rainfall stations with significantly different rainfall distributions, a rapid decay in rainfall intensity and a low density of rain gauge network. They further suggested that a more pragmatic solution for daily catchment rainfall was a driver rainfall gauge weighted by the correction factor.

A limited number of distributed sub-catchments in this study had a rain gauge density adequate to support the application of the ACRU-300 trend surface approach - the overwhelming majority of the sub-catchment did not. The driver station approach was consequently applied for all sub-catchments in this study.

Infilling of missing rainfall data

Smithers *et al*. (1995) described two methods of infilling missing daily rainfall data, *viz*. a manual infill method with data from nearby stations and a 12-parameter synthetic rainfall generator developed by Zucchini and Adamson (1984).

- *Manual Infill Method based on best rainfall gauges identified*

This infilling procedure relies heavily on the rainfall gauges identified during the implementation process used to identify the most appropriate station as a driver rainfall station. In this method, the days with missing rainfall data in the most appropriate rainfall gauge (driver station) are replaced with rainfall from the second-most appropriate gauge and by adjusting the infilled value by the ratio of the MAPs between the two stations. With this technique, the sequencing of the historical rainfall is preserved which is important when comparing simulated and observed flow sequences.

The disadvantage of this approach is that manual comparison of stations is required on the days that missing data occurs and this can be a time-consuming process.

- *12-parameter rainfall generator*

According to Smithers *et al*. (1995), an infilling technique developed by Zucchini and Adamson (1984) employed a random number generator and modelled parameters for each of the more than 5000 rain gauges in South Africa. Schulze *et al.* (1995) described the implementation of the approach as follows:

- A complete year of synthetic daily rainfall is generated.
- Where missing data occurs in the observed record it is replaced with a synthetic value from the corresponding day in the synthetic record.
- A synthetic value, on a particular day in the year can only be used once and should another value, in a different year, in the observed record be missing on the same day as a previously used synthetic value, a new synthetic daily sequence is generated to infill this missing observed value.

Although the statistics of such a rainfall sequence at that station are preserved, it does not account for the correct sequencing of the historical rainfall nor does it include regional influences. This infilling technique is, therefore, only useful for stochastic modelling at a point.

In this study, the *Manual Infill Method* was used because it preserves the historical sequencing of the rainfall. Most of the manual work of obtaining a ranking of the best rainfall gauges for a particular station was accomplished by using the program CALC_PPTCOR (or Daily Rainfall Data Extraction Utility), thereby eliminating the disadvantage of this approach. It also ensured that the most appropriate rainfall station was used to infill the days with missing rainfall data in the driver rainfall station.

Gauging stations G1H020 to G1H036

Using GIS, 24 stations were identified that could possibly be used as driver rainfall stations for the sub-catchments in this configuration. These are shown in **Figure 29**.

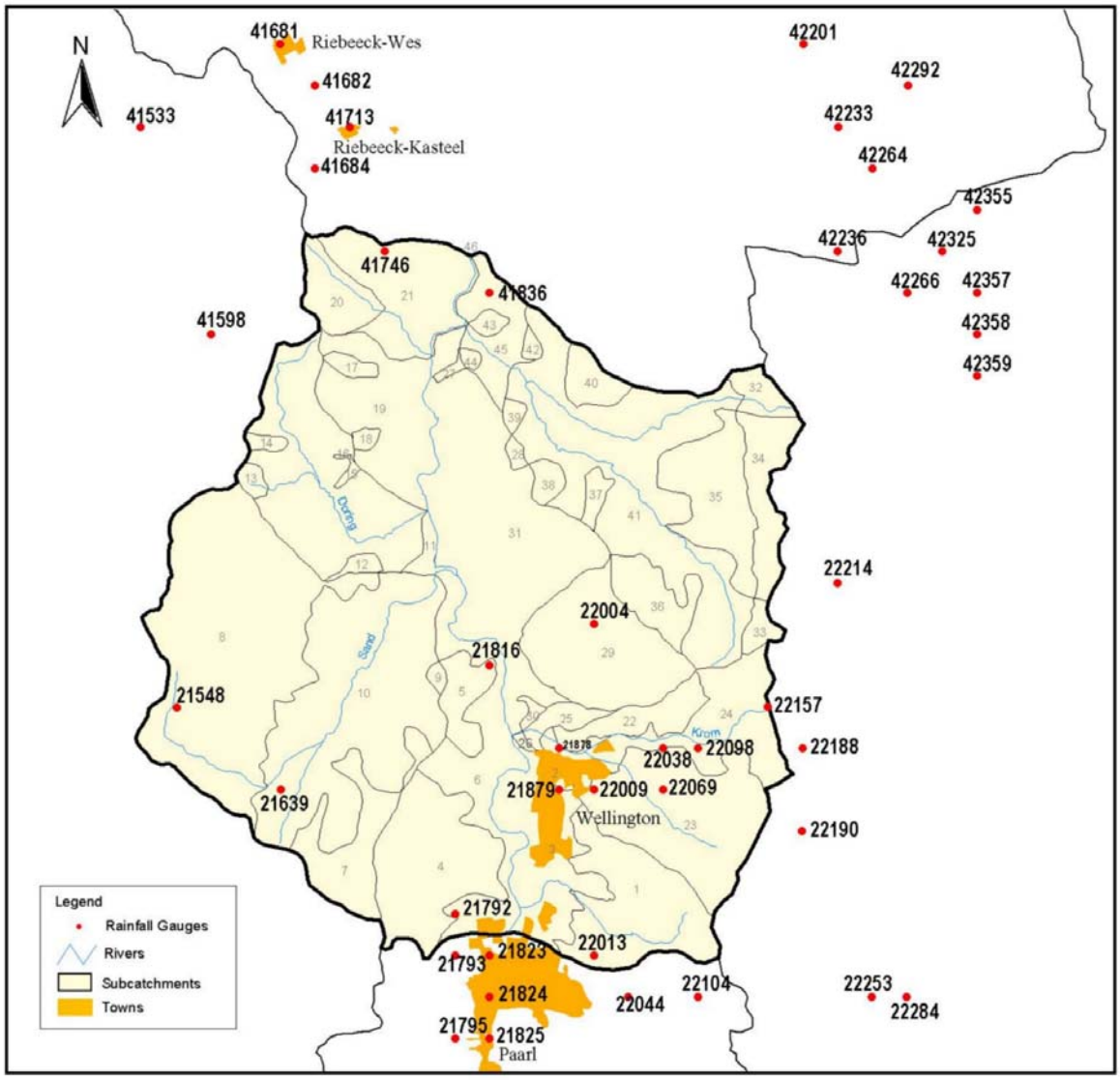

Figure 29 Possible rainfall gauges to be used as the driver rainfall stations in the various primary (distributed) catchments between G1H020 and G1H036

As stated previously, the program "CALC_PPTCOR.EXE" was then used to determine the ranking of these rainfall stations in accordance with the criteria in **Section 4.3.1** (as well as for all subsequent sub-catchments). An example of a listing showing the ranking of the rainfall station for each primary sub-catchment is shown in **Appendix A**.

Gauging Stations G1H036 to G1H013

Using GIS, the rainfall gauging stations that could possibly be used as driver stations for the sub-catchments in this configuration were identified. These are shown in **Figure 30**.

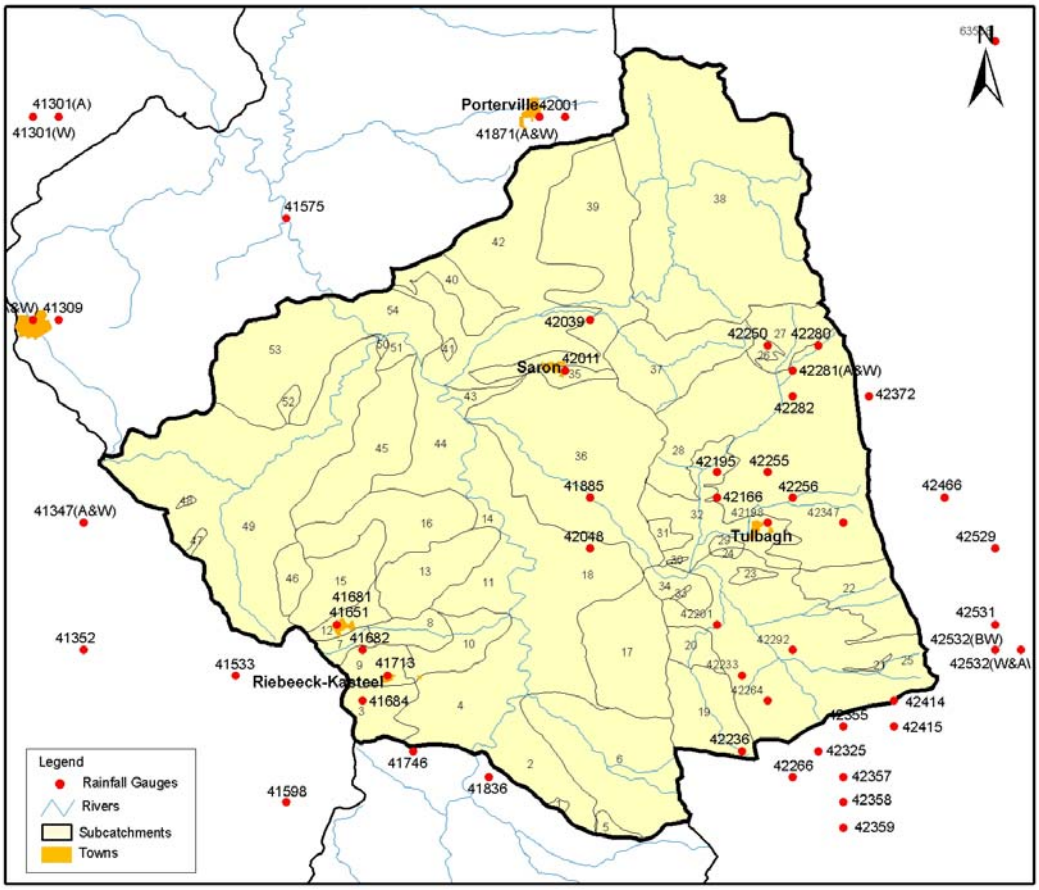

Figure 30 Possible rainfall gauges to be used as the driver rainfall stations for the primary (distributed) sub-catchments between G1H036 and G1H013

Gauging stations G1H013 to G1R003

Using GIS, the rainfall gauging stations that could possibly be used as driver stations for the sub-catchments in this configuration were identified. These are shown in **Figure 31**.

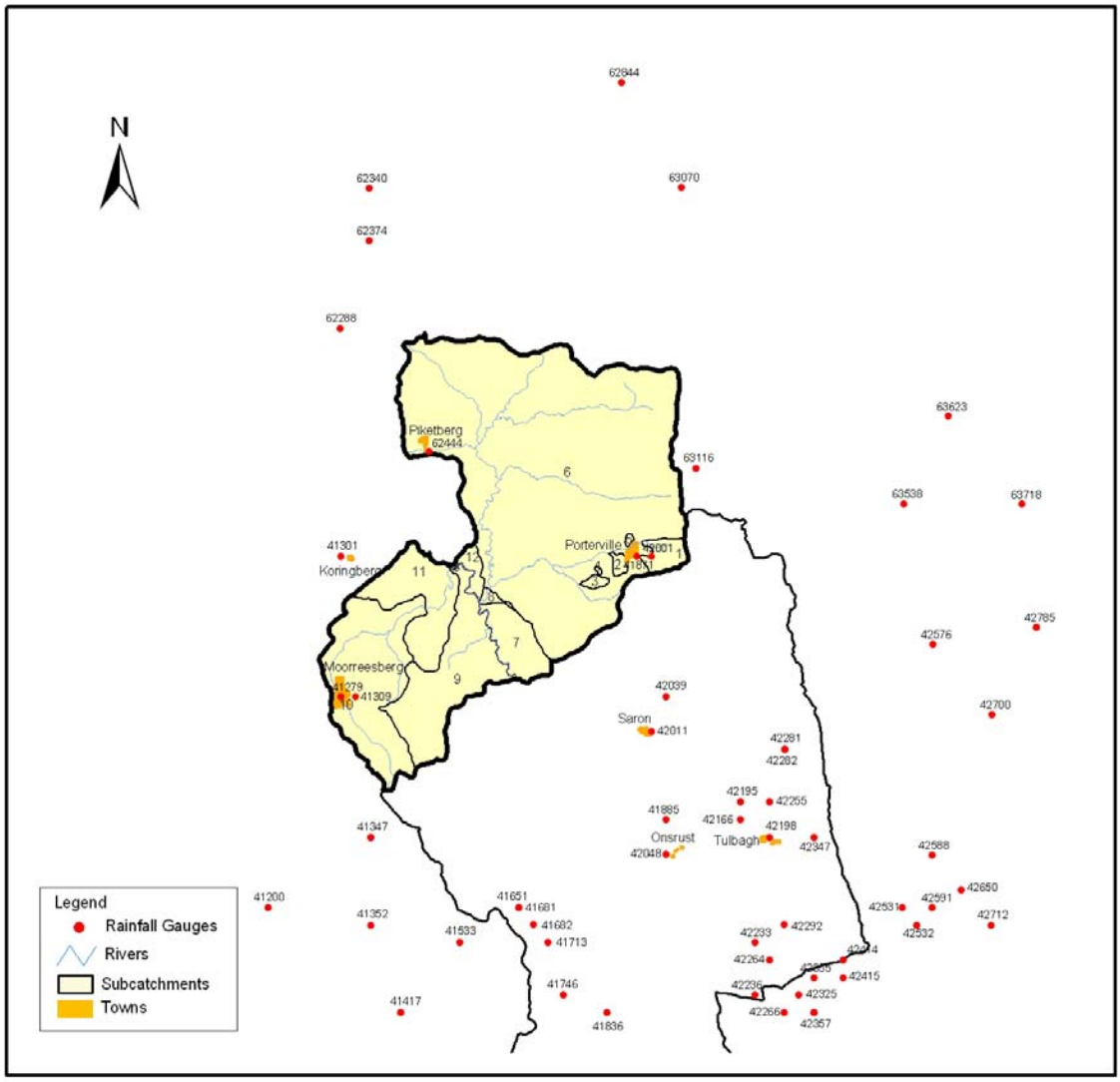

Figure 31 Possible rainfall gauges to be used as the driver rainfall stations for the primary (distributed) sub-catchments between G1H013 and G1R003

4.3.2 Land-use

Land-use data for the Berg River Catchment upstream of Misverstand Dam (G1R003) was obtained from the *Voëlvlei Augmentation Feasibility Study* (VAFS) (DWAF, 1999). In that study several sources of land-use data were considered but the irrigation data obtained from the Department of Agriculture (1997) was eventually used, because this data had sufficient detail on crop types and also compared favourably with the National Land Cover Database Project (1993) (NLCDP) (Fairbanks and Thompson, 1996). Comparison with the irrigation water use, however, revealed that the irrigated areas from the Department of Agriculture database was over-estimated and it was decided, in the VAFS study, to reduce the irrigated areas by 25 per cent. The land-use

coverage used in the VAFS study was available from gauging stations G1H020 to G1R003 and is depicted in **Figure 32**.

In this research a similar approach was adopted. The GIS coverage of the relevant sub-catchments was intersected with land-use information obtained from the Department of Agriculture to produce further sub-divisions of each primary sub-catchment. The database files produced during this intersection process were then opened in an Excel spreadsheet where they were manipulated by reducing the irrigated areas by 25 per cent and adding the excess area to the non-cultivated or natural vegetation portion of the catchment. Since the primary sub-catchments defined in this study did not correspond exactly with those in the VAFS study, it was not possible to use those irrigated areas direcly for this study.

In addition, it should be noted that areas indicated as non-cultivated were replaced with the natural vegetation as obtained from the Acocks (1975) GIS coverage to represent water use by natural vegetation.

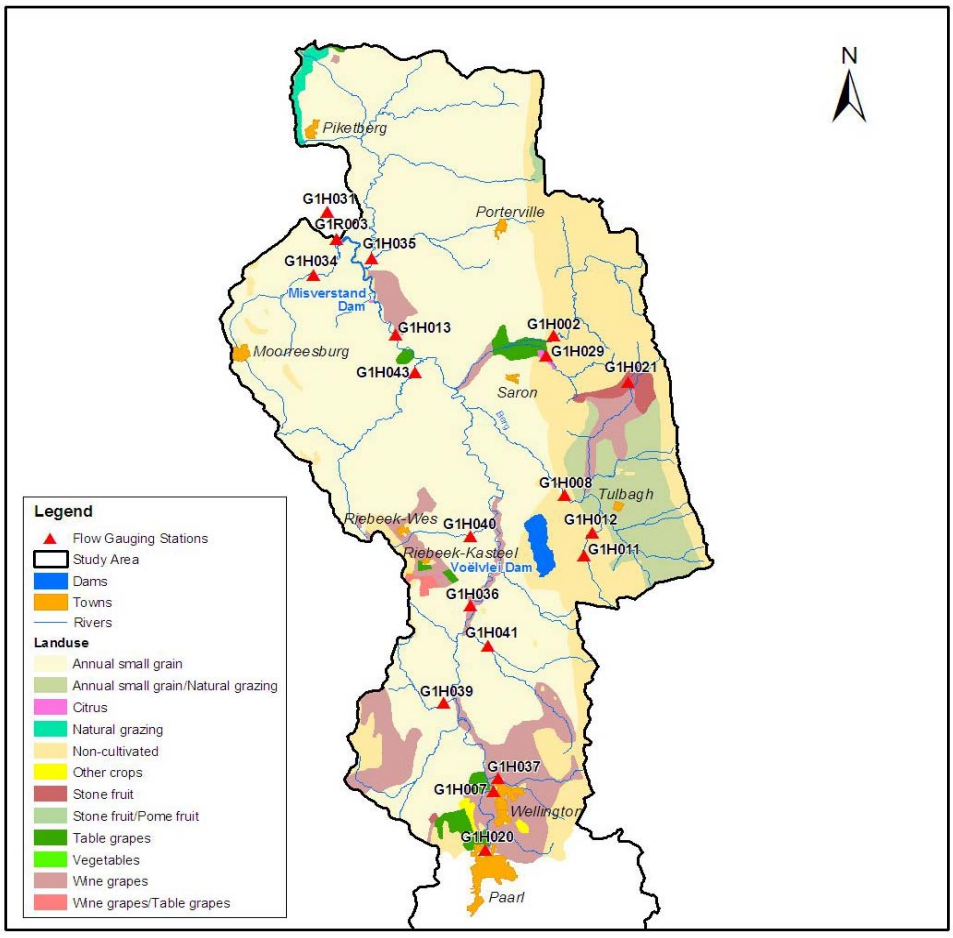

Figure 32 Land-use used in the VAFS study

Land-use information for the Berg River Catchment, downstream of Misverstand Dam (G1R003) was available from several sources. These include the following:

- Working for Water (WfW) - aerial photography.
- Council for Scientific and Industrial Research (CSIR) - satellite imagery.
- Aerial photography commissioned by DWAF in 2001.

The extent to which the WfW aerial photography covered the Berg River Catchment below Misverstand Dam is depicted in **Figure 33** (blocks). Although the aerial photography available from WfW was obtained in 2003, unfortunately only a limited number of photographs in the set had previously been geo-rectified (i.e. had the extents of the image correctly co-ordinated), thus covering a limited portion of the catchment and focusing mainly on the mainstem of the river, where it was expected the bulk of the alien vegetation growth in the catchment would occur.

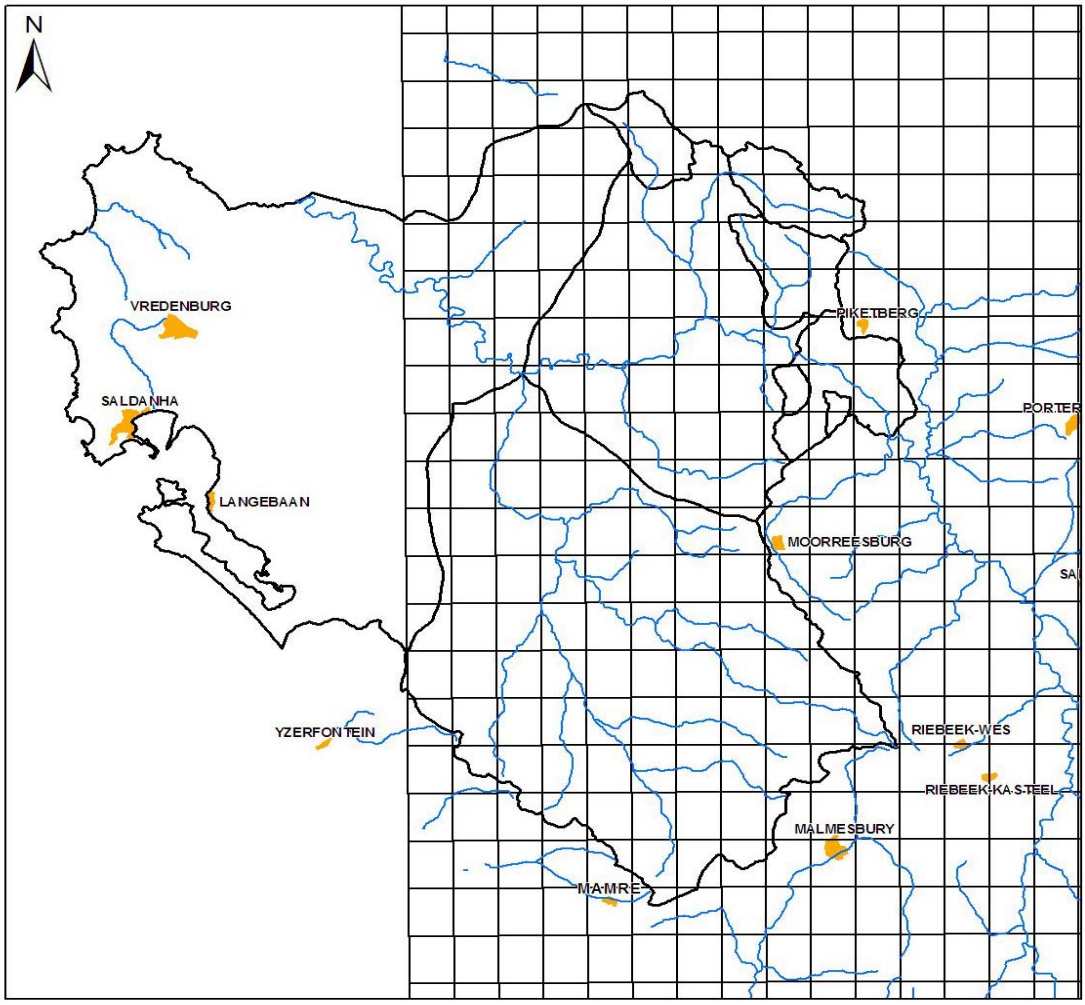

Figure 33 Extent of coverage of the the WfW aerial photography

The satellite imagery obtained from the CSIR was in LANDSAT 5 TM format and was captured in December 2004. LANDSAT 5 TM format has a pixel resolution of 30 m x 30 m and due to this fairly coarse resolution it was difficult to identify the crop types for subsequent capture of the areas on the GIS system.

The aerial photography commissioned by the DWAF in 2001 was available from the Surveyor General's office in Mowbray, Cape Town. The equivalent 1:50 000 topographical maps covered by the photography are as follows:

- 3218cd
- 3218dc
- 3218dd
- 3318aa
- 3318ab
- 3318ba and
- 3318bb

At the time, no aerial photography could be found for the southern most portion of the lower Berg River Catchment (i.e. the portion covered by topographical maps 3318ad, 3318bc) and land-use for this portion was instead obtained from the LANDSAT satellite imagery. The images were later located but not used.

The irrigated areas in the lower Berg River were eventually obtained from the 2001 aerial photography with the assistance of the agricultural extension officer (Mr Johan Meij at the time), from the Department of Agriculture's office in Moorreesburg. The extent of the dryland crops were obtained from the NLCDP with only the newly irrigated areas superseding the dryland crops. The remaining areas were then assigned the natural vegetation as indicated in the Acocks coverage. The resulting land-use coverage for the lower Berg River is shown in **Figure 34**.

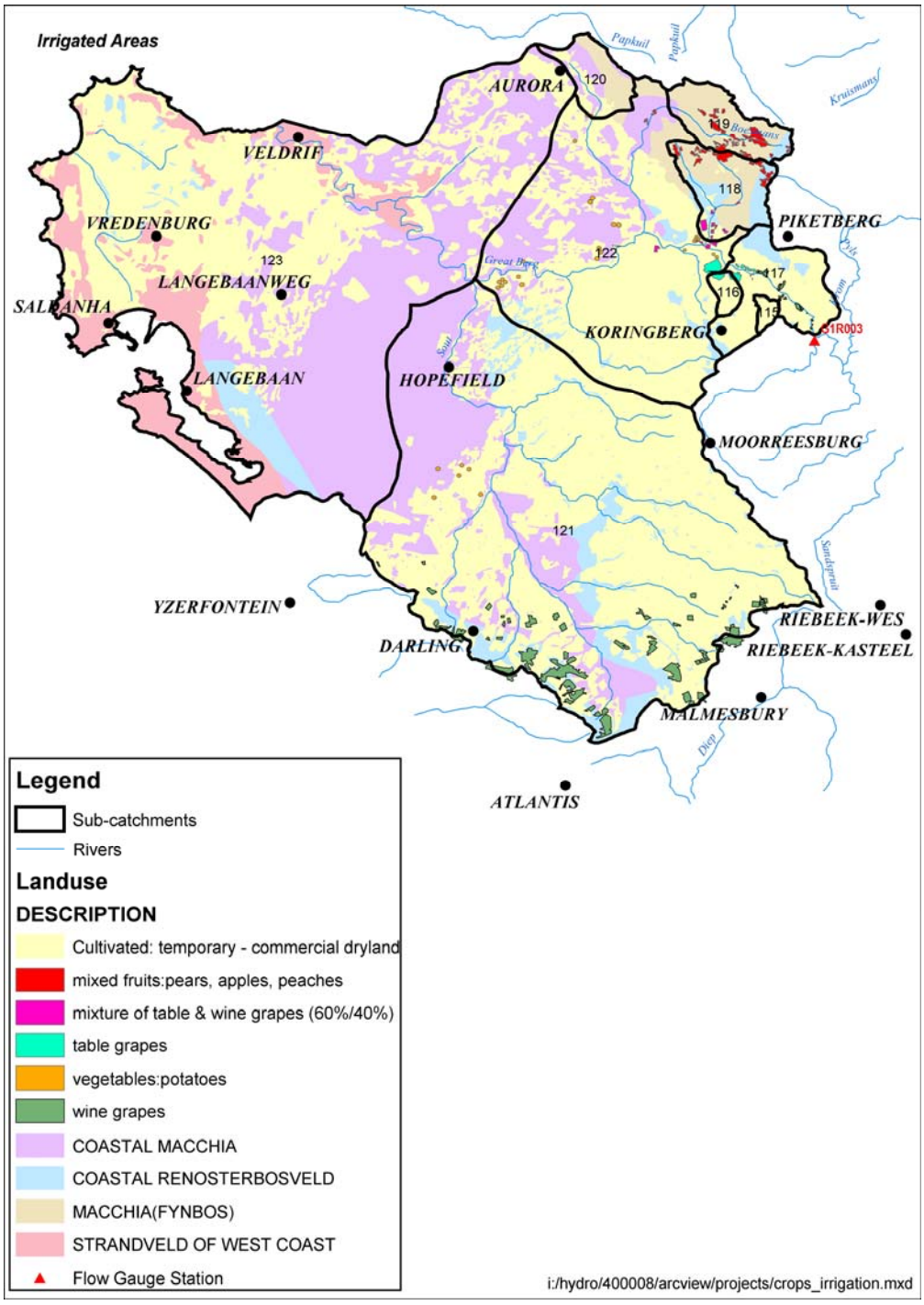

Figure 34 Land-use coverage for the lower Berg River Catchment

The ensuing sections refer to various portions of the Berg River Catchment and show the irrigated areas obtained from the Department of Agriculture's GIS coverage as well as the irrigated area after the 25 per cent reduction in this area. Due to budget limitations, no ground-truthing was undertaken to verify the extent of irrigated areas in the catchment.

G1H020 to G1H036

This portion of the Berg River Catchment was delineated into 46 primary sub-catchments. The breakdown of non-irrigated and irrigated areas is shown in **Table 5.**

Table 5 Irrigated and non-irrigated areas between gauging stations G1H020 and G1H036

Irrigated/Non-irrigated	Areas obtained from GIS coverage (km^2)	Areas after a reduction of 25% in irrigated areas (km^2)
Incremental catchment gauged by gauging station G1H036		
Irrigated area	165.7	124.3
Non-irrigated area	328.7	370.1
Total area	494.4	494.3
Catchment gauged by gauging station G1H037		
Irrigated area	34.8	26.1
Non-irrigated area	37.6	46.3
Total area	72.4	72.4
Catchment gauged by gauging station G1H041		
Irrigated area	21.9	16.4
Non-irrigated area	99.2	104.6
Total area	121.1	121.0

G1H036 to G1H013

This portion of the Berg River Catchment was delineated into 55 primary sub-catchments. The breakdown of non-irrigated and irrigated areas is shown in **Table 6**.

Table 6 Irrigated and non-irrigated areas between gauging stations G1H036 and G1H013

Irrigated/Non-irrigated	Areas obtained from GIS coverage (km^2)	Areas After a Reduction of 25% in Irrigated Areas(km^2)
Catchment gauged by gauging station G1H040		
Irrigated area	2.5	1.9
Non-irrigated area	12.9	13.5
Total area	15.4	15.4
Catchment gauged by gauging station G1H008		
Irrigated area	54.2	40.7
Non-irrigated area	321.1	334.6
Total area	375.3	375.3
Catchment gauged by gauging station G1H021		
Irrigated area	2.2	1.7
Non-irrigated area	16.4	16.9
Total area	18.6	18.6
Catchment gauged by gauging station G1H029		
Irrigated area	1.3	1.0
Non-irrigated area	34.9	35.2
Total area	36.2	36.2
Catchment gauged by gauging station G1H002/G1H028		
	No irrigated areas shown	
Catchment gauged by gauging station G1H043		
Irrigated area	1.8	1.3
Non-irrigated area	153.1	153.5

Irrigated/Non-irrigated	Areas obtained from GIS coverage (km^2)	Areas After a Reduction of 25% in Irrigated Areas(km^2)
Total area	154.9	154.8
Incremental catchment gauged by gauging station G1H013		
Irrigated area	67.5	50.6
Non-irrigated area	850.4	867.3
Total area	917.9	917.9

G1H013 to G1R003

This portion of the Berg River was delineated into 13 primary sub-catchments. The breakdown of non-irrigated and irrigated areas is shown in **Table 7**.

Table 7 Irrigated and non-irrigated areas between gauging stations G1H013 and G1R003

Irrigated/Non-irrigated	Areas obtained from GIS coverage (km^2)	Areas after a reduction of 25% in irrigated areas(km^2)
Incremental Catchment gauged by gauging station G1R003		
Irrigated area	21.8	16.3
Non-irrigated area	197.4	202.8
Total area	219.2	219.1
Catchment gauged by gauging station G1H035		
Irrigated area	9.5	7.2
Non-irrigated area	664.7	667.1
Total area	674.2	674.3
Catchment gauged by gauging station G1H034		
Irrigated area	0	0
Non-irrigated area	133.0	133.0
Total area	133.0	133.0

4.4 FARM DAMS

Farm dam information for this study was obtained from two sources:

- Western Cape System Analysis – *Hydrology of the Berg River Basin* (DWAF, 1993), and the
- Voëlvlei Augmentation Scheme : Feasibility Study – *Hydrology Report* (Volume 1) (DWAF, 1999).

The delineation of the sub-catchments required for the ACRU model was quite different from that required for the Pitman monthly modelling used in the above studies. For this reason it was necessary to develop an approach that would on the one hand satisfy the practical requirements of

the ACRU model and on the other make use of the actual land-use areas, farm dam capacities and abstractions used in previous studies for the sake of economy of time and budget.

Establishing Farm Dam Boundaries in the ACRU configuration

The major farm dams in the Berg River Valley (at a 1990 level of development) were identified and digitised during the early 1990s, as part of the Western Cape System Analysis. This process allowed for the demarcation of farm dam boundaries as well as for the determination of capacities using a numerical model and information extracted from digital terrain data (DWAF, 1993). The area-capacity relationships of these farm dams were approximated using the relationship shown below:

$$Area = A.Capacity^{B} \qquad \textbf{Equation 18}$$

Where,

Area	=	km^2 and
Capacity	=	x 10^6 m^3
A,B	=	Constants

It was considered impractical to provide each farm dam with its own sub-catchment and the "dummy dam" approach was employed instead. The "dummy dam" represents the total capacity of a group of farm dams that is clustered together spatially. The dummy dam is situated at the outlet of the concatenated catchments upstream of the farm dam cluster

In this study, the most up-to-date input data available needed to be used and in the case of farm dams this was the data from the VAFS study (DWAF, 1999), which was based at the 1996 level of development. The VAFS study showed that there had been an increase in farm dam surface area (and thus capacity) from 20.97 km^2 in 1990, to 23.39 km^2 in 1996. The VAFS study, however, gave no indication in which part of the catchment the growth in farm dams had occurred.

The approach described in the ensuing section was developed to obtain an estimate of the farm dam areas in each of the sub-catchments containing a farm dam.

The 'A' and 'B' coefficients in **Equation 18** for each calibration sub-catchment were obtained from the WCSA report (DWAF, 1999). It was then assumed that the pseudo sub-catchments that comprised these calibration sub-catchments would inherit these coefficients. Unlike the

configuration in the WCSA study where one farm dam (dummy dam) was created per calibration sub-catchment, the ACRU configuration created a dummy farm dam for each primary sub-catchment that contained a number of smaller farm dams. This meant that a calibration catchment, say the catchment gauged by G1H041, which originally contained one dummy farm dam in the WCSA now contained six farm dams in the ACRU configuration, each with a realistic representation of the area upstream of the dam.

Using the 1990 GIS coverage for the farm dams it was possible to determine the surface area of the farm dams within the sub-catchment and to convert this to the corresponding volume. It should be noted at this point that the area/volume relationship (**Equation 18**) and the appropriate coefficients are applicable to the single dummy farm dam that was created in that sub-catchment. Since this ACRU set-up resulted in the formation of more than one dummy dam, it was necessary to develop a ratio that could be used to scale up the combined capacity of the farm dams in the Berg River Catchment such that it matched the capacity quoted in the VAFS study. This ratio was developed as follows:

i) The surface areas of the farm dams in each of the catchments were determined from the GIS coverage information.
ii) The VAFS study indicated that there was growth from 1990 to 1996 in the farm dam capacity in the catchment gauged by G1H037.
iii) Using the 'A' and 'B' coefficients, a volume for each dummy dam was calculated and summed to obtain a total capacity of farm dams in the sub-catchment. For example, in the sub-catchment gauged by G1H037, this volume was 0.73×10^6 m^3.
iv) Using the surface area data (1990 level of development) from the WCSA, it was possible to calculate the total farm dam capacity in the sub-catchment gauged by G1H037 (e.g. 3.59×10^6 m^3).
v) Ratio 1, relating the capacity from the WCSA to that of this study was determined by dividing the area determined in (iv) above by that determined in (iii) to obtain 4.92.
vi) Ratio 2, relating the 1996 capacity (4.24×10^6 m^3) to the 1990 (3.59×10^6 m^3) capacity was obtained by dividing the 1996 total farm dam capacity by the 1990 capacity to obtain 1.18.
vii) Ratio 3 was then obtained by multiplying ratio 1 with ratio 2 to obtain 5.78, which was used to scale each of the total farm dam capacities in the catchment gauged by G1H037 up to the 1996 level of development.

By using the procedure described above, it was possible to obtain the 1996 capacity of farm dams as reported in the VAFS study for each of the sub-catchments used in the ACRU configuration.

It should be noted that the ACRU model requires the volume and surface area to be specified in units of m^3 and m^2, respectively. The 'A' and 'B' coefficients, however, are applicable to **Equation 18** where the units for capacity and surface area are 10^6 m^3 and km^2, respectively. The equivalent parameters, in ACRU, for the 'A' and 'B' parameters are reservoir constant (RESCON) and reservoir exponent (RESEXP). These parameters were obtained by plotting volume in m^3 against the surface area in m^2 and then fitting a curve with the form as shown in **Equation 18**, to obtain the values to be used for RESCON and RESEXP. An example of these curves for the catchment gauged by G1H008 is depicted in **Figure 35**.

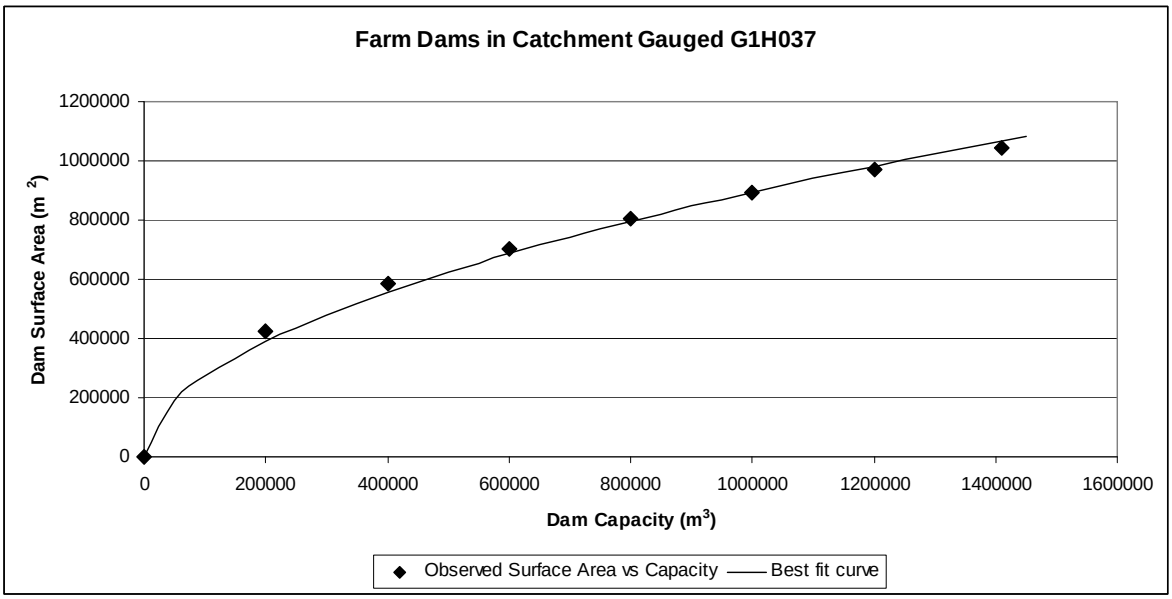

Figure 35 Relationship between farm dam surface area and capacity in catchment gauged by G1H008

4.4.1 G1H020 to G1H036

The farm dam catchment boundaries, as defined in the WCSA study (DWAF, 1993), were used in this application and are depicted in **Figure 36.**

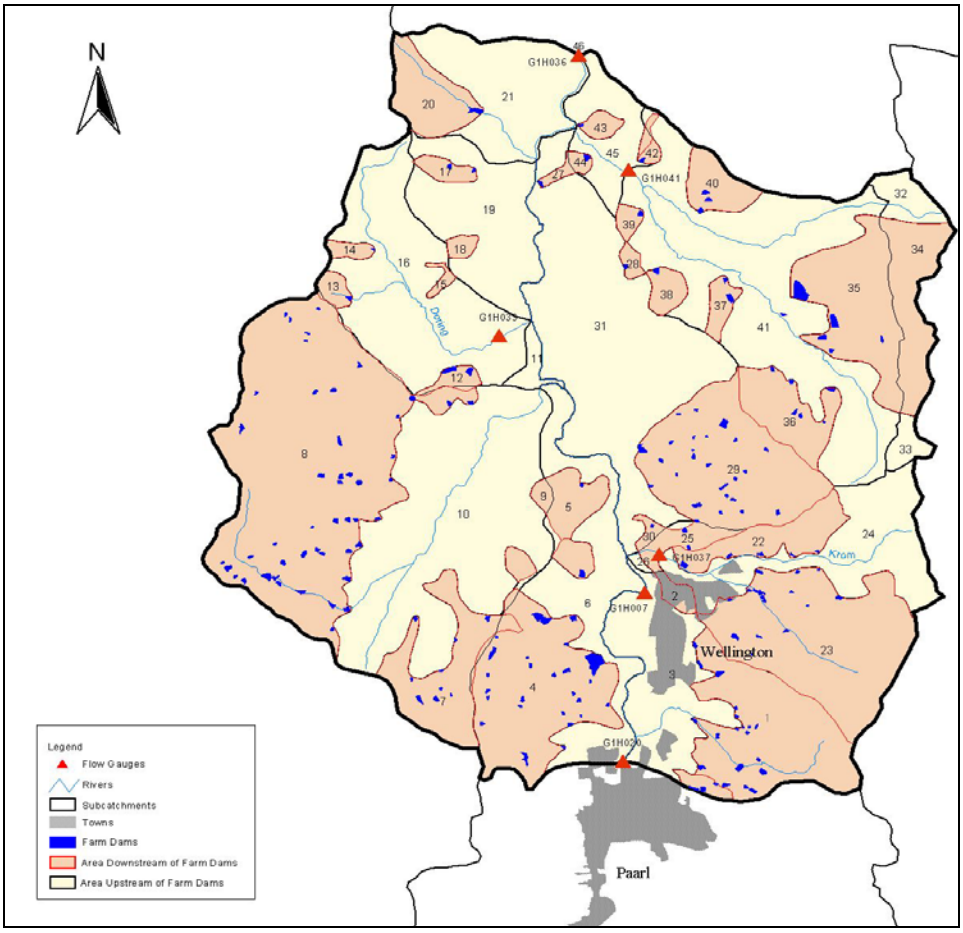

Figure 36 Farm dam catchment boundaries for the Berg River Catchment between gauging stations G1H020 and G1H036

Table 8 lists the values of the coefficients A (RESCON) and B (RESEXP) determined for the farm dams located in this sub-catchment.

Table 8 Coefficients used to relate farm dam capacity to surface area for the catchment between G1H020 and G1H036

Incremental sub-catchment	A (RESCON)	B (RESEXP)
Incremental G1H036 catchment	389.41	0.57
G1H037 catchment	274.71	0.52
G1H041 catchment	180.32	0.58

4.5 FLOW VERIFICATION OF THE ACRU MODEL

The approach whereby model parameters are adjusted to produce outputs that are representative of an observed record is referred to as calibration. Görgens (1983) explained three approaches that are commonly used for the estimating the values of parameters in view of calibration. These include:

- *A priori approach* – this approach essentially involves the estimation of model parameters based on inferences made from measurable catchment characteristics. Görgens (1983) explained that this approach was usable when the model was physically realistic so that certain model parameters could roughly be associated with (and thus be inferred from) a measured catchment characteristic.

- *Goodness-of-fit approach* – this approach essentially relies on the correspondence of simulated values with an observed record and subsequent adjustment of calibration parameters until an acceptable fit is obtained. Quantification of this closeness-of-fit usually relies on the definition of statistical entities which are collectively known as *objective functions* (Görgens, 1983). Roberts (1987) described the objective function as a "mathematical function expressing the most desired characteristics between the model's simulated output and the real world observations". Visual inspection, which is difficult to quantify and cannot be completely defined, is also used in this approach.

- *Combination of a priori and goodness-of-fit* – this is essentially a mixed approach and is dependent on the extent of the model's physical nature and the resources available to obtain *a priori* estimates (Görgens, 1983).

Since ACRU is essentially a *physical conceptual* model, most of the inputs are sourced from databases populated with measurable catchment characteristics (e.g. soils information) and adjustment of flow-related parameters would be required only in a limited number of cases. This is of course based on the assumption that a representative driver rainfall station was used in the first instance. Additionally, the salinity-related parameters in the salinity module of ACRUS*alinity* could potentially have been determined based on the *a priori* approach. In this study, however, a combination of the *a priori* and goodness-of-fit was adopted to circumvent the restriction imposed by the excessive costs in determining these. The objective function criteria used in the study will be defined in the following sections.

4.5.1 Objective functions

A suite of objective functions are available as criteria for measuring the goodness-of-fit (Görgens, 1983), but only those which were specifically used in this study will be presented here. It should be noted that the objective functions were employed only for outputs that had been aggregated from a daily to a monthly basis.

The flow routing option in ACRU was not invoked and because of this, the simulated stormflow peaks could possibly occur earlier than those expected to occur in reality. Since the timing of daily simulated peaks was shifted relative to observed flow peaks, an objective function approach was not possible on a daily basis and a comparison was done by visual inspection of the goodness-of-fit and by using a daily flow duration curve. A similar approach was adopted by Tarboton *et al.* (1992) in the hydrological modelling of the Mgeni catchment.

When employing the visual inspection of the goodness-of-fit, the following aspects were specifically examined:

- The occurrence of peaks, taking into consideration the effect of neglecting flow routing as well as the rainfall driver station used to produce the simulated flow
- The recession of the simulated stormflow (1-4 days after rainfall) in comparison with that of the observed flow
- The baseflow recession of the simulated flow in comparison with that of the observed flow

Difference in Mean Monthly Runoff (MMR)

This objective function shows the extent of conservation of the mean, and for representative simulated outputs and observed flows, this parameter has to tend towards zero (Görgens, 1983).

$$\Delta MMR = \frac{100.(MMR_s - MMR_o)}{MMR_o} \qquad \textbf{Equation 19}$$

Where,

MMR_s = Simulated MMR and
MMR_o = Observed MMR

It should be noted that **Equation 19** could equally be applied to salt load by replacing the MMR with monthly salt loads. The discussion below makes reference only to the flow component of the model outputs.

Coefficient of Determination (r^2)

This coefficient measures the simulated values as estimated by a linear regression model (Schulze *et al.*, 1994). In simpler terms, the r^2 measures the extent to which the simulation model reproduces the variance of the observed flows. It is represented as follows (Schulze, 1995):

$$r^2 = \frac{\sum_{i=1}^{n}\left(y_i - \bar{y}\right)^2 - \sum_{i=1}^{n}\left(y_i - \hat{y}_i\right)^2}{\sum_{i=1}^{n}\left(y_i - \bar{y}\right)^2} \qquad \textbf{Equation 20}$$

Where,

y_i = the simulated time series value

$\bar{y}$ = the mean of the simulated values

$\hat{y}_i$ = the estimated value from the regression line of y on x

Coefficient of Efficiency (E_c)

Görgens (1983) explains that the coefficient of efficiency, E_c, is used as a dimensionless measure of the one-to-one fit, sensitve to systematic errors.

$$E_c = \frac{\sum_{i=1}^{n}\left(y_i - \bar{y}\right)^2 - \sum_{i=1}^{n}\left(y_i - x_i\right)^2}{\sum_{i=1}^{n}\left(y_i - \bar{y}\right)^2} \qquad \textbf{Equation 21}$$

Where,

x_i = the observed time series value

All other parameters have the same meaning as before.

The value of E_c should be optimised to be as close as possible to the value of r^2. The difference between the E_c and r^2 values is considered to be the degree of systematic error in the simulated values. According to Schulze *et al.* (1995) obtaining a coefficient of efficiency close to r^2 is frequently more important, hydrologically, than a high r^2.

The evaluation of the comparison between the daily simulated and observed flows presented in the ensuing sections will be based on the criteria outlined above.

4.5.2 Verification at G1H037 (Krom River at Wellington)

Flow verification at this gauge (see **Figure 23**) was completed over the period 1982 to 1992, using land-use data obtained at the 1998 level of development. The modelling process did not account for the variation in land-use during the verification period and it was therefore necessary to identify the possible effects of this on the simulated streamflow record.

Irrigation water use was identified as the biggest user of water in this sub-catchment and because of this, it was expected that there would be some differences between the observed record and the simulated flow records, especially for the period prior to 1990, when the 1998 irrigated area (26.91 km^2 based on the area obtained from the GIS coverage) was approximately 400% more than the irrigated area in 1990.

In the WCSA (DWAF, 1993 (1)), it was reported that water was transferred from the adjacent Breede River Catchment at an estimated 0.22 x 10^6 m^3/month. In the ACRU configuration this import enters the catchment upstream of the abstractions made for run-of-river (directly from the river) irrigation, increasing the possibility of satisfying that irrigation demand. Winter abstraction to fill the farm dams was not modelled due to the lack of up-to-date information on this.

Observed flow data at gauging station G1H037 was available from 1978 until 1992. A large portion of the dataset (June 1980 to October 1981), however, was missing and consequently only the latter portion of the record was used for flow verification. No patching of the observed record was required after January 1982.

The monthly comparison of the simulated and observed flows at G1H037 is depicted in **Figure 37**, which shows that for most of the winter months, the simulated flows are below the observed flows with the exception of winter in 1985, when the simulated flows marginally

exceeded the observed flows. This could be due to the catchment not being delineated into sufficient primary sub-catchments that could adequately capture the spatial variability of the catchment rainfall.

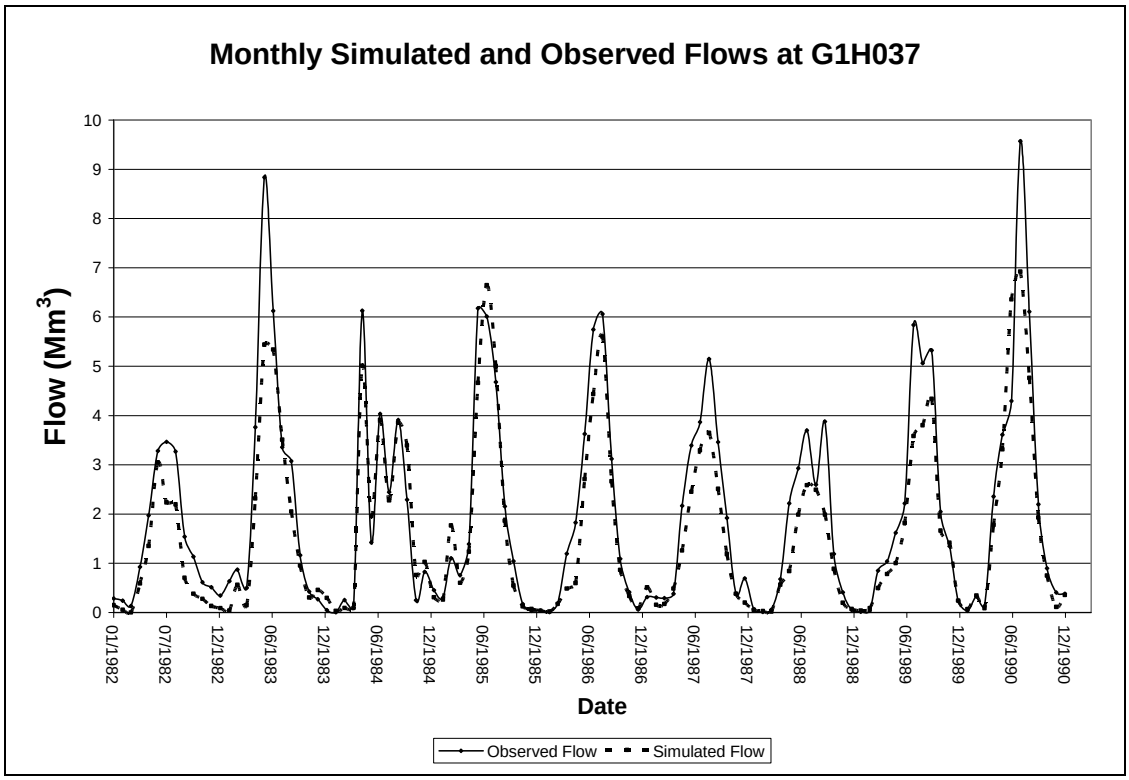

Figure 37 Monthly simulated and observed flows at gauging station G1H037

A comparison of the simulated and observed daily flows is depicted in **Figure 38** which shows the daily simulated and observed trends. For those particular months shown in **Figure 38** the simulated daily peak flows exceeded the observed flow. This was, however, not a general occurrence, since most of the montly simulated flows shown in **Figure 37** under-estimated the observed time series.

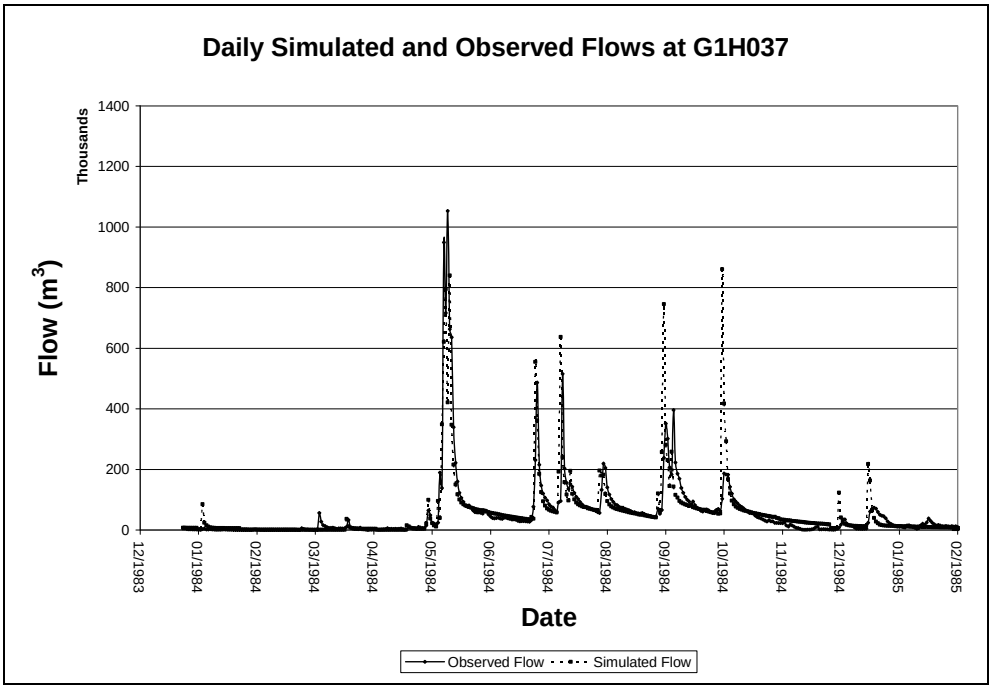

Figure 38 Daily simulated and observed flows at gauging station G1H037

A comparison of the daily flow duration curves for the observed and simulated flows is depicted in **Figure 39**. The figure shows that percentage exceedances at the various flows are not always comparable possibly caused by the under-simulated daily flows for the winters of 1983, 1989 and 1990.

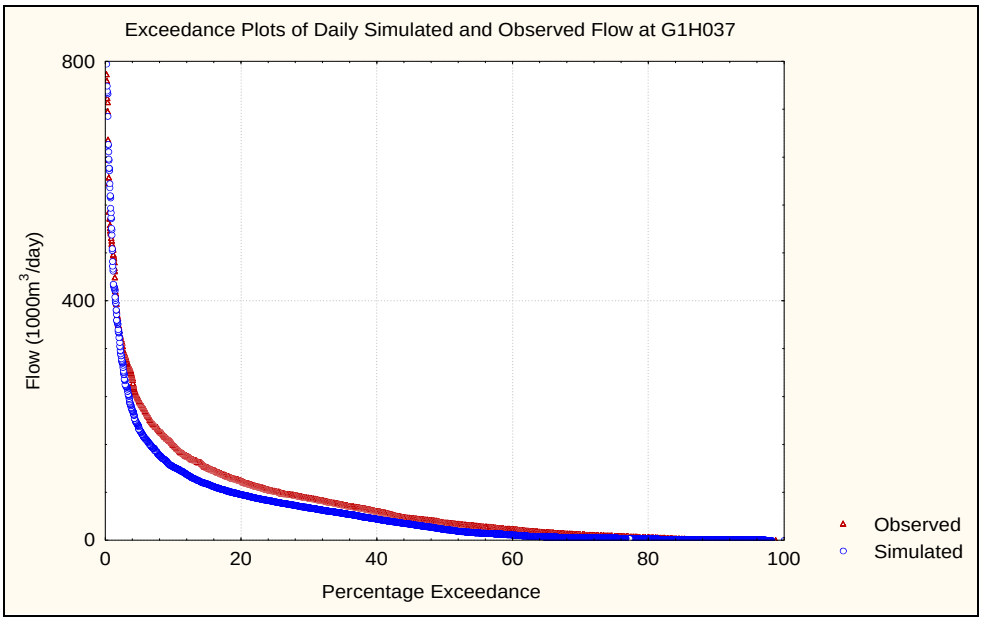

Figure 39 Daily flow duration curves for simulated and observed flows at G1H037

To test the extent of the under-simulation effect, the winter of 1990 was removed from the flow duration analysis and an improved correspondence shown in **Figure 40** was obtained.

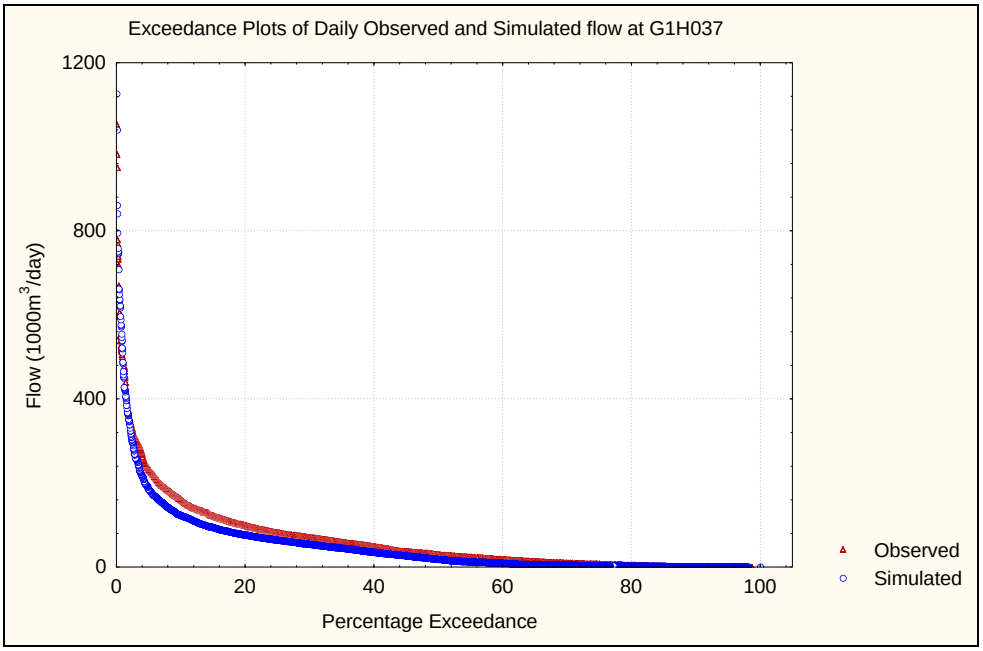

Figure 40 Daily flow duration curves for simulated and observed flows at G1H037 (flow of winter 1990 removed)

Pertinent objective function values for the monthly observed and simulated flows at gauging station G1H037 are shown in **Table 9,** which shows an 11% under-simulation of MMR over the 10 year period from 1982 to 1992. Acceptable values (Schulze *et al.*, 1995) for the coefficient of determination, r^2 and coefficient of efficiency of 0.8 and 0.78 were obtained, respectively.

Table 9 Objective function values for simulated and observed flows at G1H037

Statistics for G1H037 (1980 –1994)	Monthly totals of daily simulation
Mean observed streamflow (10^6 m^3/month)	1.8
Mean simulated streamflow (10^6 m^3/month)	1.6
% difference in standard deviation	1.53
Coefficient of determination (r^2)	0.80
Coefficient of efficiency	0.78

4.5.3 Verification at G1H041 (Kompanjies River at De Eikeboomen)

Based on the WCSA report (DWAF, 1993 (1)) the mean annual rainfall in this sub-catchment varies from 500 mm in the west to 1 800 mm in the east and this can clearly be seen from **Figure 41** which shows the rainfall distribution for this portion of the Berg River Catchment. The increased rainfall in the eastern parts of the catchment can be attributed to the topography of this region.

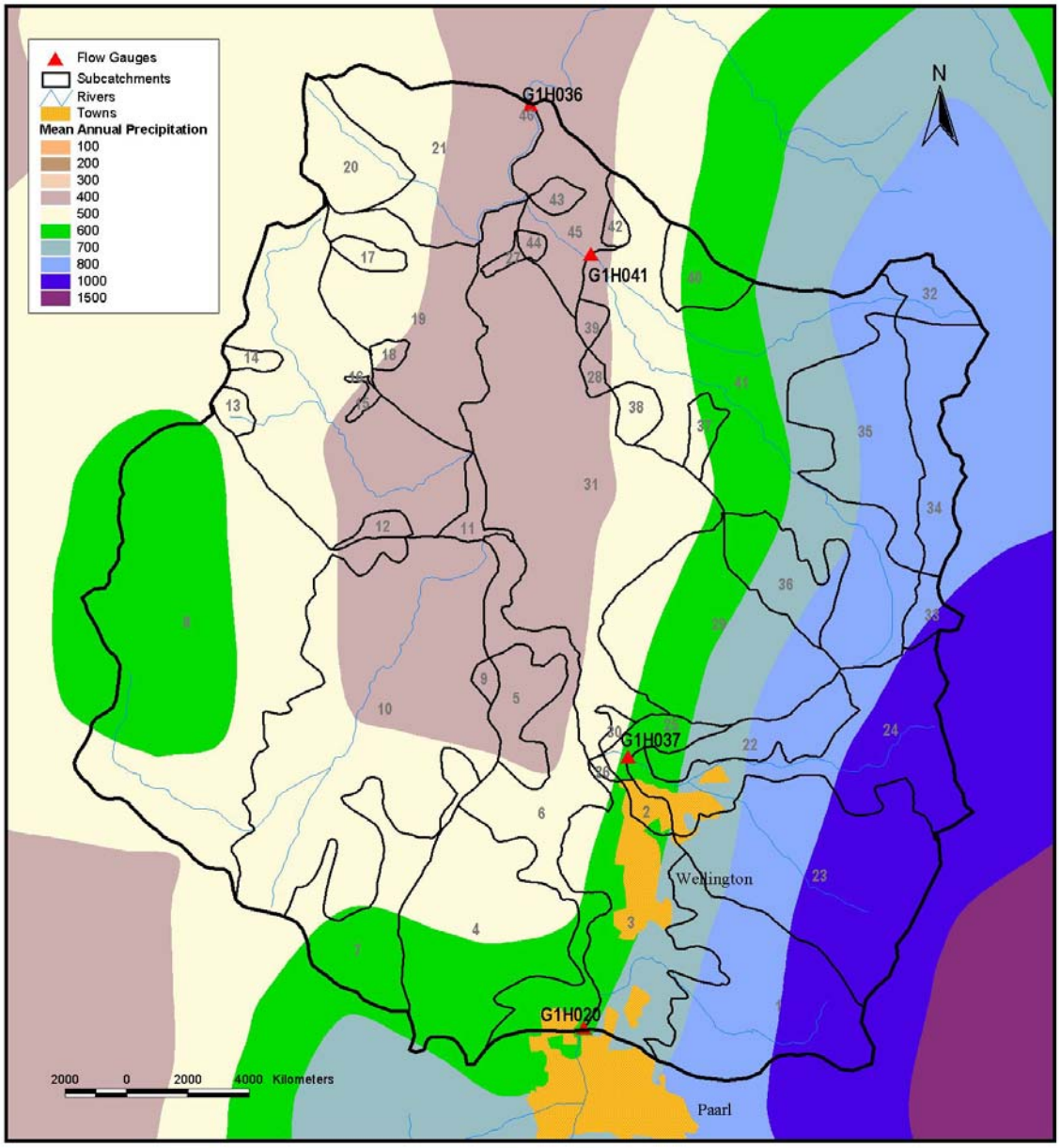

Figure 41 Rainfall distribution in the Berg River Catchment between gauging stations G1H020 and G1H036

As a result of the above, the catchment was split into a *high Mean Annual Precipitation (MAP)* and *low MAP* region with different driver rainfall stations being assigned to each of these regions. In this way, it was possible to capture the observed spatial variability in rainfall in the catchment.

The available land-use information at the 1998 level of development showed that 15.73 km^2 were irrigated as opposed to the 2.72 km^2 in 1990 (DWAF, 1993 (1)) which indicates an increase of approximately 480%. Since the ACRU model was run at a static level of development it was expected that this would affect the streamflow volumes simulated during the summer months when the over-estimated irrigation demand would be imposed on the water resources in ACRU. Winter abstractions to fill farm dams were not modelled because of the small volumes compared to the natural inflow.

The monthly comparison of observed and simulated flows is shown in **Figure 42**.

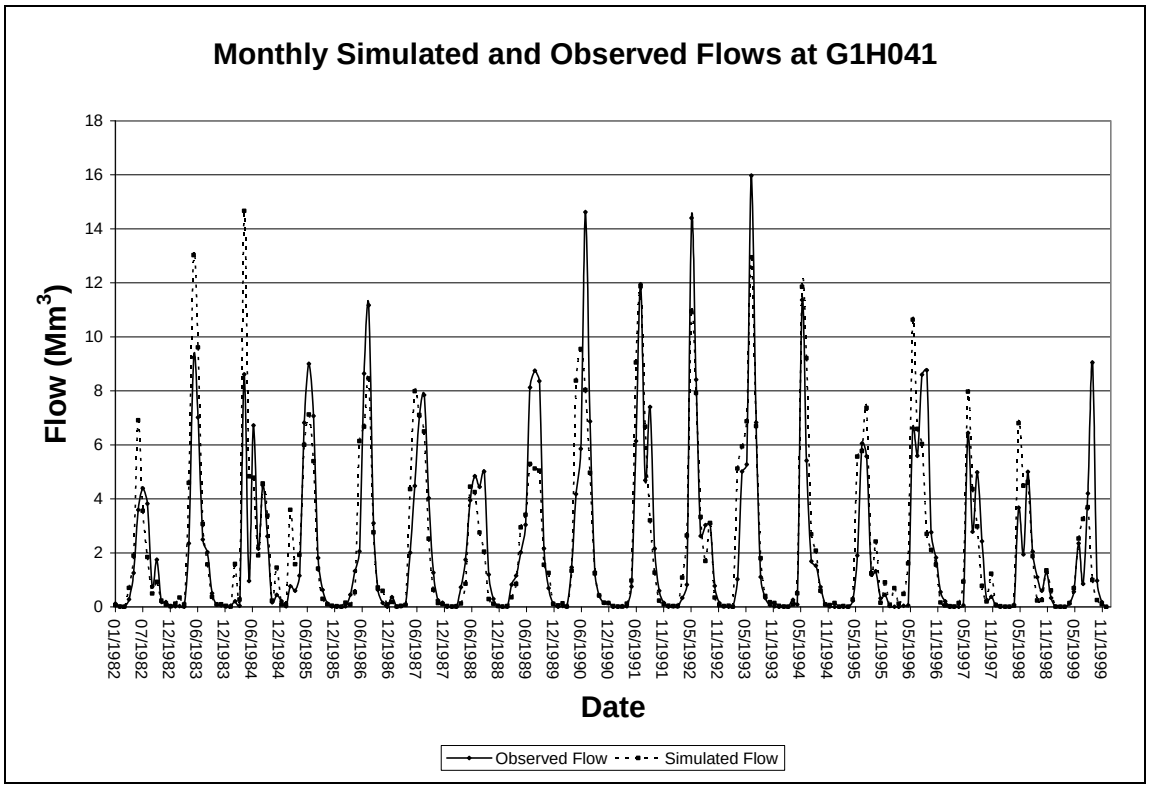

Figure 42 Monthly simulated and observed flows at G1H041

The differences in, particularly, the simulated and observed winter flows could mainly be ascribed to the rainfall measured at the driver rainfall station. In **Figure 29** it was shown that no rainfall gauges were located within this catchment and that the appropriate driver rainfall station

for each primary sub-catchment was selected based on the criteria presented in **Section 4.3.1**. Further sub-division of the catchment upstream of G1H037 could possibly be attempted if refinement was required. Although this may not result in the selection of a different driver rainfall station for the new sub-catchment it would at least provide different monthly Rainfall Adjustment Factors (CORPPT) which could in turn lead to different aerial rainfall and run-off patterns. Adjusting the values of the flow-related parameters did not significantly improve the fit between the simulated and observed flow records.

A comparison of daily simulated and observed flows is depicted in **Figure 43**, which shows that daily simulated trends are representative of the observed trends, both for high flows and recession flows.

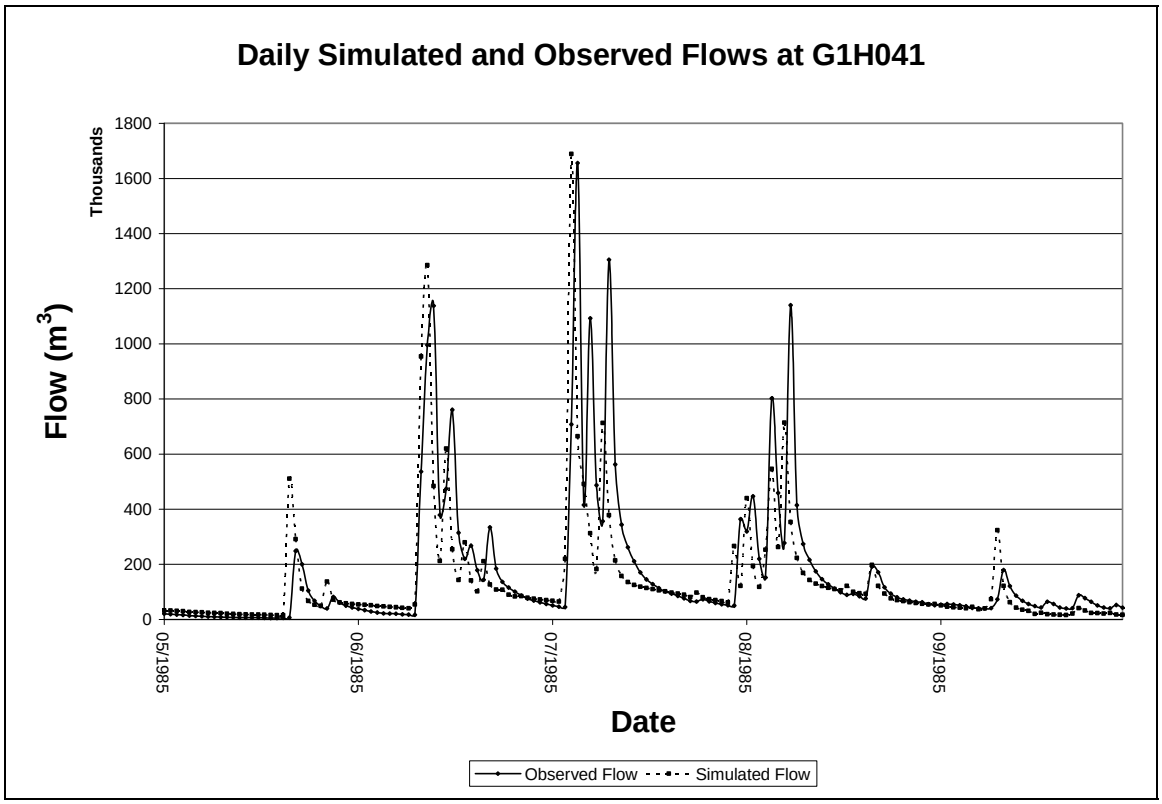

Figure 43 Daily simulated and observed flows at gauging station G1H041

The daily flow duration curve for the simulated and observed flows at gauging station G1H041 is depicted in **Figure 44,** from which it can be seen that the flow duration curve of the simulated flows is representative of the flow duration curve of the observed flows over the entire range of flows.

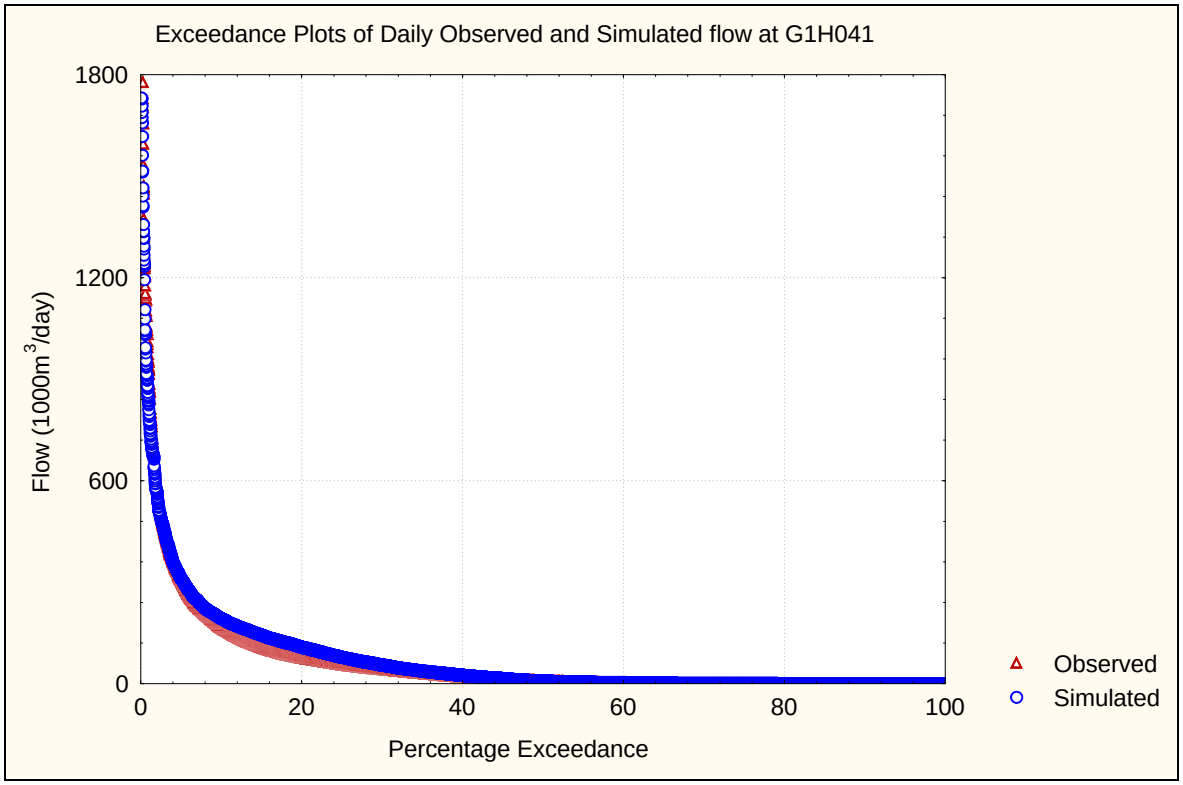

Figure 44 Daily flow duration curves at gauging station G1H041

Pertinent objective function values for the monthly observed and simulated flows at gauging station G1H041 are shown in **Table 10** which shows a 6% over-simulation of streamflow over the 19 year period from 1980 to 1999. Acceptable values for r^2 and coefficient of efficiency of 0.74 and 0.72 were obtained, respectively.

Table 10 Statistics for simulated and observed flows at G1H041

Statistics for G1H041 (1980 –1999)	Monthly totals of daily simulation
Mean observed streamflow (x 10^6 m^3/month)	2.1
Mean simulated streamflow (x 10^6 m^3/month)	2.2
% difference in standard deviation	1.4
Coefficient of determination (r^2)	0.74
Coefficient of efficiency	0.72

4.5.4 Verification at G1H036 (Berg River at Vleesbank)

In order to verify the simulated flows at gauging station G1H036 (see **Figure 23**), observed flows measured at gauging station G1H020 were used as a specified input from the Upper Berg River, while the simulated flows at gauging stations G1H037 and G1H041 were used as the tributary inflows.

The irrigated area, at the 1990-level of development, reported for the incremental G1H036 catchment (i.e. excluding the flows measured at gauging stations G1H037, G1H041 and G1H020) in the WCSA (DWAF,1993 (1)) was 57.04 km^2 as opposed to the 124.26 km^2 obtained from the Department of Agriculture Survey (1998). This was an increase of approximately 117% and would affect the comparison of the simulated and observed flows in the early years of the calibration period, especially during the summer months when an increased irrigation demand would be imposed on the water resources in ACRU.

Discharges into the catchment included the Paarl and Wellington wastewater treatment works return flows, while abstractions included that for the Malmesbury water treatment works and the winter abstractions to farm dams. The magnitudes of these imports as obtained from the WCSA (DWAF, 1993 (1)) are shown in **Table 11**.

Winter abstractions to farm dams were split based on the percentage of the total cultivated area irrigated from farm dams which occurred in the particular primary sub-catchment.

Table 11 Water imported and exported to the catchment gauged by G1H036 (DWAF, 1999)

	Jan	Feb	Mar	Apr	May	Jun	Jul	Aug	Sep	Oct	Nov	Dec
Paarl and Wellington return flows (transferred in)												
10^6 m^3	0.5	0.5	0.6	0.5	0.6	0.7	0.8	0.8	0.7	0.6	0.5	0.5
1000m^3/day	16.1	16.1	19.4	16.7	19.4	23.3	25.8	25.8	23.3	19.4	16.7	16.1
Malmesbury Abstraction (transferred out)												
10^6 m^3	0.02	0.02	0.02	0.02	0.02	0.01	0.02	0.02	0.03	0.03	0.03	0.02
1000m^3/day	0.6	0.6	0.6	0.7	0.6	0.3	0.6	0.6	1.0	1.0	1.0	0.7
Winter Abstractions to Farm Dams (transferred out)												
10^6 m^3	0	0	0	0	7.16	3.17	0.41	0	0	0	0	0
1000m^3/day	0	0	0	0	231	106	13.2	0	0	0	0	0
Net Imports to Catchment												
10^6 m^3	0.48	0.48	0.58	0.48	-6.57	-2.49	0.78	0.78	0.67	0.57	0.47	0.48
1000m^3/day	15.5	15.5	18.7	16.0	-212	-83	25.2	25.2	22.3	18.4	15.7	15.5

The comparison of the monthly simulated and observed flows is shown in **Figure 45**.

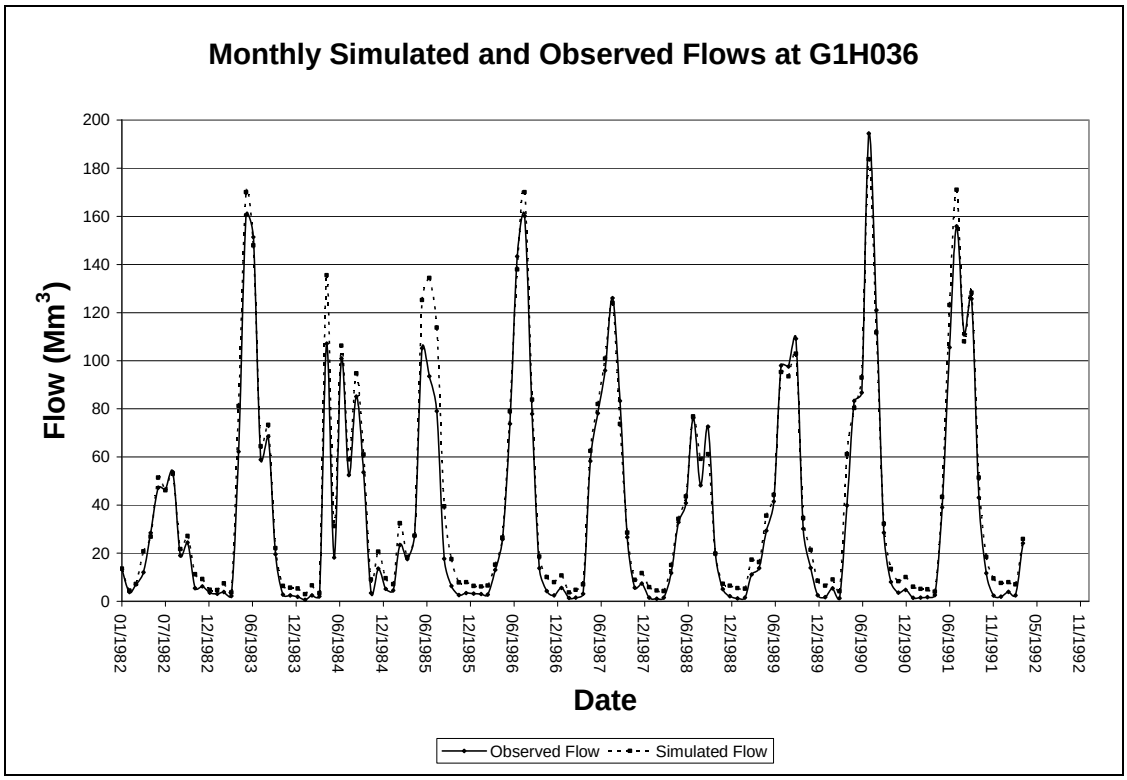

Figure 45 Monthly simulated and observed flows at G1H036

Visual inspection of **Figure 45** suggests that the monthly simulated flows are representative of the observed flows. This was, however, to be expected because of the observed flows at gauging station G1H020 being used as a specified inflow to the incremental catchment. It was noted that the volume of flows generated in ACRU upstream of gauging station G1H020 was much bigger than that generated from the incremental catchment gauged by gauging station G1H036 and, as a consequence, the flow-related parameters in incremental catchment G1H036 could be insensitive to changes in their respective values.

Pertinent objective function values for the monthly observed and simulated flows at gauging station G1H036 are shown in **Table 12** which shows a 13% over-simulation of streamflow over the 12 year period from 1982 to 1994. Relatively high values for r^2 and coefficients of efficiency of 0.96 and 0.95 were obtained, respectively.

Table 12 Objective function values for simulated and observed flows at G1H036

Statistics for G1H036 (1982 –1992)	Monthly totals of daily simulation
Mean observed streamflow (10^6 m^3/month)	50.9
Mean simulated streamflow (10^6 m^3/month)	57.9
% difference in standard deviation	1.87
Coefficient of determination (r^2)	0.96
Coefficient of efficiency	0.95

A comparison of the simulated and observed daily flows is depicted in **Figure 46**, which shows that the daily trends in the observed flow pattern are mimicked by the simulated flow record.

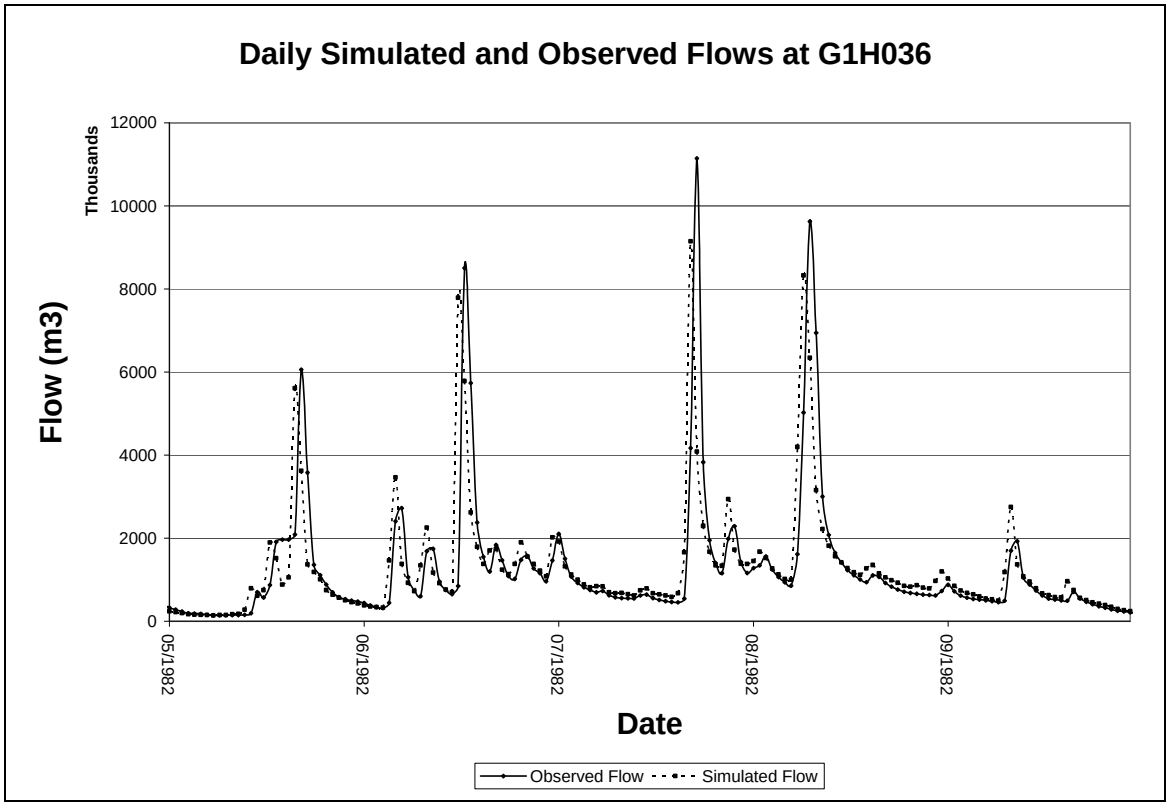

Figure 46 Daily Simulated and Observed Flows at Gauging Station G1H036

The daily flow duration curve for the simulated and observed flows at gauging station G1H036 is depicted in **Figure 47.** Visual inspection of this figure shows that the flow duration curve of the simulated flows is representative of the flow duration curve of the observed flows over the entire range of flows.

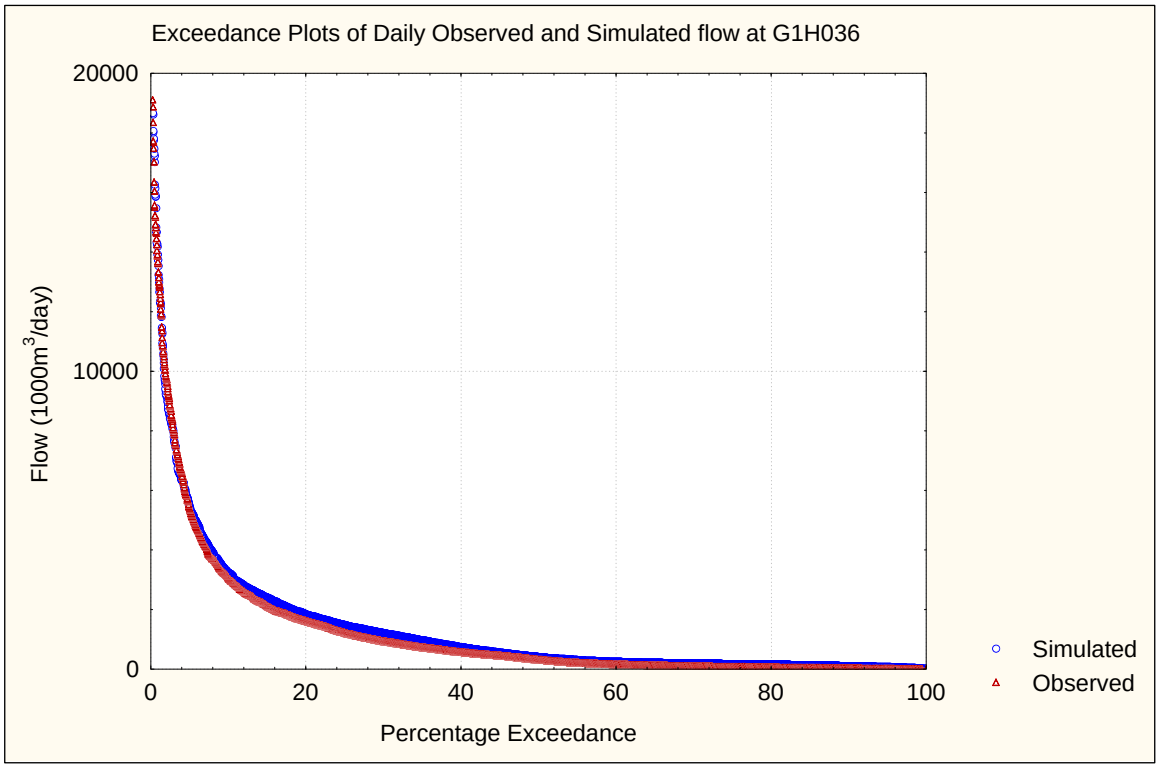

Figure 47 Simulated and Observed Flow duration curves at Gauging Station G1H036

4.5.5 Verification at G1H002/G1H028 (24 Rivers at Drie-Das Bosch)

This is the site of the streamflow diversion into the Voëlvlei Canal. The flow verification at this gauge did not include the variation in land-use over the verification period but was instead completed with land-use data at a static 1998 level of development. The available land-use data for 1998 showed that no crops were cultivated upstream of the gauging station G1H002 (see **Figure 25**) while in the WCSA study (DWAF, 1993 (1)), relatively small areas of irrigation (0.048 km^2 – 0.112 km^2) were used for calibration purposes.

According to previous studies on the hydrology of the Berg River Catchment (DWAF(1), 1993(1)) and DWAF, 1999), flow recordings at gauging station G1H002 were available from 1951 and extended up until 1970 when the station was closed and replaced with gauging station G1H028, situated just upstream of the original G1H002 gauging station. Flow records at gauging station G1H028 were available from 1972 and consisted of the following two components:

- The flow over the weir (measured by gauging station G1H028).
- The flow in the diversion canal to Voëlvlei Dam (G1H058).

Although land-use at a 1998 level of development was used, verification could possibly be conducted over a much longer period taking into account the fact that minimal development had occurred in the catchment since 1950. Both the WCSA (DWAF,1993(1))) and VAFS (DWAF, 1999) studies, however, reported that a sizeable portion of the flow entering the diversion canal was allowed to spill from a silt trap located upstream of gauging station G1H058, leading to some under-estimation of total flow at gauging station G1H028 if these two records were added together. For this reason, these studies did not use the flow records from 1972 onwards in their calibration process and instead opted for the observed flows recorded at gauging station G1H002 during the period 1951 to 1970.

For this study, the model was verified for the period 1951 to 1963 and was then checked (in recognition of the inaccuracies in flow measurement) over the period 1972 to 1994.

Verification (Period : 1951 – 1963)

Initial delineations of the catchment upstream of gauging station G1H002 proved too coarse (see **Figure 25**) and further sub-division was required to allow for the usage of different monthly Rainfall Adjustment Factors (CORPPT) which could in turn lead to different aerial rainfall and run-off patterns. The monthly comparison of observed and simulated flows is shown in **Figure 48**, which highlights a number of short-comings in the simulation, i.e. the ACRU recessions are often too fast, while the wetter months are sometimes over-simulated. The high flow-over-simulations are directly related to over-estimated daily rainfalls, whereas the imperfect recessions are related to non-optimal soil water and groundwater constants in this ACRU configuration.

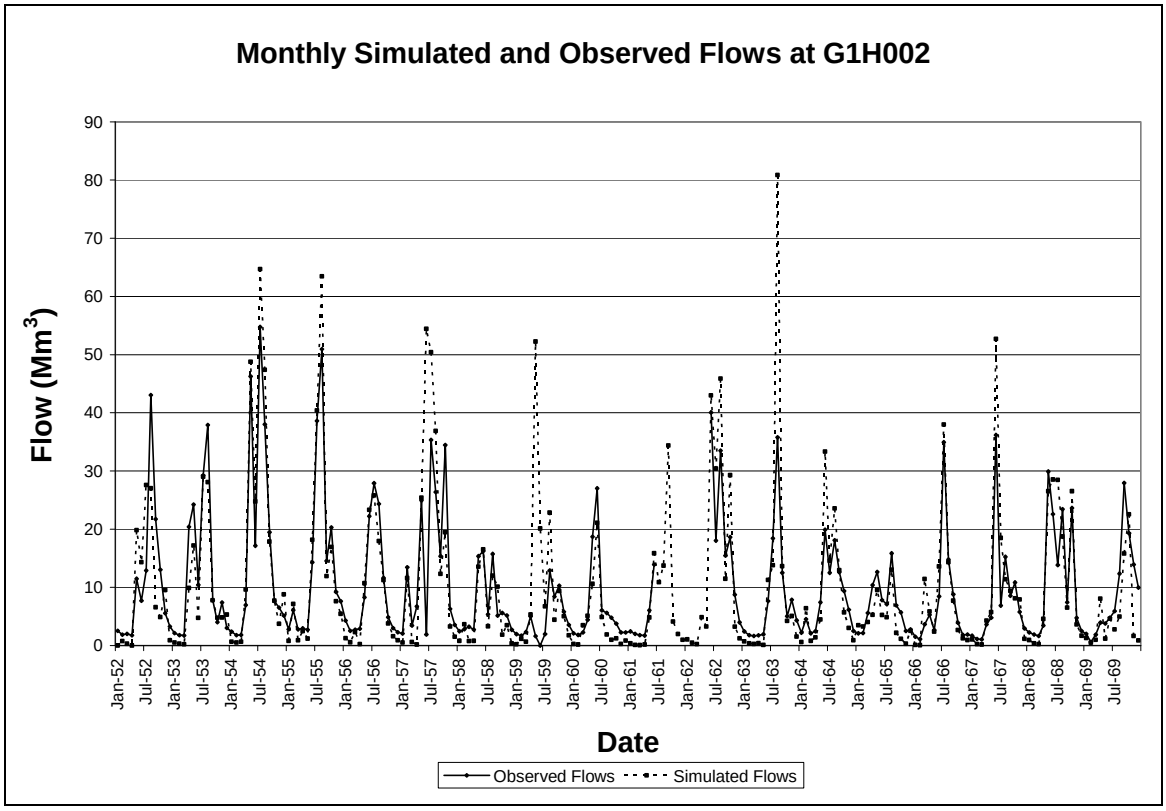

Figure 48 Comparison of observed and simulated flows at G1H002

Pertinent objective function values for the monthly observed and simulated flows at gauging station G1H002 are shown in **Table 13** which shows that the simulated flow over-estimated the observed flow by 8%. The lower values of r^2 and coefficients of efficiency of 0.62 and 0.61, respectively, reflected the short-comings of the simulated flows.

Table 13 Objective functions for simulated and observed flows at G1H002

Statistics for G1H002 (1951 –1963)	Monthly totals of daily simulation
Mean observed streamflow (10^6 m^3/month)	10.1
Mean simulated streamflow (10^6 m^3/month)	10.9
% difference in standard deviation	16.26
Coefficient of determination (r^2)	0.62
Coefficient of efficiency	0.61

The daily flow duration curve for the simulated and observed flows at gauging station G1H002 is depicted in **Figure 49** where it is evident that the low flows are consistently under-estimated.

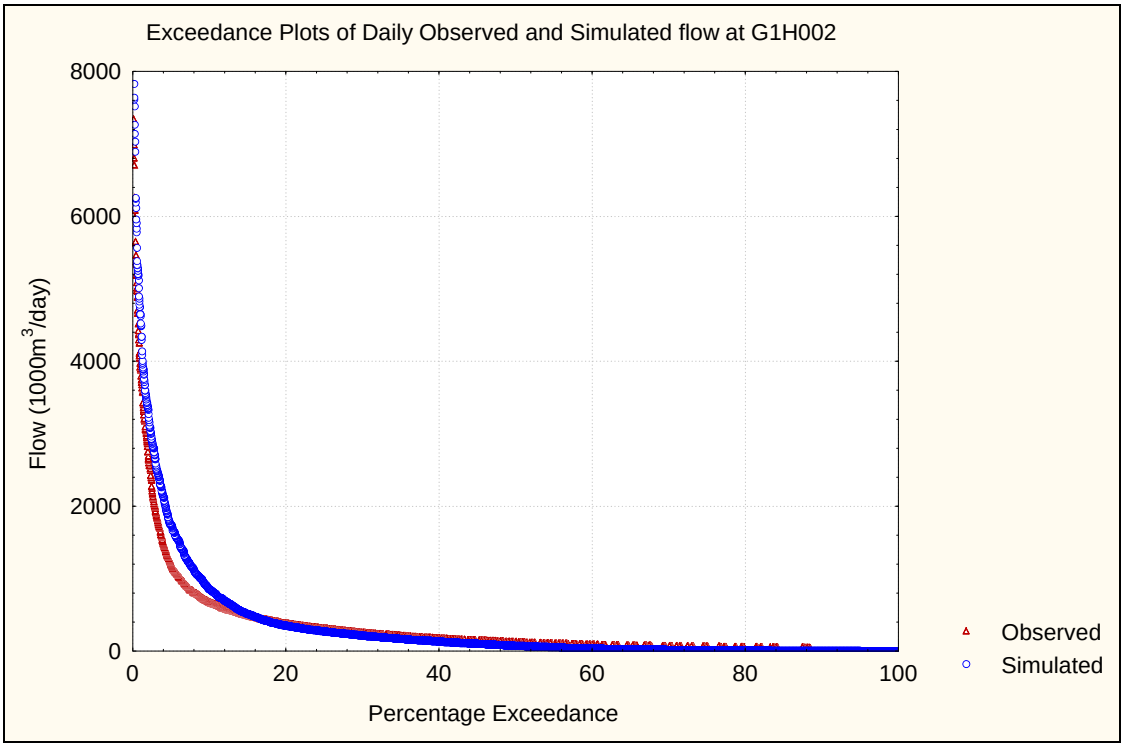

Figure 49 Daily flow duration curve for simulated and observed flows at gauging station G1H002

Verification (Period: 1972 – 1994)

Despite the fact that the observed record for G1H028 was unreliable (DWAF,1993 (1) and DWAF, 1999), the model was also verified for the period 1972 to 1994. In this way it was possible to confirm whether the flow-related objective function values obtained from the 1951 to 1963 verification were in fact applicable to this catchment. The observed flow record used was constructed as the sum of the flows measured at gauging stations G1H028 and G1H058.

A number of gaps in the observed record occurred during the winter months when it was more likely that there would be some streamflow rather than zero streamflow. These gaps were subsequently patched with simulated flows. Although gaps of several months existed in certain cases, it was still useful to evaluate the models performance relative to the portion of the observed flow record that was intact.

The monthly flow comparison of simulated and observed flows at gauging station G1H002 is depicted in **Figure 50**. It is evident that over-simulation of wet months occurred less frequently than for the earlier period and that simulated recession was mimicked better by the ACRU model. These "improvements" in the simulation are reflected in the "improved" r^2 and C_e values shown in **Table 14.** However, these apparent "improvements" simply reflect the changes in the nature of the observed sequence between 1951 to 1963 and 1972 – 1994.

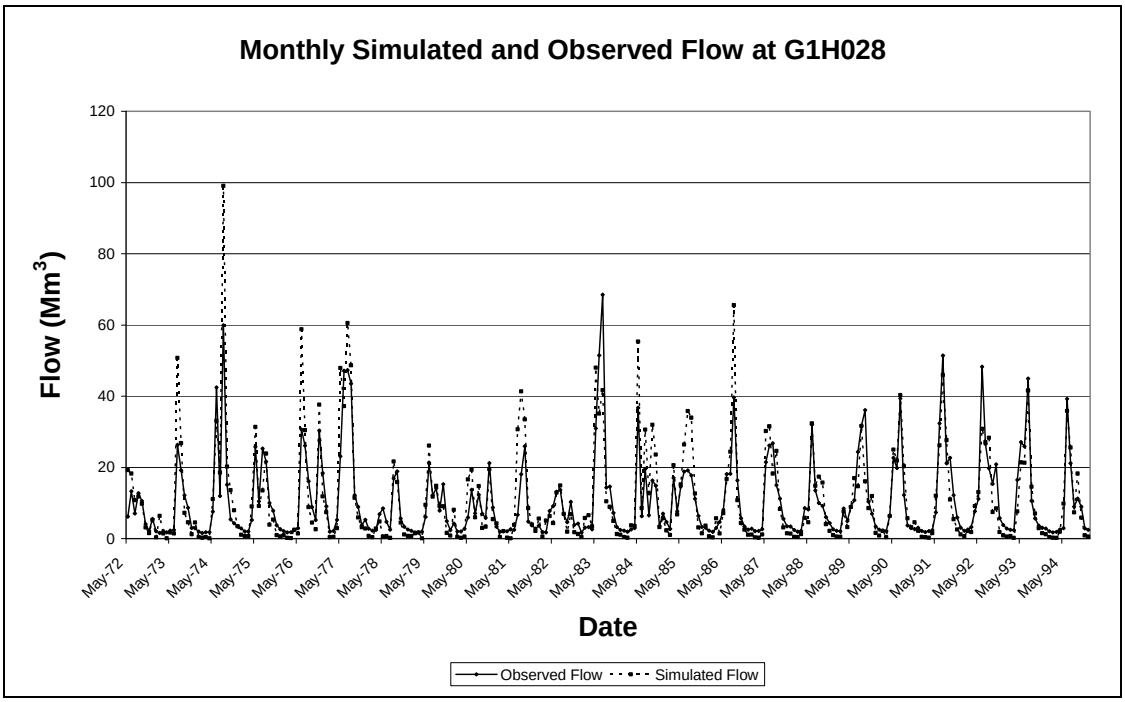

Figure 50 Monthly simulated and observed flows at gauging station G1H028

Pertinent objective function values for the monthly observed and simulated flows at gauging station G1H028 are shown in **Table 14** which shows that the simulated flow over-estimated the observed flow by 8%. Acceptable values for r^2 and coefficients of efficiency of 0.76 and 0.76 were obtained, respectively. These results indicate that the flow-related model parameters and driver rainfall stations are applicable to the catchment, resulting in a realistic representation of run-off in response to the rainfall, but with some concerns about low flows.

Table 14 Statistics for simulated and observed flows at G1H028

Statistics for G1H028 (1951 –1969)	Monthly totals of daily simulation
Mean observed streamflow (10^6 m^3/month)	10.1
Mean simulated streamflow (10^6 m^3/month)	11.0
% difference in standard deviation	17.45
Coefficient of determination (r^2)	0.76
Coefficient of efficiency	0.76

The daily flow duration curves for the simulated and observed flows at gauging station G1H028 are depicted in **Figure 51.**

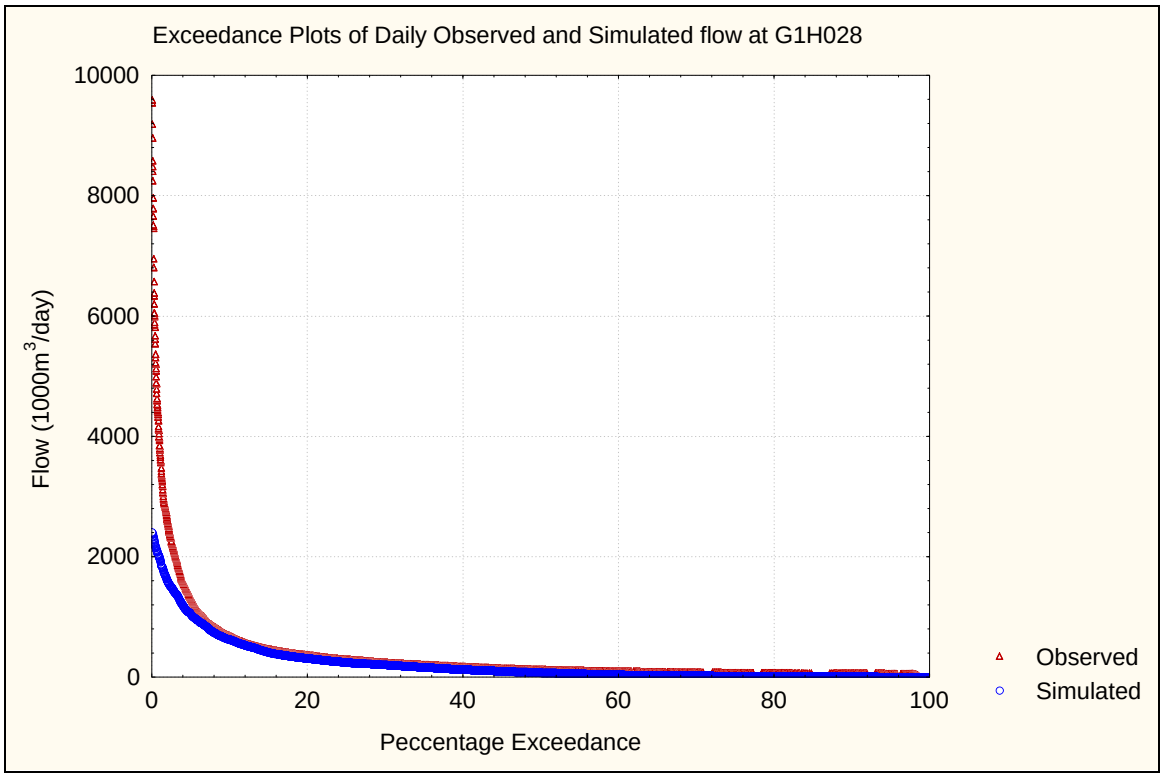

Figure 51 Daily flow duration curves for simulated and observed flows at G1H028

Figure 51 shows that the simulated flows are fairly representative of the observed flows for the low flow portion of the flow record. The model, however could not replicate the higher flows satisfactorily, this is probably directly related to the rainfall events driving these simulated events. Finer primary sub-catchment delineation combined with re-selection of driver rainfall stations may result in more representative simulated flows.

4.5.6 Verification at G1H008 (Klein Berg River at Nieuwkloof)

This gauging station is situated on the Klein Berg River (see **Figure 25**) and measures the flow generated in the catchment upstream of the diversion to Voëlvlei Dam. Verification was undertaken at a constant 1998 level of development which indicated that the irrigated area had increased from 19.27 km^2 in 1990 to 42.35 km^2 in 1998. Imports to the catchment were assumed to consist of the "White Bridge Import", which is diverted from a Breede River tributary at a constant rate of 0.53 x 10^6 m^3/month for irrigation and urban use.

The comparison of monthly simulated and observed flows at G1H008 is depicted in **Figure 52** which shows that the monthly simulated flows are representative of the observed flows. It is, however, obvious that low flows are consistently being over-simulated during the summer months which can possibly partially be attributed to an over-estimation of the flows imported from the Breede River during this period.

The pertinent objective function values for the monthly simulated and observed flow at G1H008 are depicted in **Table 15** which shows that the simulated flow under-estimated the observed flow by 6%. Sound values for 'r^2' and coefficients of efficiency of 0.87 and 0.82 were obtained. The catchment would probably require limited further refinement to obtain a more representative areal distribution of rainfall and to reduce the magnitude of under-simulation.

Table 15 Objective function values for the Simulated and Observed flows at G1H008

Statistics for G1H008 (1960 – 1999)	Monthly totals of daily simulation
Mean observed streamflow (10^6 m^3/month)	6.0
Mean simulated streamflow (10^6 m^3/month)	5.6
% difference in standard deviation	12.19
Coefficient of determination (r^2)	0.87
Coefficient of efficiency	0.82

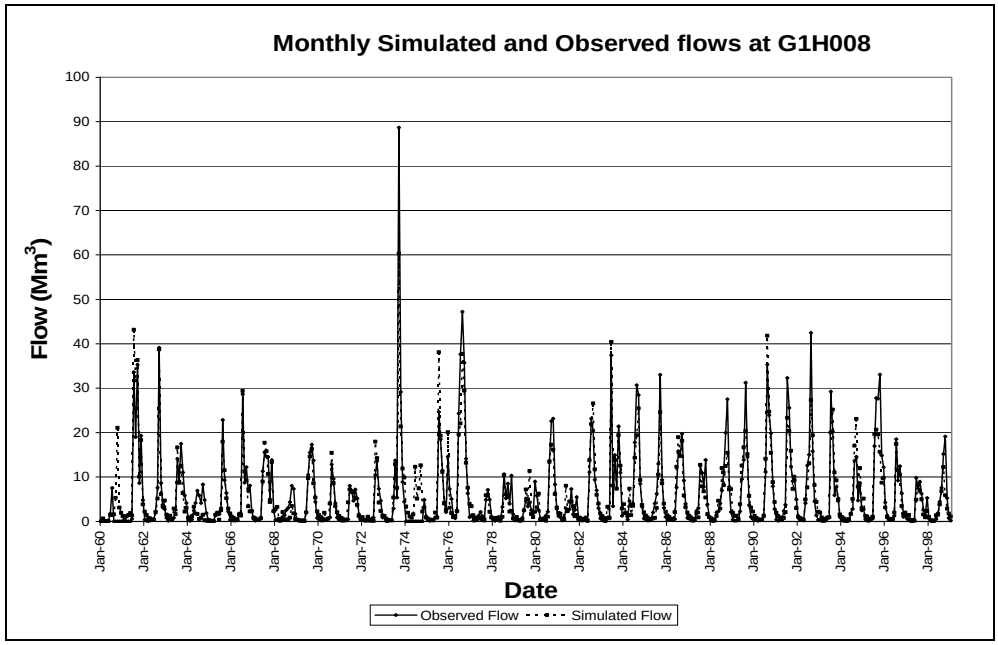

Figure 52 Simulated and observed monthly flows at gauging station G1H008

A comparison of daily simulated and observed flows is depicted in **Figure 53**. As with the monthly flows there is an over-estimation of daily flows during the summer months. The daily comparison also reveals that, compared to the observed record, the recession in simulated baseflows is not fast enough, thus contributing to the flows introduced by the "White Bridge Import".

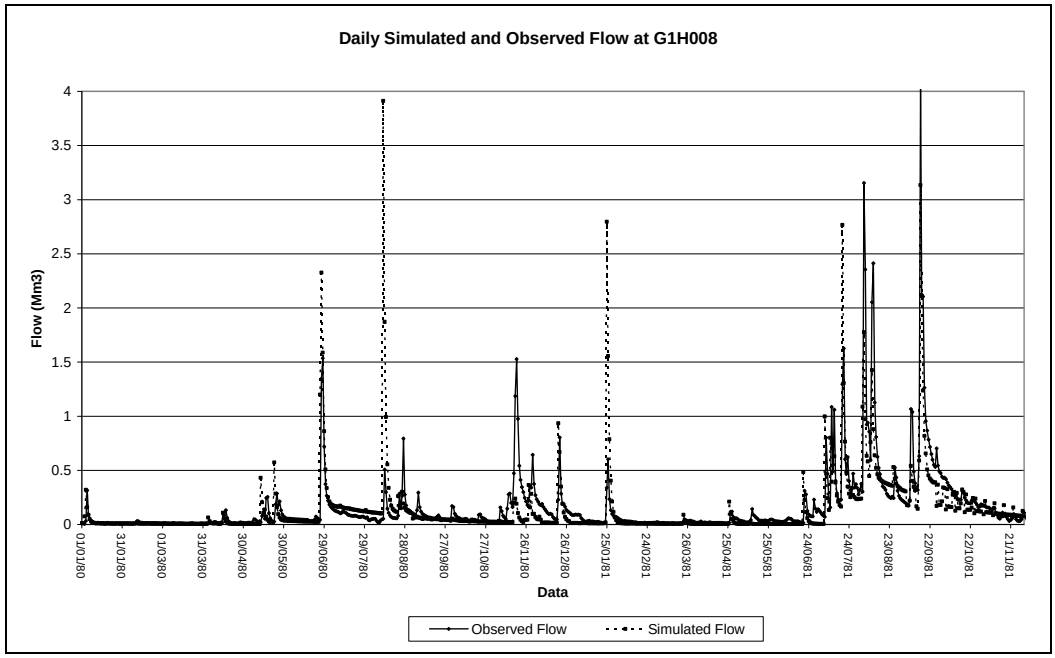

Figure 53 Daily simulated and observed flows at gauging station G1H008

The daily flow duration curves for the simulated and observed flows at gauging station G1H008 are depicted in **Figure 54**.

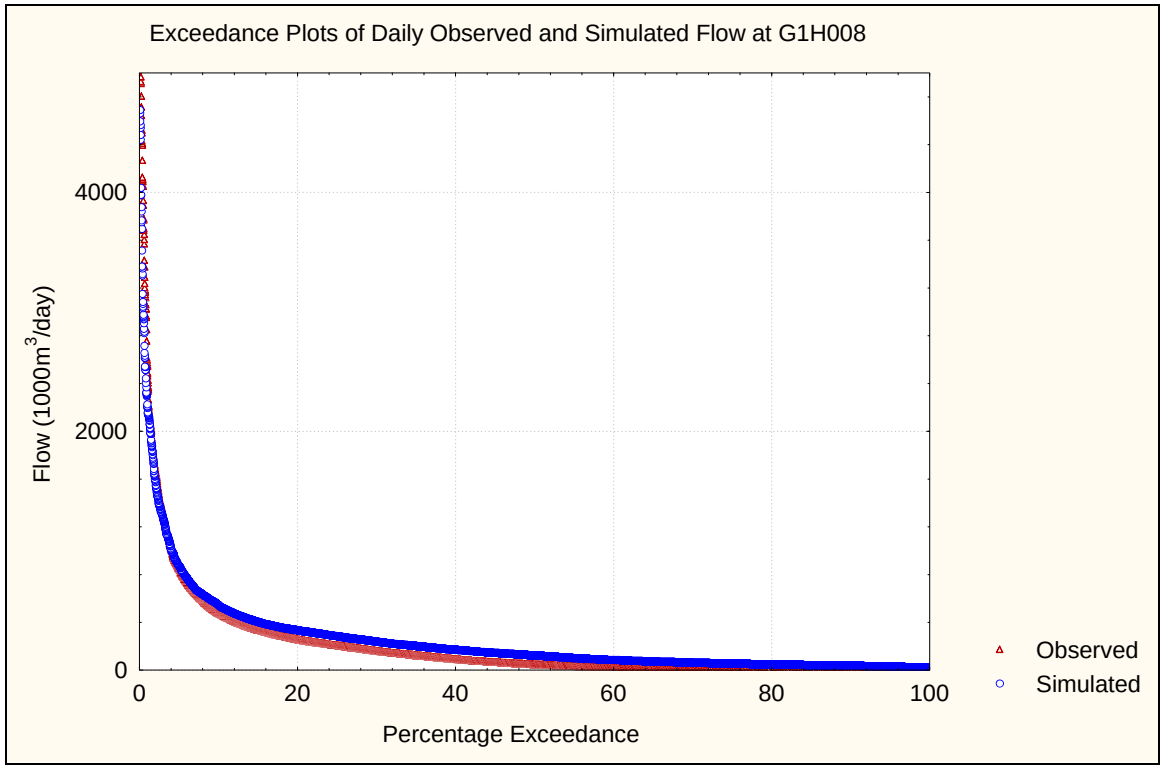

Figure 54 Daily flow duration curves for simulated and observed flows at G1H008 (1977 to 1994)

As expected, the higher simulated flow rates have an exceedance percentage comparable to the observed flows but the lower simulated flow rates have higher exceedances compared to those of the observed.

4.5.7 Verification at G1H043 (Sandspruit River at Vrisgewaagd)

Although the unit run-off generated in this sub-catchment is relatively small compared to that generated in the upper portions of the Berg River Catchment, it is the most upstream gauging station (see **Figure 25**) which measures flow from a catchment underlined by Malmesbury Shale and it was consequently necessary to obtain the most representative simulated flows to ensure that the salt loads entering the Berg River mainstem could be realistically represented. Verification for this sub-catchment did not account for the variation in irrigated area with time and was instead completed at a constant 1998 level of development. The irrigated area in the catchment increased from 0.07 km^2 in 1990, to 1.75 km^2 in 1998.

The comparison of monthly simulated and observed flows is depicted in **Figure 55** which shows that the simulated monthly flows are often not representative of the observed flows. Particularly, the wet months during 1990 – 1995 were markedly under-simulated. This is mainly the result of the absence of a driver rainfall station within the catchment boundaries. The driver stations actually used, 41684W and 41347A, are some distance away from the approximate centroid of the catchment (see **Figure 30**). A particular short-coming of the monthly flows is the very slow recession of the simulated response. This indicates non-optimal soil-water-related and groundwater-related settings in ACRU for this case.

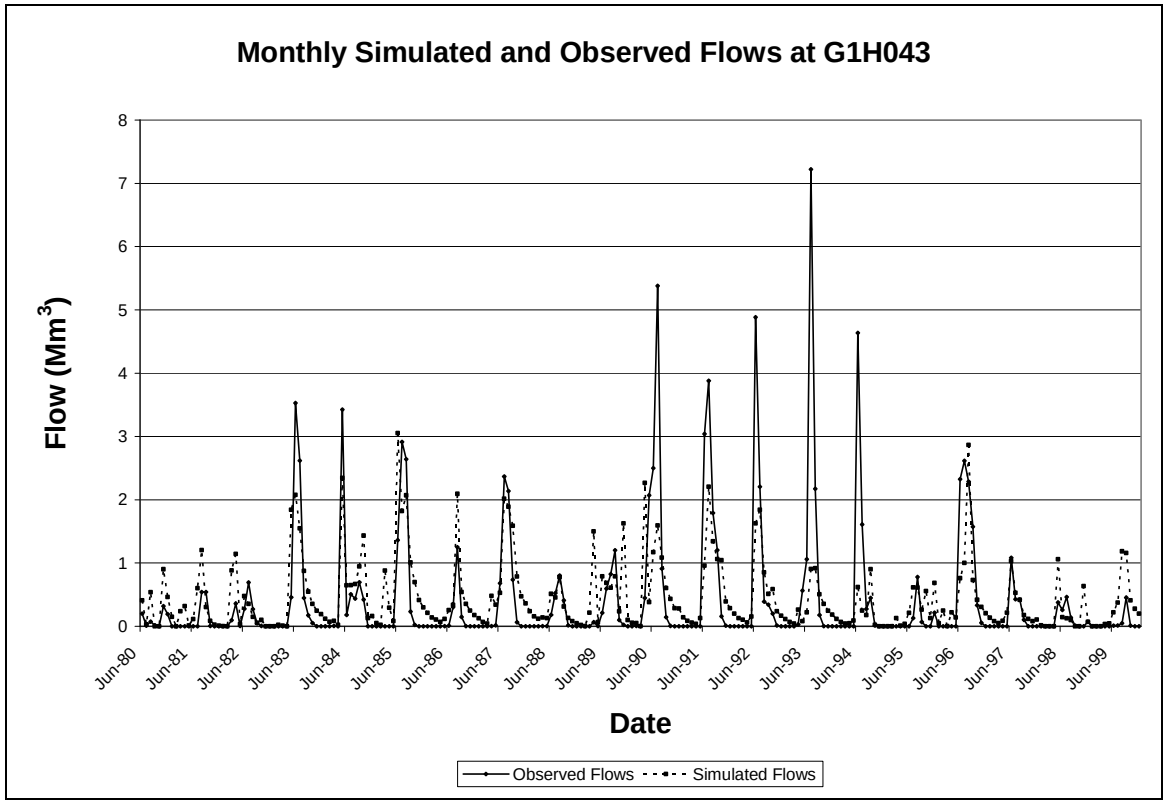

Figure 55 Monthly simulated and observed flows at gauging station G1H043

The values of the objective functions are shown in **Table 16.** The simulated flow exceeds the observed flow by 5%. Unacceptable values for 'r^2' and coefficients of efficiency of 0.40 and -0.86 were obtained, respectively. As expected, statistical parameters echo the poor fit seen between the observed and simulated flows depicted in **Figure 55**.

Table 16 Objective values for simulated and observed flows at G1H043

Statistics for G1H043 (1980 – 1999)	Monthly totals of daily simulation
Mean observed streamflow (10^6 m^3/month)	0.42
Mean simulated streamflow (10^6 m^3/month)	0.44
% difference in standard deviation	43.0
Coefficient of determination (r^2)	0.40
Coefficient of efficiency	-0.86

A comparison of the daily simulated and observed flows is shown in **Figure 56**. It can be seen that the model is responding to the various storm events, but that the magnitude of the response is not entirely representative of the observed flows. As mentioned previously, the major reason for the poor simulated outputs is probably the choice of driver rainfall station, which is not within the confines of the catchment boundary.

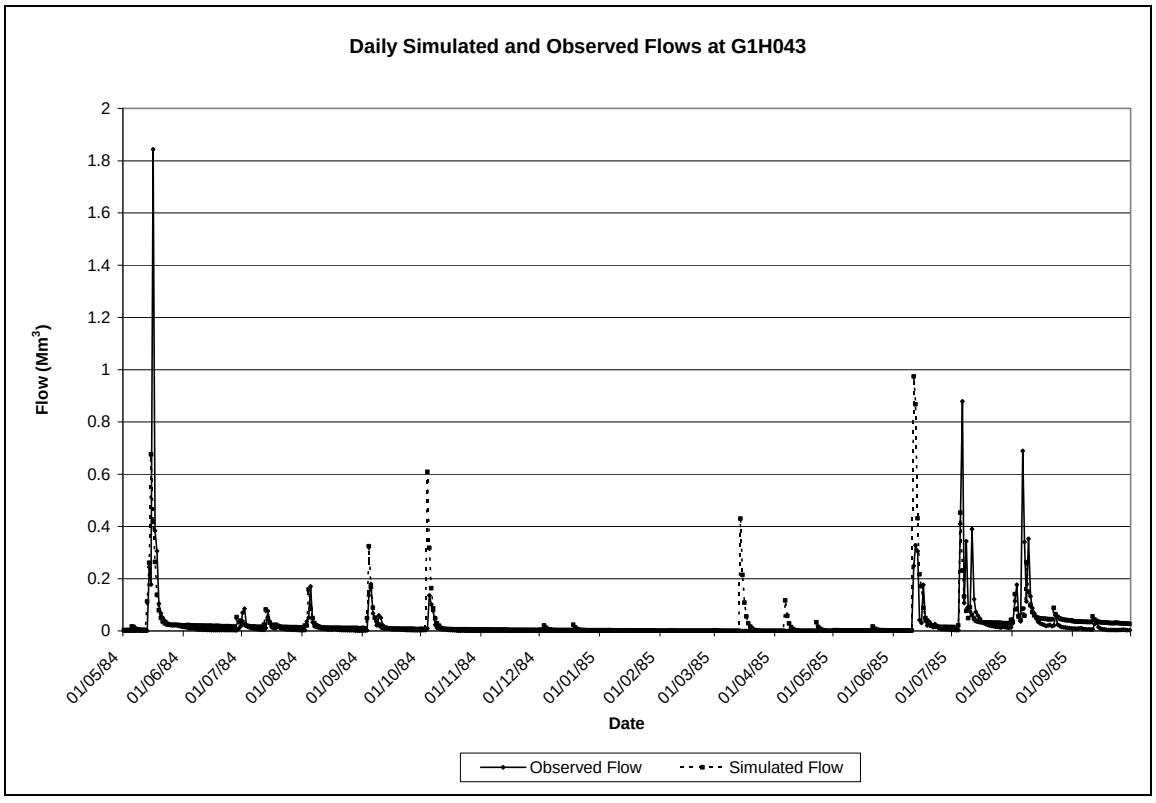

Figure 56 Daily Simulated and Observed Flows at G1H043

The flow duration curves for the simulated and observed flows at gauging station G1H043 are depicted in **Figure 57**. The plot reflects the differences seen in the daily time series comparison.

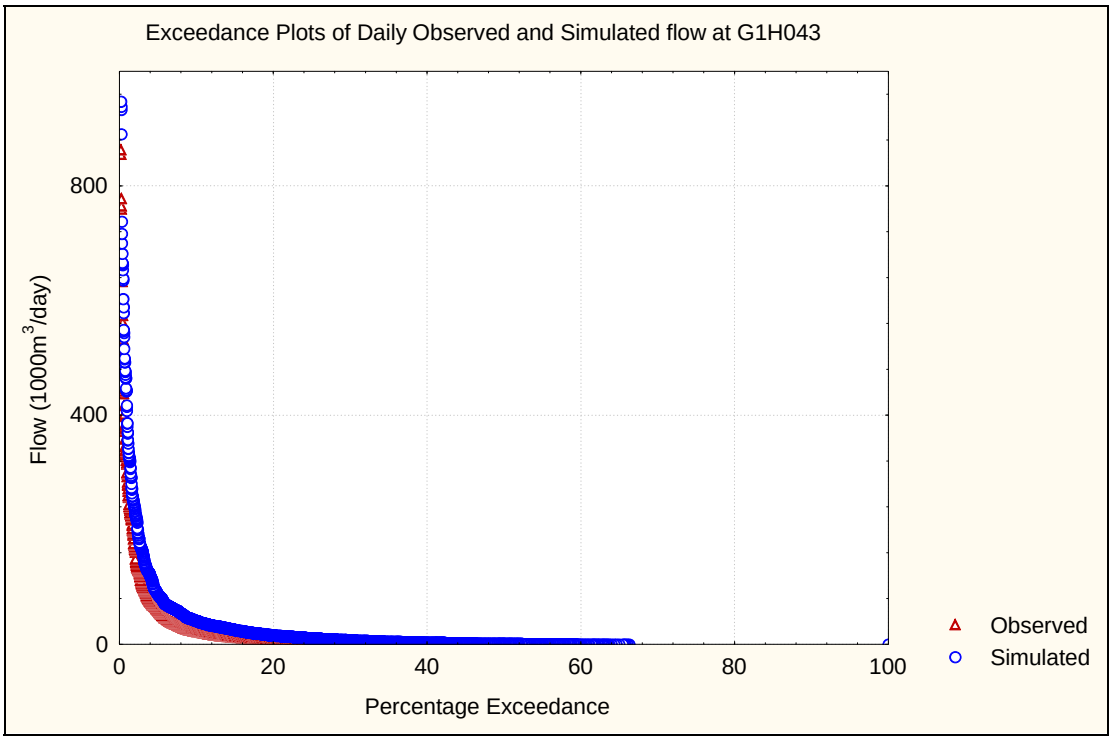

Figure 57 Flow Duration Curves Simulated and Observed Flows at G1H043

4.5.8 Verification at G1H013 (Berg River at Drieheuwels)

Gauging station G1H013 is the last gauging station before Misverstand Weir. The comparison between monthly simulated and observed flows at this gauge is depicted in **Figure 58**.

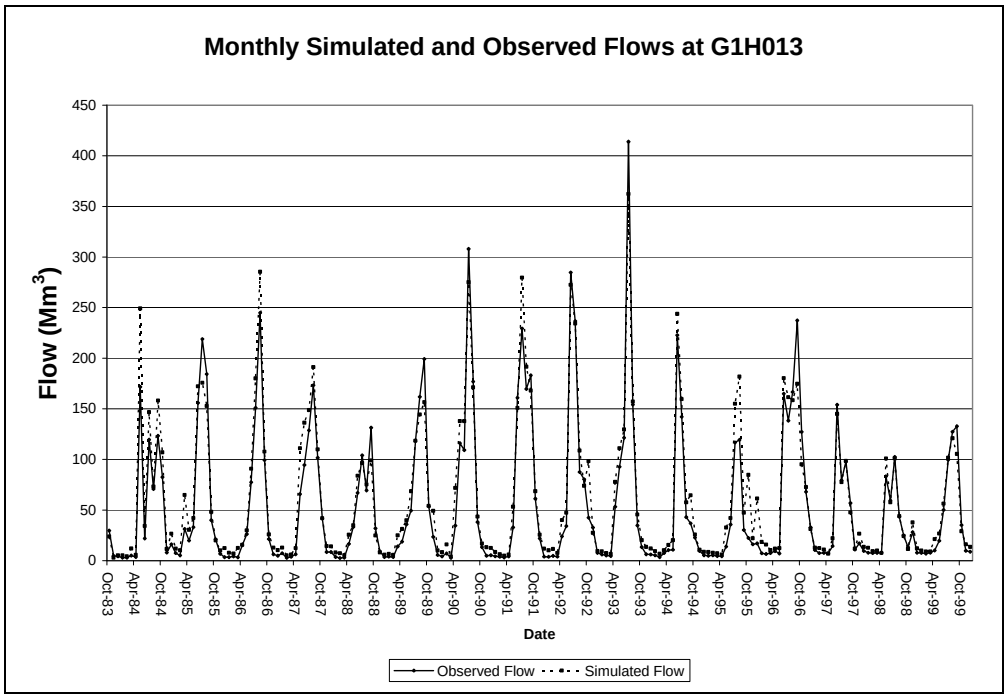

Figure 58 Monthly simulated and observed flows at gauging station G1H013

Figure 58 shows that the simulated monthly flows are representative of the observed flows. This was, however, expected since the observed record at G1H036 was used as input to the ACRU configuration between gauging stations G1H036 and G1H013.

The objective function values are shown in **Table 17**, which shows that the simulated flow over-estimated the observed flow by 10.7%. Sound values for 'r^2' and coefficients of efficiency of 0.95 and 0.94 were obtained, respectively.

Table 17 Objective function values for simulated and observed flows at G1H013

Statistics for G1H013 (1983 – 1999)	Monthly totals of daily simulation
Mean observed streamflow (10^6 m^3/month)	55.0
Mean simulated streamflow (10^6 m^3/month)	60.9
% difference in standard deviation	1.17
Coefficient of determination (r^2)	0.95
Coefficient of efficiency	0.94

4.5.9 Verification at G1H035 (Matjies River at Matjiesfontein)

As with the Sandspruit River (G1H043) this catchment produces very little run-off but is the most important tributary affecting the TDS concentration at Misverstand Dam (G1R003). This catchment was not verified with a changing irrigated area but was instead verified at a constant 1998 level of development. The irrigated area in this catchment had changed from 5.01 km^2 in 1990, to 4.51 km^2 in 1998.

The comparison of monthly simulated and observed flows is depicted in **Figure 59** which shows that the simulated flows are responding to the rainfall, but that a more appropriate driver rainfall station is probably required to produce representative simulated flows. Additionally, finer delineation of the catchment may still be possible. It is particularly important to capture the higher flows that occur in winter because these flows are associated with high TDS values and consequently high salt loads.

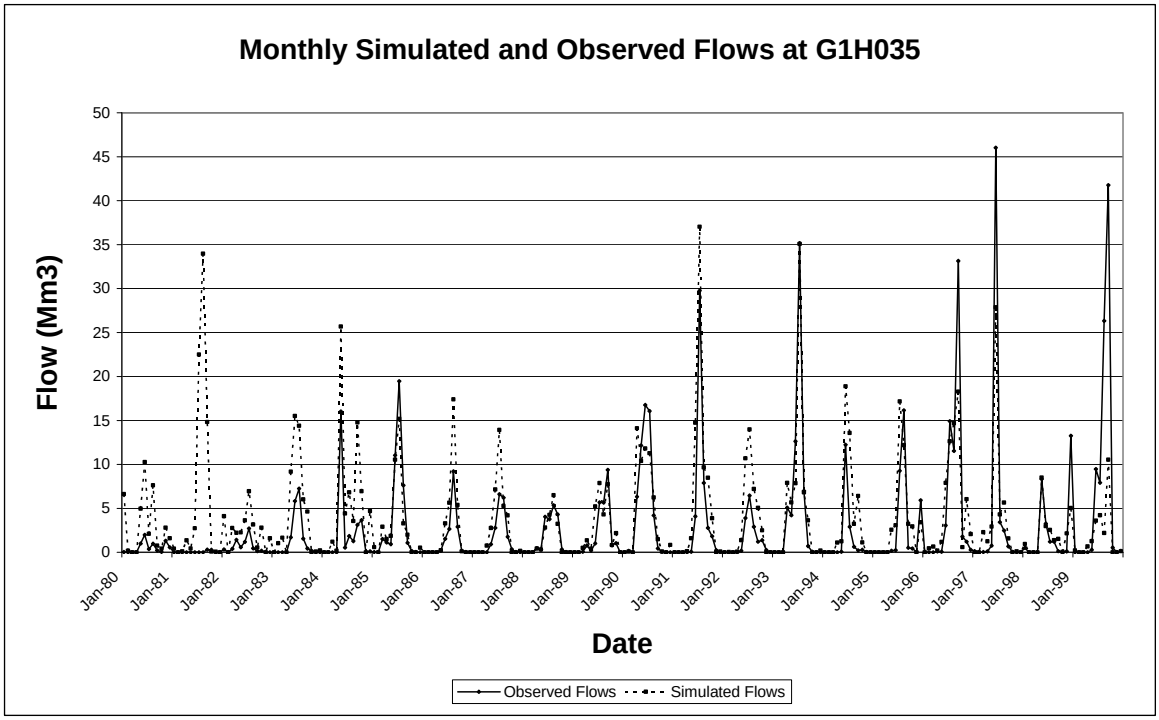

Figure 59 Monthly simulated and observed flows at G1H035

The comparison of daily simulated and observed flows is depicted in **Figure 60** which also shows that the simulated flows are responding to the rainfall input but that the magnitude is not always representative. This could probably, to a greater extent, be ascribed to the selection of driver rainfall stations for each of the primary sub-catchments comprising the calibration catchment and to a lesser extent to the delineation of the catchment.

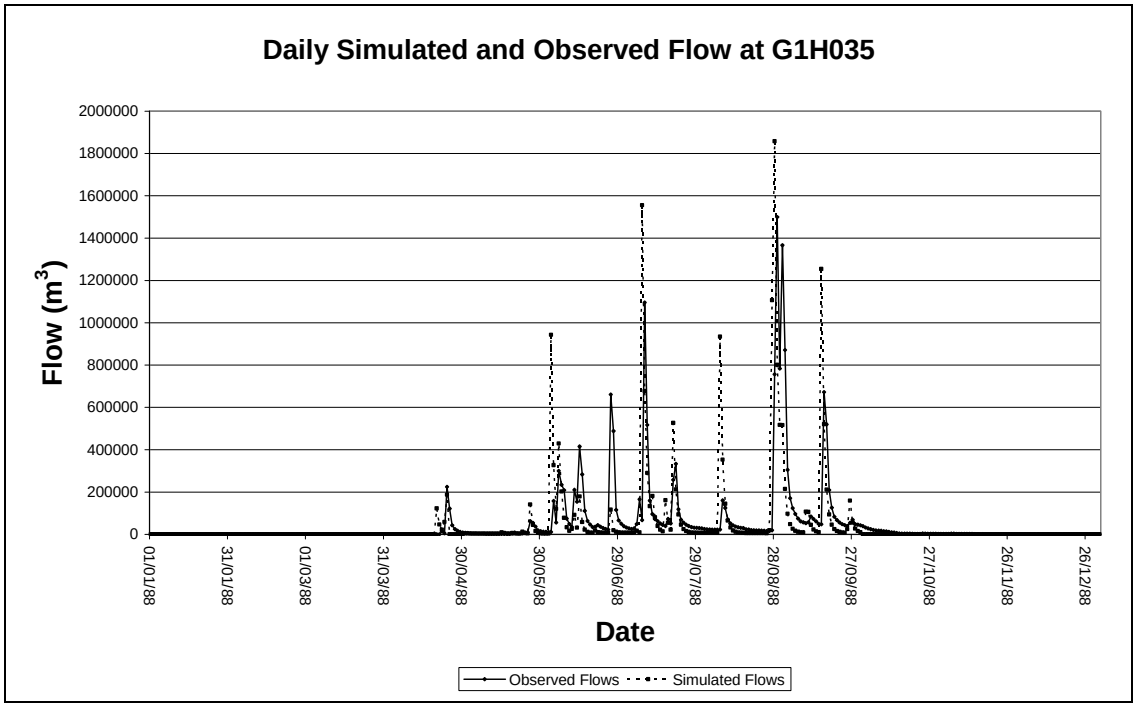

Figure 60 Daily simulated and observed flows at G1H035

The values of the objective functions for the observed and simulated flows are shown in **Table 18,** which shows that the simulated flow over-estimated the observed flow by 27%. Unacceptable values for 'r^2' and coefficients of determination of 0.60 and 0.45 were obtained, respectively. As expected, statistical parameters echo the poor goodness-of-fit between the observed and simulated flows depicted in **Figure 59**.

Table 18 Objective function values for simulated and observed flows at G1H035

Statistics for G1H035 (1980 – 1994)	Monthly totals of daily simulation
Mean observed streamflow (10^6 m^3/month)	2.8
Mean simulated streamflow (10^6 m^3/month)	3.5
% difference in standard deviation	12.35
Coefficient of determination (r^2)	0.60
Coefficient of efficiency	0.45

The flow duration curves for the simulated and observed flows at gauging station G1H035 are depicted in **Figure 61** which shows a considerable difference between the simulated and observed daily flows. This difference can possibly only be addressed by finer scale delineation and re-selection of the driver rainfall stations.

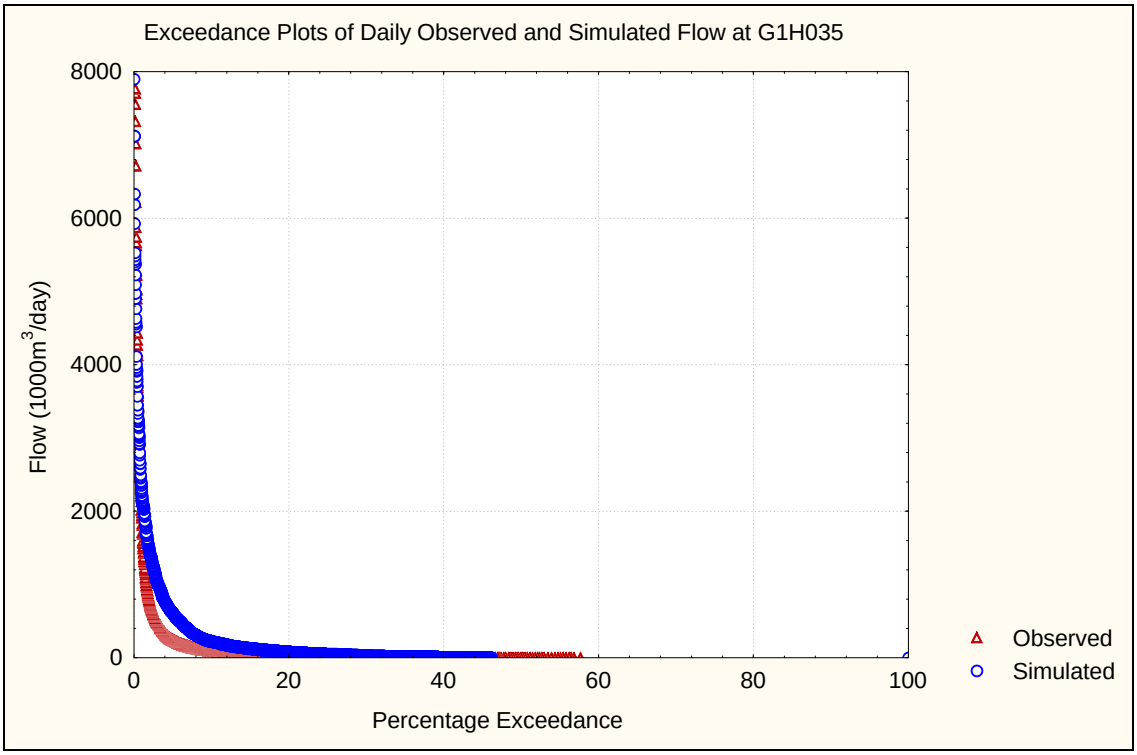

Figure 61 Flow duration curves simulated and observed flows at G1H035

4.5.10 Simulated naturalised flow sequences

Simulated naturalised flow sequences for the period 1921 to 1999 were produced at various gauges for comparison with the Pitman Model-based flow sequences developed for earlier DWAF (1993) and WRC (1994 and 2005) studies. For these runs, the irrigated and dryland land-use was replaced with the Acocks (Acocks, 1975) veld types, all transfers of water were removed and all dams were removed, resulting in an un-impacted catchment. A comparison of the simulated naturalised Mean Annual Runoffs (MARs) obtained from the ACRU configurations, the *Western Cape System Analysis* (DWAF, 1993(1)) the *Surface Water Resources of South Africa 1990* (WRC, 1994) and the *Surface Water Resources of South Africa 2005* (WRC, 2005) is shown in **Table 19**.

Table 19 Simulated naturalised MARs

Gauge	ACRU MAR ($\times 10^6$ m^3) (1921-1999)	WR 90 MAR ($\times 10^6$ m^3) (1920 – 1989)	WCSA MAR ($\times 10^6$ m^3) (1926 -1988)	WR2005 ($\times 10^6$ m^3) (1920 -2004)
	This thesis	**WRC (1994)**	**DWAF (1993(1))**	**WRC (2005)**
G1H020	403	412	384	329
G1H036	493	528	521	453
G1H013	789	Approx. 782	871	Approx. 615
G1R003	832	825	904	728

Table 19 shows that the naturalised MAR obtained from the individual studies are comparable, although not exactly the same. It should be noted, however, that the WR2005 study indicates substantially less naturalised flows than the other three studies. The possible reason for this is not clear at this stage.

CHAPTER 5: APPLICATION OF ACRU*SALINITY* TO THE BERG RIVER FOR SALINITY SIMULATION

5.1 INTRODUCTION

During the application of the ACRU*Salinity* model several approaches for estimating the initial values of the salanity-related parameters were considered. Eventually, the salt saturation constant (SALTSAT) was estimated from the the average concentrations during the low flow periods and the values for the salt generation constant (SALTUPT) was adjusted until a suitable fit between simulated and observed TDS concentrations were obtained on an exceedence basis.

5.2 APPROACH TO DAILY AND MONTHLY SALINITY CALIBRATIONS

5.2.1 Approach to daily TDS calibrations

The fact that the flow routing option was not envoked in the ACRU model, coupled with the inherent variablity of daily simulated TDS concentrations necessitated the application of an alternative approach for the meaningful comparison of daily simulated and observed TDS concentrations.

Since a one-to-one comparison of TDS concentrations on a daily basis was not practical, a comparison based on percentage exceedence was opted for. This approach is currently used as part of the Basin Salinity Management Strategy for controlling salinity in the Murray-Darling basin in Australia, where salinisation of the rivers has become a major threat to agricultural activities. A key feature of the strategy is the adoption of TDS concentrations as well as percentage allowable exceedence of this concentration, as indicators of the measure of success of the strategy (Rossouw *et al*., 2006).

The calculation of objective function values for the simulated and observed daily TDS concentrations and loads was also not practical since the flow routing option was not envoked and the artificial lag or premature peaking of flows introduced as a result of this would give rise to objective function values that were not applicable due to a lack of 1:1 comparison.

5.2.2 Approach to monthly salinity calibrations

The summation of daily TDS concentrations to provide a monthly value gives rise to a value with no physical meaning and the calculation of objective function values for these outputs would provide no insight into the goodness-of-fit between the simulated and infilled-observed TDS sequences. Instead, the monthly TDS loads of the simulated and infilled-observed TDS sequences were calculated and objective function values calculated for each, were then compared. Futhermore, the seasonal variation of the simulated TDS concentrations was compared with that of the observed record to qualitatively assess whether the seasonal trends in the simulated record was representative of those in the observed record.

5.3 SENSITIVITY ANALYSIS

To simplify the calibration process it was necessary to determine which salt-related parameters had the most significant effect on the simulated TDS concentrations. This was achieved by performing a sensitivity analysis on the salinity-related parameters of the ACRU*Salinity* model.

The original version of ACRU*Salinity* has two salinity-related parameters which could be varied to obtain desired streamflow TDS values (*viz*. SALTSAT and SALTUPT). These parameters are, however, applicable to both the A and B soil horizons and could thus be adjusted independently of each other, resulting in the availability of four parameters which could be used for salinity calibration.

For the purposes of this sensitivity analyses it was assumed that these parameters were equal for the A and B Horizons. The salinity-related parameter SALTUPT is not applicable to the surface soil layer. In addition to the parameters SALTSAT and SALTUPT, only three other salinity-related parameters pertaining to the surface soil layer (see **Table 3)** were subjected to the sensitivity analyses (*viz*., DEPSS, SALTCTIME and SALTSATSS). This was based on the assumption that these would be calibrated parameters that could not easily be inferred from the properties of a given soil.

The sensitivity of a parameter was assessed by varying the value of a particular parameter by ± 50% from its original value.

5.3.1 Effect of varying the salt uptake rate (SALTUPT)

As mentioned in **Chapter 1** of this thesis, the salt uptake rate can be estimated by analysing the rate of change in solute concentration (*C*) during an inter-event period after mixing had occurred in the soil. The proposed method would then require a least squares straight line regression fit of the differential form of the Nernst equation (**Equation 7**). Due to time constraints, this approach was not adopted for this study and the final values for SALTUPT was obtained by iteratively changing its intermediate value until a representative TDS time-series was obtained. The sensitivity of these results to the variation in SALTUPT will now be explored.

Sensitivity of quickflow salinity to variation in SALTUPT

Initial sensitivity analyses undertaken by Teweldebrhan (2003) showed that a change in this parameter was unlikely to affect the salinity of the quickflow component in ACRU, unless there was a contribution from saturated upward flow. With the addition of the thin surface layer, in this study, unsaturated salt movement and subsequent surface salt crusting is now represented and the variation in the value of SALTUPT may have a greater effect on quickflow salinity.

Initial simulations in the Berg River, with the ***Beta version*** of ACRU*Salinity*, revealed that the salt concentration in the observed runoff from saline catchments could not be matched by the simulated values. Further investigation of this phenomenon revealed that the daily runoff often contained a significant proportion of quickflow which had limited interaction with the soil profile. **Figure 62** shows the impact that varying the value of SALTUPT, the additional thin surface soil layer and unsaturated salt movement have on the TDS concentrations. It should be noted that the surface soil layer does not have a salt generation parameter.

Figure 62 shows a marked increase and decrease in TDS concentrations of the quickflow, contrary to what was presented by Tewldebrhan (2003). This was expected though, since the newly added soil surface layer algorithm allows for the interaction of rainfall with the salts which accumulate in this layer. The changes in pertinent statistical parameters obtained from this sensitivity analysis are shown in **Table 20**. The percentage variation of the modelled output values over the winter months only (May to September) did not differ significantly from those presented in **Table 20** and are therefore not shown separately – both for this comparison as well as all subsequent comparisons below.

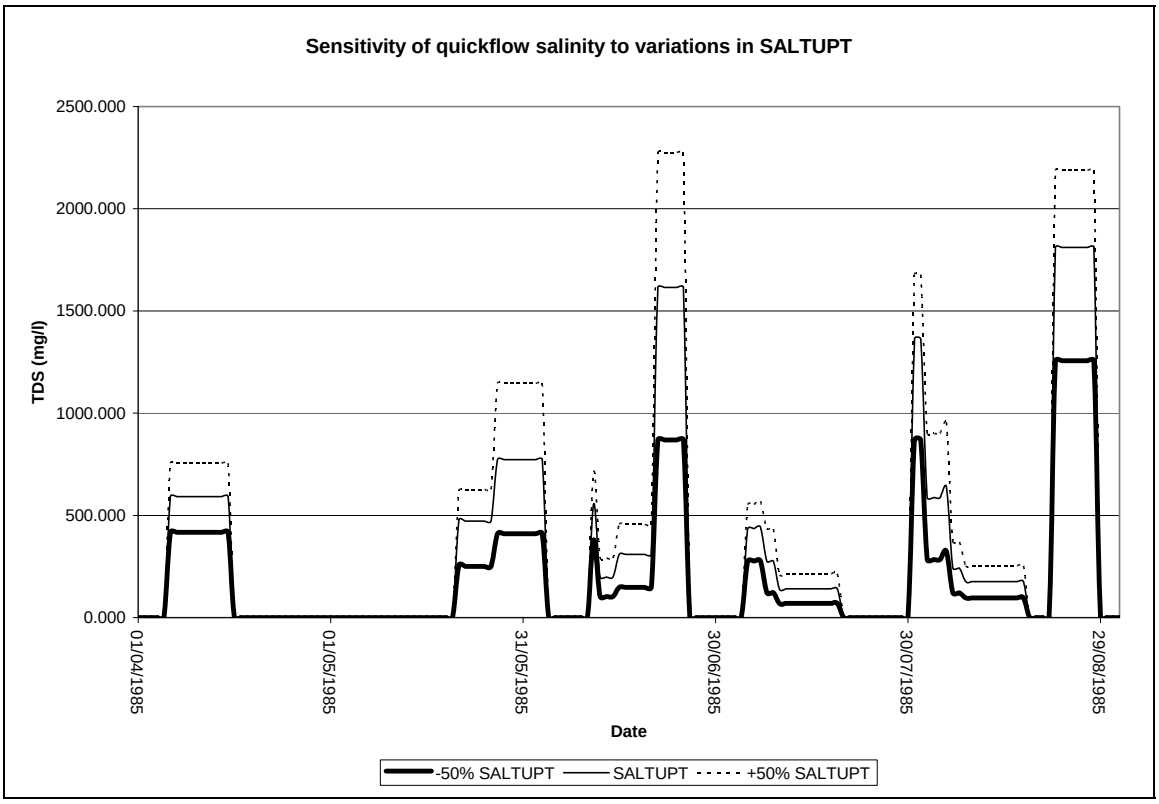

Figure 62 Variation in quickflow salinity in response to variation in SALTUPT value in the A and B Horizons

Table 20 Sensitivity of daily simulated TDS statistics to variations in the value of SALTUPT (for quickflow)

Statistical Parameter	Percentage change from calibrated value	
	-50% Change	+50% Change
Mean	-39.4	30.8
Standard Deviation	-36.7	27.1

Sensitivity of baseflow salinity to variations in SALTUPT

Since runoff is constituted of both quickflow and baseflow it can be expected that the variation in the SALTUPT parameter would have a significant impact on the response of the baseflow TDS concentrations. **Figure 63** shows this variation.

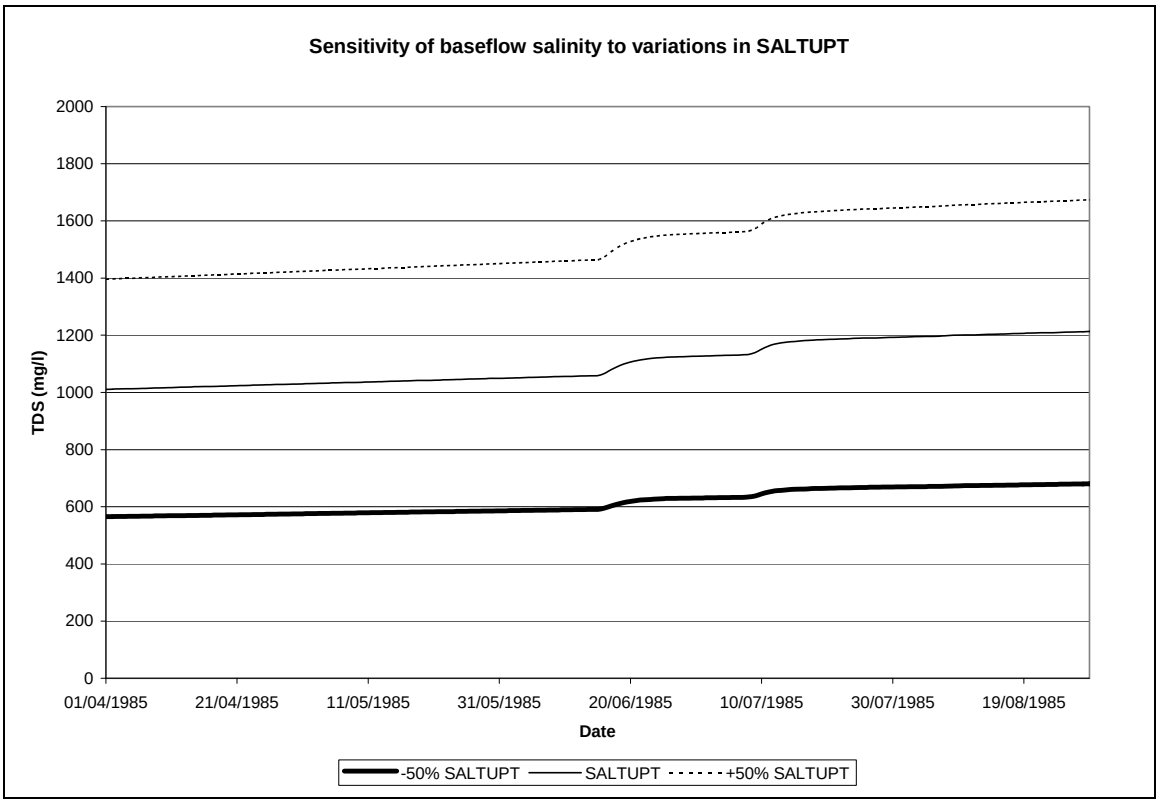

Figure 63 Variation in baseflow salinity in response to variation in SALTUPT value

Teweldebrhan (2003) showed that by changing the value of SALTUPT by 50%, a percentage change of only 15% was observed in the baseflow salinity. The values showed in **Table 21** do not correlate with the finding by Teweldebrhan (2003), but it should be noted that several algorithm additions and code modifications have been effected during the current study.

Table 21 Sensitivity of daily simulated TDS statistics to variations in the value of SALTUPT (for baseflow)

Statistical Parameter	Percentage change from calibrated value	
	-50% Change	+50% Change
Mean	-41.4	25.0
Standard Deviation	-39.6	21.9

5.3.2 Effect of varying soil surface layer depth (DEPSS)

Thorton-Dibb *et al.* (2005) undertook a preliminary sensitivity analysis on varying the surface layer depth but did not quantify the percentage change which could be expected in the salinity of

the flow components which constitute the runoff. The ensuing sections will attempt to quantify the change in TDS concentration which could be expected when increasing or decreasing DEPSS.

Sensitivity of quickflow salinity to variations in DEPSS

The variation in quickflow salinity in response to a variation in DEPSS is depicted in **Figure 64**.

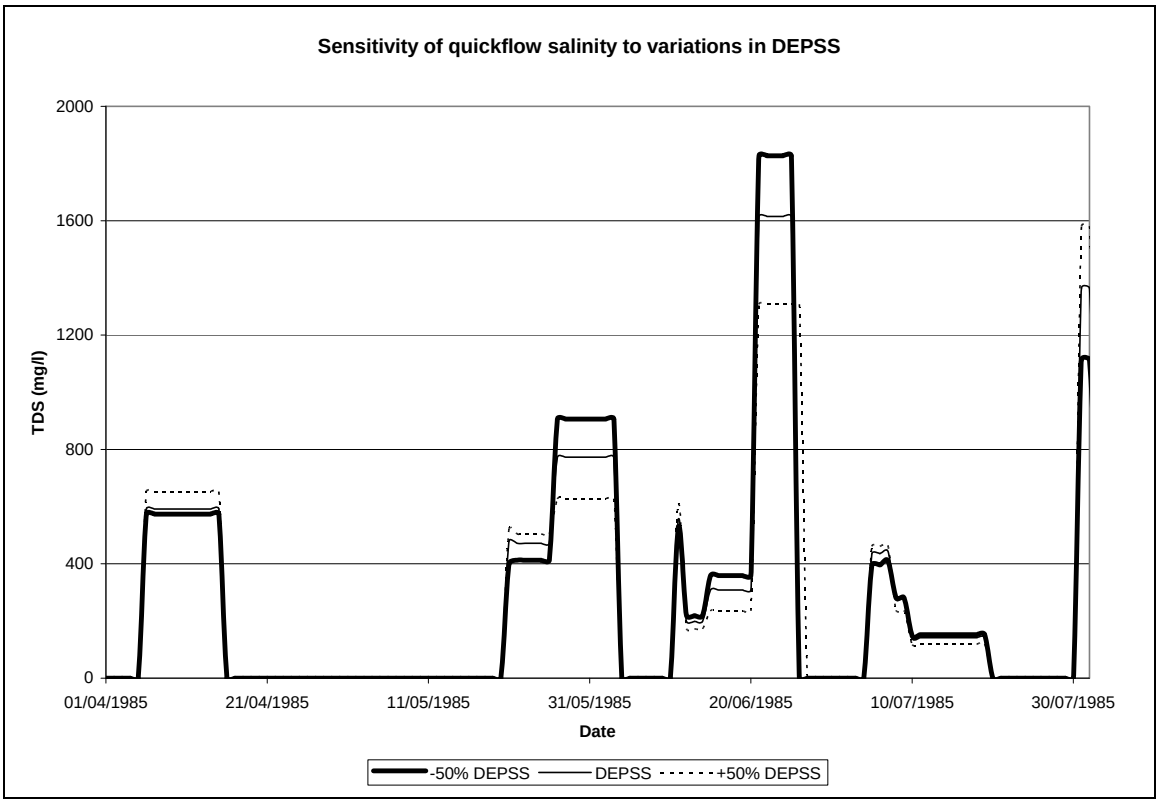

Figure 64 Variation in quickflow salinity in response to variation in DEPSS

The quantification of the variation in the modelled outputs is shown in **Table 22** which shows that even with a 50% decrease in the value of DEPSS, the mean TDS concentration of the quickflow decreased by only 4%. **Equation 1**, however, suggests that when all parameters remain constant, increasing the surface layer depth would decrease the mass of dissolved salts from the precipitated salt store in the soil surface layer.

Table 22 Sensitivity of daily simulated TDS statistics to variations in the value of DEPSS (for quickflow)

Statistical Parameter	Percentage change from calibrated value	
	-50% Change	+50% Change
Mean	-4.0	1.0
Standard Deviation	-4.8	1.0

Sensitivity of baseflow salinity to variations in DEPSS

Based on the relative position of the soil surface layer in relation to B-horizon (where the contact time of baseflow will be the longest) it is intuitively expected that the depth of the soil surface layer will have less of an effect on the salinity of the baseflow then it has on that of the quickflow component of the runoff. **Figure 65** indicates that this is in fact so and that only slight variations resulted from this analysis.

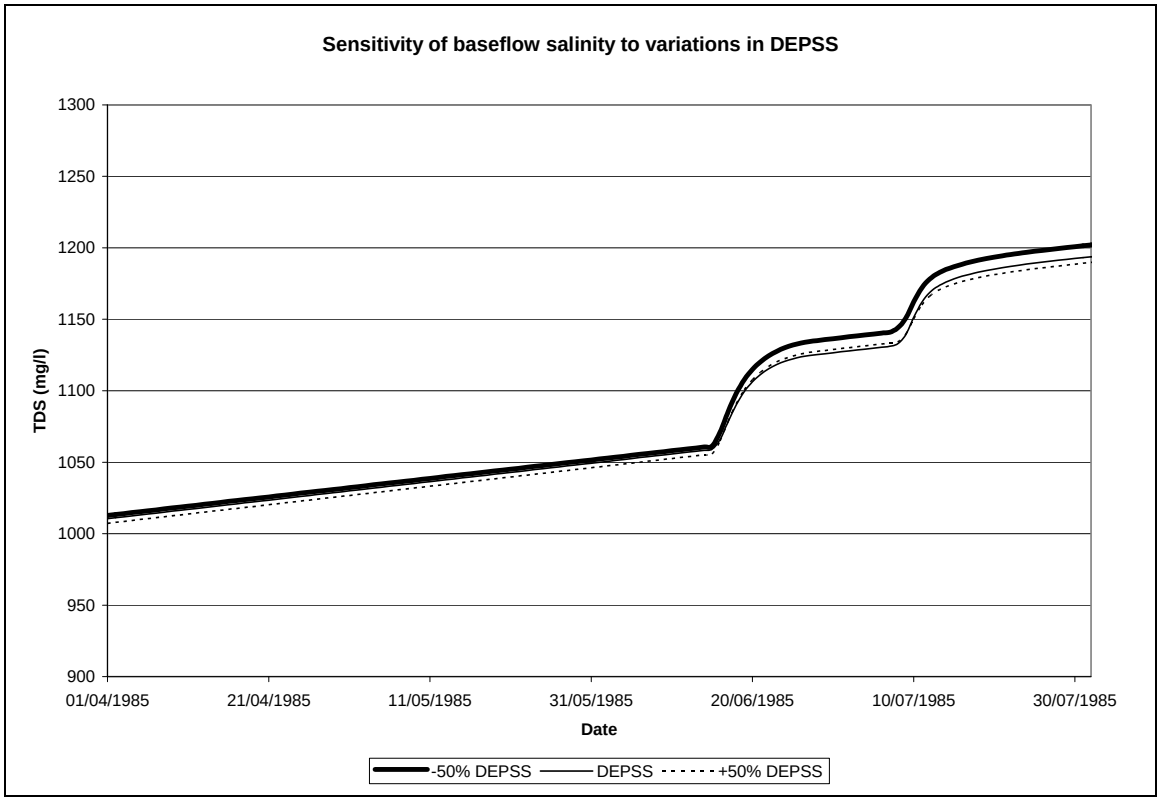

Figure 65 Sensitivity of baseflow salinity to variations in DEPSS

The variation in the TDS of the baseflow in response to variations in DEPSS is shown in Table 23 which shows neglible variations in TDS.

Table 23 Sensitivity of daily simulated TDS statistics to variations in the value of DEPSS (for baseflow)

Statistical Parameter	Percentage change from calibrated value	
	-50% Change	+50% Change
Mean	0.79	-0.69
Standard Deviation	1.46	-1.37

5.3.3 Effect of varying runoff event contact time (SALTCTIME)

Levenspiel (1972) explains the concept of contact time (or more correctly, Residence Time Distribution) using the example of an irreversible first order reaction. He showed that as the contact time increased, the concentration of product also increased. The salinity response of the various components of runoff will be explored in the ensuing sections.

Sensitivity of quickflow to variations in SALTCTIME

Based on the defining equation (**Equation 1**) for the salt contribution from the soil surface layer, it can be inferred that the response of salt concentration from the soil surface layer would increase with an increase in contact time. **Figure 66** shows, however, that the change in quickflow concentration in response to the contact time is negligible.

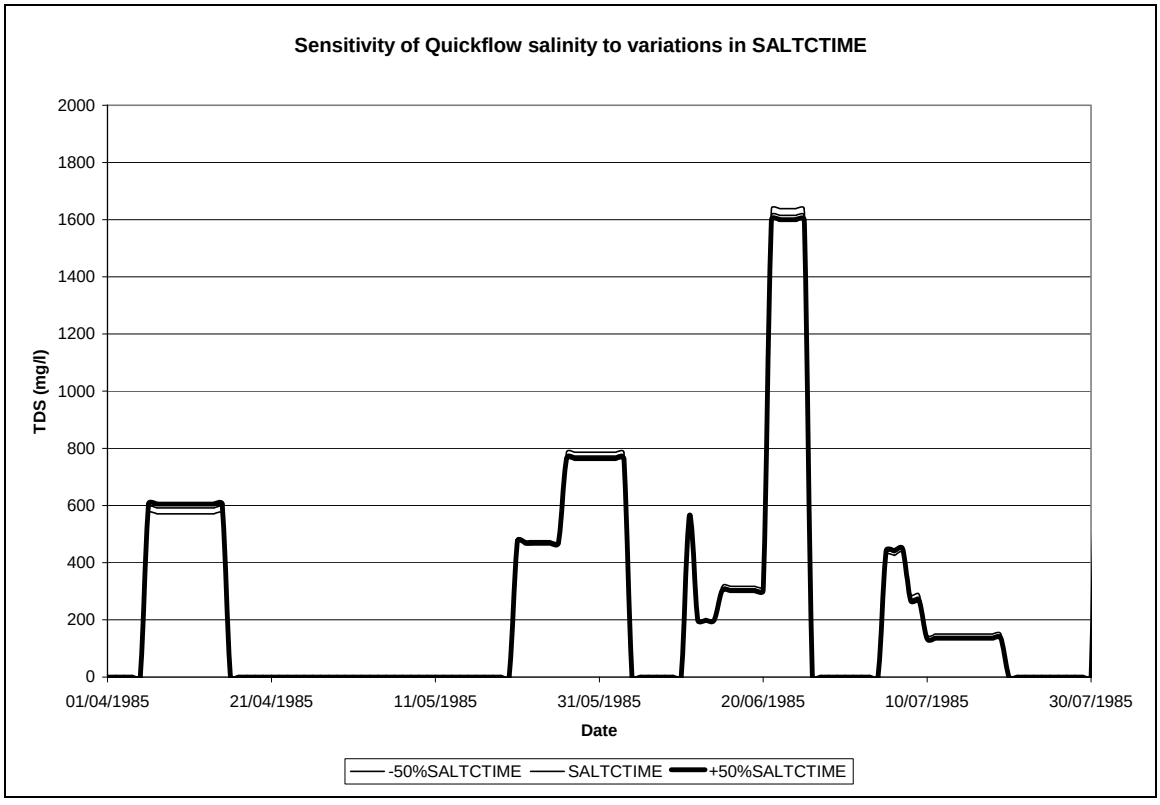

Figure 66 Sensitivity of quickflow salinity to variations in SALTCTIME

As with the graphical representation of the sensitivity of the analysis, **Table 24** shows that the simulated TDS values are insensitive to the variation in the value for SALTCTIME. This is probably caused by the default value of the dissolution constant (α), 0.2, used in the study.

Table 24 Sensitivity of daily simulated TDS statistics to variations in the value of SALTCTIME (for quickflow)

Statistical Parameter	Percentage change from calibrated value	
	-50% Change	+50% Change
Mean	-0.24	0.15
Standard Deviation	-0.75	0.48

Sensitivity of baseflow salinity to variations in SALTCTIME

As for parameter DEPSS, the SALTCTIME parameter was specifically introduced to effect changes in the values of the quickflow salinity and was not expected to have a significant impact on the baseflow salinity. This is reflected in **Figure 67** which shows negligible variation in baseflow salinity.

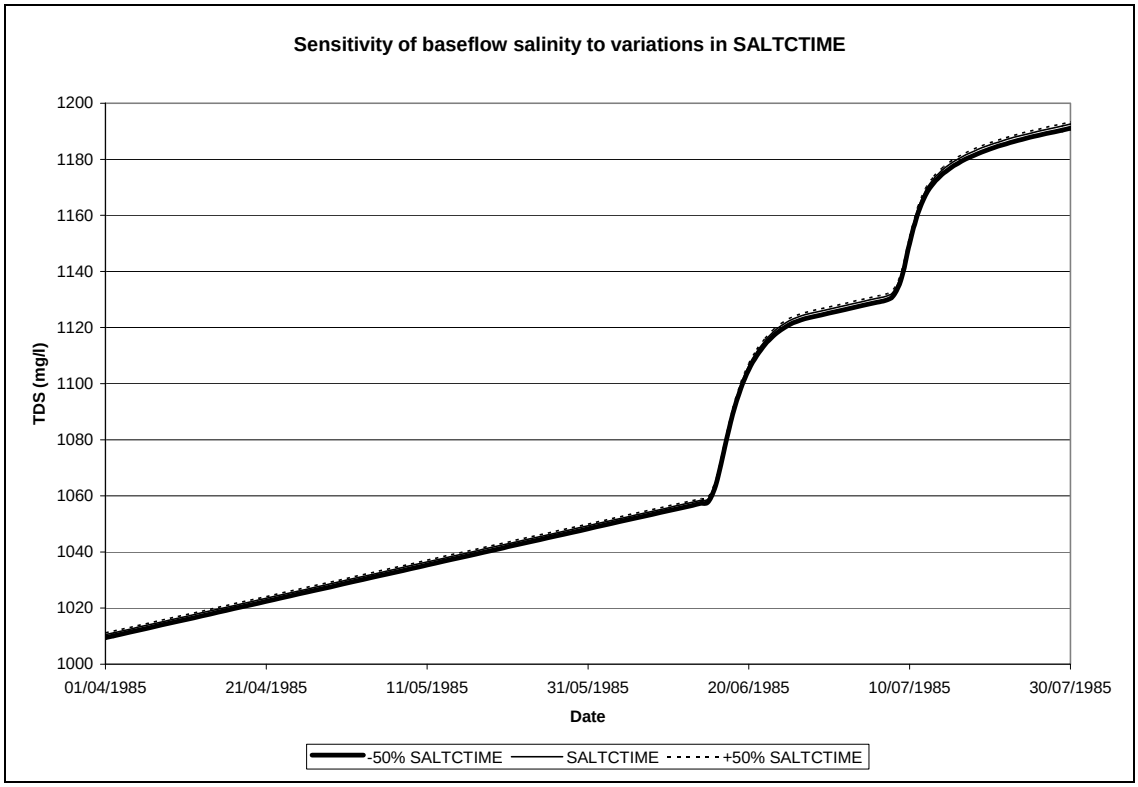

Figure 67 Sensitivity of baseflow salinity to variations in SALTCTIME

As with the graphical representation of the sensitivity of the analysis, **Table 25** shows that the output parameters are insensitive to the variation in the value for SALTCTIME. This is probably caused by the default value of the dissolution constant (β), 0.2, used in the study.

Table 25 Sensitivity of daily simulated TDS statistics to variations in the value of SALTCTIME (for baseflow)

Statistical Parameter	Percentage change from calibrated value	
	-50% Change	+50% Change
Mean	0.01	-0.01
Standard Deviation	0.06	-0.04

5.3.4 Effect of varying the monthly salt saturation (SALTSAT)

The SALTSAT value represents the maximum value of soil (sub-surface) salinity concentration above which no additional salt production occurs. In practices, this value can be inferred from the streamflow concentrations during a lowflow period, over a dry spell. In this study, the SALTSAT for the entire soil profile was kept the same to avoid introducing additional degrees-of-freedom during the calibration process.

Sensitivity of quickflow salinity to variations in SALTSAT

The sensitivity of quickflow salinity to variations in the value of SALTSAT was not previously assessed. Quickflow salinity could only be influenced by the rainfall salinity or the salinity of the saturated upward flow when the the soil moisture content of the A and B horizons was exceeded. It was subsequently concluded, by Tewldebrhan (2003), that the response of the quickflow salinity to variations in SALTSAT would be small to negligible.

In this study, the inclusion of the soil surface layer, a parameter for the surface soil saturation value (SALTSATSS) and the activation of unsaturated salt movement, however, are expected to change the sensitivity of quickflow salinity to variations in SALTSAT. **Figure 68** shows the response of the quickflow salinity in response to the variation in SALTSAT, indicating that this output is highly sensitive to these variations.

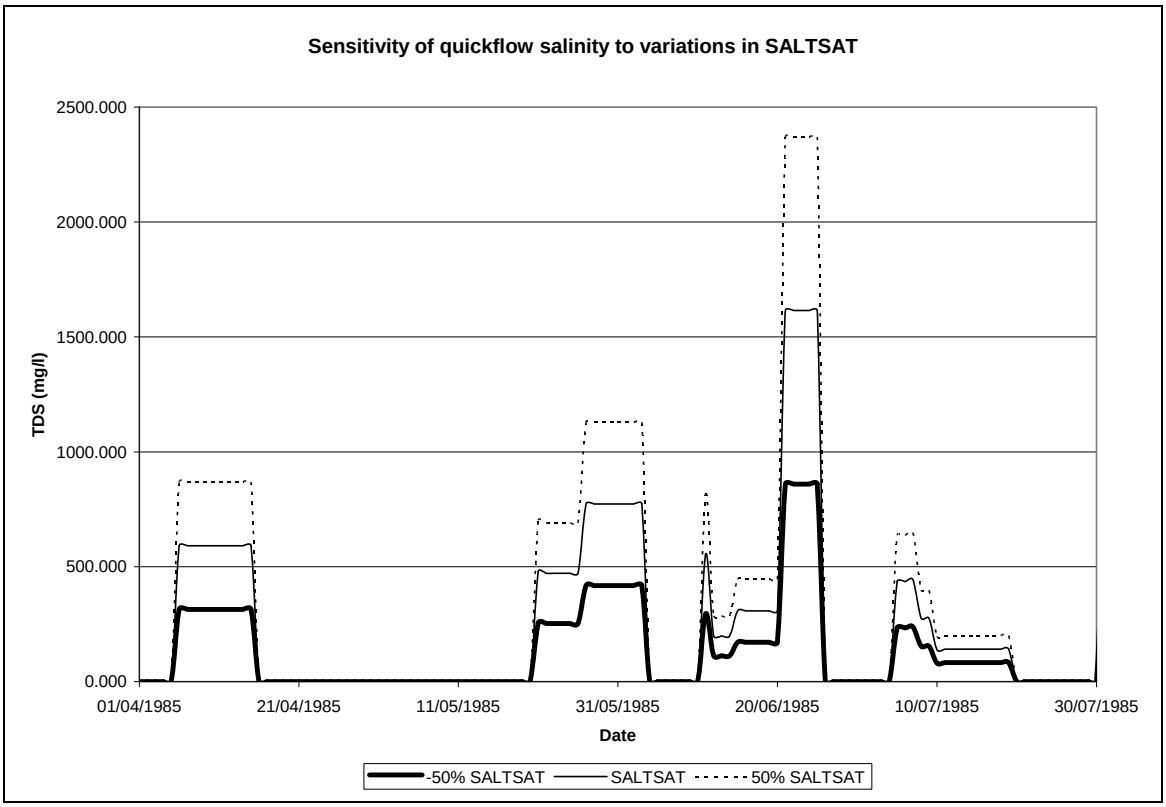

Figure 68 Sensitivity of quickflow salinity to variations in SALTSAT

As with the graphical representation of the sensitivity of the analysis, **Table 26** shows that the quickflow TDS statistics are highly sensitive to the variation in the value for SALTSAT.

Table 26 Sensitivity of daily simulated TDS statistics to variations in the value of SALTSAT (for quickflow)

Statistical Parameter	Percentage change from calibrated value	
	-50% Change	+50% Change
Mean	-46.95	46.94
Standard Deviation	-47.87	47.88

Sensitivity of baseflow salinity to changes in SALTSAT

Teweldebrhan (2003) showed only a 15% change in the runoff and baseflow salinity in response to a 50% change in the value for SALTSAT. This is important since initial attempts to calibrate the ***Beta version*** of ACRU*Salinity* with Berg River data required unrealistically large changes in the values of SALTSAT, to produce runoff TDS concentration representative of the observed records. **Figure 69** depicts the typical variations that could be expected for changes in the value of SALTSAT.

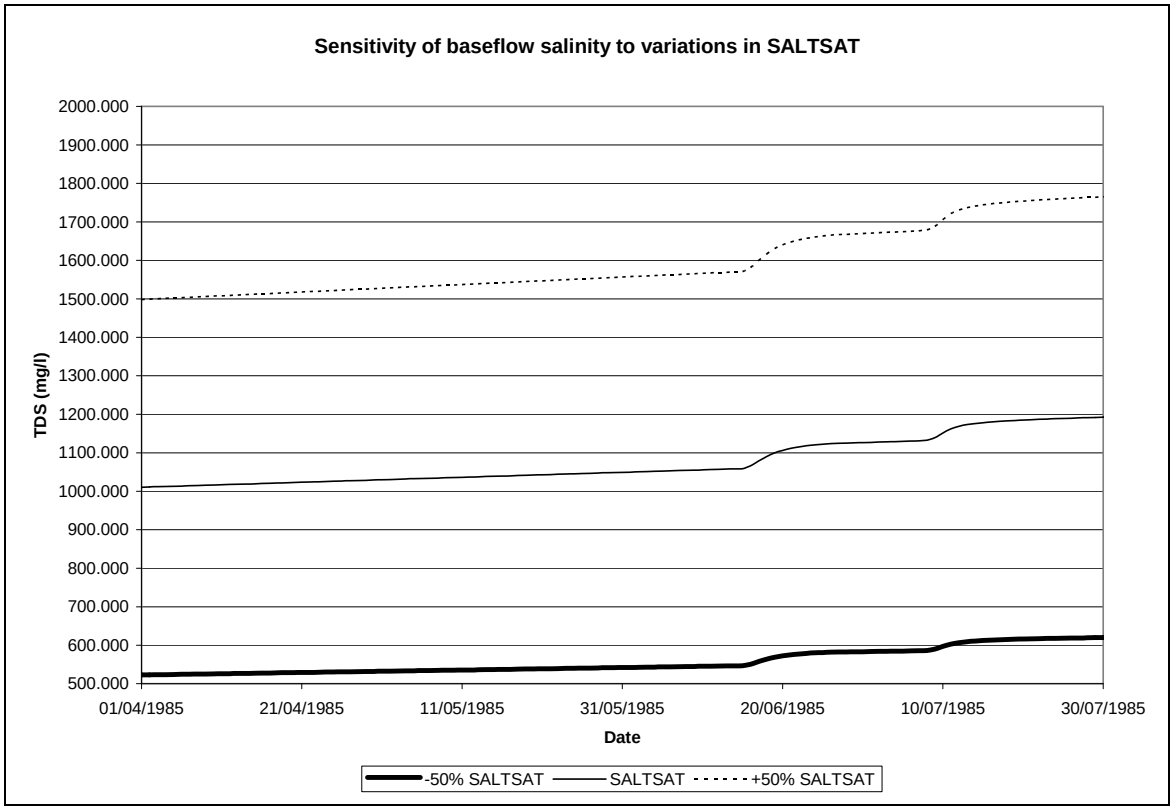

Figure 69 Sensitivity of baseflow salinity to variations in SALTSAT

As with the graphical representation of the sensitivity of the analysis, **Table 27** shows that the baseflow salinities are highly sensitive to the variation in the value for SALTSAT.

Table 27 Sensitivity of daily simulated TDS statistics to variations in the value of SALTSAT (for baseflow)

Statistical Parameter	Percentage change from calibrated value	
	-50% Change	+50% Change
Mean	-48.16	48.16
Standard Deviation	-49.95	49.99

Contrary to the findings by Teweldebrhan (2003), **Table 27** shows that a variation of 50% in the value for SALTSAT resulted in an almost equal change in the mean TDS concentrations for baseflow. This could possibly be attributed to the additional surface layer and code modifications that were undertaken as part of this study.

5.3.5 Summary of sensitivity analysis outcomes

A summary of the sensitivity of the daily simulated TDS values to the changes in various salinity-related calibration parameters are shown in **Table 28**, which indicates that efforts in calibration should be focused on a sound estimation of the values for SALTUPT and SALTSAT. The inter-dependence between these parameters, SALTUPT and SALTSAT, will now be explored.

Table 28 Summary of sensitivity of daily simulated TDS statistics

Model Parameter changed	Statistical parameter	Quickflow		Baseflow	
		50% increase in model parameter value	50% decrease in model parameter value	50% increase in model parameter value	50% decrease in model parameter value
SALTUPT	Mean	-39.4	30.8	-41.4	25.0
	Std. Dev.	-36.7	27.1	-39.6	21.1
DEPSS	Mean	-4.0	1.0	0.8	-0.7
	Std. Dev.	-4.8	1.0	1.5	-1.4
SALTCTIME	Mean	-0.2	0.2	0.01	-0.01
	Std. Dev.	-0.8	0.5	0.06	-0.04
SALTSAT	Mean	-46.9	46.9	-48.2	48.2
	Std. Dev.	-47.9	47.9	-50.0	50.0

5.4 INTER-DEPENDENCE OF SALINITY-RELATED PARAMETERS

Based on the outcome of the foregoing sensitivity analysis it was decided to test the inter-dependence of only the most sensitive salinity-related parameter, *viz*. SALTUPT and SALTSAT. Görgens (1983) described the problem of uniqueness of parameter value sets for rainfall-runoff modelling, which would be equally applicable to the hydrosalinity modelling exercise undertaken in this study. The non-uniqueness of salinity parameters in the model is related to the availability of several of these parameters which could be specied in various ratios to one another with each set producing the desired results.

The process whereby the final parameters were selected during this study relied on successive iteration of the parameters SALTUPT and SALTSAT until the value of the objective functions were considered acceptable. To investigate the response of the objective function to the variation in the salinity-related parameters, a two-dimensional response surface was constructed for the various value sets of parameters SALTSAT and SALTUPT. If more than two parameters are considered significant in influencing the value of the objective function, a multi-dimensional co-ordinate system would be required to evaluate the objective function's response.

The response surfaces depicting the variation of the coefficient of determination (r^2), as well as the variation of the ratio of r^2 to the coefficient of efficiency, for the salinity calibration at G1H037, are shown in **Figure 70** and **Figure 71**. These plots have been based on a limited number of model runs (44 runs) and are shown merely to illustrate the process which could be followed to implement a systematic calibration process or even autocalibration routines.

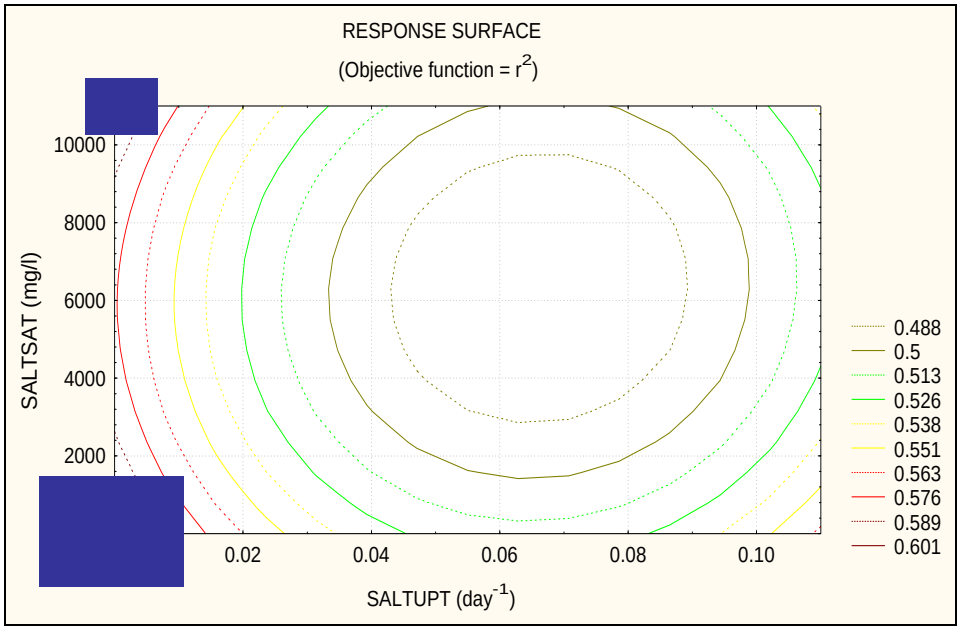

Figure 70 Two-dimensional response surface (objective function = r^2)

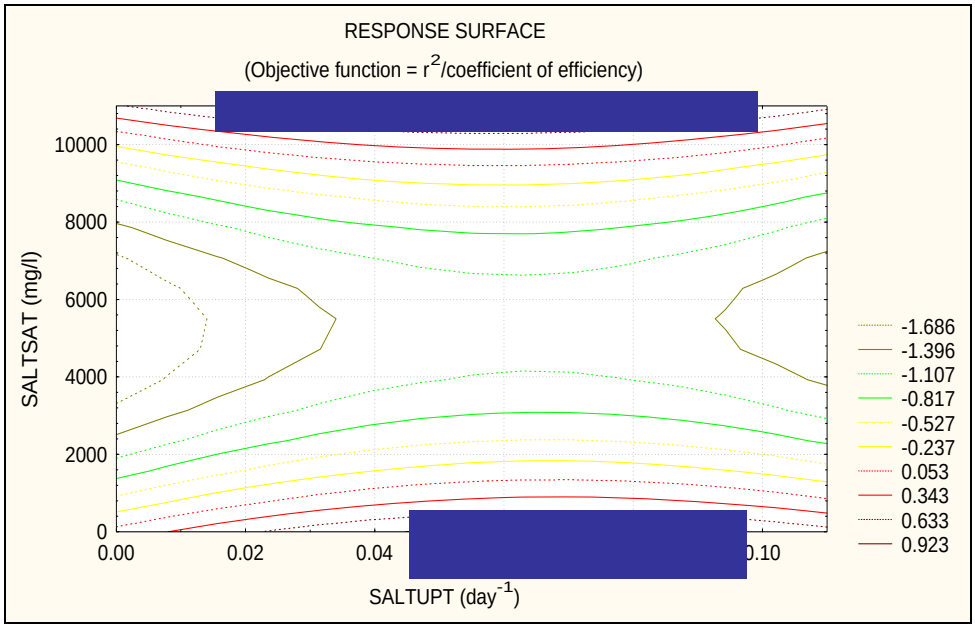

Figure 71 Two-dimensional response surface (objective function = r^2/coefficient of efficiency)

Based on **Figure 70** and **Figure 71**, the calibration strategy would rely on maximising the value of r^2 and then attempting to obtain a final value for r^2/coefficient of efficiency which is as close as possible to unity without significantly reducing the value of r^2. The second step in the aforementioned process is important because it is an attempt to increase the 1:1 fit of the simulated and observed records, while avoiding any systematic errors.

According to Görgens (1983), the phenomenon whereby quite different parameter sets yield similar values of the same objective function are quite common in rainfall-runoff models and by analogy, the Salinity module in ACRU*Salinity* would probably present the same phenomenon. Görgens grouped the possible reasons for this phenomenon as follows:

- Inter-dependence between model parameters.
- Indifference of the objective function to parameter values such that appreciable changes in the value of one parameter may cause little or no change in the objective function.
- Discontinuities or points on the response surface at which the objective function, while still continuous, is non-differentiable.
- Local optima of objective function values which could lead to premature declaration of convergence.
- Scaling of parameters – the particular scale used for different parameters may result in unfavourable configurations of the response surface for optimal search progress.

Although **Figure 70** and **Figure 71** were based on only a limited number of simulated daily TDS sets, it can be seen that a number of different value sets for SALTUPT and SALTSAT could be used to obtain acceptable values of the objective functions. Both figures suggest that a band of values (i.e. blue blocks on **Figure 70** and **Figure 71)** may exist for which the objective functions can be optimised.

For the paricular catchment tested (G1H037), the values for SALTUPT and SALTSAT should tend towards the lower region of their respective scales because the observed average TDS concentration of the streamflow is 95 mg/l and it would be unlikely that the salt saturation constant (SALTSAT) would be an order of magnitude larger than the average stream flow concentration. In this case, the value for SALTSAT should be as close as possible to that of the stream flow salinity after a prolonged dry spell, with SALTUPT then being varied to produce the desired value for the objective function, resulting in the most realistic dataset being used.

5.5 SALINITY CALIBRATION OF THE ACRU*SALINITY* MODEL

Salinity calibrations were only undertaken at gauges where a sufficient number of grab samples were taken. The gauges used for verification of the salt module and the periods of verification are given in **Table 29**.

Table 29 Gauges used for the calibration of the Salt Module in ACRU*Salinity*

Gauge	Period of Verification
G1H037	1982 – 1992
G1H041	1980 – 1999
G1H036	1980 – 1999
G1H043	1980 – 1997
G1H013	1983 – 1999
G1H035	1980 – 1999
G1R003	1980 – 1999

The final salinity-related parameters for the calibration catchments are shown in **Table 30**.

Table 30 Values of salinity -related parameters used in the Berg River

Gauge No.	SALSAT*	SALTUPT01	SALTUPT02
G1H037	1500	1e-5	7e-6
G1H041	3000	1e-4	5e-5
G1H036 incremental	11000	1e-5	7e-6
G1H008+	16000	1e-7	5e-8
G1H002+	10	1e-7	7e-8
G1H029+	10	1e-7	5e-7
G1H043	13000	7.5e-4	5e-4
G1H013 incremental	6000	1.5e-5	9.5e-6
G1H035	7500	1.5e-3	1e-4
G1H034	9000	10.5e-5	6e-5
G1R003	50	10.5e-5	6e-5

* These values are applicable to the surface soil layer, A-horizon and B-horizon

Specific comments regarding the appropriateness of the calibration set will be made in each section where the calibration is discussed. These parameters are, in part, related to the underlying geological formation and tillage practices which augment the mobilisation of salts.

5.5.1 Salinity calibration at G1H037 (Krom River at Wellington)

Analysis of the TDS grab sample record for the period 1979 to 1992 shows that the average, maximum and minimum recorded TDS concentrations at this gauge were 95 mg/l, 692 mg/l and 36 mg/l, respectively. The seasonal variation of the TDS values is depicted in **Figure 72** which is typical of what is expected from a winter rainfall region with slightly higher TDS concentrations during the summer months. This was as a result of the evapo-concentrating effect, irrigation return flows and comparatively lower TDS values during the wet winter months.

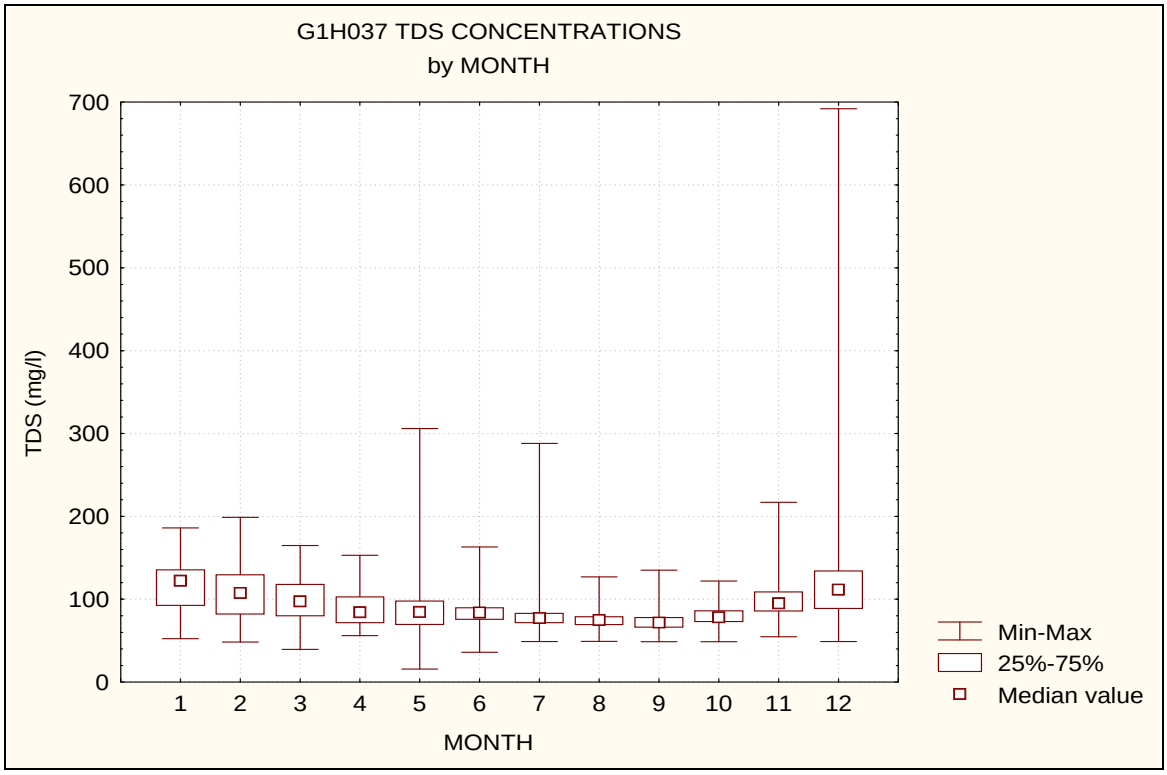

Figure 72 Seasonal distribution of observed (grab sample) TDS concentrations at gauging station G1H037

As discussed previously, the water from the Wit River (in the Breede River catchment) was assumed to be imported to this sub-catchment at a constant monthly flow rate of 0.22×10^6 m^3/month.

The comparison of daily simulated and infilled observed TDS exceedance percentages at gauging station G1H037 is depicted in **Figure 73** which shows that TDS concentrations rarely exceed 150 mg/l and that fairly good quality water (with regard to TDS) is discharged from this catchment. The simulated record closely replicates the observed record except for exceedances of less than 3% and greater than 85%, however the departures are relatively small (less than

50 mg/l) compared with the effects of the downstream saline tributary inflows on the salinity at Misverstand.

Eventhough a representative fit between the simulated and observed exceedance percentages were obtained, the final values of the salinity-related calibration parameters (see **Table 30**) are probably not the most appropriate values for this catchment. Particularly when one considers that the average TDS concentration in this catchment is only 95 mg/l. The fact that, on an exceedence basis, the simulated TDS concentrations are representative of reality is probably due to the inter-dependence between the SALTSAT and SALTUPT parameters.

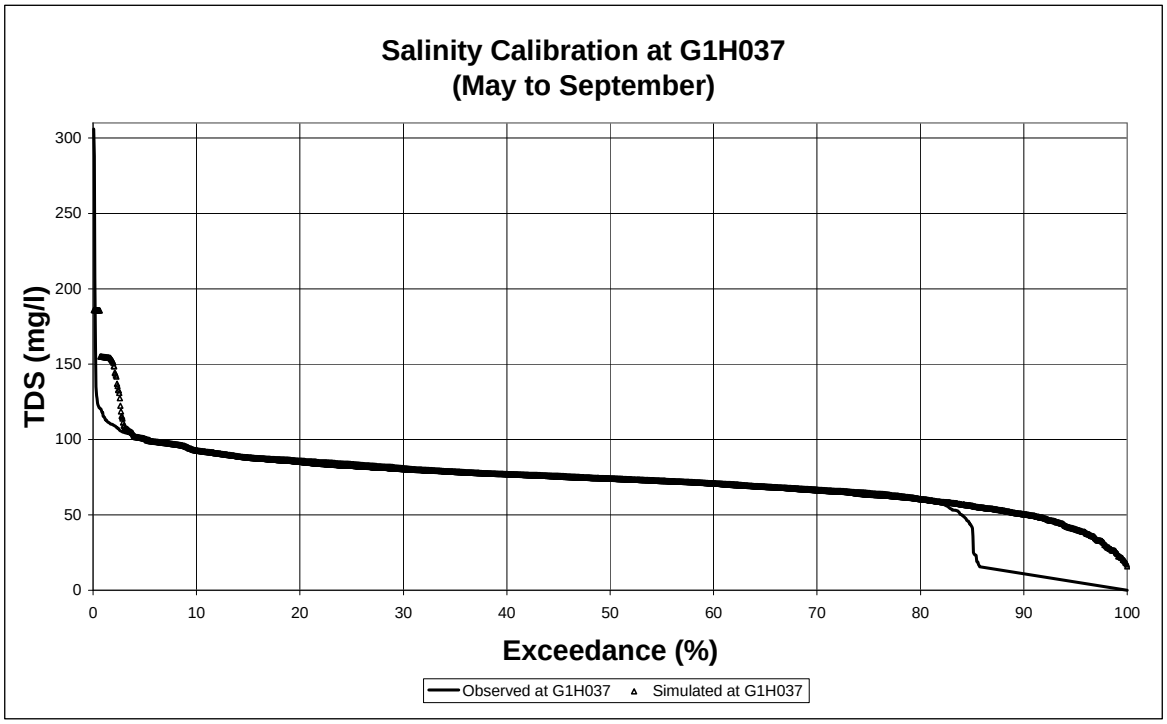

Figure 73 Exceedance of observed and simulated daily TDS at gauge G1H037

A comparison of daily observed and simulated TDS concentrations is shown in **Figure 74**. Visual inspection of this figure shows that the daily observed trends are reasonably mimicked by the simulated values, but that isolated high TDS values in the observed record are not always reflected in the simulated record. The inability of the simulated TDS values to match each peak and valley in the observed TDS record can in part be attributed to the less than perfect fit between the daily simulated and observed flows.

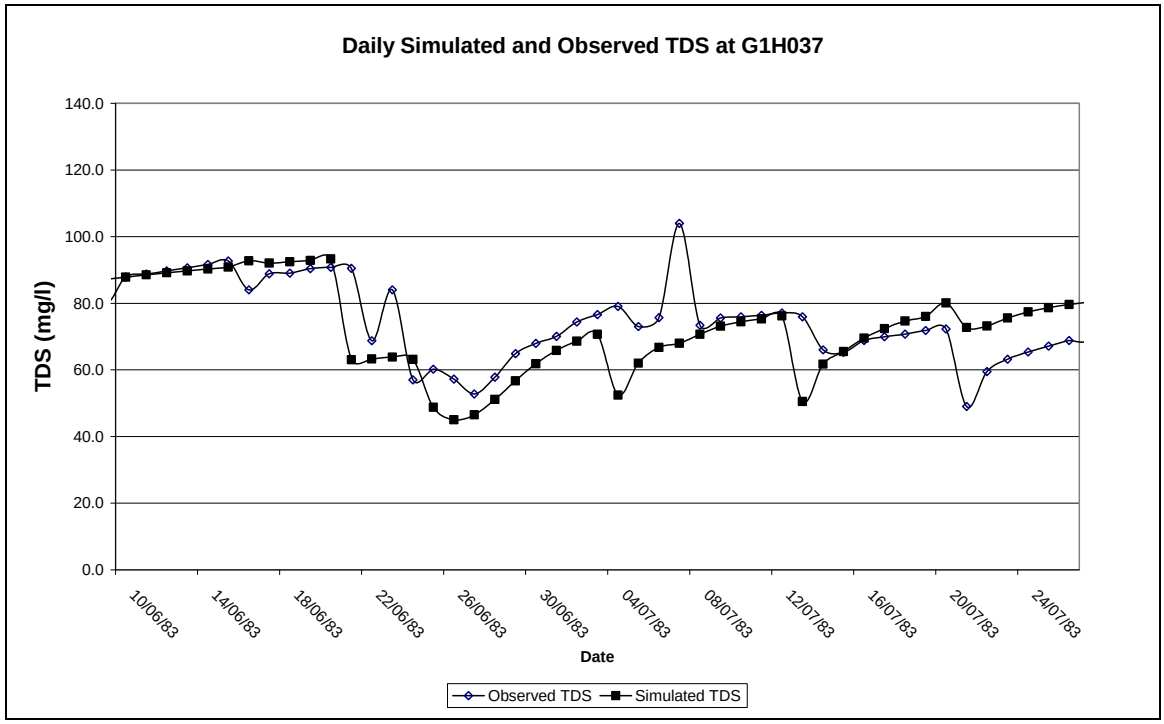

Figure 74 Daily Simulated and Observed TDS Concentrations at G1H037

A comparison of the seasonality of the daily infilled observed TDS series and simulated TDS series is depicted in **Figure 75** where month 1 is January. The figure shows a reasonable comparison of the median values over the winter months, but the infilled observed record has more natural variation.

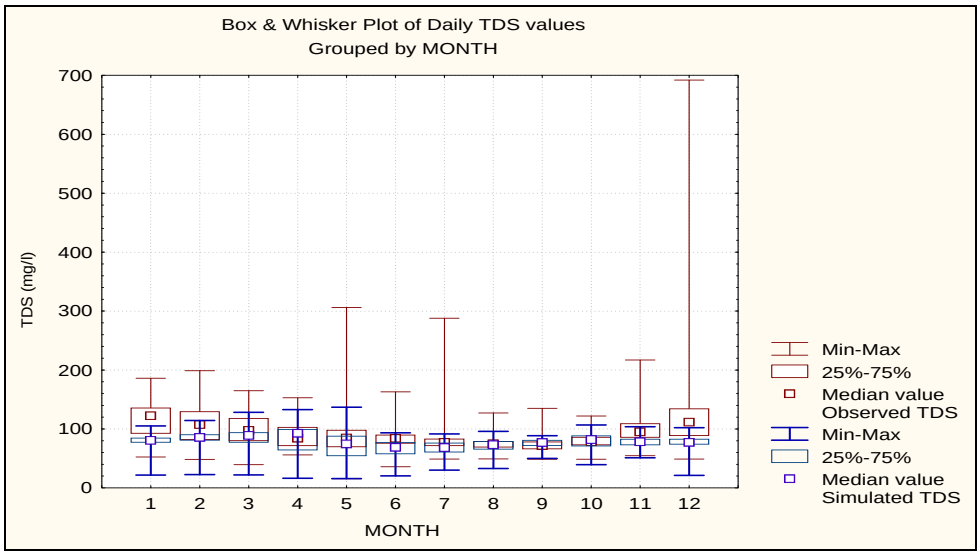

Figure 75 Comparison of seasonality of simulated and infilled observed TDS values at G1H037

5.5.2 Salinity calibration at G1H041 (Kompanjies River at De Eikeboomen)

Analysis of the TDS grab sample data for the period 1979 to 2002 showed that the average, maximum and minimum TDS concentrations were 164 mg/l, 5 499 and 39 mg/l, respectively. The seasonal distribution of the TDS concentrations at the gauge is depicted in **Figure 76**. As is typical of this part of the Berg River Catchment, the higher TDS concentrations occur during the summer months with the lower TDS concentrations occurring in the winter months.

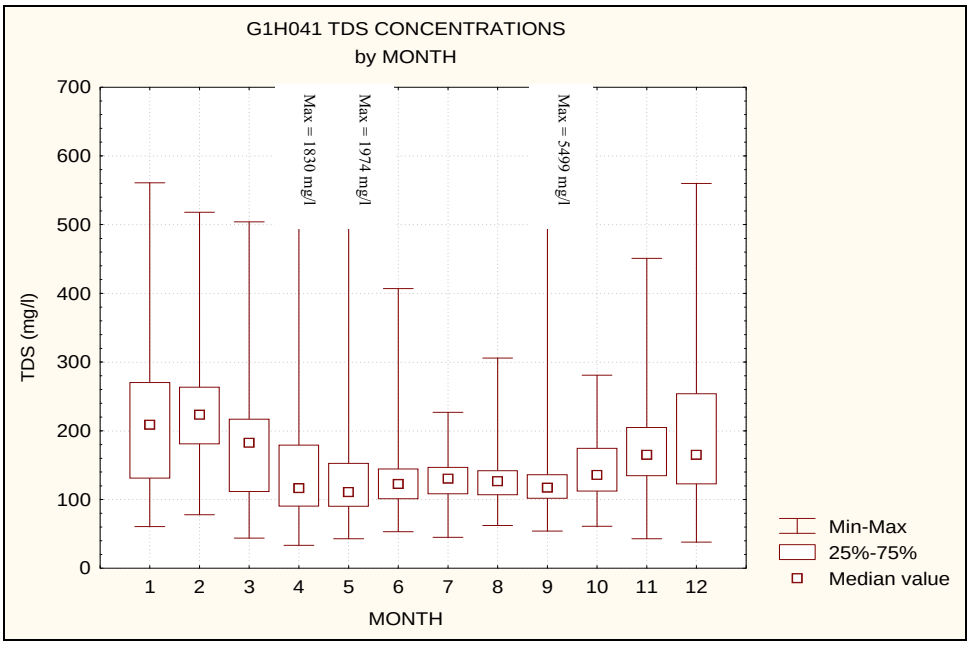

Figure 76 Seasonal distribution of observed (grab sample) TDS concentrations at Gauge G1H041

The comparison of the daily simulated and observed TDS exceedance percentage at gauge G1H041 is depicted in **Figure 77** which shows that the exceedance percentage of the simulated TDS is representative of the infilled observed record with a slight under-estimation of the exceedance percentage for simulated TDS values above 200 mg/l.

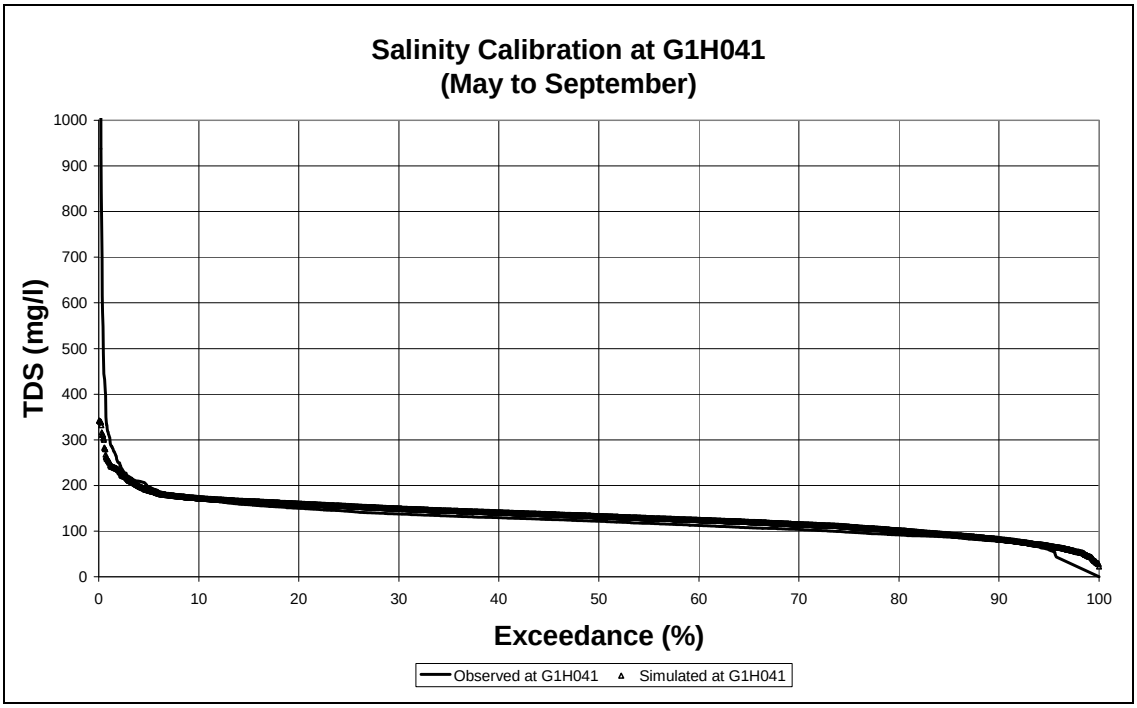

Figure 77 Exceedance of observed and simulated daily TDS at gauge G1H041

The final values of the salinity-related calibration parameters (see **Table 30**) used in this calibration are not appropriate, considering that the average TDS concentration in this catchment is only 164 mg/l. The fact that, on an exceedence basis, the simulated TDS concentrations are representative of reality is probably due to the inter-dependence between the SALTSAT and SALTUPT parameters.

A comparison of daily observed and simulated TDS concentrations is shown in **Figure 78**. Visual inspection of this figure shows that the daily observed trends are reasonably mimicked by the simulated values, but that isolated high TDS values in the observed record are not always reflected in the simulated record. For periods of the flow record where an unsatisfactory comparison between the daily simulated and observed flows were obtained, the comparison between daily simulated and observed TDS values is likely to be less favaourable.

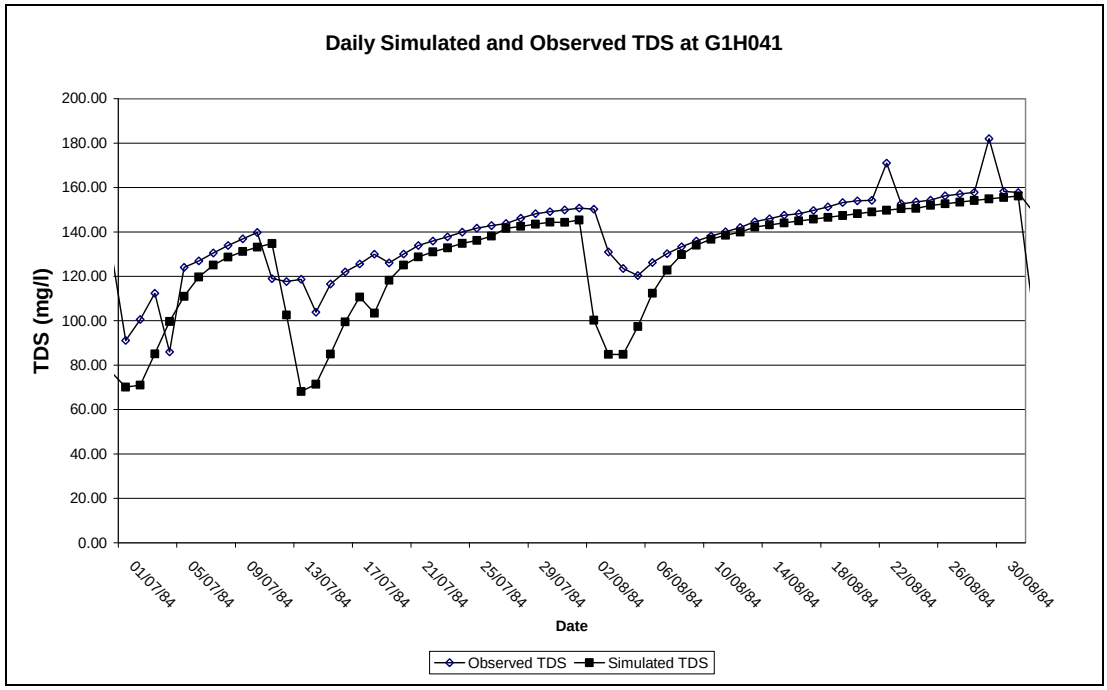

Figure 78 Daily Simulated and Observed TDS Concentrations at G1H041

A comparison of the seasonality of the daily infilled observed TDS series and simulated TDS series is depicted in **Figure 79** where month 1 is January. The figure shows a reasonable comparison of the median values over the winter months, but the infilled observed record has more natural variation.

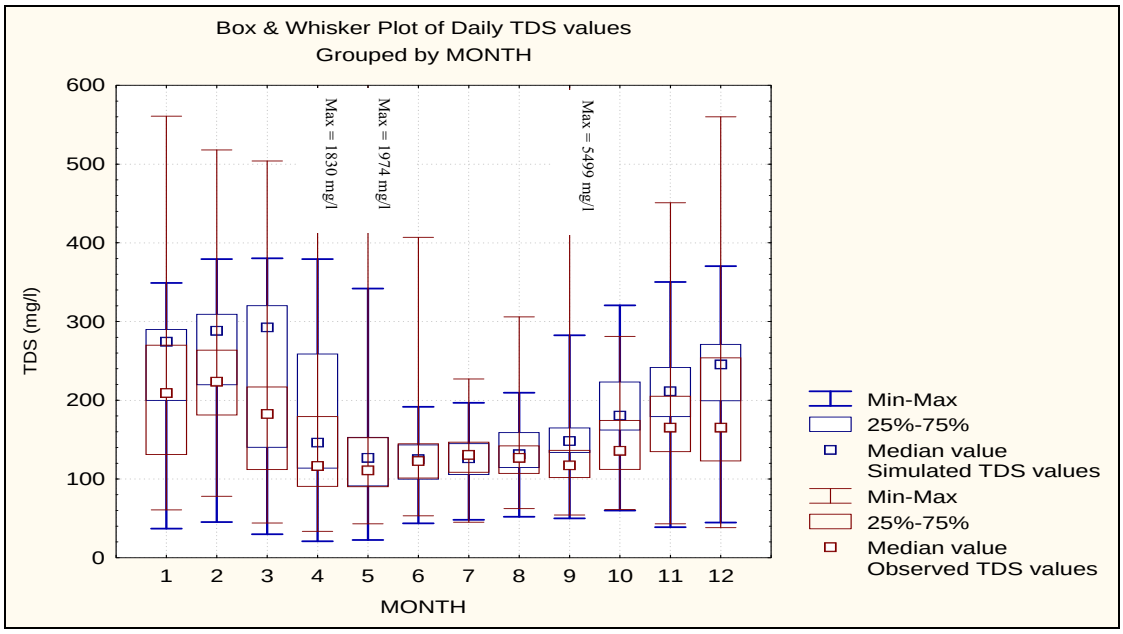

Figure 79 Comparison of seasonality of simulated and infilled observed TDS values at G1H041

5.5.3 Salinity calibration at G1H036 (Berg River at Vleesbank)

Salinity calibration at gauge G1H036 was essentially completed to ensure that the values of the salinity-parameters transferred from the rest of the catchment resulted in representative TDS concentrations at gauge G1H036. During the calibration process the observed flow and TDS measured at gauging station G1H020 were used as specified inflows, while the calibrated model for the sub-catchments gauged by G1H037 and G1H041 was used to generate input from these sub-catchments.

Analysis of the TDS grab sample data over the period 1978 to 2002 revealed that the average, maximum and minimum TDS concentrations were 123 mg/l, 418 mg/l and 35 mg/l, respectively. The seasonal distribution of the TDS concentration at gauge G1H036 (see **Figure 80**) shows that no marked increase in TDS is experienced over the winter months with 75% of the observed TDS values in winter being less than 150 mg/l.

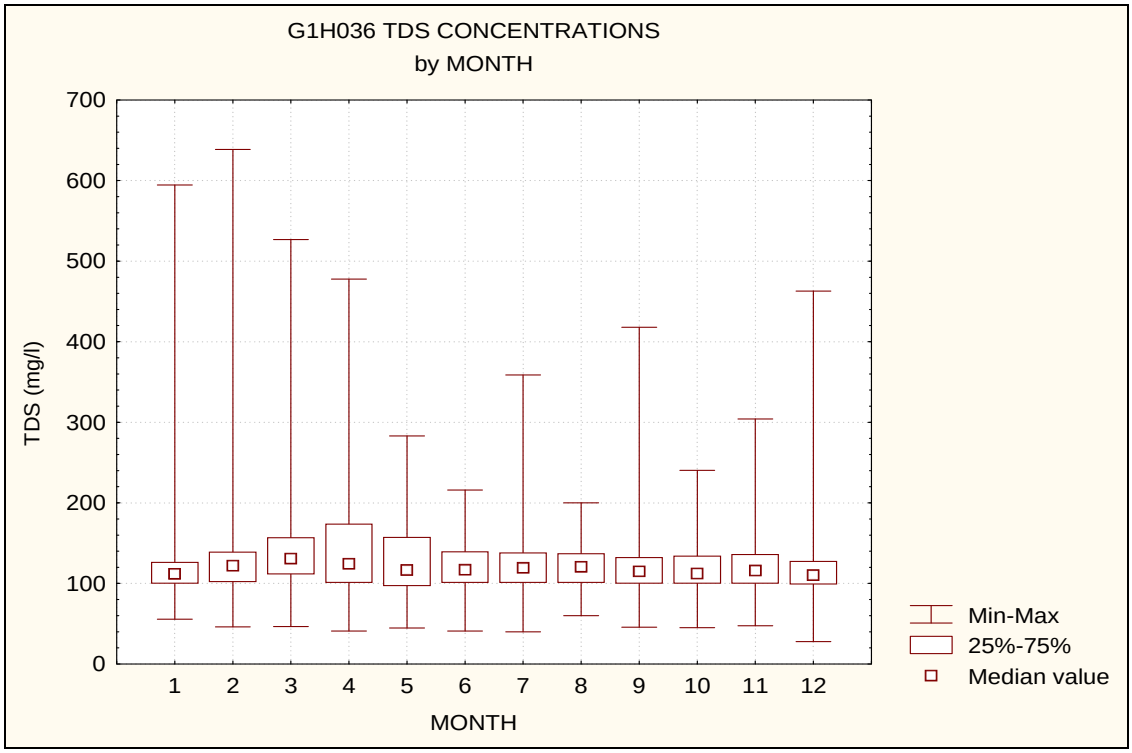

Figure 80 Seasonal distribution of observed (grab sample) TDS concentrations at gauge G1H036

The comparison of the daily simulated and observed TDS exceedance percentage at gauge G1H036 is depicted in **Figure 81** which shows that the exceedance percentage of the simulated

TDS is representative of the infilled observed record over a large portion of the range of TDS values. Where there are significant deviations, i.e. between 130-200 mg/l, the simulated values are more conservative.

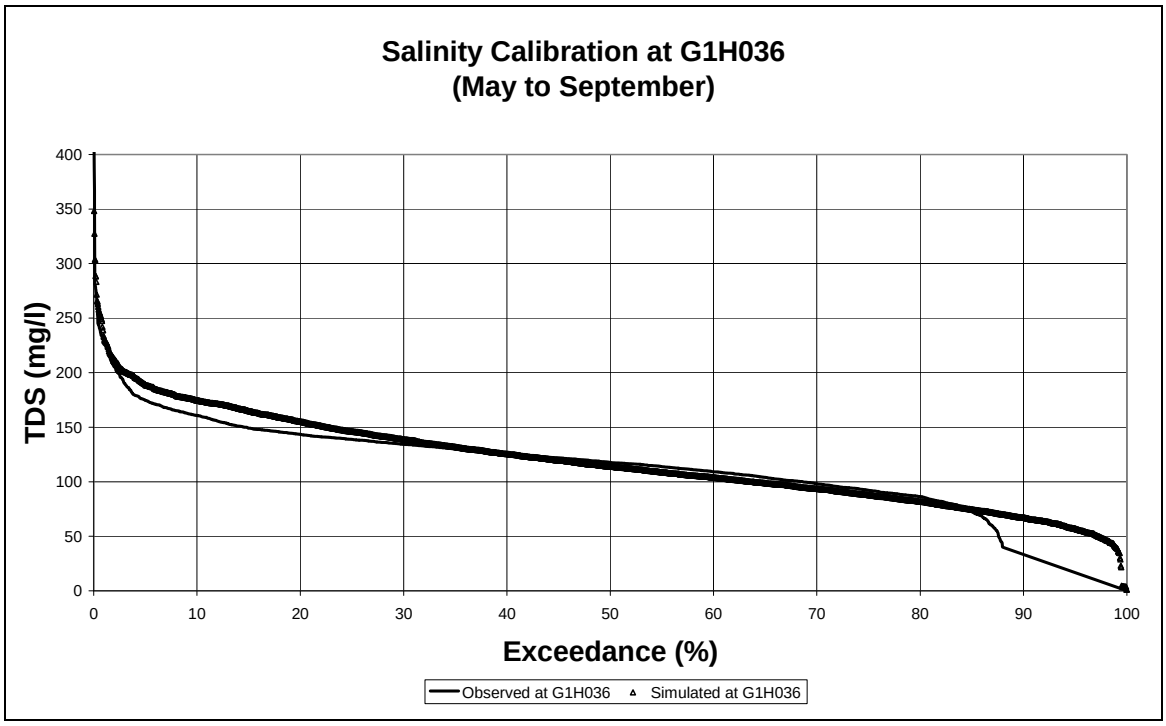

Figure 81 Exceedance of observed and simulated daily TDS at Gauge G1H036

The final values of the salinity-related calibration parameters (see **Table 30**) used in this calibration are not appropriate, considering that the average TDS concentration in this catchment is only 123 mg/l. The fact that, on an exceedence basis, the simulated TDS concentrations are representative of reality is probably due to the inter-dependence between the SALTSAT and SALTUPT parameters.

A comparison of daily observed and simulated TDS concentrations is shown in **Figure 82**. Visual inspection of this figure shows that the daily observed trends are reasonably mimicked by the simulated values, but that isolated high TDS values in the observed record are not always reflected in the simulated record. In general, the simulated TDS concentrations had a faster rate of increase after dilution, possibly indicating under-simulation of flows on the recession limb of the daily hydrograph or a value of SALTUPT which has been overestimated.

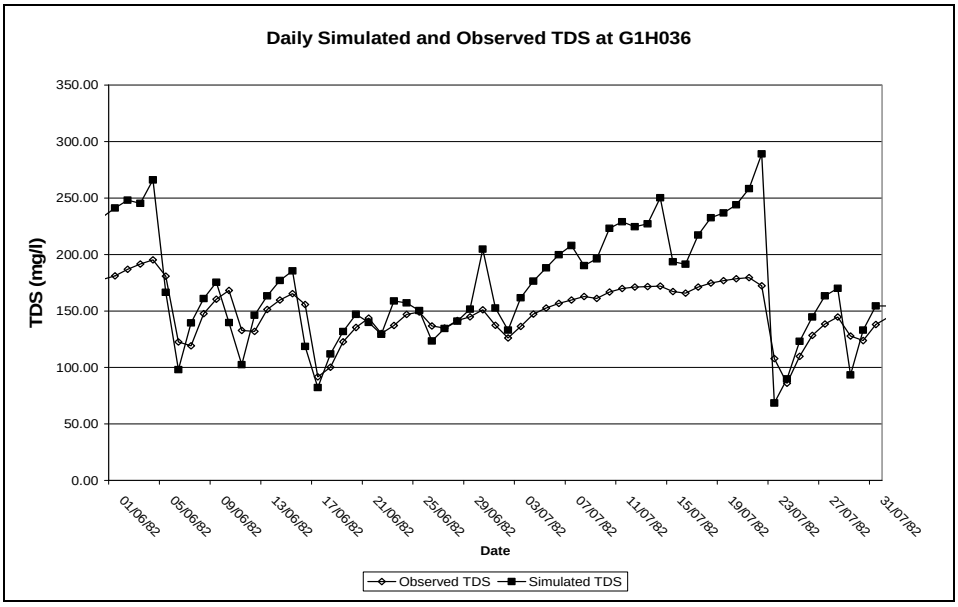

Figure 82 Daily Simulated and Observed TDS Concentrations at G1H036

A comparison of the seasonality of the daily infilled observed TDS series and simulated TDS series is depicted in **Figure 83** where month 1 is January. The figure shows that the median values of the daily simulated TDS series, during the winter months, are pessimistic. Since the comparison of the seasonal variations at gauging stations G1H037 and G1H041 are acceptable, this effect could probably be ascribed to the choice of parameters in the G1H036 incremental catchment.

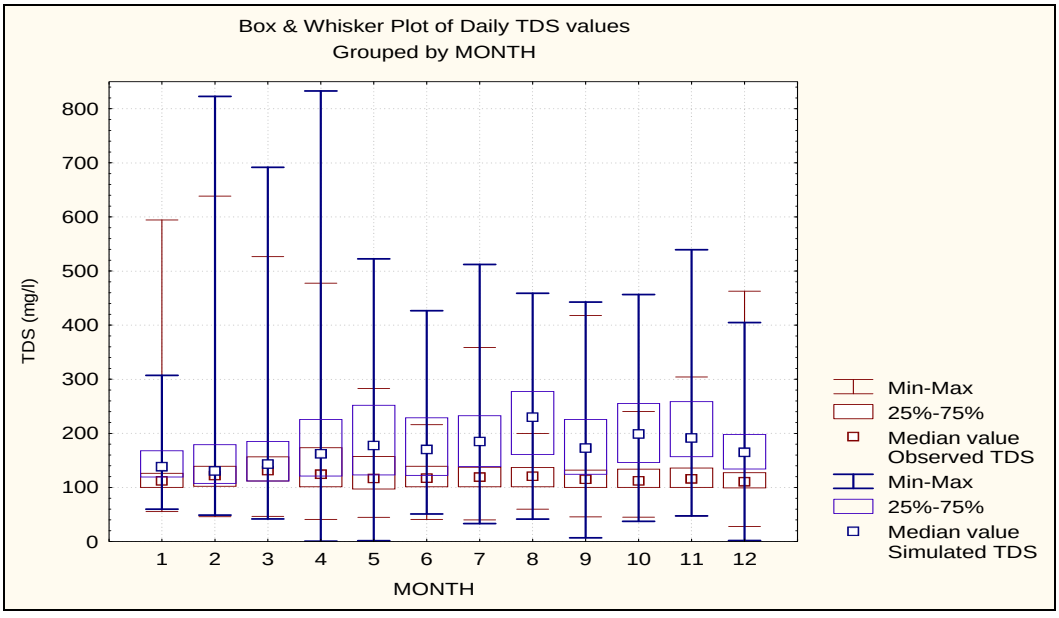

Figure 83 Comparison of seasonality of simulated and infilled observed TDS values at G1H036

5.5.4 Salinity calibration at G1H043 (Sand Spruit at Vrisgewaagd)

As mentioned previously in the report, this catchment naturally produces high TDS concentrations during the winter months when previously dissolved salts are mobilised. Analysis of the grab sample TDS record spanning the years 1980 to 1997 showed that the average, maximum and minimum TDS concentrations of the run-off produced in this catchment were 5 039 mg/l, 10 989 mg/l and 1 005 mg/l, respectively. The seasonal distribution of TDS concentrations are depicted in **Figure 84**. It should be noted that, the TDS concentration increases over the later winter months, into spring, implying that high TDS loads can be expected from this catchment.

The final values of the salinity-related calibration parameters (see **Table 30**) used in this calibration are appropriate, considering that the average TDS concentration in this catchment is 5 039 mg/l. This is based on the assumption that the equilibrium salt concentration (see **Equation 7**) would be closer to the highest observed streamflow concentration. The values of the parameters are also consistent with the fact that the soils in this sub-catchment overlay the Malmesbury Shale geological formation known for having a high salt content in its weathered state.

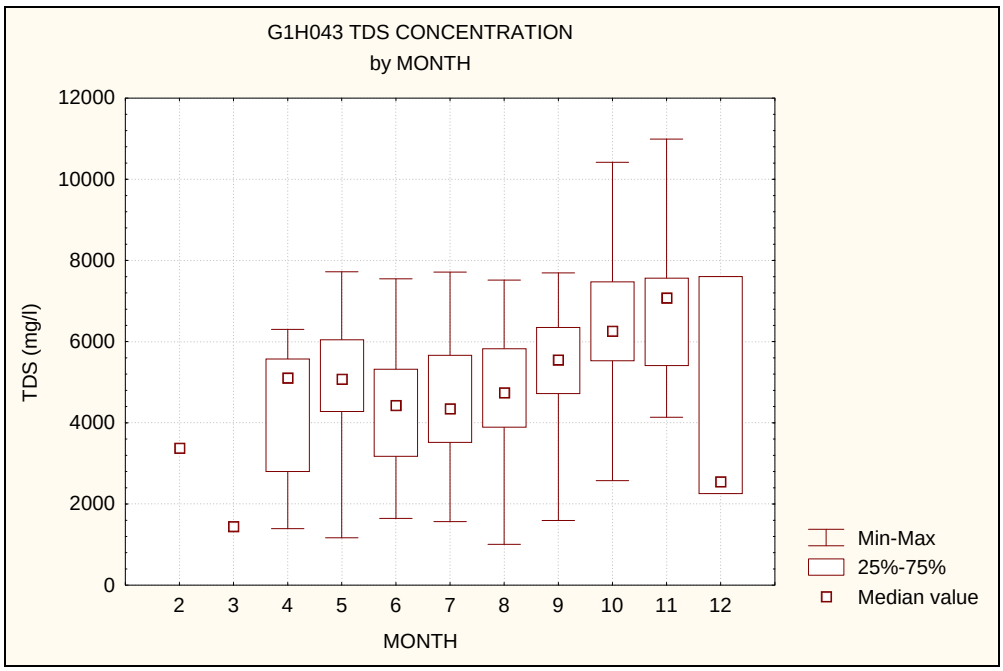

Figure 84 Seasonal variation of observed (grab sample) TDS concentration at gauging station G1H043

The salinity calibration of the daily TDS concentrations is depicted on an exceedance basis in **Figure 85**, which shows that for TDS concentrations above 5 000 mg/l, the simulated exceedance percentage is representative of the exceedance percentage displayed by the infilled observed record. Below 5 000 mg/l, however, simulated TDS values have a lower exceedance percentage.

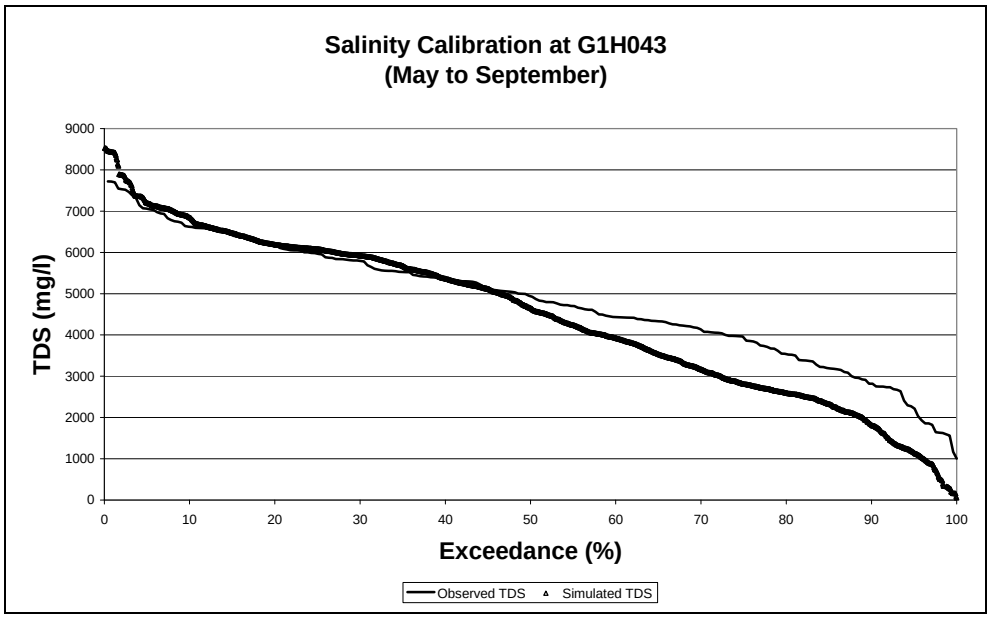

Figure 85 Exceedance of simulated and observed daily TDS concentrations at G1H043

A comparison of daily observed and simulated TDS concentrations is shown in **Figure 86**. Visual inspection of this figure shows that the daily observed trends are reasonably mimicked by the simulated values, but that isolated high TDS values in the observed record are not always reflected in the simulated record. In general, the simulated TDS concentrations had a faster rate of increase after dilution. This rising limb of TDS concentrations also did not exhibit the natural variability of that in the observed record.

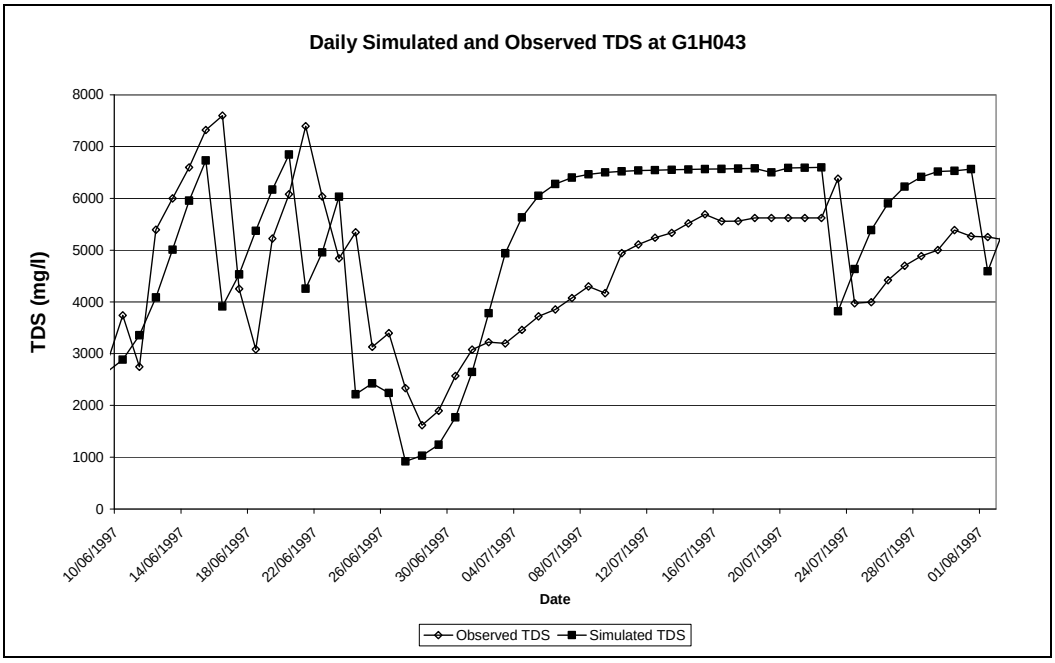

Figure 86 Daily Simulated and Observed TDS Concentrations at G1H043

A comparison of the seasonality of the daily infilled observed TDS series and simulated TDS series is depicted in **Figure 87** where month 1 is January. The figure shows that the median values of the daily simulated TDS series, during the winter months show sound correspondence with the infilled observed median values. In particular, the model manages to capture the increase in TDS concentration over the winter months.

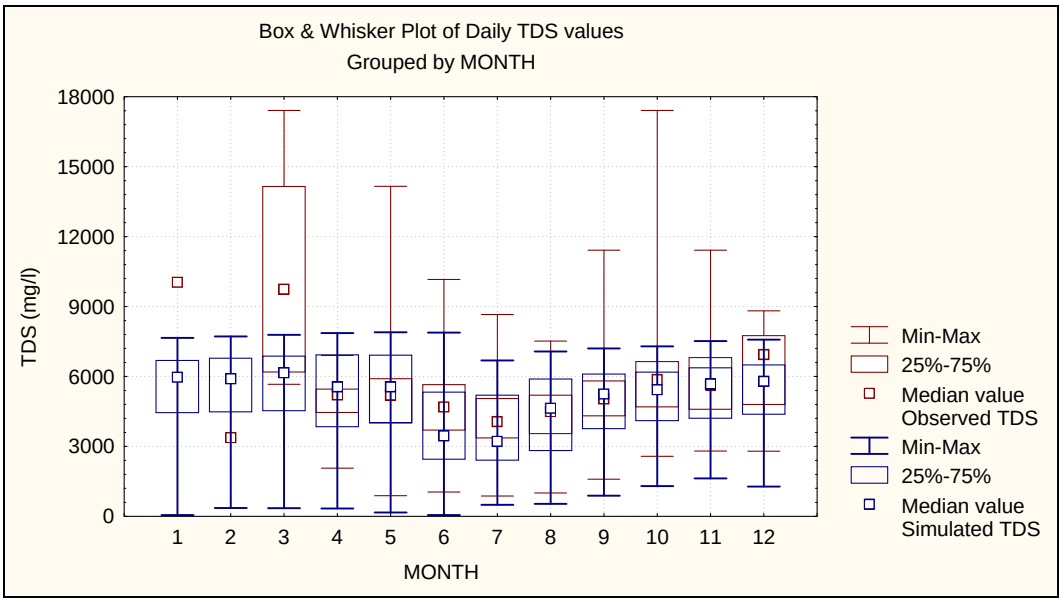

Figure 87 Comparison of seasonality of simulated and infilled observed TDS values at G1H043

5.5.5 Salinity calibration at G1H013 (Berg River at Drieheuwels)

Previous studies (Fourie and Görgens, 1977 and DWAF, 2005) have shown that two peaks in TDS concentration occur in the Lower Berg River and postulated that the winter peak was probably caused by the mobilisation of salts from the downstream catchment. In the current analysis of the TDS grab samples for the period 1965 to 2002 it was found that the average, maximum and minimum TDS concentrations at this gauge were 142 mg/l, 1 170 mg/l and 18 mg/l, respectively. The seasonal distribution of the TDS concentrations is shown in **Figure 88**.

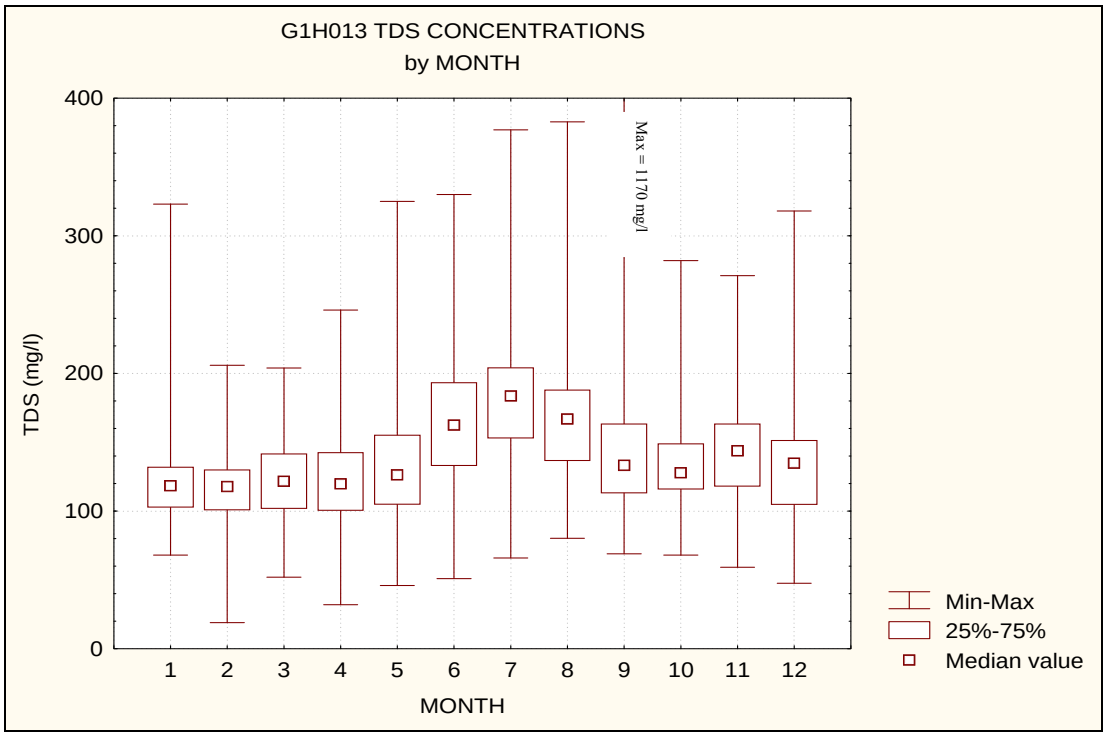

Figure 88 Seasonal distribution of observed (grab sample) TDS concentration at Gauge G1H013

This shows that a significant increase in daily TDS concentrations is experienced over the winter months, partially consistent with the increase in TDS observed at gauging station G1H043. It can be accepted that the salt concentration of the run-off generated in the catchment gauged by G1H043 has a marked effect on the TDS in the Berg River mainstem. The daily winter salinity calibration results for G1H013 is depicted in **Figure 89**, which shows a reasonable correspondence between the infilled observed and simulated exceedance percentages for TDS, but with the simulated values conservative above 200 mg/l and optimistic below 100 mg/l.

The final values of the salinity-related calibration parameters (see **Table 30**) used in this calibration are realistic on a regional scale, eventhough the average TDS concentration in this catchment is only 164 mg/l. It could be argued that the average TDS concentrations are as a result of the low-salinity in the upstream inflow to this part of the catchment and that the values of the salinity-related parameters are appropriate for describing the localised effect of the incremental catchment.

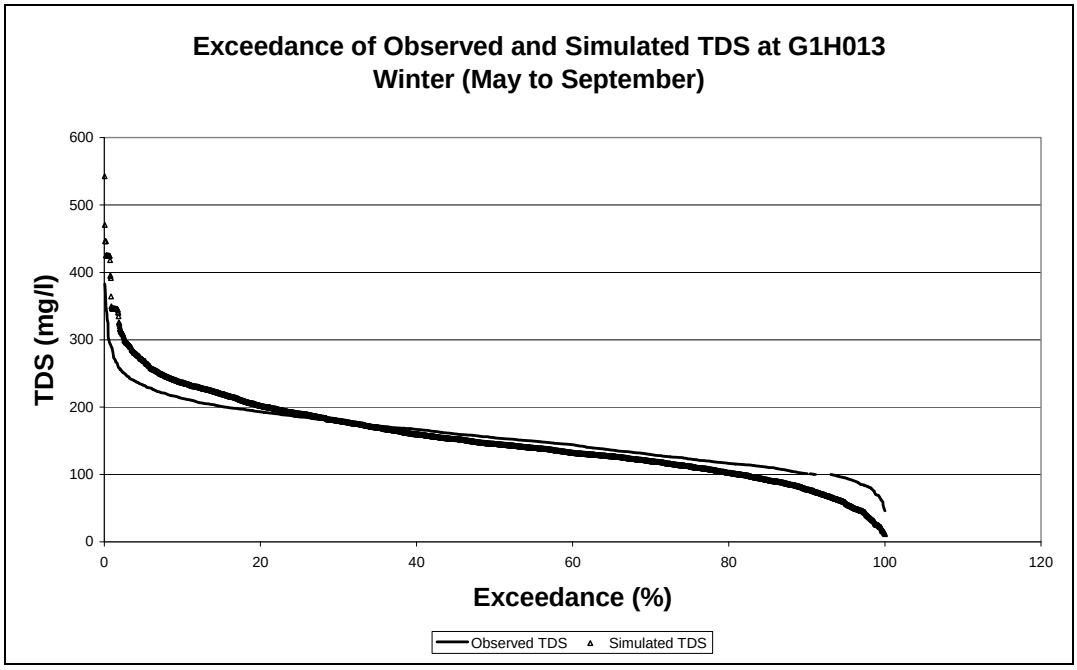

Figure 89 Exceedance of simulated and observed daily TDS concentrations at G1H013

A comparison of daily observed and simulated TDS concentrations is shown in **Figure 90**. Visual inspection of this figure shows that the daily observed trends are reasonably mimicked by the simulated values, but that the simulated TDS concentrations generally underestimate the observed record. The underestimation is probably "corrected" for in other portions of the record where oversimulation occurs.

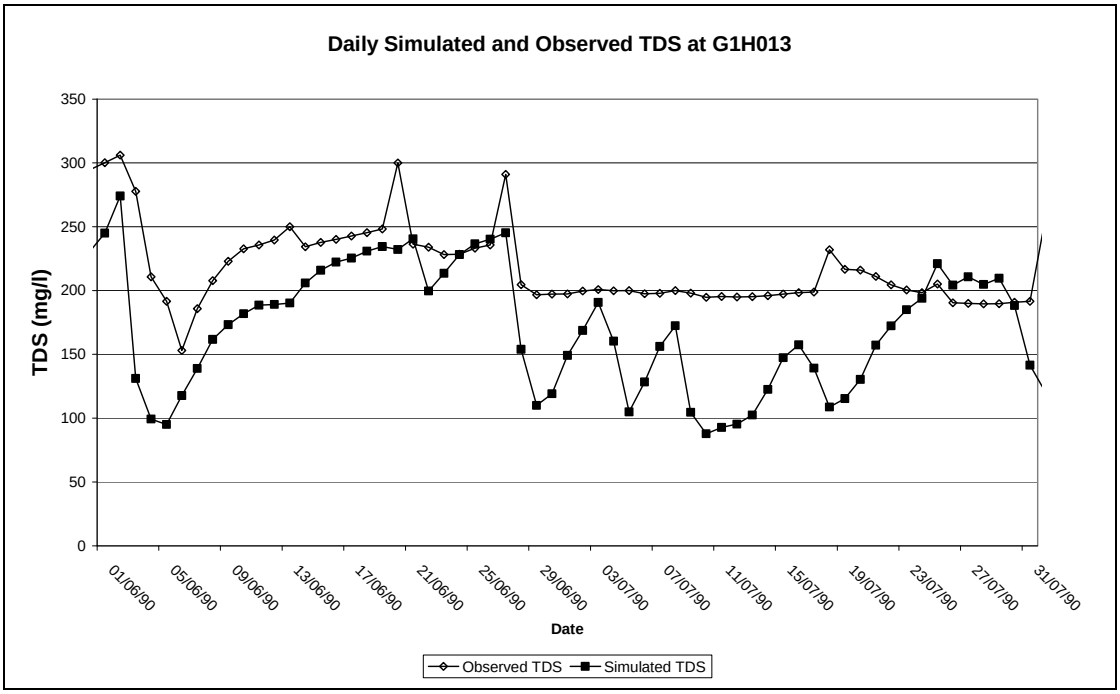

Figure 90 Daily Simulated and Observed TDS Concentrations at G1H013

A comparison of the seasonality of the daily infilled observed TDS series and simulated TDS series is depicted in **Figure 91** where month 1 is January. The figure shows sound correspondence of the median TDS values of the daily simulated TDS series with that of the infilled observed series over the winter months. In particular, the model manages to capture the increase in TDS concentration over the winter months.

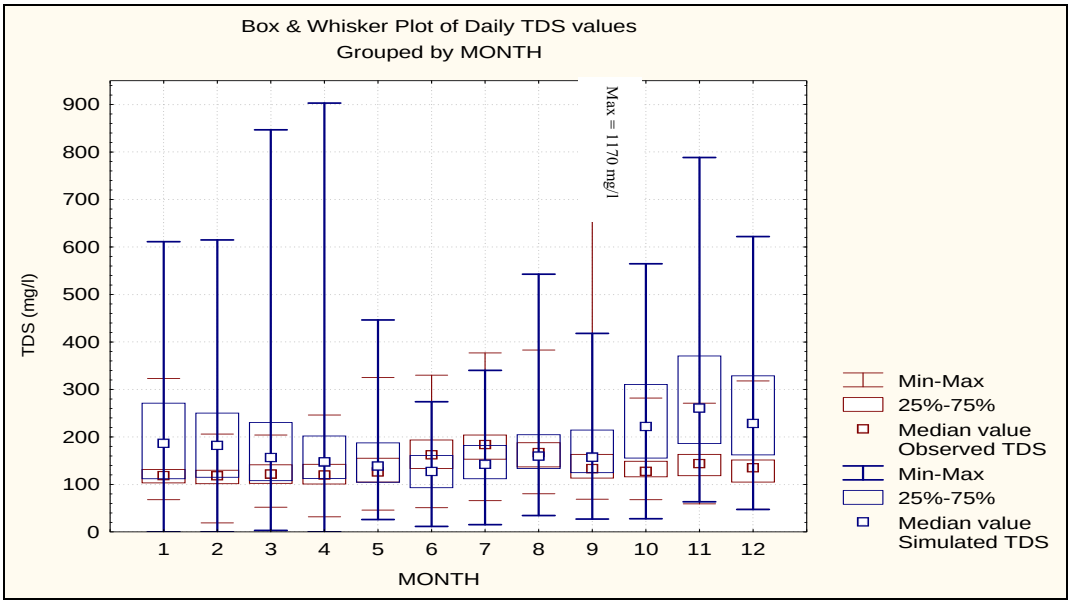

Figure 91 Comparison of seasonality of simulated and infilled observed TDS values at G1H013

5.5.6 Salinity calibration at G1H035 (Matjies River at Matjiesfontein)

According to Bath (DWAF, 1993), the largest salt load contribution to the Berg River mainstem is from the Matjies River (G1H035). Analysis of the TDS grab sample record for the period 1971 to 2002 showed that the average, maximum and minmum TDS concentrations were 1 814 mg/l, 5 669 mg/l and 25 mg/l, respectively. The seasonal distribution of TDS concentrations at gauge G1H035 is depicted in **Figure 92**, which shows that more than 75% of the winter grab samples had TDS concentrations over 1 000 mg/l while at least 25% of the observations had concentrations above 2 000 mg/l.

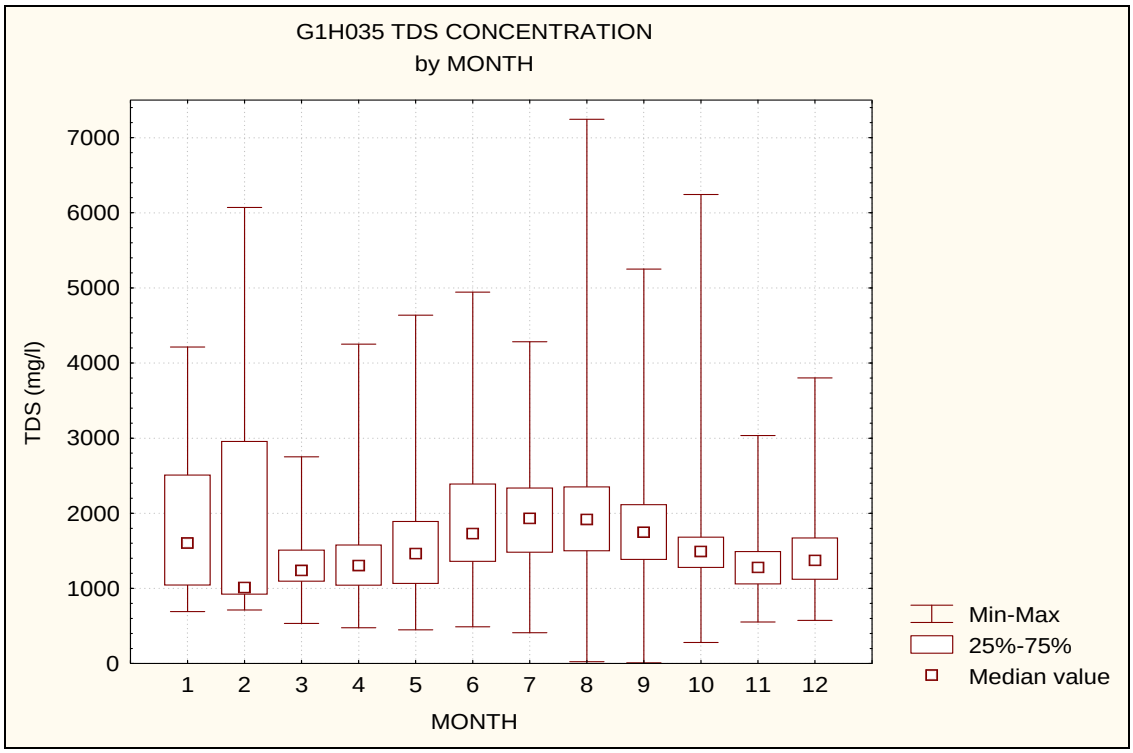

Figure 92 Seasonal distribution of observed (grab sample) TDS concentration at G1H035

The daily salinity verification at G1H035 is depicted in **Figure 93** which shows a reasonable correspondence of infilled observed and simulated exceedance percentages for TDS.

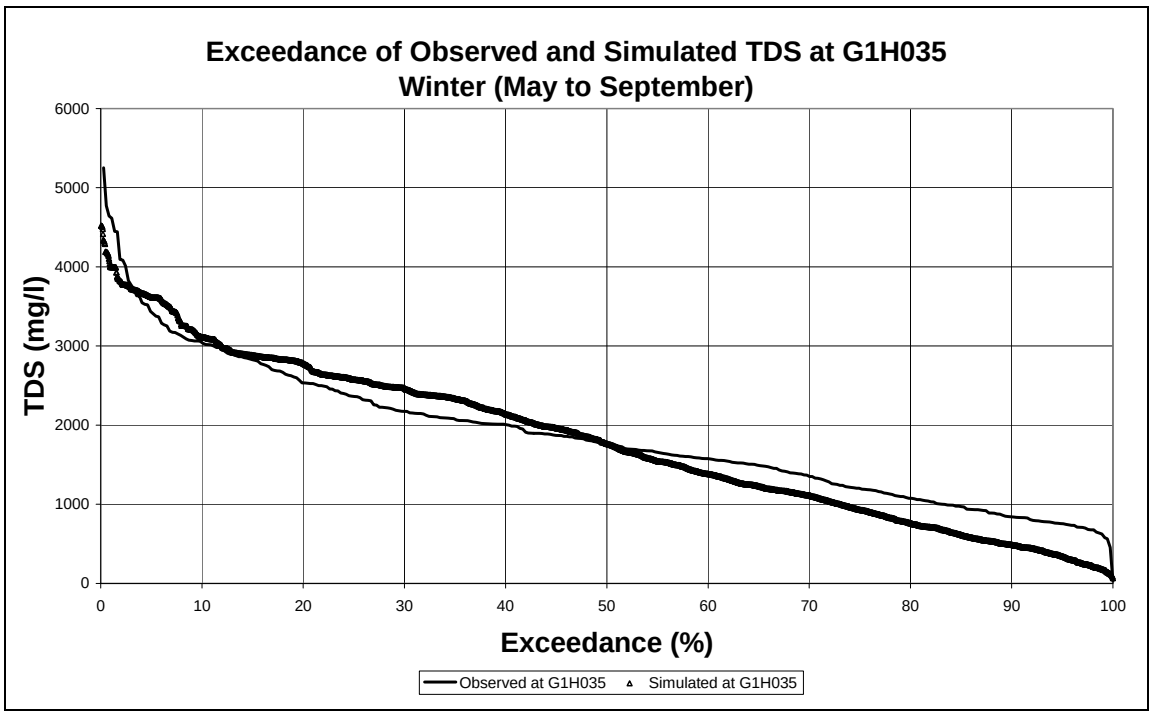

Figure 93 Exceedance of observed and simulated daily TDS at G1H035

The final values of the salinity-related calibration parameters (see **Table 30**) used in this calibration are realistic, considering that the average TDS concentration in this catchment is 1 814 mg/l. The values of the parameters are also consistent with fact that the soils in this sub-catchment overlay the Malmesbury Shale geological formation known for having a high salt content in its weathered state.

A comparison of daily observed and simulated TDS concentrations is shown in **Figure 94**. Visual inspection of this figure shows that the daily observed trends are reasonably mimicked by the simulated values, but that the simulated TDS concentrations generally lack the variability exhibited in the observed TDS series.

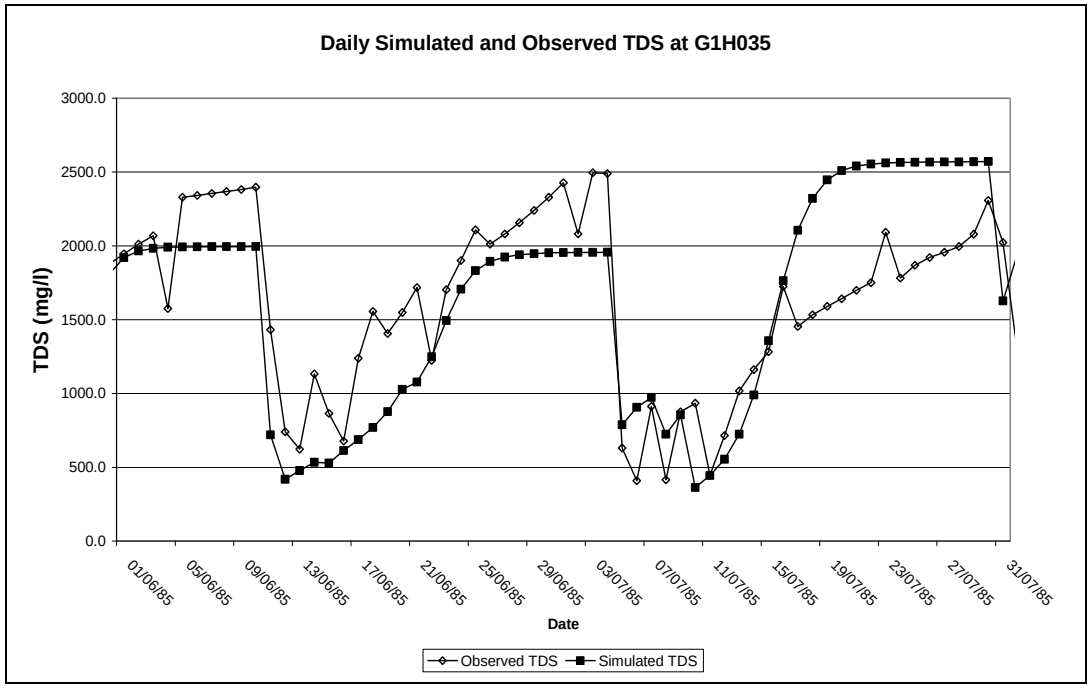

Figure 94 Daily Simulated and Observed TDS Concentrations at G1H035

A comparison of the seasonality of the daily infilled observed TDS series and simulated TDS series is depicted in **Figure 95** where month 1 is January. The figure shows that the median values of the daily simulated TDS series, during the winter months show sound correspondence with those of the infilled observed TDS values. In particular, the model manages to capture the increase in TDS concentration over the winter months, being optimistic in June and July and pessimistic in September.

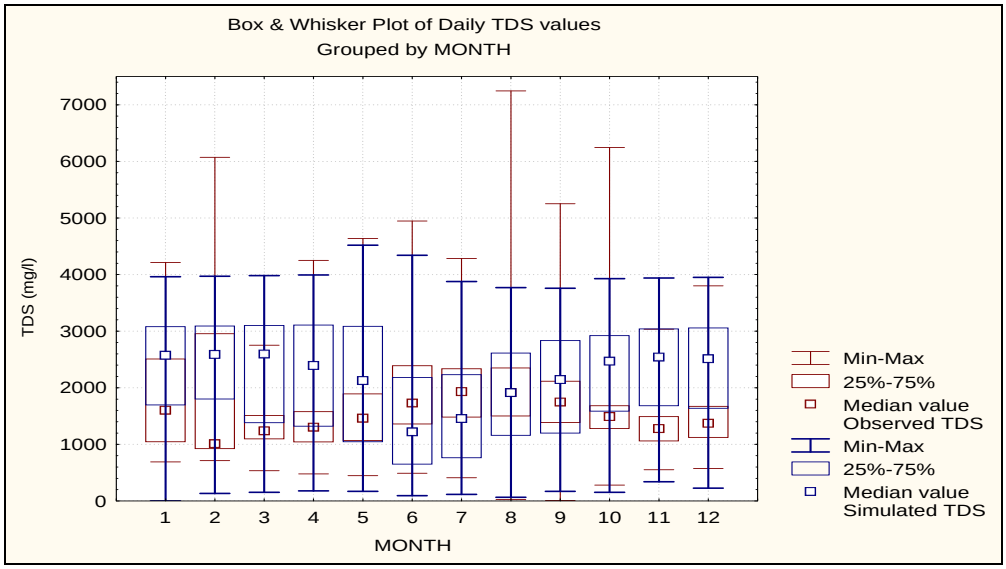

Figure 95 Comparison of seasonality of simulated and infilled observed TDS values at G1H035

5.5.7 Salinity calibration at G1R003 (Berg River at Misverstand Dam)

Analysis of the TDS grab sample record for the period 1977 to 2002 showed that the average, maximum and minimum TDS concentrations were 197 mg/l, 615 mg/l and 22 mg/l, respectively. The seasonal distribution of TDS concentrations at gauge G1R003 is depicted in **Figure 96** which shows that more than 75% of the winter grab samples had TDS concentrations less than 300 mg/l and that 500 mg/l was seldom exceeded.

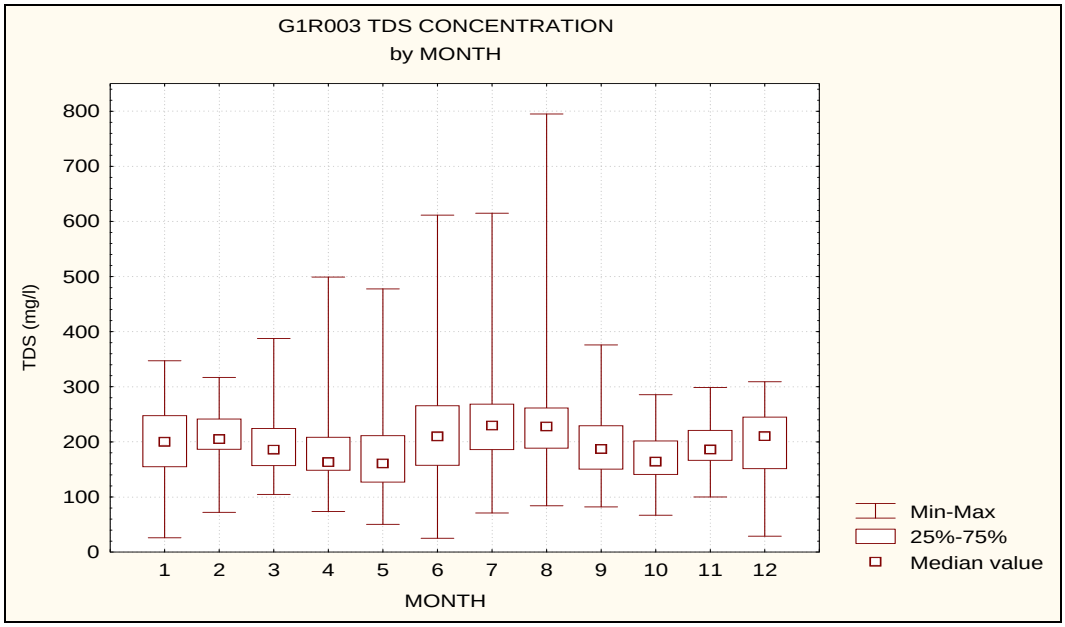

Figure 96 Seasonal distribution of TDS concentration at Gauge G1R003

The daily salinity verification at G1R003 is depicted in **Figure 97** which shows a sound correspondence between the observed and simulated exceedance percentages for TDS over almost the entire range of concentrations.

The final values of the salinity-related calibration parameters (see **Table 30**) used in this calibration are realistic on a regional scale, eventhough the average TDS concentration in this catchment is only 197 mg/l. It could be argued that the average TDS concentrations are as a result of the low-salinity in the upstream inflow to this part of the catchment and that the values of the salinity-related parameters are appropriate for describing the localised effect of the incremental catchment.

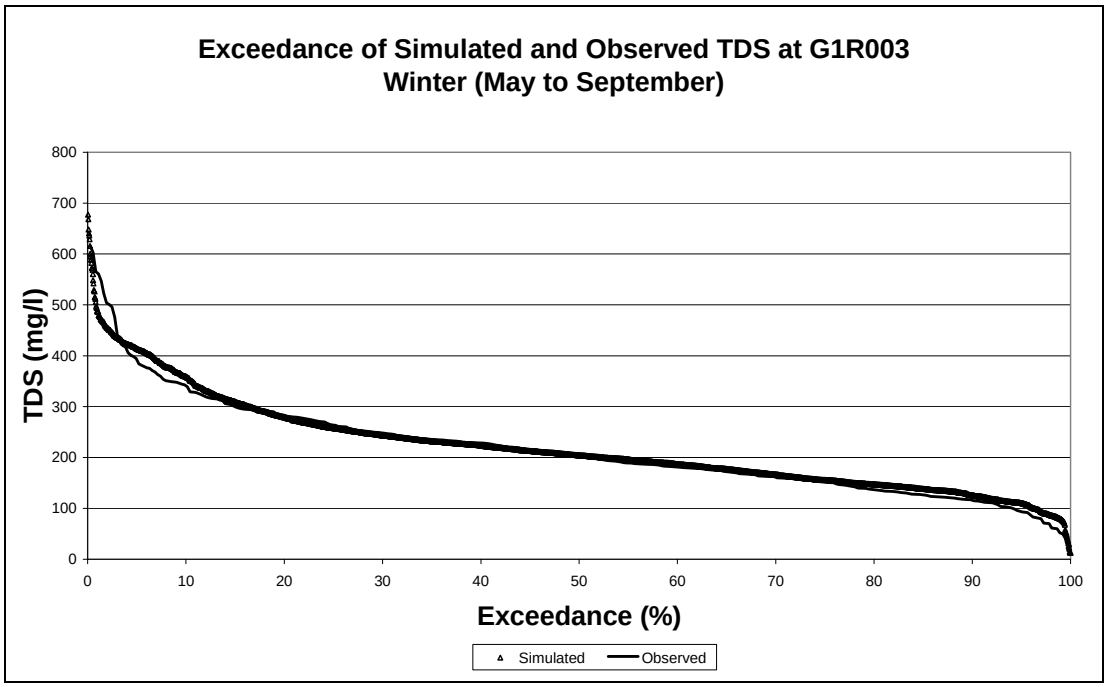

Figure 97 Exceedance of observed and simulated TDS at G1R003

A comparison of daily observed and simulated TDS concentrations is shown in **Figure 98**. Visual inspection of this figure shows that the daily observed trends are reasonably mimicked by the simulated values, but that the the variability exhibited in the observed TDS series is not completely captured by the simulated values. The order of magnitude of the simulated values is, however, comparable with that of the observed TDS values.

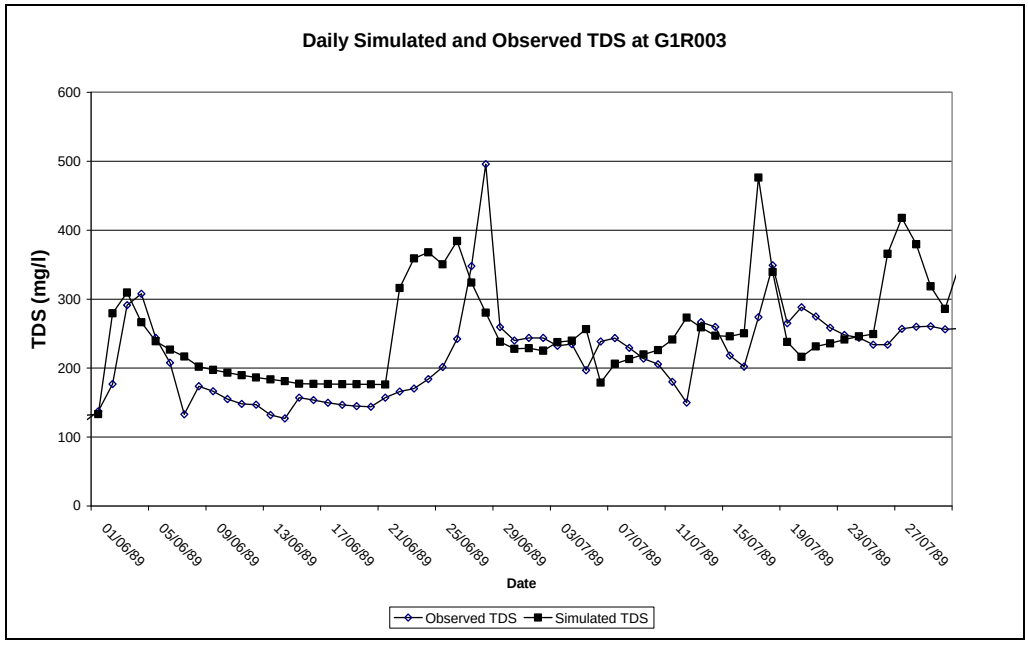

Figure 98 Daily Simulated and Observed TDS Concentrations at G1R003

A comparison of the seasonality of the daily infilled observed TDS series and simulated TDS series is depicted in **Figure 99** where month 1 is January. The figure shows that the median values of the daily simulated TDS series, during the winter months show sound correspondence with those of the infilled observed record. In particular, the model manages to capture the increase in TDS concentration over the winter months.

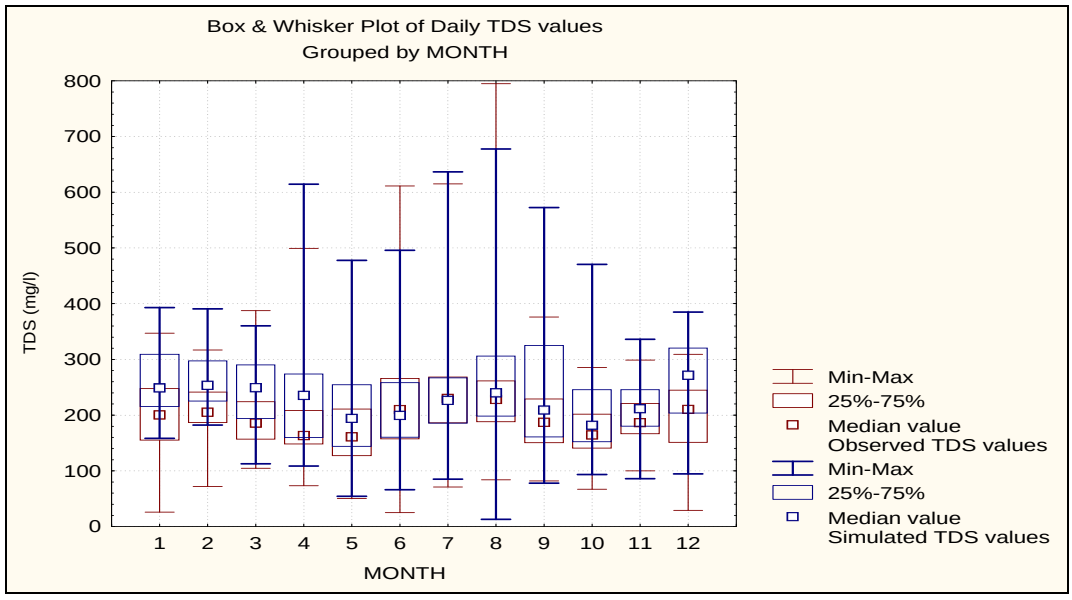

Figure 99 Comparison of seasonality of simulated and infilled observed TDS values at G1R003

5.5.8 Summary of objective function values for salinity calibrations

The objective function values which allow a goodness-of-fit assessment between the daily simulated and infilled observed TDS values are listed in **Table 31**. The objective functions indicate a relatively poor 1:1 correspondence between the simulated and observed TDS concentrations. This is, however, expected since:

- The salinity module is a highly simplified representation of salt-soil dynamics.
- Simulation errors in high flows were common due to poor availability of driver rainfall stations – this led to large errors in TDS on those particular days.
- Small errors in low flows would result in relatively large errors in TDS, and
- Flow routing had not been activated; therefore the model would not simulate the correct lag time for either flow or salts.

It would thus seem in this case, that visual comparison of exceedance percentages would be an appropriate technique for evaluating the model's performance in terms of replicating the daily observed TDS concentration patterns. If the flow routing capability was activated a 1:1 comparsion of flow and subsequently TDS would be possible. In such a case comparison of daily simulated and observed objective functions should be employed to quantify the goodness-of-fit.

Table 31 Objective functions values for comparison of daily TDS concentrations (May to September)

Gauge	% difference in mean TDS concentration	Coefficient of determination (r^2)	Coefficient of efficiency
G1H037	8.7	0.01	-0.94
G1H041	-4.1	0.01	-10.16
G1H036	4.9	0.24	0.10
G1H043	14.7	0.05	-0.42
G1H013	16.7	0.73	0.36
G1H035	-1.1	0.02	-0.30
G1R003	-11.7	0.20	0.01

The objective function values for goodness-of-fit of the monthly simulated and observed loads are shown in **Table 32**. The statistics suggest a more favourable correspondence between the simulated and observed sequences which is probably due to the aggregation process which masks the lack of a 1:1 fit of the daily simulated values to the observed data. The statistics for the monthly loads at G1R003 were not calculated given the poor observed flow record at this gauge.

Table 32 Objective function values based on the comparison of monthly TDS loads (May to September)

Gauge	% difference in mean monthly TDS loads	Coefficient of determination (r^2)	Coefficient of efficiency
G1H037	-16.3	0.59	0.46
G1H041	-24.6	0.49	-0.83
G1H036	-16.2	0.70	0.42
G1H043	-43.7	0.23	-1.72
G1H013	-16.7	0.73	0.36
G1H035	-31.7	0.13	-6.8
G1R003	NOT CALCULATED		

5.6 DISCUSSION

The proposed hypothesis underlying the approach for determining the effect of upstream bulk water scheme developments on the TDS concentration at Misverstand Dam, has stated that the abstraction of more fresh water in the upper reaches of the Berg River would result in a deterioration of the water quality at Misverstand Dam, because of the high TDS loads contributed by the Matjies and Sandspruit Rivers during the winter months.

In this project, ACRU*Salinity* had been configured in distributed mode allowing for the run-off from each primary sub-catchment to be driven by the most appropriate rainfall station. In this way it was possible to capture the spatial variation in MAP which exists in the Berg River and to capture the relationship between timing of daily rainfall/run-off events in the lower Berg which produce highly saline run-off and those in the upper Berg which produce relatively low salinity run-off, by comparison.

To increase the level of confidence in the model and to keep the model spatially as close to reality as possible, flow verifications were undertaken at most of the important gauging stations in the catchment and only, once this had been completed satisfactorily, was the salinity calibration undertaken. Since the module which describes salt generation and mobilisation is physically-based, it was necessary to calibrate the values of the salt generation parameters to obtain simulated TDS concentrations which were reasonably representative of the observed TDS values. It was also argued that, in the absence of daily flow routing in the model, the most appropriate technique to assess the correspondence of the simulated and observed TDS concentrations was by exceedance percentage plots. A 1:1 comparsion of daily TDS concentrations together with the

calculation of daily objective function values would of course be desirable when the flow routing option is activated.

Different values for salt generation have been selected based on whether the catchment produces highly saline, moderately saline or low salinity water and whether it was uncultivated, under dryland agriculture or irrigated. This differentiation would allow for the effect of a change in land-use on TDS simulated concentrations.

Since the model was verified for flow and calibrated for salinity at this stage in the study, various development scenarios could subsequently be tested for the effect on the salinity at Misverstand Dam, as presented in **Chapter 6**.

CHAPTER 6: EVALUATION OF ENGINEERING OPTIONS FOR SALINITY MANAGEMENT OF THE BERG RIVER

6.1 INTRODUCTION

This chapter describes how the ACRU*Salinity* model can be used to investigate the impact of the proposed BRD as well as the Voëlvlei Augmentation Scheme (VAS) on the salinity at Misverstand Dam and the possible mitigating options that could be considered to address the concerns of the West Coast District Municipality (WCDM) and some of the industries that obtain their water from Misverstand Dam. A more detailed description of the evaluation of the engineering options for the Berg River is presented by Cullis and Kamish (2006).

6.2 OUTLINE OF THE BERG RIVER DAM AND VOËLVLEI AUGMENTATION SCHEMES

6.2.1 The Berg River Dam scheme

The BRD scheme was put forward as one of the schemes for further investigation in the WCSA study (DWAF, 1993(1)). The Dam has been constructed in the upper reaches of the Berg River (G1H004) in 2007 and has a capacity of 127 x 10^6 m^3 and an estimated yield of 56 x 10^6 m^3/a. Flow can also be returned to the Dam from the Supplement Scheme which is located on the Berg River Downstream of its confluence with Dwars River. The Supplement Scheme is an off-channel balancing dam, from which water can be pumped back at a maximum rate of 4 m^3/s. With the implementation of the Supplement Scheme in 2007 the yield of the system increased to 81 x 10^6 m^3/a.

6.2.2 The Voëlvlei Augmentation scheme

The Voëlvlei Dam is an off-channel storage with a capacity of 172 x 10^6 m^3 and a yield of 105 x 10^6 m^3/a Currently the Dam is supplied with flows diverted from the Klein Berg River, Twenty Four Rivers River and the Leeu River via a system of canals. The VAS scheme would involve augmentation of the inflows by pumping from the Berg River, during the winter months, to increase the yield of the Dam.

6.3 FLOW SCENARIOS AND MANAGEMENT OPTIONS

The following flow scenarios were considered to demonstrate the use of hydrosalinity modelling in engineering planning for the Berg River development.

- Current day simulated flow and salinity.
- Simulated flow after the construction of the Berg River Project (BRP) (this would include the supplement scheme).
- Future simulated flow after the construction of the VAS and the Berg River Project (BRP).

The following management options were considered to mitigate the potential impact of the BRP and the VAS on the salinity at Misverstand Dam:

- The use of a conditional abstraction of flow to Withoogte treatment works based on the salinity in Misverstand Dam.
- The provision of off-channel storage at Withoogte water treatment works (WTW) to bridge the periods of high salinity.

As mentioned previously, the ACRU model was configured for this project from G1H020, located on the Berg River at Daljosafat near Paarl, to the estuary. While another ACRU model had previously been configured for the Berg River Catchment upstream of G1H020, it was for an entirely different purpose and was thus not used in this evaluation.

For this study the ACRU model downstream of G1H020 with a specified inflow at G1H020 representing the total inflow from the upper catchment was used. As the bulk of the salinity impacts occur below this point, running the model from this point would be sufficient to analyse the salinity impacts at Misverstand weir.

The specified input flow files required at G1H020 were produced as described below.

6.3.1 Current Day flow at G1H020

For the current day flow, the observed record at G1H020 from 1/1/1980 to 31/12/1999 (i.e. 20 years) was used. This flow record required only minor patching. A total of 25 days of missing

data were patched using linear interpolation after comparison with the observed flow rates at G1H004. The current day MAR at G1H020 for the period was 354 x 10^6 m^3/a.

6.3.2 Post Berg River Dam flow for G1H020

For the post BRP flow, the observed record at G1H020 was adjusted to account for the impact of the BRP, which consists of the Dam and the Supplement Scheme, from this point winter flows are pumped back to BRD, at Drakenstein. Only the winter flows were adjusted to account for the impact of the Dam as it was assumed that similar irrigation releases would in future have to be made in the summer as are currently made from the Theewaterskloof Dam tunnel.

The impact of the Berg River Dam on the winter flows was determined by subtracting the observed record at G1H004, upstream of the Dam site. Additionally, the anticipated inflow to the dam from the Supplement Scheme, from G1H020, was also added. Anticipated release patterns from the Berg River Dam, which incorporated environmental base flows, environmental flood releases and the spills from the Dam, as well as minor irrigation releases in August (0.2 m^3/s) and September (0.8 m^3/s) was added to the record. This was done for the period 1st May to 31st September.

A spreadsheet program for estimating the releases from the Berg River Dam was developed and it incorporated the following features (TCTA, 2007):

- The median monthly baseflows for G1H004 were used as the inflows to the Dam from 1st November to 24th May. This was to account for the irrigation releases from Theewaterskloof Dam, which form part of the observed flow at G1H004. For the rest of the time the patched and extended flow record for G1H004 was used.
- The urban abstractions from the Berg River Dam were taken as 80% of 81 x 10^6 m^3/a (i.e. 64.8 x 10^6 m^3/a) for the first three years of the flow record, and as 100% of 81 x 10^6 m^3/a after that.
- No releases for irrigation were included as it was assumed that these would be made from Theewaterskloof directly through the Supplement Scheme pipeline.
- The capacity of the Berg River Dam was 125 x 10^6 m^3 and the dam was assumed to start at 60% capacity (i.e. 75 x 10^6 m^3), corresponding to the start of the flow record.

- The incremental inflow to the Supplement Scheme was calculated as 88% of the flow at G1H004 excluding the irrigation releases. This was based on the proportion of mean annual flows currently used in the Western Cape System Model.
- The capacity of the Supplement Scheme is 4 m^3/s.
- The environmental baseflow requirements at the Supplement Scheme are given in **Table 33**. The baseflow requirements are constant for each month.

Table 33 Baseflow requirements for the Supplement Scheme

Month	Flow (m^3/s)	Month	Flow (m^3/s)	Month	Flow (m^3/s)	Month	Flow (m^3/s)
January	0.46	April	1	July	2.86	October	1.54
February	0.46	May	2	August	2.86	November	0.61
March	0.46	June	2.86	September	2.86	December	0.46

- The environmental baseflow requirements from the Berg River Dam are given in **Table 34**. The baseflow requirements are dependent on the historical inflow to G1H004 excluding the irrigation releases. The baseflow information for BRD as well as the Supplement Scheme was obtained from the document, *Preliminary Determination of the Reserve and Resource Class in Terms of Section 14(1) and 17(1)(b) of the National Water Act*, 1998 (Act No. 36 of 1998).

Table 34 Environmental baseflow releases (m^3/s) from Berg River Dam based on historical average daily natural inflow (m^3/s)

October		November		December		January		February		March	
Inflow	**Release**	**Inflow**	**Release**	**Inflow**	**Release**	**Inflow**	**Release**	**Inflow**	**Release**	**Inflow**	**Release**
0.743	0.503	0.44	0.324	0.175	0.175	0.082	0.082	0.058	0.058	0.049	0.049
1.247	0.503	0.59	0.324	0.31	0.184	0.149	0.149	0.083	0.083	0.116	0.116
1.542	0.587	0.76	0.417	0.366	0.24	0.198	0.183	0.141	0.141	0.161	0.161
2.005	0.733	0.957	0.579	0.485	0.379	0.258	0.236	0.198	0.198	0.265	0.262
2.401	0.845	1.246	0.702	0.653	0.523	0.329	0.291	0.248	0.248	0.302	0.302
2.811	0.909	1.609	0.773	0.706	0.621	0.403	0.329	0.422	0.328	0.429	0.338
3.289	0.939	1.836	0.806	0.993	0.671	0.541	0.348	0.537	0.348	0.586	0.351
4.114	0.952	2.292	0.821	1.206	0.693	0.665	0.356	0.806	0.356	0.866	0.357
4.73	0.957	2.944	0.826	1.579	0.7	0.937	0.359	1.343	0.359	1.602	0.359
6.623	0.957	2.944	0.826	2.378	0.7	1.93	0.359	2.298	0.359	2.117	0.359
April		**May**		**June**		**July**		**August**		**September**	
Inflow	**Release**	**Inflow**	**Release**	**Inflow**	**Release**	**Inflow**	**Release**	**Inflow**	**Release**	**Inflow**	**Release**
0.313	0.262	1.744	0.504	3.58	1.006	3.58	1.006	4.958	1.006	2.631	1.005
0.61	0.302	2.912	0.632	4.178	1.292	5.496	1.292	5.444	1.292	3.14	1.151
1.269	0.338	4.077	0.855	4.811	1.599	6.25	1.599	6.313	1.599	3.893	1.406
1.763	0.351	5.32	1.025	6.543	1.768	7.038	1.768	6.84	1.768	4.24	1.6
2.303	0.357	6.299	1.121	7.793	1.851	9.476	1.851	7.799	1.851	5.15	1.71
2.758	0.359	7.027	1.168	9.877	1.889	11.13	1.889	8.957	1.889	6.084	1.763
3.268	0.359	8.654	1.188	12.72	1.907	12.578	1.907	9.431	1.907	6.721	1.786
4.252	0.359	11.156	1.195	16.647	1.914	15.438	1.914	11.156	1.914	7.82	1.795
6.975	0.359	14.531	1.195	20.089	1.914	17.884	1.914	13.008	1.914	11.034	1.795

- Additional flood releases were made in the model to simulate the required operating rule which aims to provide floods with an average daily discharge of 5 m^3/s in April, 30 m^3/s in June, 65 m^3/s in July and 4.5 m^3/s in November and December. These releases are linked to observed natural events.

6.3.3 Post Voëlvlei abstraction scheme

A third flow scenario taking into account the impact of Phase I of the VAS was also considered. The objective of the VAS would be to abstract a total of 20 x 10^6 m^3/a from the Berg River for supply to the City of Cape Town (CCT) through the existing treatment works and supply pipeline from Voëlvlei Dam. The abstraction for the VAS would be based on an operating rule that is conditional on the flow in the river (CCT, 2002) (see **Table 35**).

The latest version of ACRU*Salinity* (v1.2.5), developed for this study, includes the functionality which allows abstraction from a reservoir or river based on either salinity or flow-related criteria and has been termed ***conditional abstraction***.

Table 35 Operating rule for the Voëlvlei Augmentation Scheme

Upstream River Flow (m^3/s)	Abstraction (m^3/s)	Number of Pumps	Downstream River Flow (m^3/s)
< 2	0	0	< 2
≥ 2; < 3,1	1,0	1	≥ 1; < 2,1
≥ 3,1; < 4,2	2,1	2	≥ 1; <2,1
≥ 4,2	3,2	3	≥ 1

6.4 SIMULATED FLOWS AT MISVERSTAND DAM

The ACRU model was run for the middle and lower Berg River sections using the above flow sequences as inputs at G1H020 and using the observed salinity at G1H020, thus producing two scenarios of inflow to Misvertsand Dam, *viz*. "Current Day" and "Post Berg River Dam".

6.5 EVALUATION OF MANAGEMENT OPTIONS

With the ACRU*Salinity* model configured it was possible to analyse and evaluate several management options for mitigating the potential deteriorating effects in water quality as a result of the Berg River Dam. These options will be discussed further in the ensuing sections.

6.5.1 Spreadsheet model developed for the evaluation of management options

To evaluate the various management options for the Berg River, a further spreadsheet model was developed (Cullis and Kamish, 2006). The model is based on a daily time-step with the inputs to the model as the simulated flow and TDS sequences from ACRU*Salinity* for the three scenarios. The model assumes perfect mixing of the inflows and incorporates both a conditional abstraction and a conditional scour based on the salinity levels in the reservoir. It provides, however, an option of applying a factor to adjust the TDS at the abstraction point and the scour to accommodate any possible stratification or uneven mixing of the salinity in the reservoir.

The following set of variables was used in the spreadsheet model to allow for the analyses of different scenarios:

- The TDS threshold of the conditional abstraction.
- The maximum daily pumping rate.
- The off-channel storage capacity at Withoogte.
- The gross and live storage capacity of Misverstand Dam.
- The average annual demand from Withoogte WTW as well as the monthly and daily peaking factors.
- The threshold TDS and discharge capacity for the conditional scour.
- The environmental baseflow release requirements.

6.5.2 Analysis of the salinity impact of a conditional abstraction at Misverstand Dam

For the conditional abstraction from Misverstand Reservoir, two salinity thresholds were considered. The first was based on 450 mg/l, the upper limit for TDS for domestic water use. The second was a much lower threshold of 300 mg/l (DWAF, 2005), which was considered in recognition of the needs of certain industries that are highly sensitive to saline water, such as Saldanha Steel.

To bridge periods when poor quality water occurs at Misverstand Dam, additional storage would be required at Withoogte. The following additional storages were considered for analyses.

- 250 000 m^3 – this is the current capacity of the raw water storage reservoir at the Withoogte treatment works.
- 500 000 m^3 – this would be the total capacity if a second raw water storage reservoir at Withoogte were to be lined and used.
- 1 500 000 m^3 – this would require the lining of a second reservoir at Withoogte plus an additional storage capacity of 1 x 10^6 m^3 which could be provided through aquifer recharge.
- 5 000 000 m^3 – this would require substantial off-channel storage, and is an unlikely scenario, but was considered in order to assess the requirements for providing a 100% level of assurance of supply.

In terms of the demands from the Withoogte WTW, only the following scenario was considered.

- 20 x 10^6 m^3/a – this corresponds to the likely future demand to be reached some time between 2010 and 2015, by which time the Berg Water Project would be in full operation.

Using the ACRU*Salinity* outputs obtained from the conditional abstraction runs for "Current Day" and "Post BRD" scenarios as input to the spreadsheet model, it was possible to evaluate the number of days on which the salinity in Misverstand was above the threshold level or/and the number of days for which the daily demand could not be met from the off-channel storage.

As the focus for this study is the winter period only, the average number of days of no abstraction and shortfall were calculated in terms of the percentage of all winter days from May to September during the analysis period. While the simulation was run for the period January 1980 to December 1999, the analysis was done only for the period from 1984 to 1999. This allowed for a "warm up" period for the spreadsheet model. The longest continuous period of no abstraction or shortfall was also determined for this period.

The results for the "Current Day" and "Post BRD" flow simulation for both the 300 mg/l and 450 mg/l salinity thresholds using the estimated current demand of 20 x 10^6 m^3/a, are shown in **Table 36**.

Table 36 Impact of conditional abstraction: current demands (20 x 10^6 m^3/a)

		Current Day Simulated		Post BRD Flow	
Annual Demand from Withoogte WTW (Mm^3/a)		20		20	
Salinity threshold at Misverstand Dam for abstraction to Withoogte WTW (mg/l)		300	450	300	450
Days* of no abstraction from Misverstand Dam: Winter		486 (20%)	38 (1.6%)	592 (24%)	48 (1.6%)
Longest continuous period of no abstraction to Withoogte WTW off-storage (days)		45	14	46	24
Days* of shortfall in winter (i.e. when daily demand cannot be met from off-channel storage)	0.25 Mm^3 storage	354 (14%)	17 (0.7%)	427 (0.7%)	27 (1.1%)
	0.5 Mm^3 storage	253 (10%)	8 (0.3%)	304 (0.3%)	14 (0.6%)
	1.5 Mm^3 storage	47 (1.9%)	0 (0%)	71 (0%)	0 (0%)
	5 Mm^3 storage	0 (0%)	0 (0%)	0 (0%)	0 (0%)
Longest period of shortfall in meeting the winter demand (days)	0.25 Mm^3 storage	40	10	41	20
	0.5 Mm^3 storage	34	4	35	14
	1.5 Mm^3 storage	27	0	28	0
	5 Mm^3 storage	0	0	0	0

* This refers to the total number of winter days out of the sixteen-year simulation period, i.e. out of 2448 days.

Table 36 shows that the number of days of no abstraction to Withoogte WTW as a result of unacceptable water quality at Misverstand Dam, decreases as the bridging capacity at the Withoogte WTW, increases. It also shows that the number of days of no abstraction as well as the longest continuous period of no abstraction increases after the implementation of the BRP. It should be noted that to have no days of shortfall in meeting the winter demand from Withoogte WTW the additional storage required would be larger than 1.25 x $10^6 m^3$.

6.5.3 Analysis of the salinity impact of the VAS on conditional abstraction at Misverstand Dam

The impact of the Voëlvlei Augmentation Scheme, when considered in addition to the impact of the construction of the BRP, was found to be significant. The results of this scenario are given in **Table 37** on annual demand of 20 x $10^6 m^3$/a.

Table 37 Impact of salinity on the abstraction at Misverstand Dam post BRP and post VAS

		Post VAS and Post BRP	
Annual Demand from Withoogte WTW (Mm^3/a)		20	
Salinity Threshold at Misverstand Dam for abstraction to Withoogte WTW (mg/l)		300	450
Days* of no abstraction from Misverstand Dam: Winter		637 (26%)	72 (2.9%)
Longest continuous period of no abstraction to Withoogte WTW off-channel storage (days)		47	24
Days* of shortfall in winter (i.e. when daily demand cannot be met from off-channel storage)	0.25 Mm^3 Storage	468 (19%)	43 (1.8%)
	0.50 Mm^3 Storage	333 (14%)	16 (0.7%)
	1.50 Mm^3 Storage	73 (3.0%)	0 (0%)
	5.00 Mm^3 Storage	0 (0%)	0 (0%)
Longest period of shortfall in meeting the winter demand (days)	0.25 Mm^3 Storage	42	20
	0.50 Mm^3 Storage	36	14
	1.50 Mm^3 Storage	28	0
	5.00 Mm^3 Storage	0	0

* This refers to the total number of days out of the sixteen years simulation period (i.e. out of 2448 winter days).

Using the formula:

Average Level of Assurance (%) = 100% - Average percentage of days of shortfall (%)

it was possible to calculate the level of assurance of supply during the winter months for each of the flow scenarios. These are represented graphically in **Figure 100** and **Figure 101**.

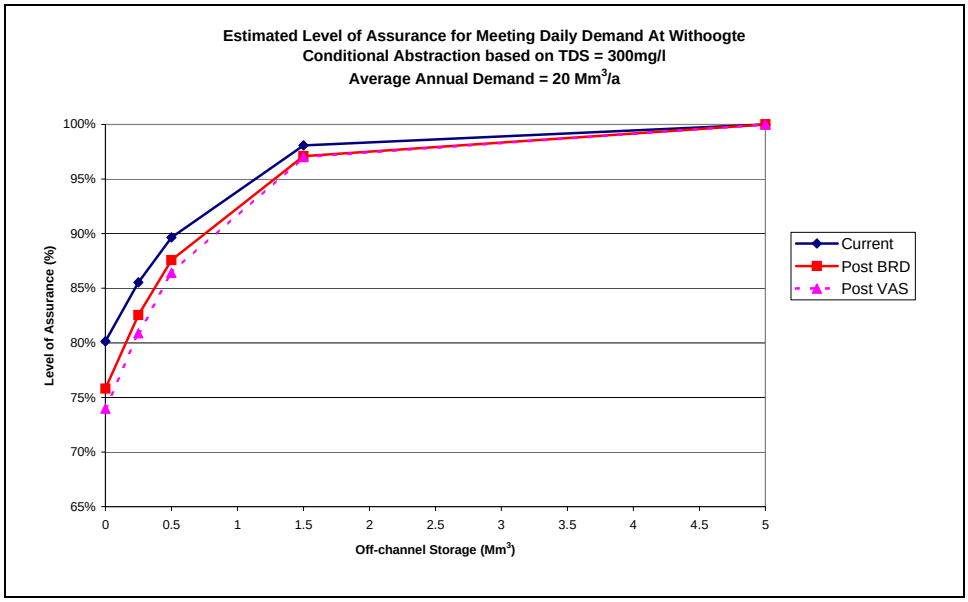

Figure 100 Estimated level of assurance based on a conditional abstraction based on TDS = 300 mg/l (extracted from Cullis and Kamish, 2006)

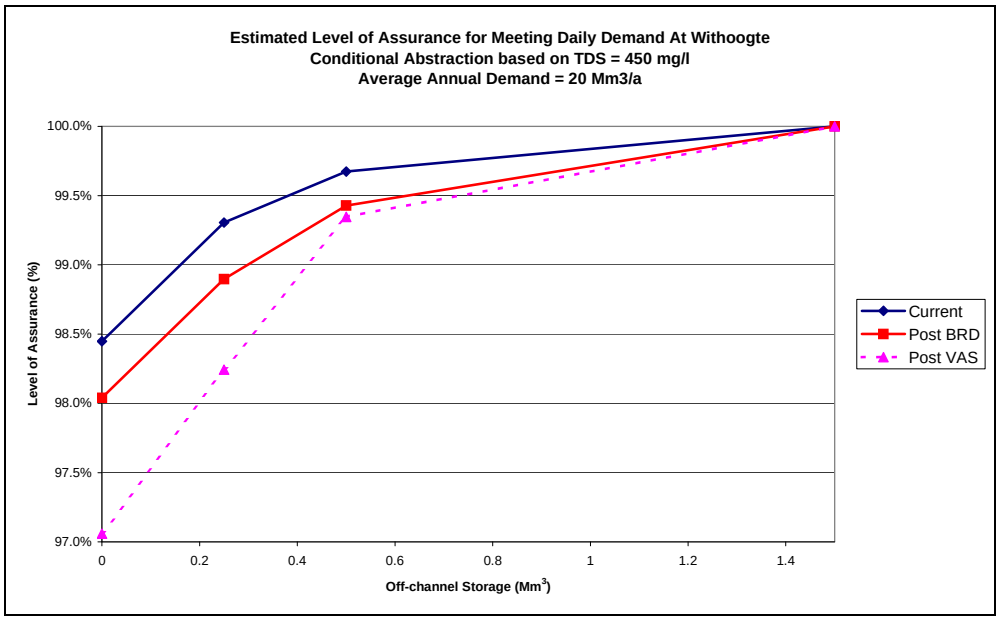

Figure 101 Estimated level of assurance based on a conditional abstraction based on TDS = 450 mg/l (extracted from Cullis and Kamish, 2006)

If one assumes a 98% level of assurance of supply is acceptable, **Figure 100** shows that for the 300 mg/l case, at least 1.5 x 10^6 m^3 additional storage would be required at the Withoogte WTW to ensure this for the "Current Day" scenario. With the current infrastructure of 0.25 x 10^6 m^3 for raw water storage at Withoogte, a 300 mg/l salinity threshold would be impractical, since this

would require lining of a second 0.25 x 10^6 m^3 reservoir and then locating a suitable additional 1 x 10^6 m^3 of storage. Using a threshold of 450 mg/l, however, would result in a 98% assurance of supply by lining only the already existing 0.25 x 10^6 m^3 reservoir at the Withoogte WTW.

6.6 DISCUSSION

This application demonstrates the role that ACRU*Salinity* can play in the evaluation of engineering options for salinity management. In many respects, this application was the ideal testing platform for the model since it included almost the entire range of problems which could be experienced in other catchments in South Africa. These include:

- Steep rainfall gradients related to topographical weather systems.
- Steep TDS gradients related to underlying geology.
- Highly saline catchments which give rise to seasonal streamflow salinity patterns that differ from those normally expected in a semi-arid catchment.
- A fast-response river which demands analysis on a daily rather than monthly basis.
- Development of significant bulk water supply infrastructure in the catchment which could potentially result in the deterioration of water quality in the downstream reaches.

The salinity-related outputs from the model have proven invaluable in quantifying and evaluating the potential negative salinity-related effect that the the Berg River Dam, as well as the Voëlvlei Augmentation Scheme may have on the the water quality at Misverstand Dam and provided the basis for assessing the extent of intervention required to mitigate this effect. Futhermore, this application has highlighted the need for and led directly to the eventual development and implementation of the conditional abstraction routines (based on flow and/or salinity) in the ACRU*Salinity* model.

CHAPTER 7: CONCLUSIONS AND RECOMMENDATIONS

7.1 CONCLUSIONS

Based on the findings and discussions in the preceding sections, the following conclusions can be drawn about the application of the ACRU*Salinity* model to the Berg River System:

7.1.1 Salinity situation of the Berg River

- The observed salinity record shows that there is a possibility that TDS concentrations at Misverstand Dam could exceed 500 mg/l for periods of a few weeks. This could be detrimental to certain industrial users. Events like this might not be reflected in the monthly flow-averaged TDS data. However, the available DWAF grab-sample-based data shows that such events occur infrequently, i.e. only one 3-consecutive-week-period was recorded in 24 years (1977 to 2002) in which the TDS appears to have been sustained above 500 mg/l.

- The impact of tributaries such as the Matjies (G1H035), Moorreesburg Spruit (G1H034) and the Sandspruit (G1H043) on the salt concentrations of the Berg River cannot be under-estimated. This is particularly important when one considers that the highest concentrations in these streams actually occur in winter when stream flows are high.

7.1.2 ACRU*Salinity* modelling

- Calibration of the salinity module was completed on an iterative basis by first choosing a representative value for the SALTSAT parameter and then varying the value of the SALTUPT value, in successive calibration runs, until an acceptable visual fit between simulated and observed TDS exceedances sequences were obtained. This, however, is a time consuming process and if the initial value for SALTSAT is not of the same order of magnitude as the highest observed streamflow concentrations, salinity calibration may be declared with an inappropriate set of values for the salinity related parameters.

- The most sensitive salinity-related parameters in the model were SALTSAT and SALTUPT. These values characterise the salinity response from the sub-catchments and are most probably linked to the salt mobilisation and generation dynamics of the

underlying geology. In this study, higher values of the salinity-related parameters were associated with the soils overlaying the Malmesbury Shale while the lower values were associated with the Table Mountain Group geology.

- The patterns of salinity production and mobilisation as observed in the highly saline catchments of the middle to lower Berg River Basin can be adequately simulated using the current salinity module in the ACRU*Salinity* model, which had been modified for this study. In the case of the Berg River Catchment, some sub-catchments and tributaries do not have driver rainfall stations available in or near the sub-catchments. This undermined simulation of both daily flows and daily TDS concentrations.

- A calibrated ACRU*Salinity* model would enable the quantification of the effects of further development (e.g. new dams or changes in land-use) on the quantity as well as the quality of the run-off by taking into account the spatial distribution of rainfall, abstractions, imports, irrigation demands and the effect of dams.

- Since ACRU*Salinity* operates on a daily timestep, the rainfall input data requirements are quite substantial. Also, the lack of availability of sufficiently detailed electronic land-use information for a catchment could severely hamper the application of the model.

- When TDS concentrations are the driving concern within a catchment, the delineation of sub-catchment should be guided by the level of detail required to address the problem. In the Berg River Catchment, the concern is the quality of discharge from the various tributaries and the catchment was delineated accordingly.

- Pseudo-sub-catchments should be based on the land-use types of non-cultivated, dryland agriculture and irrigated lands. In this way, distinction can be made between the values of the salt generating parameters used in each of these pseudo-sub-catchments.

7.1.3 Evaluation of engineering options using ACRU*Salinity*

- The use of a conditional abstraction at Misverstand Dam can address the bulk of the salinity concerns at Misverstand Dam. It was found that a conditional abstraction based on a TDS of 300 mg/l was not feasible, but that one based on 450 mg/l would be feasible. There would still, however, be some shortfalls in terms of meeting the demand, but this

could be addressed through the provision of additional storage capacity, pumping from the additional storage for a few days when the TDS is in excess of 450 mg/l and utilising the dilution capacity of the off-channel storage.

- The impact of the construction of the BRP and the VAS on the salinity at Misverstand can be off-set through the provision of an additional 0.25×10^6 m^3 off-channel storage capacity. This would require lining of the second existing reservoir at Withoogte.

7.2 RECOMMENDATIONS

Based on the preceding findings, discussions and conclusions, the following recommendations for future research in this domain can be made:

- Regular (grab-sample) monitoring of water quality variables in the Berg River should continue, but continuous recording at strategically important sites of electrical conductivity should be used to "infill" the daily salinity values between grab samples.

- A more mechanistic module for salinity generation and mobilisation should be incorporated in the ACRU*Salinity* model. In this way, the simulation of saline run-off will use measurable (or literature-quoted) salinity-related parameters, specific to the natural geology, vegetation or type of cultivation. The current Water Research Commission project Land-use impacts on Salinity in Western Cape Waters (K5/1503) could deliver the deterministic model which could be used in ACRU*Salinity* as well as the typically expected ranges for the salinity-related parameters.

- Additional field studies (focusing on a wider range of land-use), to determine the typical ranges of salinity-related parameters, should be undertaken to provide a database that can be used with an updated ACRU*Salinity* model.

- In the absence of a database of typical salinity related values, the selection of values should be based on the method proposed by Ferguson *et al*. (1994). This would eliminate the use of unrealistic values, as a result of parameter inter-dependence.

- Recession flow behaviour by the ACRU model was less than satisfactory on a few tributaries. The interflow-groundwater dynamics in the model should be further developed.

In conclusion, it is believed that the application of ACRU*Salinity* in this thesis was successful in highlighting many conceptual and logistical considerations which should be addressed in future model applications. It is further the opinion of the author that implementation of the classical kinetic theory (i.e. interpretation of the change in salinity concentration data) in the determination of salinity-related parameters, SALTSAT and SALTUPT, would partly eliminate the problem of non-uniqueness of salinity parameter sets and should be the point of departure for salinity module calibration in future ACRUSalinity model applications. The aforementioned approach, coupled with the activation of the flow routing option in ACRU, would also allow for the direct comparison of daily observed and simulated time series records, providing a basis for quantitative assessment of the goodness-of-fit.

REFERENCES

Acocks, J.P.H. 1975. *Veld Types of South Africa*. Mem. Bot. Surv. S. Afr., 40. Dept. Agric. Tech. Services, Pretoria.

Aris, R. 1975. *The mathematical theory of diffusion and reaction in permeable catalysts – Volume I : The theory of steady state*. Clarendon Press, Oxford.

Addiscot, T M and Wagenet, R J. 1985. *Concepts of solute leaching in soils: a review of modeling approaches*. Journal of soil science. Vol. 36. 411-424.

Bowie, G L *et al*. 1985. *Rates, constants and kinetic formulations in surface water quality modelling*, EPN600/3-85/040, U.S. Environmental Protection Agency, ORD, ERL, Athens, Ga

Bicknell, B.R., Imhoff, J.C., Kittle, J.L., Jr., Donigian, A.S., Jr., and Johanson, R.C., 1997, *Hydrological Simulation Program--Fortran: User's manual for version 11*: U.S. Environmental Protection Agency, National Exposure Research Laboratory, Athens, Ga., EPA/600/R-97/080, 755 p.

Chapra, S C. 2003. *Engineering Water Quality Models and TMDLs*. Journal of Water Resource Planning and Management. ASCE July/August 2003. 247 – 256.

City of Cape Town (CCT). 2002. *Voëlvlei Augmentation Scheme Phase I.* Prepared by Ninham Shand (Pty) Ltd as part of the CMA Bulk Water Supply Study. Ninham Shand Report No. 3245/9531.

Cole, T M and Wells, S A. 2001. CE-QUAL-W2: A *Two-dimensional, laterally averaged, hydrodynamic and water quality model, Version 3.1*. US Army Corps of Engineers Instruction Report EL-00-1 (Draft).

CSIR. 1976. *An investigation into the deteriorating water quality related to drainage from cultivated lands along selected catchments with special reference to the Great Berg River*. Prepared by J.M Fourie.

Cullis, J and Kamish, W. 2006. *Analysis of Management Options at Misverstand Weir to mitigate the potential impact on salinity of the Berg Water Project and Voëlvlei Augmentation Scheme.* Prepared by Kwezi V3 Engineers in association with Ninham Shand Consulting Services for the Department of Water Affairs and Forestry. Draft Final Report.

De Clercq, W P, Ellis, F, Fey, M V, Van Meirvenne, M, Engelbrecht, H and de Smet, G. 2005. *Research on Berg River Water Management – Vol 3 – Water and soil quality information for integrated water resource management: Berg River Catchment*. Prepared by the Department of Soil Science, University of Stellenbosch for the Water Research Commission. WRC Report No : 951/3/05.

Dent, M C, Lynch, S D and Schulze, R E. 1989. *Mapping mean annual and other rainfall statistics over southern Africa*. Water Research Commission, Pretoria, Report 109/1/89.

Department of Water Affairs and Forestry, South Africa. 1996. *South African Water Quality Guidelines (Second Edition). Vol 1: Domestic Use*.

Department of Water Affairs and Forestry, South Africa. 2005. *Review of Observed and Simulated TDS Patterns at Misverstand Dam, Berg River*. Prepared by W Kamish of Ninham Shand (Pty) Ltd.

Department of Water Affairs and Forestry, South Africa. 2005(1). *Updating of FLOSAL Parameters for the Berg River*. Prepared by W Kamish of Ninham Shand (Pty) Ltd.

Department of Water Affairs and Forestry, South Africa. 2005(2). *Review of Dr Fourie's Calculation of Projected TDS concentrations at Misverstand Dam as a Result of the Berg River Dam*. Prepared by W Kamish of Ninham Shand (Pty) Ltd.

Department of Water Affairs and Forestry, South Africa. 1999. *Hydrology. Volume I*. Prepared by GIBB Africa (Pty) Ltd in Consultation with Fongoqa Skade Toyi & Associates cc as part of the Voëlvlei Augmentation Scheme: Feasibility Study. DWAF Report Number PB G100-03-0799.

Department of Water Affairs and Forestry, South Africa. 1997. *Main Report*. Prepared by Ninham Shand as part of the Skuifraam Feasibility Study. DWAF Report No. P G100/00/0596.

Department of Water Affairs and Forestry, South Africa. 1994. *Flow Gauging Stations : Calibration and Evaluation, Volume III : Particulars of Gauging Stations*. Prepared by Ninham Shand Inc. in association with BKS Inc. as part of the Western Cape System Analysis. DWAF report no. P G000/00/1090.

Department of Water Affairs and Forestry, South Africa. 1994 (1). *Flow Gauging Stations : Calibration and Evaluation, Volume IV : Particulars of Gauging Stations*. Prepared by Ninham Shand Inc. in association with BKS Inc. as part of the Western Cape System Analysis. DWAF report no. P G000/00/1090.

Department of Water Affairs and Forestry, South Africa. 1993. *Water Quality, Volume I : General*. Prepared by Ninham Shand Inc. in association with BKS Inc. as part of the Western Cape System Analysis. DWAF Report No.P G000/00/2891.

Department of Water Affairs and Forestry, South Africa. 1993 (1). *Hydrology of the Berg River Basin*. Prepared by Ninham Shand in association with BKS Inc. as part of the Western Cape System Analysis. DWAF report no. P G000/00/2491.

Department of Water Affairs and Forestry, South Africa. 1993(2). *Hydro-salinity Modelling of the Berg River Basin*. Prepared by Ninham Shand Inc. in association with BKS Inc. as part of the Western Cape System Analysis. DWAF Report No. P G000/00/3392.

Dupuit, J. 1863. *Estudes Thèoriques et Pratiques sur le mouvement des Eaux dans les canaux dècouverts et à travers les terrains permèables*, Second Edition, Paris: Dunod, 304 p.

Dzvukamanja, T N, Görgens, A H M and Jonker, V. 2005. *Streamflow Reduction Modelling in Water Resources Analysis*. Water Research Commission, Pretoria, WRC Report no. 1221/1/05. ISBN No. 1-77005-338-7.

Fairbanks, D H and Thompson, M. 1996. *Assessing land-cover map accuracy for the South African Land-Cover Database*. South African Journal of Science Volume 92:Pg 465-470.

Fourie, J M. 1976. *Mineralisation of Western Cape rivers: An investigation into the deteriorating water quality related to drainage from cultivated lands along selected catchments, with special reference to the Great Berg River*. Thesis presented for the degree of Doctor of Philosophy in Agriculture at the University of Stellenbosch.

Fourie, J M and Görgens, A H M. 1977. *Mineralization Studies of the Berg River (1974 to 1976)*. A research report of the National Institute for Water Research of the Council for Scientific and Industrial Research.

Ferguson, R. I, Trudgill, S T and Ball, J. 1994. *Mixing and uptake of solutes in catchments: Model development*. Journal of Hydrology. Vol. 159. 223-233.

Fey, M V, De Clercq W P and Jovanovic N. 2008. *Research on Berg River Water management – Landuse impact on salinity in Western Cape waters*. Draft report to the Water Research Commission.

Görgens, A H M. 1983. *Conceptual Modelling of the Rainfall-Runoff Modelling Process in Semi-Arid Catchments*. HRU Report No. 1/83 to the Water Research Commission. Rhodes University, Grahamstown.

Görgens, A H M, Jonker, V, and Beuster, H. 2001. *The DISA hydrosalinity model*. Water Research Commission, Pretoria, Report No. 369/1/01.

Hall, G C and Du Plessis, H M. 1981. *User's guide to FLOSAL, Vol. 3*. Pretoria : Water Research Commission.

Herold, C E. 1980. A *Model to Compute on a Monthly Basis Diffuse Salt Loads Associated with Runoff*. Prepared by the Hydrological Research Unit, University of Witwatersrand, Johannesburg for the Water Research Commission. Report No. 1/80.

Herold, C E. 1990. *Vaal River Water Quality Management Study – Calibration Procedures for the monthly time-step Hydro-Salinity Model*. Compiled by Stewart, Sviridov and Oliver Consulting Engineers for the Department of Water Affairs – Directorate of Project Planning. Report No. P C000/00/9490.

Herold, C E and Görgens, A. 1991. *Vaal Dam Salinity Assessment with Particular Reference to Atmospheric Deposition*. Pretoria : Stewart Sviridov & Oliver in co-operation with Ninham Shand Inc. Report No. NC120/13/DEQ0391, Hydrological Research Institute, Department of Water Affairs and Forestry.

Jewitt, G.W.P. 1998. *Resolution of scale issues in an integrated catchment information system for the rivers of the Kruger National Park*. PhD Thesis. University of Stellenbosch.

Jurinak, J J, and Suarez, D L. 1990. *The chemistry of salt-affected soils and waters*. Chapter in "Agricultural Salinity Assessment and management". American Soc. Of Civil Eng. New York, pp619.

Kienzle, S W, Lorentz, S A and Schulze, R E. 1997. *Hydrology and water quality of the Mgeni Catchment*. Water Research Commission, Pretoria. Report No. TT87/97.

Kunz, R. 2004. *Daily Rainfall Data Extraction Utility: User Manual. Version 1.3.* Institute for Commercial Forestry Research in conjunction with the School of Bioresources Engineering and Environmental Hydrology, University of Kwazulu-Natal, Pietermaritzburg.

Levenspiel, O. 1972. *Chemical Reaction Engineering - Second Edition*. John Wiley & Sons.

Lynch, S D. 2001. *The development of an improved gridded database of annual, monthly and daily rainfall*. Water Research Commission, Pretoria, South Africa, Project K5/1156/0/1.

Matji, M P. 2000. *Comparative Modelling of Phophorous Production in Rural Catchments*. MSc EngSc Thesis. Department of Civil Engineering, Faculty of Engineering, University of Stellenbosch, South Africa.

Mulvaney, T.J. 1850. *On the use of self-registering rain and flood gauges in making observations on the relations of rainfall and flood discharges in a given catchment*. Transactions of Institution of Civil Engineers Ireland, 4, 18-31.

Nestorov, I S, Hadjitodorov, S T, Petrov, I, Rowland, M. 1999. *Empirical Versus Mechanistic Modelling: Comparison of an Artificial Neural Network to a Mechanistically Based Model for*

Quantitative Structure Pharmacokinetic Relationships of a Homologous Series of Barbiturates. *AAPS PharmSci*. 1999; 1 (4): Article 17. DOI: 10.1208/ps010417.

Neitsch, S L. Arnold, J G, Kiniry, J R, Williams, J R, King, K W. 2002. *Soil and Water Assessment Tool – Theoretical Documentation – Version 2000*. Grassland, Soil and Water Research Laboratory, Temple, Texas. GSWRL Report 02-01.

Ninham Shand Inc. (NSI). 1990. *Breede River System: Development of a Daily Hydrosalinity Model (DISA)*. Department of Water Affairs. Report No. H 000/00/0790.

Nernst, H.W., *Z. Physik. Chem.* 1889, 4 , 129.

Nitsche, N C. 2000. *Assessment of a Hydrodynamic Water Quality Model, DUFLOW, for a Winter Rainfall River*. MSc Thesis, Department of Civil Engineering, University of Stellenbosch, South Africa.

Novotny, V and Olem, H. 1994. *Water Quality: Prevention, identification and management of pollution. Van Nostrand Reinhold*, New York.

Pike A. 2004. *CreateMenuFromGIS. Pre-processor program to automatically delineate primary sub-catchments into finer pseudo sub-catchments*. Obtainable on-line from www.beeh.unp.ac.za/acru under the heading "Utilities".

Pike, A. 2004(1). *Personal communications*. University of Kwa-zulu Natal, Pietermaritzburg, South Africa.

Pike, A. 2004(2). *Personal communications*. *CALC_PPT_COR*. Pre-processor program to prioritize driver rainfall stations. Obtainable on-line from www.beeh.unp.ac.za/acru under the heading "Utilities".

Roberts, P J T. 1987. *The Role of Objective Functions in Digital Simulation Modelling*. In: Thornton, J A. (Ed) Proceedings, Symposium on Modelling of Aquatic Systems. Ecosystem Programme, FRD-CSIR, Pretoria. Occasional Report 24, 159-171.

Ross, S. 1989. *Soil processes: A systematic approach*. Routledge, Chapman and Hall Inc.USA.

Rossouw, J N, Kamish, W and Görgens, A HM. 2006. *Technical Instruments to Support Water Quality Use Allocation*. WRC Report No. K5/1301/1/07, Water Research Commission, Pretoria.

Schäfer, N W. 1991. *Modelling the Areal Distribution of daily rainfall*. MScEng dissertation. University of Natal, Pietermaritzburg, South Africa.

Schultz, C B. 1987. Integrated *Studies of the Generation of Runoff, Solutes and Sediment in Tributary Catchments of the Great Fish River*. Prepared for the Water Research Commission. WRC Report No. 100/1/88. ISBN 0-947447-02-4.

Schulze, R E, Schäfer, NW and Lynch, SD. 1989. *An assessment of regional run-off production in Qwa Qwa*. University of Natal, Pietermaritzburg, Kwazulu-Natal, South Africa.

Schulze, R E. 1995. *Hydrology and Agrohydrology* : A text to accompany the ACRU 3.00 Agrohydrological Modelling System. Water Research Commission, Pretoria, Report TT69/95.

Schulze, R E and Smithers, J C. 1994. *Procedures to Improve and Verify Streamflow Simulations*. In Smithers, J C and Schulze, R E. ACRU Agrohydrological Modelling System User Manual Version 3.00. Water Research Commission, Pretoria, Report TT70/95. pp AM9-1 to AM9-14.

Schulze, R E, Dent, M C, Lynch, S D, Schäfer, N W, Kienzle, S W and Seed, A W. 1994. *Rainfall*. In Schulze, R E. Hydrology and Agrohydrology : A text to accompany the ACRU 3.00 Agrohydrological Modelling System. Water Research Commission, Pretoria, Report TT69/95. pp AT 3-1 to AT 3-38.

Schulze, R E. 1994. *Soil water budgeting and total evaporation*. In *Hydrology and Agrohydrology: A Text to Accompany the ACRU 3.00 Agrohydrological Modelling System*. ed. R E Schulze. Water Research Commission, Pretoria, Report TT69/95. pp AT7-1 to AT7-21.

Seed, A W. 1992. *The generation of spatially distributed daily rainfall database for various weather modification scenarios*. Unpublished report to the Water Research Commission, Pretoria.

Simunek, J, Sejna, M and The. van Genuchten, M. 1996. HYDRUS-*2D. Simulating water flow and solute transport in two-dimensional variably saturated media*. U.S. Soil Salinity Laboratory. USDA-ARS. Riverside, California.

Smithers, J C, Dent, M C, Lynch, S D, Schulze, R E. 1995. *Preparation of daily climate input file*. In : Smithers, J.C. and Schulze, R.E. *ACRU Agrohydrological modeling S System : Users manual Version 3.00*. Water Research Commission, Pretoria, Report no. TT70/95. pp AM4-1 to AM5-10.

STOWA/EDS. 1998. *Duflow for Windows*. Version 3.0. EDS, Leidschendam, The Netherlands.

Tarboton, K C and Schulze, R E with contributions by Lynch, S D, Smithers, J C, Schmidt, E J, Guy, R M and Maharaj, M. 1992. *Distributed hydrological modelling system for the Mgeni catchment*. Water Research Commission, Pretoria, Report no.234/1/92.

Teweldebrhan, A T. 2003. *The Hydrosalinity module of ACRU Agrohydrological modelling System (ACRUSalinity) – Module Development and Evaluation*. Submitted in partial fulfilment of the

requirements for the degree of MSc in Hydrology, School of Bioresources Engineering and Environmental Hydrology, University of Natal, Pietermaritzburg.

Teweldebrhan, A T, Lorentz, S A and Schulze, R E. 2003. *The Hydrosalinity module of ACRU Agrohydrological modelling System (ACRUSalinity): User Manual*. ACRUcons Report 47. School of Bioresources Engineering and Environmental Hydrology, University of Natal, Pietermaritzburg.

Thornton-Dibb, S, Clark, D, Lorentz, S. 2005. *The Addition of a Soil Surface Layer and Corresponding Processes to ACRUSalinity*. School of Bioresources Engineering and Environmental Hydrology, University of KwaZulu-Natal, Pietermaritzburg.

Trans Caledon Tunnel Authority. 2007. *Berg River Dam : Further Water Quality Studies*. Prepared by the Berg River Consultants. Report No. C201.51-17IR.

Walling, D E and Webb, B W. 1986. *Solutes in river systems. In Solute processes*, ed. S TTrudgil. 251-317. John Willey & Sons Ltd., Chichester.

Water Research Commission. 1994. *Surface Water Resources of South Africa 1990*. Volume IV. Report no. 298/4.1/94.

Water Research Commission. 2005. *Surface Water Resources of South Africa 2005.* Draft report prepared by Middleton, B and Bailey, A.

Zucchini, W, Adamson, P T. 1984. *The occurrence and the severity of droughts in South Africa*. Water research Commission, Pretoria, Report no. 91/1/84.

C:\Wageed\final report masters\Final Report_Wageed_Masters.doc

APPENDIX A

Example of Rainfall Station Ranking
for Primary Sub-catchments

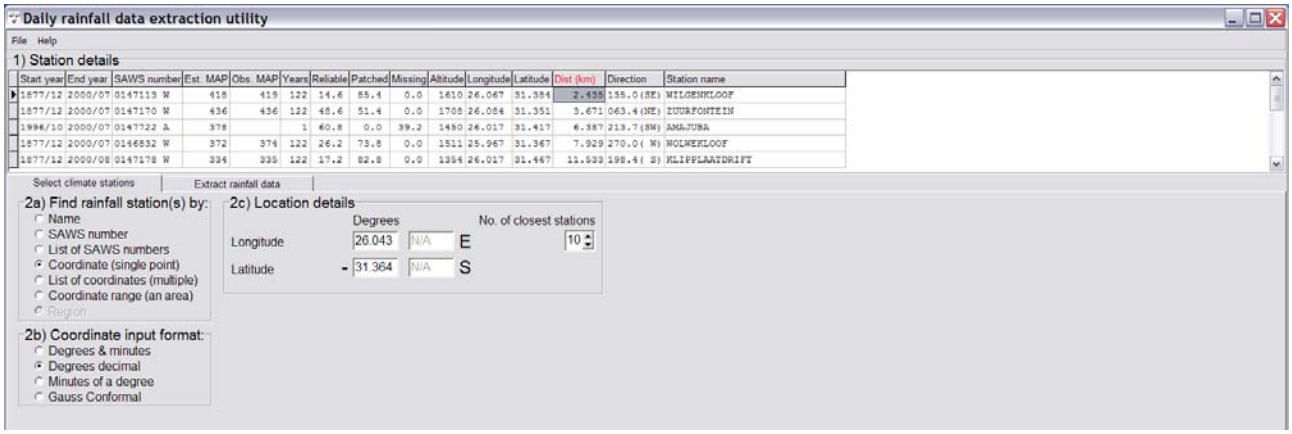
Daily rainfall data extraction utility
File Help
1) Station details
Start year End year SAWS number Est. MAP Obs. MAP Years Reliable Patched Missing Altitude Longitude Latitude Dist (km) Direction Station name
1877/12 2000/07 0147113 W 418 419 122 14.6 85.4 0.0 1610 26.067 31.384 2.435 135.0(SE) WILGENKLOOF
1877/12 2000/07 0147170 W 436 436 122 48.6 51.4 0.0 1708 26.084 31.351 3.671 063.4(NE) ZUURFONTEIN
1996/10 2000/07 0147722 A 378 1 60.8 0.0 39.2 1480 26.017 31.417 6.387 213.7(SW) AMAJUBA
1877/12 2000/07 0146832 W 372 374 122 26.2 73.8 0.0 1511 25.967 31.367 7.929 270.0(W) WOLWEKLOOF
1877/12 2000/08 0147178 W 334 335 122 17.2 82.8 0.0 1354 26.017 31.467 11.533 198.4(S) KLIPPLAATDRIFT
Select climate stations
Extract rainfall data
2a) Find rainfall station(s) by:
Name
SAWS number
List of SAWS numbers
Coordinate (single point)
List of coordinates (multiple)
Coordinate range (an area)
Region
2b) Coordinate input format:
Degrees & minutes
Degrees decimal
Minutes of a degree
Gauss Conformal
2c) Location details
Degrees
No. of closest stations
Longitude 26.043 N/A E 10
Latitude - 31.364 N/A S

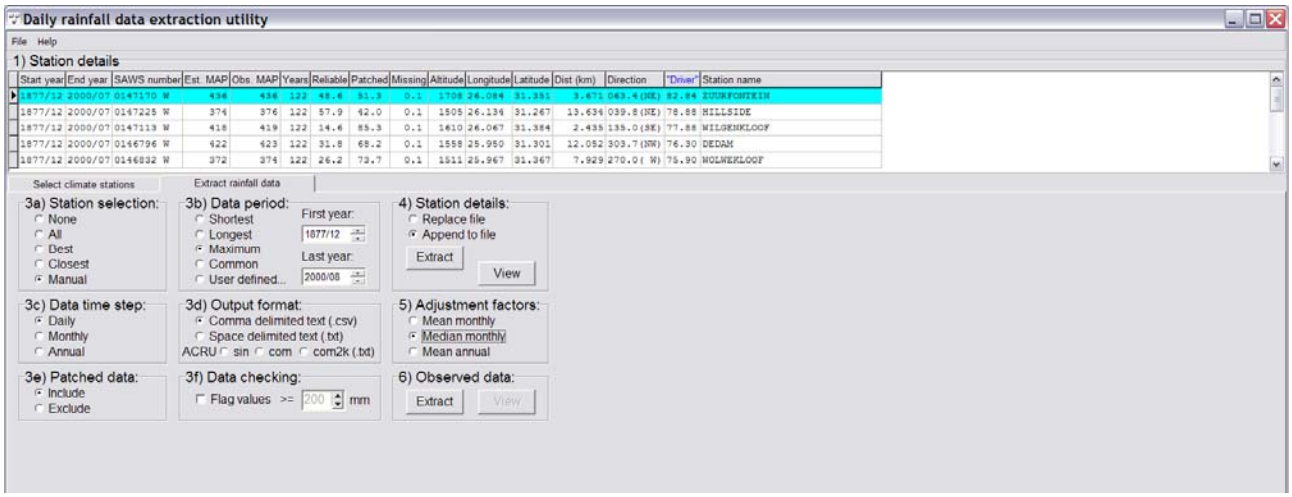
Daily rainfall data extraction utility
File Help
1) Station details
Start year End year SAWS number Est. MAP Obs. MAP Years Reliable Patched Missing Altitude Longitude Latitude Dist (km) Direction "Driver" Station name
1877/12 2000/07 0147170 W 436 436 122 48.6 51.3 0.1 1708 26.084 31.351 3.671 063.4(NE) 82.84 ZUURFONTEIN
1877/12 2000/07 0147225 W 374 376 122 57.9 42.0 0.1 1505 26.134 31.267 13.634 039.8(NE) 78.88 HILLSIDE
1877/12 2000/07 0147113 W 418 419 122 14.6 85.3 0.1 1610 26.067 31.384 2.435 135.0(SE) 77.88 WILGENKLOOF
1877/12 2000/07 0146796 W 422 423 122 31.8 68.2 0.1 1558 25.950 31.301 12.052 303.7(NW) 76.30 DEDAM
1877/12 2000/07 0146832 W 372 374 122 26.2 73.7 0.1 1511 25.967 31.367 7.929 270.0(W) 75.90 WOLWEKLOOF
Select climate stations
Extract rainfall data
3a) Station selection:
None
All
Best
Closest
Manual
3b) Data period:
Shortest
Longest
Maximum
Common
User defined...
First year: 1877/12
Last year: 2000/08
4) Station details:
Replace file
Append to file
Extract
View
3c) Data time step:
Daily
Monthly
Annual
3d) Output format:
Comma delimited text (.csv)
Space delimited text (.txt)
ACRU sin com com2k (.txt)
5) Adjustment factors:
Mean monthly
Median monthly
Mean annual
3e) Patched data:
Include
Exclude
3f) Data checking:
Flag values >= 200 mm
6) Observed data:
Extract
View